PROVENANCE OF THE ICE-CORED MORAINE AT MT. ACHERNAR, LAW GLACIER, ANTARCTICA

Nicole Ann Bader

Submitted to the faculty of the University Graduate School
in partial fulfillment of the requirements
for the degree
Master of Science
in the Department of Earth Sciences,
Indiana University

June 2014

Accepted by the Graduate Faculty, Indiana University, in partial fulfillment of the requirements for the degree of Master of Science.

Master's Thesis Committee

Kathy J. Licht, PhD, Committee Chair

Michael R. Kaplan, PhD

R. Jeffrey Swope, PhD

ACKNOWLEDGEMENTS

I would like to express my gratitude to my advisor, Dr. Kathy Licht for this amazing opportunity to work on this research. She was extremely helpful with any and all questions, and offered excellent guidance, encouragement, enthusiasm, and support throughout this entire process. I could not have asked for a better advisor or friend. I cannot express how much I am truly grateful to Kathy for giving me this amazing opportunity and introducing me to the Antarctic world.

I would also like to thank my committee members, Dr. Michael Kaplan and Dr. Jeffrey Swope for their guidance and suggestions throughout this project. Thank you as well to an honorary committee member, Dr. Timothy Flood. Without your support and encouragement I would not have had this amazing opportunity at IUPUI.

I am also extremely grateful for my fellow lab mates and friends, Theresa Dits and Beth Welke. We have been through so much in these past few years and I would not have made it through the good times nor the bad without your support, laughter, and endless coffee runs. I love you both and thank you for the countless memories!

In my daily work at IUPUI, I am so thankful for such a wonderful support group of both graduate and undergraduate students including Clint Broach, James Harris, Fotios Kafantaris, Shiva Laden, Samapriya Roy, Owen Rudloff, Anna Samuels, Austin Stanforth, Mick Thomas, Rachael Gehrman, Justin Hodgson, and others. I simply could not have done this without their friendship, support, and company on those countless coffee trips. A thank you must also go out to the entire staff in the Earth Sciences Department at IUPUI for their assistance over the past three years.

In addition, a thank you to Mark Pecha, Clay Loehn and other staff at the University of Arizona Laserchron Center for their assistance in zircon imaging and U/Pb

analyses. Thank you to collaborators Michael Kaplan, Gisela Winckler, and Claire Mathieson for sharing unpublished exposure age data used for interpretation. Thank you also to Sandra Passchier, Anne Grunow at the Polar Rock Repository, the staff at the Polar Geospatial Center, ActLabs, and the United States Antarctic Program.

I literally might not have survived field work in Antarctica without the amazing guidance of mountaineer, Mike Roberts (aka Shorty). I now have a deeper appreciation for peas, milk, and not falling into crevasses, so thanks to you!

I would also like to thank my parents Mark and Cheryl, brother Eric, and friend Beth Gregorich for their support and encouragement. No matter what it was, you all knew just what to say to help me through.

This research was supported by the National Science Foundation Office of Polar Programs grant NSF-0944578, an IUPUI Educational Enhancement Grant and IUPUI School of Science Graduate Student Council Grant.

Nicole Ann Bader

Provenance of the Ice-Cored Moraine at Mt. Achernar, Law Glacier, Antarctica

Glacial till from the Mt. Achernar moraine (MAM) records pre- and post- last glacial maximum (LGM) compositional variability of an East Antarctic moraine sequence through time and space. Pebble lithology, detrital zircon geochronology, and till geochemistry were analyzed on samples from a 6.5 km transect. Hummocky topography occurs with the most recently exposed material along the active ice margin (Zone 1), followed by a relatively flat and low region (Zone 2), and then a series of ~2 m high parallel/sub-parallel ridges and troughs accompanied by distinct color changes that are directly related to the dominant lithology of the region (Zones 3–5). Zone 3 is dominated by ~38% more sedimentary rocks than adjacent zones and has an overall shape of a broad arch superimposed with smaller ridges. Zone 4 is composed of distinct colored bands that alternate between dominant sedimentary and mafic igneous lithologies. These dominant sedimentary and intermediate/mafic igneous rocks for all Zones are interpreted to be primarily the Beacon and Ferrar Supergroup rocks respectively. The U/Pb data from the till is consistent with a Beacon Supergroup source as samples consistently show significant populations from the Permian ~250-260 Ma, the Proterozoic ~565–600 Ma, ~950–1270 Ma, and ~2300-2320 Ma, as well as (and) the late Archean ~2700-2770 Ma. The Pagoda, Mackellar, Buckley, and Fremouw Formations are potential sources of the detrital zircons. When paired with surface exposure ages, the U/Pb data indicates that the debris source has been consistent over the past ~555 ka, implying relatively stable ice sheet behavior. However, ice sheet change is indicated by a trim line present on Mt. Achernar that can be traced back to the boundary between Zones 3 and 4, as well as a change in pebble lithology, geochemistry, and morphology of Zone

3. Zone 3 records a time of ice sheet thickening and a change in provenance during the LGM. Zone 4 is pre-LGM, Zone 2 records deglaciation, and Zone 1 is still actively connected to the Law Glacier. This study reveals the broader importance of using multiple provenance techniques when interpreting provenance changes in till over time.

Kathy J. Licht, PhD, Committee Chair

TABLE OF CONTENTS

LIST OF TABLES

LIST OF FIGURES

LIST OF APPENDICES

INTRODUCTION

Antarctica is the reservoir for 70% of the world's fresh water and plays a potentially vital role in climate change and ocean circulation patterns. The Transantarctic Mountains (TAM) divide the continent of Antarctica into two regions, the East and West. The East Antarctic Ice Sheet (EAIS) overrides the TAM in places and drains into the Ross Sea via a series of outlet glaciers. The behavior of the EAIS has been considered relatively stable due to the fact that most of the ice sheet rests on bedrock above sea level and is therefore less susceptible to changes in climate and sea level rise (Pollard and DeConto, 2009). However, recent studies show widespread lakes and water beneath the ice (e.g., Siegert et al., 2005; Wingham et al., 2006; Stearns et al., 2008), as well as evidence of past ice sheet collapse as a response of climatic warmth during the Pliocene (e.g., Cook et al., 2013), indicating a much more dynamic behavior than once thought. In contrast, the West Antarctic Ice Sheet (WAIS) is a marine based ice sheet that is mostly grounded below sea level, which makes it much more susceptible to changes in sea level and variations in ocean temperatures (Joughin and Alley, 2011). Reconstructions of the EAIS and WAIS provide modelers with essential parameters that are used to predict Antarctica's response to changes in climate. One such response is the 65-meter rise in sea level that would occur if both the WAIS and EAIS were to completely melt (Pollard and DeConto, 2009; Fretwell et al., 2012). This drastic rise in sea level would undoubtedly have worldwide detrimental economical and societal impacts. While this drastic rise in sea level is possible, the upper bound of predictions for the contribution of the WAIS to sea level rise in the 21st century ranges from 0.2–0.4 m (Joughin and Alley, 2011).

Antarctic ice sheet evolution both during and since the last glacial maximum (LGM) has been studied extensively (e.g., Denton and Hughes, 2002; Anderson et al., in press). However, pre-LGM glacial deposits and ice sheet flow reconstructions are less common because readvance and thickening of downstream ice destroys previous records of glacial events. Limited constraints on pre-LGM fluctuations of the EAIS are directly related to this relative lack of data (Bromley et al., 2010). Evidence now suggests that pre-LGM records may be preserved in the blue ice regions at the head of outlet glaciers in the TAM (Bromley et al., 2010; Ackert et al., 2011, 2013).

Compositional and provenance studies of glacial till and pebbles deposited in blue-ice moraines can not only reveal what is being deposited from beneath the ice, but also provide insight to past ice sheet configurations. This study focuses on the blue-ice moraine sequence of Mt. Achernar, located in the Queen Alexandra Range along the Law Glacier, Antarctica (Figure 1). Multiple provenance techniques, as well as cosmogenic surface exposure dating, are utilized in order to test three hypotheses: (1) the moraine sequence at Mt. Achernar contains a mixture of subglacially derived sediment and locally-derived debris eroded from nearby outcrops, (2) till composition within the moraine varies through time, (3) and moraine morphology reflects Quaternary changes in the ice flow dynamics of the EAIS. The results indicate that the Mt. Achernar moraine (MAM) is not only a vital source of information regarding what rock types lies upstream beneath the EAIS, but also changes in Late Quaternary ice sheet dynamics. This research, combined with a similar project at Mt. Howe, head of the Scott Glacier, (Dits et al., 2012; in prep) results in the first systematic dataset that documents compositional variability of East Antarctic moraine sequences through time and space, and how that variability relates to changes in climate. The results of both studies help to provide a

more detailed understanding of the dynamics of the EAIS, which in turn provide modelers with additional constraints that lead to more accurate models to explain past and predict future ice sheet dynamics.

BACKGROUND AND GEOLOGIC SETTING

Early Antarctica

East Antarctica (EA) is one of the Earth's largest, intact Precambrian continental interiors, containing some of the Earth's oldest continental crust (Goodge et al., 2010). The formation of the core of EA began in the Archean and concluded in the Mesoproterozoic (Tingey, 1991; Goodge and Finn, 2010) and was an integral part of two major supercontinents, Rodinia and Gondwana. Rodinia assembled in the Neoproterozoic between 1300–900 Ma and is associated with the global mountain building event known as the Grenville Orogeny (Goodge et al., 2010). Rodinia lasted ~150 Ma before it began to break apart between 825 and 740 Ma as a result of rifting caused by a superplume (Li et al., 2008). The supercontinent of Gondwana ultimately formed between 600 and 530 Ma as a result of oblique plate collision and subduction-related intrusions of the Neoproterozoic Beardmore and Pan-African Orogenies, as well as the Cambrian-Ordovician Ross Orogeny (Fitzgerald, 2002; Veevers, 2003). The Ross Orogeny is characterized by the deformation and metamorphism of Neoproterozoic and Cambrian sedimentary and volcanic basement rock as well as the intrusion of granitoid batholiths known as the Granite Harbour Intrusives (Stump, 1995; Fitzgerald, 2002). The Ross Orogeny ceased around 480 Ma and was followed by exhumation and ~15–20 km erosion of the basement rock, which is currently known as the Kukri Erosion Surface (Stump, 1995).

Following the erosion of the metamorphic and igneous basement rock was the extensive sedimentation of the Beacon Supergroup, which is preserved in two main sedimentary basins: the McMurdo and Ellsworth Basins (Barrett, 1991). These basins were surrounded by a pre-Cambrian craton on one side and highlands that included a

magmatic arc on the other (Barrett, 1991). The oldest rocks of the Beacon Supergroup are the Taylor Group. The Taylor Group is dominated by alluvial and glacial systems in the Devonian as seen by the stream deposited quartzose sandstones of the Alexandra Formation (Barrett, 1991; Faure and Mensing 2010). The Victoria Group consists of sedimentary formations deposited in the Permian–early Jurassic (Figure 2). The oldest formation of the Victoria Group is the Pagoda Tillite and was deposited in the late Carboniferous–early Permian and is characterized by massive, poorly sorted sandstones/diamictites (Barrett, 1991; Faure and Mensing, 2010). The glacial sediments of the Pagoda were deposited during retreat of the large continental ice sheet in Gondwana (Faure and Mensing, 2010). The remaining formations of the Victoria Group, the Mackellar, Fairchild, Buckley, Fremouw and Falla Formations, are all are indicative of alluvial sedimentation originating from the reactivation of the Paleozoic magmatic arc as subduction occurred along the Pacific Plate margin in West Antarctica (Barrett, 1991; Faure and Mensing, 2010). Increasing proportions of eroded Ross-age granites from East Antarctica were contributed to Beacon Supergroup sediments as the source regions shifted throughout the Permian (Elliot and Fanning, 2008). The Mackellar Formation is dominated by carbonaceous shales interbedded with sandstones. The Fairchild Formation is dominated by arkosic sandstones with minor siltstones and shales. The Buckley Formation is characterized by thick-bedded sandstones interbedded with carbonaceous shale and coal (Barrett, 1991; Faure and Mensing, 2010). Deposition of the Victoria Group ended in the Triassic with the Fremouw and Falla Formations (Barrett, 1991) (Figure 2). These Triassic strata are attributed to the late Permian–early Triassic uplift associated with the Gondwanide Orogeny and were deposited by low-sinuosity rivers (Barrett, 1991). The Fremouw Formation consists of 3 parts: the basal beds are

composed of quartz sandstone and greenish-grey mudstone, and the middle beds are composed of mudstone that is capped by upper beds of volcanic sandstone (Faure and Mensing, 2010). The Falla Formation is a sequence of sandstones and shales capped by tuffaceous sandstones (Faure and Mensing, 2010).

The onset of rifting of Gondwana that began in the Jurassic involved the rotation of microplates as East Gondwana stretched away from West Gondwana (Fitzgerald, 2002). The formation of a basin in the Ross Embayment began with stretching, subsidence, and possible strike-slip motion (Fitzgerald, 2002). The rifting was accompanied by tholeitic magmatism, which is noted by the intrusion of dykes and sills of the Ferrar Dolerite and its extrusive equivalent, the Kirkpatrick Basalt that extends over 3,000 km and is dated to 184–183 Ma (Elliot and Fleming, 2000)

The Transantarctic Mountains

The Transantarctic Mountains (TAM) are approximately 3,500 km long, 100–200 km wide, and reach heights up to 4.5 km (Fitzgerald, 2002). Multiple models have been proposed to explain the elevation and uplift mechanisms of the TAM, including isostatic rebound from glacial erosion that can account for as much as 2,000 m uplift in the central TAM (Stern et al., 2005), and a topographic reversal of a high elevation plateau with thicker than average crust during Cretaceous extension (Bialas et al., 2007). Using apatite fission-track thermochronology, the uplift of the TAM has been constrained. Fitzgerald (2002) suggested that the uplift of the TAM occurred in three separate events. The first of these events is the break up between Australia and Antarctica in the early Cretaceous ~125 Ma (Stagg and Willcox, 1992) and resulted in 1–2 km of uplift (Fitzgerald, 2002). The second major event is related to the main extensional phase between East and West Antarctica that took place at the end of the early and into late

Cretaceous between 105–85 Ma. The third major event associated with the exhumation of the TAM occurred in the early Cenozoic ~55 Ma and involved seafloor spreading that began in the Adare Trough region and continued southward into the continental crust underlying the western Ross Sea (Fitzgerald, 2002). Through the use of apatite fission-track thermochronology, exhumation of the TAM seems to have begun earlier in Victoria Land than farther along the southern regions of the TAM: ~55 Ma in north and south Victoria Land, ~50 Ma in the Beardmore and Shackleton Glacier regions, and ~45 Ma near Scott Glacier (Fitzgerald, 2002). Not only does the exhumation age decrease southward along the TAM, but this younging trend is also noted as age dates were taken farther inland. This inland younging trend is noted in the Shackleton Glacier region where the exhumation age is ~50 Ma along the coast and ~45 Ma further inland (Fitzgerald, 2002). There is little known about the exhumation history between 40 and 15 Ma. Due to the cooling climate and glaciation of the continent, it is hypothesized that the rate of exhumation, as well as the rate of erosion, began to decline (Fitzgerald, 2002). The modern day features and faulting of the TAM were mostly complete by ~15 Ma (Fitzgerald, 2002).

Antarctic Ice Sheet Evolution

A dramatic climate cooling occurred ~34 Ma that may have been triggered by a drop in atmospheric CO_2 levels (DeConto et al., 2008). In addition to this CO_2 decrease, Antarctica became physically isolated as the last two fragments of Gondwana drifted away from Antarctica; Australia at ~35.5–32 Ma (Lawver and Gahagan, 2003; Stickley et al., 2004) and South America between 40 and 8 Ma (Barker et al., 2007). The physical isolation allowed the Southern Ocean to surround Antarctica and create the Antarctic Circumpolar Current (ACC), which thermally isolated Antarctica even more. This

change in ocean circulation and climate cooling initiated the first Antarctic glaciation at the Eocene-Oligocene boundary ~34 Ma (e.g., Wise et al., 1991). For the subsequent ~20 Ma, Antarctic ice sheets regularly reached the continental margin and retreated every 40,000 years (Bertler and Barrett, 2010). Coinciding with a global cooling in the mid-Miocene, (Zachos, 2001), the behavior of these Antarctic ice sheets are thought to have stabilized ~14.2–13.8 (Bertler and Barrett, 2010). Today, there are two main ice sheets dominating the Antarctic continent. The WAIS is a marine-based ice sheet in which most of the bed lies beneath sea level, over 2,000 m below in some regions (Fretwell et al., 2012). In contrast, the EAIS is mostly grounded above sea level, although there are regions much further below sea level than previously thought; over 1,000 m in some regions (Fretwell et al., 2012). Combined, the EAIS and WAIS covers ~98% of the Antarctic continent and are ~5 km thick in some regions (Fretwell et al., 2012).

Both the EAIS and WAIS drain into the Ross Embayment (Denton and Hughes, 2000). The EAIS drains through the TAM via outlet glaciers and flow into either the Ross Ice Shelf (RIS) or the Ross Sea. The WAIS drains through ice streams into the RIS. The amount and speed of ice draining from the EAIS and WAIS both rely on location of the grounding line and thickness of the RIS. As the RIS thickens, the grounding line advances in the Ross Embayment, therefore suppressing the effect that ocean water has on subglacial melting and slowing overall ice mass loss (Stearns, 2011). Studies indicate that without the Ross Ice Shelf acting as a dam for the outlet glaciers and ice streams of the EAIS and WAIS, increased fast-flow drainage could have detrimental effects for the stability of the behavior of both ice sheets (Pollard and DeConto, 2009). The damming effect caused by thickening of the WAIS and RIS during glacial events, such as the LGM, causes substantial thickening at the mouths of outlet glaciers (>1,000 m) and little

effect at the heads of the EAIS outlet glaciers (e.g., Denton and Hughes, 2000; Bromley et al., 2010; Ackert et al., 2011). As ice thickens, boulders and till are left perched along mountain faces and are deposited at successively lower elevations as ice thins. Cosmogenic dating indicates that boulders perched along vertical transects are LGM and younger, indicating records of previous periods of thicker ice were destroyed (Bromley et al., 2010). However, the boulders perched in laterally accumulating moraines at the heads of the outlet glaciers along the polar plateau can preserve records over multiple glacial cycles (Denton et al., 1989; Bromley et al., 2010).

Law Glacier and Mt. Achernar

The Law Glacier is located between the MacAlpine Hills and the Queen Elizabeth Range, is approximately 20 km wide, and feeds into the Bowden Névé (Figure 1). The Law Glacier contains blue ice areas characterized by dimpled ice that can only be maintained by sublimation and wind scouring processes dominating over snow accumulation (Bintanja, 1999). Regions, such as nunataks, with irregular surface topography can induce a microclimate of increased localized wind turbulence, which is favorable for the formation of blue ice regions while simultaneously acting as a barrier of the ice flow of the main outlet glacier and forcing the ice to flow in an upward direction (Whillans and Cassidy, 1983; Bintanja, 1999). This upward direction of ice flow, in addition to the high sublimation rates, allows for the formation of blue-ice moraines as rocks and till accumulate at the ice surface.

The MAM, the focus of this study, is in the central TAM, near the head of the Law Glacier. Mt. Achernar is located at 84^{o} 12'S and 160^{o} 56'E and its base sits at an elevation of ~2,000 m (Faure and Mensing, 2010). This nunatak is influenced by it's own microclimate of increased wind turbulence and weather patterns that may differ from

that of local areas (Figure 3), and an extensive blue-ice moraine complex has formed adjacent to Mt. Achernar as a result. This ice-cored moraine extends approximately 15 km downstream from Mt. Achernar and 7.5 km from Law Glacier to the Lewis Cliff Ice Tongue. The glacially-derived material on the MAM is thought to be concentrated in the same manner that Whillans and Cassidy (1983) described for the concentration of meteorites on the plateau of the EAIS side of the TAM, except that the rocks in the moraine have been eroded from bedrock or fallen from local outcrops rather than being originally derived from space. Whillans and Cassidy (1983) described three mechanisms for the concentration of meteorites: meteorites fall into the snow accumulation zone and are transported to the ablation zone by ice flow, they fall directly onto the ablation zone, and/or are concentrated by compressive ice flow; all three processes also likely affect the MAM.

The Mt. Achernar nunatak consists of flat-lying, Permian sandstones and coal seams of the Buckley Formation (Beacon Supergroup) (Stump, 1995). The Jurassic Ferrar Dolerite sills intruded the Buckley Formation, causing contact metamorphism (Stump, 1995). As seen in many sills of the Ferrar Dolerite throughout the TAM, these rocks at Mt. Achernar range from fine to coarse grained, and show evidence of strong jointing and hydrothermal activity (Stump, 1995).

PREVIOUS RESEARCH

Studies reveal that the thickening of the WAIS and RIS during glacial events play a large role in determining both the behavior and thickness of the EAIS outlet glaciers feeding into the Ross Sea. During the LGM, the mouths of the East Antarctic outlet glaciers thickened over 1,000 m in some places as a result of WAIS and RIS thickening, while very little change in elevation was noted at the heads of the outlet glaciers (e.g., Denton and Hughes, 2000; Bromley et al., 2010; Ackert et al., 2011). As ice thickened, boulders were left perched along nunatak faces and are deposited at successively lower elevations as ice thinned. Exposure dating indicates that boulders perched along vertical transects of the Reedy and Scott Glaciers are LGM and younger, typically showing maximum ice thickness occurring ~13–18 ka (Hall and Denton, 2000; Todd et al., 2010; Allard et al., 2011; Koffman et al., 2011).

Debris that accumulates in ablation moraines may be a combination of rock fall and subglacial derivation. Palmer et al. (2012) identified both local and exotic rock types in blue ice moraines at the Lonewolf Nunataks at the head of Byrd Glacier, Antarctica. Approximately 25% of pebbles are faceted and/or striated, which also indicates subglacial origin. Palmer et al. (2012) also reported that the particle size shows evidence of subglacial origin. Silt and clay sized sediments are more abundant (>50% fines) than in active lateral moraines located downstream (<10% fines).

Faure et al. (1992) studied the MAM during the 1990-1991 field season and found that the till is composed of dolerite, basalt, sandstone, siltstone, shale (gray, red, and black), limestone, and minimal amounts of conglomerate, hornfels, and tillites. Their studies also indicated that granitic igneous rocks and high-grade metamorphic rocks from the Precambrian shield of East Antarctica are absent. In addition, particle traps were

placed along the Lewis Cliff Ice Tongue and were used to measure the size fractions of wind-blown sediment; most samples were dominated by the 0.250-0.125mm size fraction (fine sand) (Hagen, 1995).

Previous work suggests the MAM formed in a time-progressive manner, with age increasing away from the ice margin of the Law Glacier (Hagen, 1995). Hagen calculated the exposure age of five sandstone boulders from the MAM by measuring the concentration of ^{26}Al and ^{10}Be in quartz. The results showed minimum exposure dates between 315 ± 5 ka and 14 ± 0.5 ka with age increasing away from the active ice margin of the Law Glacier (Figure 4). Hagan (1995) recalculated two of the dates to take into account thinning rate of the ice sheet and the elevation of the collection site relative to the present level of the Law Glacier; recalculated ages are 664 ± 123 ka and 577 ± 112 ka. Thus, Hagen (1995) inferred the formation of the moraine to have begun around 664 ka. They interpret their results as support for the hypothesis that the EAIS has receded after a major ice advance in early to middle Pliocene time and that ice-cored moraine ridges at the edge of the ice sheet form sequentially as the ice recedes across the landscape (Faure and Nishiizumi, 1994).

METHODS

Sample Acquisition and Provenance Tools

A topographic profile (Figure 5) was created across the MAM utilizing a Trimble GPS backpacking system in order to characterize a main transect of interest. Regions lying along this main transect were divided into five zones based on field observations: Zone 1 has hummocky topography, Zone 2 is relatively flat with little relief, and Zones 3–5 were established based on color changes. A second sampled transect, hereafter known as the "tail," is located along the ice edge of Zone 1, downstream from the main transect (Figure 1). It was sampled to assess spatial variability under a priori assumption that samples near the ice margin have similar relative age.

On various moraine crests in these zones, 1m x 1m areas were selected and all pebbles, coarse-very coarse gravel in size, on that surface were photographed and collected. More than 1500 pebbles were collected from 24 sites (Table 1, Figure 1) and were compared to a reference collection of regionally mapped bedrock obtained from the Byrd Polar Rock Repository. Cluster analysis was run on all sampling sites using Paleontological Statistics software (PAST) (Hammer et al., 2001) and was based on pebble lithologies listed in Table 2, including the criteria of faceted and/or striated pebbles (Table 3). A non-random sampling of more than 50 cobbles and large pebbles was collected from along the tail and across the main transect and targeted material that was representative of the local lithology and others that were inferred to be exotic. Approximately 1kg of bulk till was also collected from 36 sites (Table 1, Figure 1). The top 5 cm of till was removed before collection to avoid particle size biasing due to wind deflation. Each till sample was prepared for a suite of three different analytical

measurements. These analyses include particle size analysis, U/Pb dating of detrital zircons, and geochemical analysis of the silt and clay-sized fraction.

The uranium-lead decay system has played a vital role in quantifying geologic time. There are few minerals that contain high concentrations of uranium that are suitable for uranium-lead dating, yet these minerals are well known and easy to obtain. The most common of these minerals is zircon ($ZrSiO_4$). Zircon is the most commonly used mineral because of its chemical and physical stability over a wide range of lithospheric pressures, temperatures, and fluid/melt compositions (Moecher and Samson, 2006). Zircon contains concentrations of uranium well above the average of its host rock and preserves its original concentration of uranium (U) and accumulated lead (Pb) (Davis et al., 2003). Other minerals such as uraninite, thorianite, monazite, sphene, and apatite often have these same properties, yet zircon is the most abundant due to the fact that it is a trace component of felsic rocks (Davis et al., 2003; Faure, 1986). U/Pb dating of zircons is used to determine the age of igneous rocks, the maximum age of stratigraphic successions, recognize gaps in the geologic record, and determine provenance characteristics of rocks and sediments (Fedo et al., 2003).

As part of a collaborative research effort, Dr. Michael Kaplan collected samples from the tops of sandstone and dolerite boulders on various moraine crests across the main transect (Figure 1) for surface exposure dating. Claire Mathieson and Drs. Michael Kaplan and Gisela Winckler (Lamont-Doherty Earth Observatory) analyzed the quartz and pyroxene from these samples for concentrations of ^{10}Be, ^{26}Al and ^{3}He in order to estimate how long these samples were exposed at the surface of the moraine. Surface exposure ages (Figure 4) were used to establish time constraints for the evolution of the MAM.

Particle size analysis

Thirty-six bulk till samples were chosen for particle size analysis (Table 1, Figure 1). Approximately 15–100 g of sub-sampled sediment from these samples was freeze dried for 24 hours on a VirTis Benchtop freeze drier. The weight of coarse fraction (>1000 μm) was determined by dry sieving. Approximately 1.5–2 g of the fine fraction (<1000 μm) was then heated for 1–1.5 hours with 5 mL of 30% H_2O_2 added every 30 minutes to remove organic material. Once heating of the samples was completed, 8 mL of 25 g/L magnesium chloride was added to each sample. The samples were then wet sieved through a 125μm sieve. The >125 μm fraction was examined using a Leica MZ95 stereoscope and any organic material remaining was removed by hand. The <125 μm and >125 μm fractions were then recombined and placed in a 600 mL beaker filled with DI water and left to settle for 24 hours; additional MgCl was added to aid in settling of any samples in which the fine fraction was not settling. Once settled, the supernatant was siphoned from the beaker and the remaining sediment was poured into 50 mL centrifuge tubes and centrifuged for 15 minutes at 8000 rpm. The supernatant was poured out of these tubes and 20 mL of 2.5 g/L sodium metaphosphate was added before samples were stored. Following these initial preparation steps, the samples were either completely used or split from 1/2 to 1/8 and analyzed using a Malvern Mastersizer 2000 laser particle size analyzer. Each sample was measured (percent by volume) 3–6 times for its clay, silt, and sand-sized content ranging from 0.02–1000 μm. Average values are reported in Tables 4 and 5.

U/Pb analysis of detrital zircons

In preparation for U/Pb analysis, the 63-150 μm fraction of 8 till samples and 4 cobbles were sent to the Arizona LaserChron Center (ALC) for zircon separation using

heavy liquids. Once separated, the zircons of unknown age, R33 and Sri Lankan (SL) standards of known age and isotopic composition were mounted in one inch diameter epoxy pucks and polished to half the grain thickness (Gehrels, 2012). Low resolution back-scatter electron (BSE) images were taken of each sample before analysis in order to differentiate the zircons from other minerals and to aid in the selection of where to place the laser over the zircon so that any inclusions, cracks, or regions of zonation would be avoided during laser ablation.

Using laser ablation multicollector inductively coupled plasma mass spectrometry (LA-MC-ICPMS), the U/Pb isotopic ratio was measured for ~24–122 of randomly selected zircons from each of the 8 till samples. The R33 standard zircons were analyzed for calibration purposes at the beginning, middle, and end of each sample and are of known age of 419.3 ± 0.4 Ma (Black et al., 2004). The SL standard zircons were analyzed to correct for any elemental fractionation. SL zircons are 563 ± 2.3 Ma in age and were analyzed and at the beginning and end of each sample, as well as after every fifth unknown zircon analysis (Gehrels et al., 2006). This method of standard-sample bracketing yields accuracy of 1-2% (2-sigma) (Gehrels, 2012).

The ablation of zircons was completed utilizing a Nu Plasma HR ICPMS and a Photon Machines Analyte G2 Excimer laser that ablates a pit in each zircon that is 30 μm in diameter and ~15 μm deep. Analysis for each zircon consisted of measuring the background by one 15-second integration for background with the laser off, 15 one-second integrations with the laser firing, and finally a 30 second delay to purge the previous sample and prepare for the next analysis. The ablated material was carried in helium gas into the plasma source of the Nu Plasma HR ICPMS. Due to its sufficient flight tube width, this ICP-MS allows for the simultaneous measurement of U, Th, and Pb

isotopes. These measurements were collected using $3x10^{11}$ ohm Faraday detectors for ^{238}U, ^{232}Th, ^{208}Pb, and ^{206}Pb, a 10^{12} ohm Faraday collector for ^{207}Pb, and dynode ion-counting channels for ^{204}Pb and ^{202}Hg. Ion yields are ~0.8 mv per ppm (Gehrels et al., 2008).

For each analysis, the errors in determining $^{206}Pb/^{238}U$, $^{206}Pb/^{207}Pb$, $^{206}Pb/^{204}Pb$ result in a measurement error of ~1–2% (2-sigma). However, errors in measurement of $^{206}Pb/^{207}Pb$ and $^{206}Pb/^{204}Pb$ only result in ~1–2% uncertainty in age for grains that are >1.0 Ga; substantially larger margins of error occur for younger grains due to low intensity signal of ^{207}Pb (Gehrels et al., 2008).

The error of common Pb is corrected by using the measured ^{204}Pb and using Stacey and Kramers (1975) to assume an initial Pb composition, including uncertainties of 1.5% for $^{206}Pb/^{204}Pb$ and 0.3% for $^{207}Pb/^{204}Pb$. The measured value of ^{204}Pb is unaffected by the presence of ^{204}Hg because ^{202}Hg is measured on peaks during laser ablation and ^{204}Hg is subtracted based on the natural ratio of $^{202}Hg/^{204}Hg$ of 4.35 (Gehrels et al., 2006).

Interpreted ages are based on $^{206}Pb/^{238}U$ for grains <1.0 Ga and on $^{206}Pb/^{207}Pb$ for grains >1.0 Ga (Gehrels et al., 2008). By comparing these aforementioned ratios, any analyses that are >30% discordant or >5% reverse discordant are not considered further. For most detrital zircon samples, significant age populations are only defined as clusters with three or more overlapping analyses (Gehrels, 2012).

The resulting interpreted ages are shown on Pb/U concordia diagrams and relative age-probability diagrams using the routines in Isoplot (Ludwig, 2008). The normalized probability plots are formed by calculating a normal distribution from the data, totaling the probability distribution of all accepted analyses, and dividing the area under the curve

by the number of analyses (Gehrels, 2012). The peak heights of the age distribution curves are a function of the number of grains at a particular age and the precision associated with that analysis. The age-probability diagrams show each age and its uncertainty as a normal distribution and show the sum of all ages from a sample into a single curve (Gehrels, 2012).

The interpreted ages are also analyzed using the Kolmogorov-Smirnov test (K-S test) in order to evaluate the similarity between distributions. The K-S test is used to compare age population distributions to determine if they are statistically different at a 95% level of confidence. The null hypothesis, two samples are not drawn from the same population, was rejected when the "P" value exceeded 0.05.

Geochemical analysis

The major, trace, and rare earth element concentrations were determined for the <63 micron fraction of 25 till samples from across the transect (Table 1, Figure 1). Geochemical analysis was performed by Activation Laboratories in Ontario, Canada using x-ray fluorescence (XRF) and inductively coupled plasma-mass spectroscopy (ICP-MS). Samples were mixed with a flux of lithium metaborate and lithium tetraborate, fused in an induction furnace at ~1100 degrees C, and dissolved in 5% nitric acid. The samples were run for major oxides and some trace elements on a combination simultaneous/sequential Thermo Jarrell-Ash ENVIRO II ICP. The remaining trace elements were analyzed on a Panalytical Axios Advanced wavelength dispersive XRF, while the REE were digested in acid and analyzed with a Perkin Elmer Sciex ELAN 9000 ICP-MS. Major oxides, trace and rare earth elements measured are listed in Table 6. As, Mo, In, Sb, and Bi were also measured, but concentrations were below detection limit are therefore not listed in Table 6.

RESULTS

Field Observations

An extensive blue ice moraine complex lies northwest of and adjacent to Mt. Achernar and extends approximately 15 km downstream and 7.5 km from Law Glacier to the Lewis Cliff Ice Tongue (Figure 1). The MAM is characterized by a series of troughs and ridges 1–12 meters high that have formed roughly parallel to the Law Glacier margin (Figure 5). Distinct colored bands parallel to the moraine are evident and are related to the dominant pebble/cobble lithology (Figure 6). The topography of the ridges and colored bands help to separate the moraine into multiple distinct regions, or zones, that were used throughout this study. Zone 1 has hummocky topography, occasional salt crust or meltwater, and a distinct "red/grey line" (noted more so in the "tail" of Zone 1) that separates regions dominated by intermediate/mafic igneous lithologies, interpreted to be the Ferrar dolerite, that are covered in a grey coating to those that exhibit more of a red color that is associated with weathering of the dolerite. The tail of Zone 1 refers to the moraine that is located along the ice edge of Zone 1, downstream from the main transect. Zone 2 is a relatively flat region with no distinct color changes. Zones 3–5 all have parallel/sub-parallel ridges, but are different in color and broad topography. Zone 3 is dominated by sedimentary rocks and has an overall shape of a broad arch, with an ~18 m elevation increase from the Zone 2/3 boundary to the highest point and the same ~18 m elevation drop at the Zone 3/4 boundary (Figure 5). Zone 4 is composed of distinct color bands that alternate between dominant lithologies of sedimentary and mafic igneous lithologies, as well as an overall steady elevation increase of ~30 m up and away from Law Glacier. Zone 5 is characterized by its presumed oldest exposure age due to extensive varnish on the cobbles and boulders. The formation of the moraine and ridges

appears to be influenced by multiple ice tongues, which is most evident in the distortion of the ridges near the Lewis Cliff Ice Tongue (Figure 6), and the ridges in Zone 5 that are orientated in the opposite direction of Zones 1–4 (Figure 6). A potential fold feature that is also influencing the formation of the MAM is referred to as the "hook" (Figure 7). The ridges are continuous both east and west of the hook and become more distorted as they approach this feature.

Till cover ranges from 1 cm to >45 cm in thickness, and from light to dark grey along the ice margin and progresses to pale yellow and light yellowish brown towards the nunatak (Figure 5, Table 1). Various sites throughout Zone 4 and site 5A have surficial sediment crusts that overlie loose till and vary from <0.5–1 cm in thickness and platy to "knobby" in form (Figure 8). The material of the moraine ranges from clay to boulders larger than a few meters in diameter. Although a systematic analysis was not completed, the large cobbles and boulders seem to be most prominent in Zone 4, although they do appear in Zone 3 as well. Zones 1 and 2 appear to be mostly dominated by smaller cobbles, pebbles, and loose till, although some boulders are present.

Patterned ground was noted near sites 1E and 1E Red/Grey, as well as throughout Zones 3 and 4 (Figure 1). In Zone 3, the cracks of the patterned ground are ~75–125 cm deep, not sorted into well defined polygons, but are filled with mostly a matrix of loose sediment and some cobbles. On the sides of some of these polygon trenches, in areas as small as 1 m^2, a drastic color change in till from a buff to a dark grey color is evident (Figure 9a). Sites throughout Zone 4 have very well defined fine-grained paths, with cobbles dominating the higher regions and a fine-grained matrix dominating the lows (Figure 9b).

Particle Size

Particle size distribution data were collected from sub-samples of all bulk till samples collected from the MAM (Table 1, Figure 1). The averaged zone data show an overall pattern of increasing sand and decreasing silt and clay with increasing distance from the active ice margin (Tables 4 and 5, Figure 10). Despite the aforementioned overall trend, each of the size fractions along the Tail and in Zones 1 and 4 have wide range of variability. For example, the 4F outlier is distinguishable from the other zone 4 samples due to its extremely low sand and high silt and clay values (Table 5) despite its great distance from the active ice margin. In contrast, Zones 3 and 5 have the least amount of within-zone variability.

Pebbles

The pebble lithology data (Figure 11, Tables 3 and 7,) for the samples collected from the MAM shows distinct changes in dominant rock type between and within zones. The abundance of sedimentary and igneous rock fragments, primarily sandstone and dolerite, varies up to 70% between adjacent crests (i.e., 4A and 4B) and up to 38% along adjacent zones (i.e., zones 3 and 4), consistent with field observations of distinct lithologic bands. Only <2% of pebbles are exotic felsic igneous and metamorphic rocks, with the majority of the metamorphic pebbles categorized as quartzite. Most lithologies are similar in appearance to rocks from the Ferrar and Beacon Supergroups, specifically the Buckley, Fairchild, and Mackellar Formations from the Beacon Supergroup.

Overall observations include the greatest average number of pebbles per square meter nearest to the active ice margin (exception being 1A) (Table 7). Figure 12 shows an overall decrease in the percent of angular pebbles per site and an overall increase in the percentage of pebbles that are sub-rounded and sub-angular away from Law Glacier.

Faceting and/or striations indicate glacial abrasion and were seen on ~20% of pebbles overall. Of this number, 12.2% igneous, 0.9% metamorphic, and 6.9% sedimentary rock fragments showed signs of abrasion (Table 7). No clear spatial patterns were recognized for the numbers of faceted and/or striated pebbles.

Cluster analysis (CA) of all sample sites (Figure 13) is based on pebble lithologies as defined in Table 2. CA was performed twice, once with only the lithologies listed in Table 2 (Figure 13b) and once with data on the percentage of faceted and/or striated pebbles and a distinction between coarse and fine-grained igneous rocks (Figure 13a). CA results delineated 2 main groups, groups A and B, at a similarity distance of around 37 (Figure 13a). Group A consists of samples from Zones 1, 2, and 4 and is influenced by a dominant igneous component. Group B consists of samples only from Zone 3. Although there are individual sites that are dominated by sedimentary rocks rather than igneous, Zone 3 (group B) is distinguishable from the others because it is the only zone whose sample sites are consistently dominated by sedimentary rocks (Figure 11). Zone 3 also has the lowest percentage of meta-sandstones influencing the totals in the sedimentary category (Figure 11a). Samples 5A, 4B, and 4C do not fall in either of these main groups, but are noted as group C in Figure 13a for simplicity. Sample 5A is similar lithologically to the samples of Zone 3, except that 5A has a metamorphic component that Zone 3 lacks (Figure 11b). Sample 4B not only has the greatest igneous component, ~93%, but also the greatest igneous faceted/striated component at ~58% (Figure 11b). Sample 4C is characterized by a greater igneous and lesser sedimentary component than Zone 3, a metamorphic component that Zone 3 lacks, but a lesser igneous component and greater sedimentary component than all other samples with the exception of Zone 3 and sample 5A (Figure 11b). When CA is run without the faceted and/or striated or

coarse/fine-grained intermediate/mafic igneous fractions separated, the results differ slightly (Figure 13b). When compared using the same similarity distance of around 37 the results delineated 4 groups, groups A–D. Group A again consists of samples from Zones 1, 2, and 4, while groups B and C consist of samples from Zone 3 and site 4C, and group D consists only of site 5A. The CA analysis results, both with and without the coarse and fine-grained fraction of the intermediate/mafic igneous rocks and the faceted and/or striated pebble fraction acting as separate categories influencing the results, reveals a cophenetic correlation coefficient of 0.7611 and 0.8043 respectfully; the closer this value is to 1, the higher quality/less distorted the results are. A commonly accepted value of the cophenetic correlation coefficient is 0.8, so the results shown in Figure 13a are slightly distorted.

U/Pb analysis of detrital zircons

Bulk Till

In total, 938 zircons from the bulk till samples were chosen for analysis, 830 of which resulted in concordant ages that were used for interpretations. The zircon ages in till ranges from the Triassic to Archean (~205–3495 Ma) with common populations in the Permian ~250–270 Ma, the Proterozoic ~565–600 Ma, ~950–1270 Ma, and ~2270–2320 Ma, as well as the late Archean ~2670–2730 Ma (Figure 14). The Neoproterozoic population is dominant across all sites. These zircon age distributions show little variation across the moraine. Sample sites 4J and 4L show a younger age shift of ~40 Ma in the Neoproterozoic Ross/Pan-African population (Figure 14). K-S test results of the detrital zircons reveal that sample sites 4J and 4L are the only two sites that are not statistically similar to other sampled tills across the transect (Table 8).

Cobbles

(MA-11) Z3B-1 and 0Z5-1

Cobbles representing dominant sedimentary lithologies observed on the moraines were analyzed to determine U/Pb signatures of potential sources of MA till (Figure 15). Z3B-1 collected from Zone 3 is visually similar to sandstones of the Mackellar Formation, and 0Z5-1 collected from Zone 5 is consistent with the Pagoda Tillite. If both cobbles are identified correctly they are Permian in age and derive from the Beacon Supergroup. As seen in Figure 15, the U/Pb detrital zircon age population for both cobbles ranges from early Cambrian to late Archean, with the dominant peak in the Neoproterozoic ~580–600 Ma. A second dominant Mesoproterozoic population (~1190 Ma) is most pronounced in the tillite. The K-S test (Table 8) indicates that the sandstone is statistically similar to 5 of the till samples. However, the K-S test based on the detrital zircon ages (Table 8) indicates that the tillite is not statistically similar to any of the sampled tills. Although both the tillite and the tills have dominant populations in the Ross and Grenville Orogenies, the till has a greater abundance of ages in the Grenville population, as well as the late Mesoproterozoic through the Paleoarchean.

(MA-11) Z5c/d-1 and Z5c/d-2

Z5c/d-1 and Z5c/d-2 are granite and granitoid cobbles collected between sample sites 5C and 5D. 100% of the age population (n=13 and 28 respectively, or n=20 and 46 if both the core and rim measurements are counted separately) for both cobbles lies within the Mesoproterozoic between ~1400–1480 Ma (Appendix A). Grains from this Mesoproterozoic population are uncommon, but are also present in the Permian tillite cobble and in till sites 2A, 3B, 4K, 4L, and 4B (n=11). The K-S test (Table 8) indicates

that the granite and gneiss cobbles are not statistically similar to the clastic rocks nor till samples analyzed in this study.

Geochemical Analysis

The chemical data from the MAM till samples are normalized to various averaged rock samples including the Beacon and Ferrar Supergroups (Vavra, 1982; Horner, 1992; Faure and Mensing, 2010), Sirius formation till (Passchier, 2004), upper continental crust (UCC) (Rudnick and Gao, 2003) and the post-Archean Australian shale (PAAS) (Taylor and McLennan, 1985) averages (Figures 18–21). These comparisons are plotted to look for patterns across the transect to assess spatial and temporal variability (Figures 16 and 17).

Major Elements

Heterogeneity in the till's major element geochemistry is apparent from ice margin to nunatak. Figure 16 summarizes all spatial trends qualitatively. Oxides follow three general trends across the tail and transect: oxides that increase, decrease, and values that vary irregularly, sometimes with convex or concave patterns (Figures 16 and 17; Table 6). For example, the MAM tills reveal a ~17% decrease in SiO_2 and a convex trend in MnO (Figure 17). Additionally, variability is noted on a smaller scale (~15 m) where tills 1A and 1B have a 3% difference in SiO_2.

Oxides that are the most consistently enriched (>2sigma) in the till samples when normalized to standards are CaO, Al_2O_3, and Na_2O (Figures 18, 20, and 21). All other oxides are enriched depending on what the samples are normalized to, but not consistently. When normalized to surrounding sedimentary rocks (i.e., Pagoda, Mackellar, Fairchild, and Buckley Formations) (Figure 20) and Sirius Formation till (Figure 21), MA samples show enrichment (>2 sigma) in CaO, Na_2O, and MgO, all of

which increase in concentration with increasing distance from the active ice margin. 20–50% of MA samples are depleted (<2 sigma) in K_2O when normalized to the Pagoda, Mackellar, and Fairchild Formations. One third of all MAM tills are also depleted in SiO_2 when normalized to the UCC and Fremouw Formation (Appendix B-1 and B-10). However, when normalized to Ferrar dolerite bedrock samples from Mt. Achernar (Faure and Mensing, 2010) the till samples are enriched in K_2O, LOI, and depleted in CaO, MgO, Fe_2O_3, and MnO, and within 2-sigma standard deviation when compared to Al_2O_3, TiO_2, and P_2O_5 (Figure 20).

Trace Elements

The trace elements across the transect have been categorized into spatial patterns similar to the oxides (Figures 16 and 17). The majority of trace elements are either variable or decrease across the tail and transect, and increasing in only Sr, Cs, W across the transect and Th along the tail.

When normalized to the average carbonate standard reported in Mason and Moore (1982), MAM tills are enriched in all elements with the exception of Ni in site 4J and Sr in all samples (Figure 19). The majority of the MAM tills are enriched in Ba when normalized to the average shale (Mason and Moore, 1982; Krauskopf and Bird, 1994), average carbonate and the Sirius tills in the Beardmore Glacier region (Figures 19 and 21). When normalized to the UCC, only Zone 3 is enriched in Ba (Appendix B-1). Zones 2, 3 and four sites in Zone 4 are also enriched in Ba when normalized to overall TAM averages of Sirius tills (Appendix B-13). About half of the MAM tills are also enriched in Cu when normalized to the UCC; site 3 Dark is the only sample in which Cu is depleted (Appendix B-1). Site 5C, and occasionally sites 5B and 5D, are consistently enriched in Cu when normalized to most standards (Appendix B-1, B-4, B-6–9). Site 5C

is also noted for its enrichment of Zn when normalized to average shale, and the Mackellar and Fairchild Formations (Appendix B-4, B-7 and B-8). Sr is enriched in Zone 5, but depleted in East Crest, Zone 1 and Zone 4L, K, and J when normalized to the UCC as well as Zone 5 of the average shale (Appendix B-1 and B-4). Tills, with the exception of Zone 1, are also enriched in Sr when normalized to the local Ferrar outcrops at Mt. Achernar (Appendix B-11). The MAM tills have a significant enrichment of Ag, well above 2-sigma standard deviation, when normalized to all standards (Figures 18–21). Site 4G is noted for its enrichment in W, while all other sites are consistently depleted in W (Appendix B-1, B-6–B-9). Elements Be, Ge, and Ta are also consistently depleted when normalized to the standards (Figures 18 and 20).

Various trace element ratios were chosen for comparison (Table 9). The Th/U ratios range from 3.76 to 4.81, the majority of which fall below the PAAS value of 4.7, with the exception of site 3 Dark, and above the continental crust average of 3.9, with the exceptions of sites 4L, 4J, and 4E. The Zr/Sc ratios for the MAM tills, ranging from 9.9 to 24.3, fall below and above the 13.13 average value of the PAAS and 13.79 of the UCC. 5C is the only sample that is depleted in Zr (189 ppm) when normalized to PAAS and UCC, 210 and 193 ppm respectively. The Th/Sc ratios for MAM tills vary between 0.56 and 0.93, some which are well below or above the PAAS value of 0.91 and UCC value of 0.79. The Cr/V ratios of the MAM tills indicate the enrichment of Cr over other ferromagnesian trace elements, with the exception of site 4J with a ratio of 0.48. The Cr/V ratio is 0.62 +/- 0.07 on average. The Y/Ni ratio is 0.92 +/- 0.23 on average.

REE

The REE elements follow the same overall spatial trends as the oxides and trace elements (Figures 16 and 17). La–Nd follow an irregular pattern both across the tail and

transect, while Sm–Lu decrease across the transect. Sm and Gd increase along the tail while Eu and Tb–Lu vary with a concave pattern.

The chondrite-normalized REE diagram for the MAM tills (Figure 19) shows a light REE (LREE) enriched pattern, a slight negative Eu anomaly, and a relatively flat, slightly enriched, heavy REE (HREE) distribution. The Eu anomalies for the tills range from 0.58 to 0.73 with an average value of 0.66, equal to the Eu anomaly for the PAAS and less than the UCC (0.70). The Sm/Nd ratios range from 0.18 to 0.21 (Table 9), slightly higher than the average value for the PAAS (0.175) and UCC (0.174), but consistent with East Antarctic onshore tills reported in Farmer et al. (2006). With the exception of the chondrite-normalized pattern, the MAM tills are more enriched in the heavy REE than the light REE (Appendix B-1, B-2, B-6–B-9). The MAM samples that are most consistently enriched in both the light and heavy REE are the East Crest site, Zones 2 and 3, 4I, G, E, and C. The two most variable REE are La and Ce. La and Ce are the only REE consistently depleted when normalized to the Pagoda, Mackellar, and Fairchild Formations (Figure 20). Only when normalized to the Buckley Formation do all REE values of the MA samples fall within 1 sigma standard deviation of the normalized values (Figure 20), although it should be noted that the Buckley has much larger standard deviation than the other formations of the Beacon Supergroup.

Discriminant Analysis

Discriminant analysis revealed that till geochemistry is distinctive by zone (Tables 10–13, Figure 22). The top three most discriminating factors for the major oxides, trace, and rare earth elements are as follows: SiO_2, LOI, CaO, Ba, Sr, Zr, Ce, La, and Nd (Tables 10–13, Figure 22). Results indicate Zone 3 and Zone 5 tills are the most

distinct. SiO_2, Ba, Zr, Ce, La, and Nd all trend towards Zone 3, and LOI, CaO and Sr trend towards Zone 5. Sr also trends towards Zones 1 and 2.

DISCUSSION

The behavior of the EAIS has been considered stable since the middle Miocene (~14 Ma) due to thermal isolation of the continent and the fact that most of the ice sheet rests on bedrock above sea level making it less susceptible to changes in climate and sea level rise (Kennett and Hodell, 1995; Pollard and DeConto, 2009). However, recent studies show widespread lakes and water beneath the EAIS (e.g., Siegert et al., 2005; Wingham et al., 2006; Stearns et al., 2008) as well as evidence of past ice sheet collapse during the Pliocene (e.g., Cook et al., 2013). Previous studies suggest that the head of glaciers in the TAM have not been greatly affected during warming periods and therefore have remained relatively stable in behavior (Denton and Hughes, 2002). A potential trim line present on Mt. Achernar (Figure 23) implies that the head of the Law Glacier was affected to some degree by fluctuations in the EAIS. With the presence of an ice sheet with constant thickness, it is likely that the MAM would have been fed by a consistent source. An ice sheet with variable thickness could result in a shift in debris sources, which would be reflected in the moraine's composition. The provenance data collected from the MAM provides critical information for assessing ice sheet changes and their potential sources over time, as well as exploring results from different provenance methods.

Lithologic Source of the Till

The material exposed in glacial moraines originates predominately by mechanical erosion of the rocks exposed along the path of glacial drainage. In the case of an ice sheet, a large area is sampled and the composition of the sediments reflects the average composition of the bed in the glaciated area. Distinct colored bands across the MAM are evident between zones and within zones (Figure 6). These bands reflect the dominant

rock type within the till. Pebble and cobble lithology reveal that the composition of the MAM till is consistent with locally derived material, but also has minor non-local components. Pebble lithologies from these bands across the MAM tail and transect average 56.2% igneous, 3.2% metamorphic, and 40.6% sedimentary, ~20% of which indicate subglacial transport by exhibiting faceting and/or striations. Most of these lithologies are interpreted to be derived from the dolerite of the Jurassic Ferrar Supergroup and the sedimentary units of the Permian Pagoda, Mackellar, Fairchild, and Buckley Formations of the Beacon Supergroup. Only <2% of the pebbles are of an unknown felsic igneous source. There are other notable unmapped erratics that were identified in the moraine. Many erratics were noted in the non-random cobble collection survey and include coral, granite, granitoid, gneiss, granodiorite, quartzite, chert, marble, and multiple intermediate/mafic igneous cobbles. Regolith of Shackleton Limestone, relatively minor Douglas Conglomerates, and some Ferrar Dolerite is present on the east wall of the nunatak (Elliot, personal comm.) and may be the source of some regolith found in Zone 5.

In areas as small as 1 m^2 in Zone 3, dark grey till was overlain by a 2 cm buff layer (Figure 9a). Scarrow et al. (2014) noted that the dark soil colors of the bottom-most horizon in the MAM were consistently higher in carbon content than the overlying till. Scarrow interpreted these findings as an indication for different sources for the two soil layers: the uppermost layer deriving from comminution and aeolian redistribution of sand and silt weathered from surface clasts, and the bottommost till being fed into the moraine by a subglacial source. The findings from this study suggest that although this proposed idea for the source of the material could be applied to areas of the moraine closest to the nunatak walls, it seems unlikely that this same idea could be applied to all of the moraine

complex further downstream. Debris bands are seen emerging parallel to the moraine's edge (Figure 24) to supply till that is deposited in the moraine; an obvious source of supraglacial debris is lacking. The ~20% of faceted and/or striated pebbles collected from the surface of moraine crests for this study indicates that although some of the source ice does flow past the nunatak wall, subglacially transported material rests on the surface of the moraine. Therefore, although the two till colors could be an indication of multiple sources, it unlikely that the source of the uppermost till unit can be attributed solely to supraglacial rock fall sources.

Buckley Formation Input

The Mt. Achernar nunatak consists of flat-lying, Permian sandstones and coal seams of the Buckley Formation (Stump, 1995). Results from pebble lithology, geochemical, and U/Pb analysis all suggest the presence of Buckley Formation material in the MAM. The Buckley Formation is characterized by thick-bedded sandstones interbedded with carbonaceous shale, coal, and *Glossopteris*-bearing mudstones (Barrett, 1991; Faure and Mensing 2010). Multiple pebbles and cobbles matching these descriptions were noted in lithologic analyses. A permineralized wood specimen (MA-11 Z1F6) (Figure 25a) was collected from site 1F along the tail of the MAM (Table 1). The wood structure is dominated by tracheids and there is no evidence of vessel elements within the growth rings, which indicate that this specimen was most likely a gymnosperm (Thomas, 2000). The mineralization appears to be predominantly quartz, which is common in both Late Permian and Middle Triassic fossil wood from Antarctica (Taylor and Taylor, 1990). There are two plants that produced conifer-type wood in Antarctica during the late Paleozoic and early Mesozoic, *Glossopteris* (Permian) and *Dicoridium* (Triassic). However, Early Jurassic wood from Antarctica is noted to contain a

significant amount of charcoalified material and less pervasive silicification and mineralization, so this specimen doesn't appear to be consistent with the preservation style of wood from the Early Jurassic (Gulbranson, personal comm.). An *in situ* fossil forest in the Upper Permian Buckley Formation crops out at Mt. Achernar and contains *Glossopteris* fossils (Ryberg et al., 2012); due to the specimen's lack of striations and/or faceting, this specimen's source is interpreted to be local and derived from the upper Buckley Formation.

The geochemical data also suggests that the MAM till is sourced, in part, from the Buckley Formation. Spider diagrams of MAM tills normalized to the geochemical data of Buckley rocks (Figure 20) reveal that the trend of the REE of the MAM tills closely resembles that of the Buckley Formation, falling within 1 sigma standard deviation. Again, it should be noted, however, that the Buckley dataset has a much larger standard deviation than the other formations of the Beacon Supergroup. Elliot and Fanning (2008) conducted U/Pb analysis of two Buckley sandstones from the Shackleton Glacier region (Figure 15), and both are dominated by an age population and of 250–270 Ma. The U/Pb analysis of MAM tills reveals this same Permian age population ~250–270 Ma (Figures 14 and 15), indicating that this population could be derived from a Buckley Formation source. However, this Permian population is not unique to the Buckley Formation; it is noted in the Fremouw Formation as well (Figure 15). Therefore, the lack of a unique population means it is difficult to assess the extent of a Buckley contribution to till composition.

Fremouw Formation Input

Although it is the Buckley Formation that outcrops at Mt. Achernar (Stump, 1995), there is evidence that the Triassic Fremouw Formation is influencing the

composition of the MAM. When compared to surrounding sites, the section of the Upper Buckley that outcrops at Mt. Achernar is equivalent to ~50 m below the Buckley-Fremouw contact (Gulbranson et al., 2012). The Fremouw Formation occurs throughout the central TAM, including in the Queen Alexandra and Queen Elizabeth ranges, as well in the Dominion and Supporters ranges at the head of the Beardmore Glacier (McGregor, 1965). The total thickness of the Fremouw Formation is between 670–800 m (Barrett et al., 1986). The basal beds of the Fremouw Formation are composed of quartz sandstone and greenish-gray mudstone (Faure and Mensing, 2010). Cobble MA-11-6 (Figure 25b) is visually similar to a Fremouw sandstone (PRR-4145) collected from the Coalsack Bluff area (Figure 1) just east of Mt. Achernar within the Queen Alexandra Range and multiple sandstone pebbles appear quite similar to Fremouw samples collected from the Lewis Cliff. The Fremouw influence is also inferred from comparison of detrital zircon ages in the MAM till to those of a Triassic Fremouw sandstone, cobble 96-36-4 (Elliot and Fanning, 2008). Zircons from sandstones from both the Buckley and Fremouw Formations were analyzed by Elliot and Fanning (2008) and K-S test results (Table 8) indicate that only sites 1A and 4J are statistically similar to the Triassic Fremouw sandstone with dominant population peaks in the middle Permian to the early Triassic and Neoproterozoic to early-Ordovician, and small population in late Mesoproterozoic to early Neoproterozoic. Site 4L has a p-value of 0.049, and is likely of similar source. Likewise, there is also geochemical evidence supporting the input of Fremouw material into the moraine. When normalized to the major oxides of the Fremouw, the MAM tills are only enriched in MgO and Fe_2O_3, element ratios that can be accounted for when combined with the geochemical data of the Mt. Achernar Ferrar dolerite (Figure 20). Given that the Ferrar dolerite outcrops at Mt. Achernar and the Fremouw Formation

outcrops nearby, it is likely this mixture of Ferrar/Fremouw mixture has some influence on the composition of the MAM till.

Pagoda and Mackellar Formation Input

The Pagoda and Mackellar Formations are exposed in fault slices on the east-facing wall of the nunatak in Zone 5 (Elliot, personal comm.). When compared to rocks from known outcrops, some of the pebble fraction in Zones 1–4 were visually similar to the Mackellar Formation, while rocks from the Pagoda Formation were only noted only in the cobble fraction of only Zone 5 and site 1I (Table 1).

Data from geochemical and U/Pb of zircons also suggests that the till may be sourced from the Pagoda and Mackellar Formations. Spider diagrams of MAM tills normalized to the geochemical data of Pagoda and Mackellar rocks reveal that the trend of the REE of the MAM tills resemble that of the Pagoda Formation with most elements falling within 2 sigma standard deviation (Figure 20; Appendix B-6 and B-7). When normalized to the Mackellar Formation, about two-thirds of the samples are depleted (greater than 2 sigma) in La and Ce (Appendix B-7). Likewise, the U/Pb data indicates that the zircon populations of MAM tills most closely resemble that of the Pagoda Formation, although the Mackellar Formation zircon age distribution is similar and could be contributing zircons as well. Similar to the MAM tills, the zircons analyzed from the Pagoda Formation have a bimodal peak in the Grenville population as well as a minor population ~1400–1480 Ma (Figure 14). Like the MAM tills, both the Pagoda and Mackellar Formations have multiple populations pre-Mesoproterozoic, including the Paleoproterozoic (~2270–2320 Ma), and the neo-Archean (~2670–2730 Ma) populations. Although the Fremouw Formation does contain a few minor pre-Mesoproterozoic populations, the Buckley and Fremouw Formations completely lack these

Paleoproterozoic and Neoarchean populations of interest. So with the Permian population ~250–270 Ma attributed to a Buckley source, it seems probable that the Pagoda and Mackellar are also likely contributors to zircon population in the till.

Distinct Zones

The tail, and Zones 1, 2, and 4 are similar both lithologically and geochemically. Although each zone has it's own set of distinct characteristics, Zones 3 and 5 are unique for various reasons and are discussed separately, in detail, below.

Zone 3: A drastic change

Cluster analysis results of pebble lithology indicates that Zone 3 is the most distinguishable of these zones, with all Zone 3 samples clustering in their own group (Figure 13). Zone 3 is dominated by sedimentary rocks whereas the dominant lithology for the other zones and tail section is intermediate/mafic igneous (Figure 11). Zone 3 is not only distinguishable lithologically, but also geochemically. Discriminant analysis (Figure 22) of all elements reveals 6 out of the 9 most discriminating elements, SiO_2, Ba, Zr, Ce, La, and Nd, trend towards Zone 3 indicating that these elements are the most useful in discriminating Zone 3 samples from all others. The highest Ba concentrations are found in shales (~580 ppm), while carbonate rocks and sandstones contain only 10 ppm on average (Mielke, 1979). The average Ba concentration for Zone 3 is 782.3 +/- 50.9, well above the average carbonate, sandstone, and shale, while tills analyzed from other zones are much closer to the average Ba concentrations in shales. So although it is sandstone and meta-sandstones that dominate the lithology, it was noted during collection that mudstones would be underrepresented in Zone 3 because they broke easily into sheets and were unable to be collected. The distinct ~18 m high arch morphology of Zone 3 (Figure 5), combined with provenance variation, implies a change in ice sheet

behavior and flow into the moraine. This change in morphology and its implications will be further discussed below in the "Temporal Evolution of the Mt. Achernar Moraine" section.

Zone 5: A different source

Evidence suggests that Zone 5 is derived from a different source than the rest of the MAM. The material in the tail and Zones 1–4 are thought to be fed primarily by Law Glacier, whereas the orientation of ridge crests in Zone 5 indicates that this area was likely fed by the unnamed ice tongue seen in Figure 6. Geochemical analyses reveal that Zone 5 is likely fed from a more mafic source than the rest of the moraine as it contains higher concentrations of Cu, Ni, Co, Zn, and MgO, and lesser concentrations of SiO_2 and Zr. Likewise, the U/Pb data of detrital zircons reveals that Zone 5 is the only zone to not have a population of grains younger than the Ross/Pan-African grains (Figure 15). In addition, the nunatak walls in Zone 5 are the only place where the local rock types include Shackleton Limestone and Douglas Conglomerate float exposed on the west facing hillside, as well as Pagoda, Mackellar, and Fairchild Formations exposed in at least three fault slices on the east facing wall (Elliot, personal comm.) The granite and deformed granitoid suite collected in Zone 5 are unique to Zone 5. Zircon grains from one granite (Ma-11 Z5 c/d-1) and one deformed granitoid (Ma-11 Z5 c/d-2) were analyzed and ages are tightly clustered with peaks ~1400–1480 Ma (Appendix A). The K-S test (Table 8) indicates that the zircon grains from these granite and granitoid cobbles are nearly statistically identical to each other. Interestingly, zircon grains of this age are absent in the Zone 5 till sample analyzed, but present in other sites across the transect (Figure 14). One explanation for the presence of the ~1400–1480 Ma grains, but lack of granite/granitoid cobbles in the Zones 1–4 till is that this population of grains is

derived from the Pagoda Formation. As discussed in section 6.1.3, the Pagoda Formation is a potential source of the till in the MAM and the zircons analyzed from the Pagoda tillite is the only other sample that shows the ~1400–1480 Ma population (Figure 15). Another possible explanation is that the Law Glacier catchment area is eroding into this igneous source, but pebbles and/or cobbles of this igneous suite were simply missed and not collected. The granite and granitoid cobbles are interpreted to have an origin associated with that of sample TNQ reported in Goodge et al. (2008). The source of these Rodinian-aged cobbles are not exposed in the TAM, but further geochemical and petrographic analyses were conducted on both Z5 c/d-1 and 2 and were found to be indistinguishable from TNQ and Laurentian granites (Hodgson et al., 2013). Therefore, these Rodinian-aged cobbles originated from an igneous suite buried within the continental interior of East Antarctica and were transported to the MAM via the glaciers of the EAIS.

Temporal Evolution of the Mt. Achernar Moraine

Based on observations from photographs, pebble lithology, and geochemical data, the following model is proposed for the formation of the MAM complex for Zones 1–3:

The trim line present on Mt. Achernar (Figure 23) implies ice at the head of the Law Glacier was thicker in the past and affected to some degree by fluctuations in the thickness of the EAIS, and specifically damming of the Law Glacier by thicker ice in the Ross Sea. The intersection of the trim line and the moraine can be traced back to the boundary between Zones 3 and 4. Based on the presence and position of the trim line, combined with the surface exposure ages of boulders reported from Mathieson et al. (2012) and Kaplan (personal comm.) (Figure 4), it is concluded that the time represented at the Zone 3/4 boundary is the beginning of the LGM, with initial thickening of the ice

sheet beginning before ~50 ka. The geomorphology of Zone 3, the broad arch feature (Figure 5) peaking at ~18 m above the moraine surface with superimposed smaller ridges, is either a result of compression from more ice flowing into the moraine during the LGM, or ice sheet thickening and the arch is a remnant of thicker ice from the LGM. The absence of ridges in Zone 2 represents a period of deglaciation; a period in which there was simply not enough ice (i.e., pressure) feeding into the moraine and the ridges were not formed and/or preserved. Zone 1 is the region of the moraine that is still connected to the active Law Glacier and therefore contains the most recently deposited material of the moraine. The hummocky morphology of Zone 1 is due to a differential ablation, which is a function of minimal till thickness (1–3 cm) and dark till color (grey–very dark grey); melt ponds and liquid water was observed.

Based on this model, it its concluded that there was a change of till provenance during the LGM. Lithologic studies of discrete pebble samples reveal a change from intermediate/mafic igneous lithologies in Zone 4, to a sedimentary-rock dominated source for the material in Zone 3 (Figure 11). The field observations of a few closely spaced lithologic bands alternating between dark, igneous dominated color bands and lighter, sedimentary dominated lithologies (Figure 6) represents a transitional time of ice sheet thickening and a change in debris type, ultimately suggesting a different source of the ice feeding into the moraine. A change in provenance is also noted in the till geochemistry of the <63 micron fraction. As stated previously, Zones 2 and 3 are distinguishable geochemically; these zones consistently contain the highest concentrations of all REE, and some of the trace and major elements. There is little change seen in the U/Pb ages of the detrital zircons. The U/Pb data reflect a Beacon signature, so despite the decrease of intermediate/mafic igneous rocks (Ferrar Dolerite),

the change in provenance is not expected to be apparent in the U/Pb data because the Ferrar Dolerite typically lacks zircons.

Cosmogenic, or surface-exposure, dating is based on the production of cosmogenic nuclides in surficial rock samples due to exposure to cosmic rays (Ackert and Kurz, 2004). The amount of nuclides, such as ^{3}He, ^{10}Be and ^{26}Al determines how long a given rock sample was exposed to the atmosphere prior to sampling (Ivy-Ochs and Kober, 2007). Cosmogenic dating is a popular method for dating glacial deposits in Antarctica because erosion rates are so low that the record from multiple glacial deposits is preserved (Ackert and Kurz, 2004). Glacial deposits at the mouths of large outlet glaciers of the TAM (i.e., Reedy and Scott), dated with cosmogenic nuclides typically show maximum ice thickness occurring ~13–18 ka (Hall and Denton, 2000; Todd et al., 2010; Allard et al., 2011; Koffman et al., 2011). However inland sites, such as the Ohio Range and upper reaches of Reedy Glacier, show maximum ice surface elevation occurring ~7–10 ka (Ackert et al., 2007, 2013; Todd et al., 2010) and in some locales ~35–45 ka (Ackert et al., 2013). Most ice sheet thinning at Reedy and Scott Glaciers took place after 10 ka, (Stone et al., 2009; Todd et al., 2010), but significant retreat was noted near Quartz Hills as early as ~13 ka (Todd et al., 2010). Near present-day levels of ice thickness did not occur until ~2 ka (Todd et al., 2010). Likewise, Stone et al. (2009) report that maximum glaciation along the coasts of the Scott and Beardmore Glaciers occurred ~15–17 ka, and was too followed by rapid ice sheet thinning in the early Holocene. The exposure ages of ~11–14 ka reported by Mathieson et al., (2012) (Figure 4) along the Zone 2/3 boundary and the deglaciation period proposed by the model are in agreement with the reported time-transgressive manner in deglaciation both along the coast and inland. The exposure ages of ~5 and 6 ka are likely ages that are too young,

and can be explained due to rolling of the boulders caused by decreased stability of the Zone 3 front as a result of moraine surface slope changes caused by decreased compressional stress along what is now the Zone 2/3 boundary during the period of thinning after the LGM.

The morphology of Zone 4 shows an overall steady elevation increase of ~30 m through the series of parallel ridges and lacks additional broad arch features. The series of ridges in Zone 4 suggests a continuous supply of sediment because the ridges would likely not be preserved if there were an interruption of ice flow; material would have been carried out of the moraine as the ice retreated during a warming event and therefore would not have preserved the ridges (i.e., Zone 2) (Fogwill et al., 2012). The reversal apparent in surface exposure ages in this zone makes it unclear how much time Zone 4 represents. If the 191 ± 2.8 ka age is accepted as the accurate exposure age, it suggests that an extensive amount of material (~2 km) was deposited into the moraine in a short period of time (~7 ka) and spans only until MIS 6, whereas the 553 ± 15.4 ka age suggests Zone 4 spans multiple glacial-interglacial cycles, to ~MIS 13–14. If the younger date of 191 ± 2.8 ka is assumed to be correct, it is likely that the lithologic changes in the pebbles across this zone reflects the geometry and/or the thickness of the bedrock buried upstream. For example, if the source ice is flowing over a contact that alternates between the intermediate/mafic and sedimentary units, it is likely that the ice is simply eroding through this contact and depositing each layer as the alternating colored bands. However, if the older age of 553 ± 15.4 ka is assumed to be the accurate exposure age, it is possible to apply the model suggested above and assume that changes in the dominant pebble lithology and geochemistry of sampled sites could indicate changes in provenance and in turn changes in thickness of the EAIS; a dominance of sedimentary

lithologies representing past thickening of the EAIS, and dominant intermediate/mafic igneous lithologies representing past thinning of the EAIS. Although it is speculative, exposure ages of 184 ± 2.6 ka (MIS 6) and ~553 ± 15.4 ka (MIS 14) near the sedimentary dominated sample sites 4G/4H and 4C respectively, could be evidence in support of this model when applied to Zone 4.

Several possible hypotheses may be tested to determine why the change in provenance occurred during ice thickening associated with the LGM. One hypothesis is that a subglacial topographic feature, such as a ridge, is buried beneath the ice upstream and acts as a barricade against ice flow. As the EAIS thickened during the LGM, debris bands rich in sedimentary lithologies overrode this barrier, becoming the primary source of ice/debris feeding into the MAM. As the ice sheet thinned, this sedimentary-dominated ice source was blocked and the original intermediate/mafic igneous dominated ice source became the primary source for material feeding into the moraine once again. It is envisioned that at times of relatively thin ice, a shallow subglacial ridge may deflect most of this sedimentary-rich ice downstream and only allow minimal ice to flow over the ridge. Assuming the ridge is composed of the more erosion-resistant Ferrar dolerite, the result would be debris dominated by the Ferrar dolerite and with relatively minimal sedimentary lithologies. Also, assuming the englacial debris is being deposited into the MAM by shear bands similar to those described by Chinn (1991), sedimentary-rich debris bands from higher up in the ice column must have been accessed as ice thickened during the LGM and could flow over this barrier and be deposited into the MAM as a mix of dominant sedimentary lithologies and minimal dolerite deposits (i.e., Zone 3). Additional surface exposure ages and pebble lithology across the transect and ground-penetrating radar data from over the MAM and the Law Glacier would be extremely

beneficial in testing both the model and this hypothesis explaining why a change in provenance could occur.

Pebble lithology and U/Pb data from detrital zircons are both common provenance tools used to characterize ice flow. Unique zircon populations associated with upstream lithologies, or even significant missing populations have been successfully used as a tracer to determine the source of ice from TAM outlet glaciers and WAIS ice streams flowing into the Ross Sea (e.g., Schilling, 2010; Licht and Palmer, 2013; Licht et al., in press). Likewise, lithologic studies of pebble fractions have been successfully utilized to determine the extent of both the local and subglacial input of ice and debris flowing into moraines (e.g., Palmer et al., 2012; Dits, in prep). However, this study reveals that depending on where either of these provenance tools is being used, significant information regarding changes in provenance can be missed. The U/Pb data for the MAM tills reveals little change (Figure 14), indicating the same provenance over time; as discussed in the proposed model above, this may not be the case. In addition, the lithologic data of the pebble fraction proves to be a vital source of information regarding a change in provenance at the heads of outlet glaciers, whereas pebble studies further downstream are likely not as useful because offshore cores are too small to get statistically representative samples of pebbles.

Assessment of Provenance and Weathering Indicators

Trace elements are best used to determine whether or not a source is igneous, and if so, whether that igneous source is relatively mafic or felsic. Th, Sc, Zr and to some extent Cr, are good indicators of sedimentary provenance because they are quite insoluble and less affected by weathering (Potter et al., 2005). Ratios such as Th/Sc, Th/U, Zr/Sc and Cr/V, along with the REE distribution provide some of the most useful data for

provenance determination (Manassero et al., 2009). A plot of Th/Sc vs. Zr/Sc ratios in sedimentary units is becoming a popular provenance discriminator, both of which increase from mafic to felsic source areas (Potter, 2005). Interestingly, the alternating bands of the mafic, Ferrar dolerite and the more felsic derived sediments of the Beacon Supergroup that are distinct in the pebble lithology (Zone 3, 4G, 4C, 4A and 5A) are not distinct when using Th/Sc vs. Zr/Sc as a provenance tool (Figure 26).

During weathering and recycling, there is a tendency for an elevation of the Th/U ratio above upper crustal igneous values of 3.8 to 4.0, because under oxidizing conditions U4+ oxidizes to the more soluble U6+ and is therefore more easily removed from the sediments than Th (Manassero et al., 2009). The Th/U ratios of the MAM till samples range from 3.76 to 4.81 (Table 9), the majority of which fall below the PAAS value of 4.7, and above the continental crust average of 3.9. Most Th/U ratios are above 3.8-4, indicating strong weathering, but still less than that of the average shale. These ratios suggest that the origin of the till is a mixture of sandstones and mature mudstones.

Several chemical indices have been proposed to quantify weathering effects including the 'chemical index of alteration' (CIA) and 'chemical index of weathering' (CIW). The CIA and CIW indices reflect mostly the amount of feldspar relative to clay minerals, and therefore neither index strongly reflects the parent rock type (Potter et al., 2005). The CIA is defined as $[Al_2O_3/(Al_2O_3+CaO^*+K_2O+Na_2O)]\times100$. The CaO* represents the CaO content from silicate minerals only (Fedo et al., 1995). Primary minerals have low CIA values; CIA values of 45–55 indicate essentially no chemical weathering (Nesbitt and Young, 1982). A CIA of ~75 is equal to that of illite (Nesbitt and Young 1982). The presence of minerals such as kaolinite, chlorite, gibbsite, and bohemite indicate extensive weathering of feldspar to clay and have CIA values of 100

(Nesbitt and Young, 1982). A problem associated with the CIA is that it cannot account for the post-depositional addition of K to older clastic rocks during diagenesis. The CIW index excludes K all together and is defined as $[Al_2O_3/(Al_2O_3+CaO^*+Na_2O)]\times100$ (Potter et al., 2005).

Cox et al. (1995) proposed the index of compositional variability (ICV) that includes both Fe and Mg, allowing for discrimination between parent rock types. The ICV is defined as $(CaO+K_2O+Na_2O+Fe_2O_3(t)+MgO+MnO+TiO_2)/Al_2O_3$. In the ICV index, values decrease with increasing degree of weathering for a given rock type (Potter et al., 2005). Mature mudstones with mostly clay have ICV values that are <1.0 (Cox et al., 1995). Tills with the same degree of weathering (the same CIA) can often have different ICV values, indicating differences in the composition of the source area (Potter et al., 2005).

The CIA, CIW and ICV values (Table 14, Figure 27) for the MAM till range from 49.6 (5A) to 74.7 (1H), 53.6 (5A) to 83.5 (1H), and 1.71 (5A) to 0.88 (1H) respectively, indicating a wide range of the degree of weathering. Values indicating a greater degree of weathering were expected with increasing sampling distance from the active ice margin. However, results indicate that there is an overall trend of decreasing CIA with increasing distance from the Law Glacier, although there are some exceptions to this trend (Table 14, Figure 27). Krissek and Horner (1988) report that the CIA values for Beacon samples throughout the central TAM average ~72.7 for the Pagoda, 74.0 for the Mackellar, 80.0 for the Fairchild, and 79.1 for the Buckley. The majority of the MAM tills have much lower CIA values than the Beacon Supergroup, but similar values as the Sirius Group. Geochemical analysis on Sirius Group deposits throughout TAM are reported with similar CIA values ranging from 41–70 (Passchier, 2004). Passchier

(2004) concluded that the distribution of CIA values followed a consistent geographic and morphostratigraphic pattern related to multiple glacial phases, except for a wide range of CIAs from Ricker Hills. Like Passchier (2004) concluded about Ricker Hills, the wide range of CIAs from the MAM could be attributed to multiple glacial phases affecting the same nunatak. Previous studies in the central TAM suggest that the CIA is not affected by post-depositional weathering processes (Krissek and Horner, 1988) and must be a record of weathering of pre-glacial rock surfaces (Canil and Lacourse, 2011). However, these observations are not consistent with field observations of extensive varnish on the rocks in the MAM that are the furthest away from the Law Glacier. The extent of varnish and in turn the degree of chemical weathering does not appear to be represented in the CIA values. The MAM till CIA values could be correct and simply indicate that till towards the back of the moraine has been more affected by physical weathering on the surface rather than the chemical weathering. However, there are caveats that must be considered when interpreting CIA values:

1. Although the CIA is said to not be affected by post-depositional weathering processes (Nesbitt and Young, 1982), could the formation of weak acids produced by meltwater affect the CIA? The 3 sites with the highest CIA values, indicating the strongest chemically weathered material, are sites 1E, 1E Red/Grey, and 1H. Till from 1E and 1E Red/Grey were wet at time of collection, 1H was not. Multiple frozen meltwater ponds were seen along tail and near sites 1A and 1B in the regions closest to the active ice margin. Therefore, it is probable that any of the sites along the tail of the moraine could be influenced by meltwater throughout the summer, which could lead to the formation of weak acids and elevated weathering indices. No evidence of liquid meltwater was seen inward from the ice margin.

2. If clastic carbonate grains are abundant in the till, this could lead to very low CIA values unrelated to weathering. Zone 5 till has the lowest CIA values and is associated with an abundance of carbonate. Based on field observations of limestone regolith covering the nunatak wall in Zone 5 and the till's strong effervescence when exposed to HCl, there is a strong potential presence of carbonate grains in these samples. A subsample of till from site 5A with the highest percentage of CaO, was sieved to the <63 fraction (same size fraction sent in for geochemical analysis) and effervesced strongly when it was exposed to both 3% and 10% concentrations of HCl to try and dissolve any calcite. This sample was weighed and dried, but weight was added to the sample, indicating salts were added. Discriminant analysis reveals that CaO and Sr are some of the top discriminating geochemical factors and trend towards Zone 5, indicating these elements are best to distinguish Zone 5 till from other till samples (Figure 22). Both of these elements are associated with limestone, and with the Shackleton limestone pouring off the sides of the nunatak in Zone 5, the presence of calcite could be resulting in the lowest CIA values. Calcite could also be sourced from thin beds of dark gray to black limestone that have been reported in the Pagoda Formation as well as calcite cleats reported in the coal samples from the Buckley Formation (Faure et al., 2010).

3. Dominant grain size of a sample site can affect CIA results. Krissek and Horner (1989) attributed a decrease in CIA to the coarsening of the Mackellar and Fairchild Formations in their study, indicating the CIA is controlled more by grain size changes rather than weathering processes. Zone 5 shows the opposite pattern with samples having the lowest CIA values and the greatest sand content.

In addition to affecting CIA results, CaO concentration and grain size must also be taken into consideration when interpreting the remaining elements that were analyzed.

Although the geochemistry of Zone 5 suggests that it could be sourced from a more mafic source than Zone 4, the apparent depletion in SiO_2 could be a result of the addition of Ca/Al minerals and/or grain size effects. The concentration of CaO in Zone 5 could be a result of the addition of weathering minerals concentrated in Ca and Al, minerals such as prehnite, laumontite and heulandite, that occur due to weathering and resulting in cements (Vavra, 1982). The presence of these minerals are likely considering samples from at least the Mackellar are noted to contain prehnite, and Fremouw Formation specimens are noted to contain these minerals both as cements and replacements of detrital grains (Faure et al., 2010; Vavra, 1982). The relation between SiO_2 compared to $CaO + Al_2O_3$ has a negative correlation with an R^2 value of 0.6. Likewise, grain size may affect relative concentrations of elements. Overall, there is ~17% decrease in SiO_2 as well as decreasing percentage of silt/clay fraction from active ice margin to the nunatak; it is unclear why this might affect SiO_2.

Minerals that are very resilient against weathering have the potential to be eroded and deposited multiple times into younger sedimentary rock units or glacial till. Recycling of grains into the till can also cause problems when trying to interpret provenance information, not only in a geochemical sense, but also with U/Pb analyses. Potter (2005) uses the example of a mudstone that has a low CIA and a high ICV, which indicates that the source terrane is likely one of mostly juvenile igneous rocks. However, the inverse cannot be said for a mudstone with a high CIA and a low ICV because these values could be caused either by deep weathering of the source or recycling of previously weathered material. A sample with high CIA and low Th/Sc ratio indicates a mafic source that has been strongly weathered. But, does this mean the immediate source was a weathered basalt or a mudstone that was derived from a basaltic terrane?

Recycling must be considered when interpreting the results from the MAM because evidence suggests that the composition of the moraine has also been influenced by recycled sediments, in addition to weathered material. K_2O/Al_2O_3 ratios are one way to determine the degree of recycling of fine-grained sedimentary rocks (Cox et al., 1995). K/Al ratios >0.3 indicate K-feldspars, ~0.3 indicates illite, and ratios <0.3 indicate clay minerals (Cox et al., 1995). This method was used by Passchier (2004) on Sirius tills throughout TAM. With the exception of the southern TAM, Sirius Group sediments were <0.23, indicating clay and recycling of mature mudrocks. The K_2O/Al_2O_3 ratios for the MAM tills are all <0.18, indicating the moraine contains recycled material. The most likely source of a mature mudstone would be that of the Mackellar Formation. However, K/Al ratios from the Pagoda, Mackellar, Fairchild and Buckley range from 0.205–0.216 (Horner, 1992) and the ratio from the Fremouw Formation is even higher at 0.297 (Vavra, 1982), indicating the MAM tills are more dominated by clay than the local rocks.

Zr/Sc ratios are also used as an indicator of recycling as Zr is a relatively stable element that often resides in stable heavy minerals such as zircon (McLennan, 1993). Zr/Sc ratios greater than 22 and enrichments of Zr indicate recycling (Manassero et al., 2009). All till samples are enriched in zirconium when normalized to the upper continental crust, and sites East Crest, 1B, 2A, 4D and 4B have Zr/Sc ratios over 22 that should therefore indicate recycling. Interestingly, the 3 sites with the highest CIA values actually have some of the lowest Zr/Sc ratios of the moraine, indicating weathering dominant processes over recycling.

Recycling must also be considered when interpreting the results from the U/Pb analysis of MAM detrital zircons. The physical durability of zircon indicates recycled material may affect the results of U/Pb analysis. Since zircon is very resistant to

weathering, it has the potential to be eroded from a host rock and be deposited, or recycled, multiple times into younger sedimentary rock units or glacial till; U/Pb analysis would indicate the formation age of the grain, but not necessarily all the history that has affected the zircon nor the age of the deposit it is in.

Several factors may affect zircon abundance and analytical results. Zircon fertility is a function of rock type and is defined as the ability of a terrane or lithology to generate sufficient zircons of an age that represents the time of stabilization of that terrane (Moecher and Samson, 2006). The mafic igneous source would generate few zircons and would be rendered invisible in provenance studies of detrital zircons (Moecher and Samson, 2006). Even felsic igneous sources that are expected to produce an ample amount of zircon can produce rocks deficient in zircon if crystallized from a magma that was already nearly saturated in Zr. Another caveat Moecher and Samson (2006) discusses is that zircons are more likely to precipitate under magmatic conditions rather than regional metamorphism, except at upper amphibolite to granulite facies metamorphism. Likewise, zircons that may form under these conditions could simply be too small to be analyzed, therefore missing that whole age population. The last issue mentioned is the bias that can occur from excluding the rims of zircons and analyzing only the cores; only the age distribution for the core of each zircon is reported, and not the age of later metamorphic/overgrowth events (Moecher and Samson, 2006).

The local felsic igneous rocks that crop out in the TAM are a potential source of specific zircon populations in till. The majority of zircons from Granite Harbour Intrusives from the central TAM have been dated at ~485–555 Ma (Goodge et al., 2012). Interestingly, although U/Pb ages of 550–600 Ma are ubiquitous in tills across the TAM (Licht et al., in press), including from the MAM, there are no igneous outcrops of that

age. A single erratic granitic cobble (KTW) collected from the Kon-Tiki nunatak on the Nimrod Glacier dated at 589 ± 5 Ma indicates that there are rocks of this age buried upstream beneath the ice (Goodge et al., 2012). Likewise, the Pagoda and Mackellar Formation rocks sampled in this study reveal the same population peak ~580–600 Ma. Elliot and Fanning (2008) report U/Pb ages of Buckley and Fremouw Formation rocks that were collected in the southern TAM along the Shackleton Glacier. Findings reveal a shift from a dominant Permian–early Triassic population (245–260 Ma) in the Buckley Formation samples to increasing number of grains in the Ross/Pan-African population (480-600 Ma) in the Fremouw Formation samples (Elliot and Fanning, 2008). Rocks of the Fremouw Formation do not outcrop at Mt. Achernar, but are outcropped at surrounding sites throughout the central TAM, including the Queen Alexandra Range (McGregor, 1965). Given the prior evidence suggesting the Pagoda, Mackellar, and Fremouw Formations influencing the composition of the moraine, it is likely that the Ross/Pan-African peaks are grains recycled from these three formations. However, sites 4L and 4J have a ~40 Ma shift in the dominant Ross/Pan-African population, with peaks ~550 and ~555 Ma (Figure 14), and K-S test results (Table 8) indicate that these sites are statistically similar. However, the K-S test results should be interpreted with caution as well. Samples that fail the K-S test (such as 4L and 4J) have many of the same populations as other sites and look visually similar, but fail the K-S test simply because the populations are distributed slightly differently. Although granitic rocks of the Granite Harbour Intrusives and/or like the erratic granite (KTW) collected at Kon-Tiki nunatak (Goodge, 2012) were not found in the MAM, it cannot be ruled out that grains from these sources are being subglacially eroded, englacially transported, and deposited in the MAM as well.

CONCLUSIONS

The blue ice moraine adjacent to the Mt. Achernar nunatak serves as an archive of Law Glacier flow history and unmapped lithologies that are buried upstream beneath the EAIS. The presence of alternating lithologic bands, distinct morphology and relative exposure age across the MAM moraine help distinguish separate "zones" within the moraine. Hummocky topography occurs with the most recently exposed material along the active ice margin (Zone 1), followed by a relatively flat and low region (Zone 2), and then a series of ~2 m parallel/sub-parallel ridges and troughs accompanied by distinct color changes that are directly related to the dominant lithology of the region (Zones 3–5). Zone 3 is dominated by sedimentary lithologies and has an overall topography of a broad arch. Zone 4 consists of alternating bands of Ferrar and Beacon rocks and an overall steady elevation increase of ~30 m up and away from Law Glacier. Zone 5 is characterized by ridges that are curved in the opposite direction from those in Zones 1–4, as well as distinct geochemical concentrations and unique presence of felsic igneous cobbles. Provenance techniques such as pebble lithology and geochemical analysis indicate that the composition of the MAM moraine changes through time and consists of both local, and unmapped exotic material that mostly derive from weathered and/or recycled source rocks from the Beacon and Ferrar Supergroups. U/Pb ages of detrital zircons collected from MAM till and cobbles reveal that the dominant zircon populations are consistent with a Beacon source (most similarly to the Pagoda and Mackellar Formations) that is not locally exposed and show very little variation across the MAM. U/Pb data from this study, combined with surface exposure ages (Mathieson et al., 2012) indicate that the ice flow and erosion of the same source material has been consistent since at least the past ~200–554 ka; this consistent supply of sediment implies stable ice

sheet behavior. However, the distinctly colored lithologic bands and varied geochemistry across the MAM create an interesting contradiction since they indicate there is the potential for multiple sources to have fed material into the moraine. With its distinct morphology, cobble lithology, and geochemistry, it is concluded that Zone 5 is derived from a different source than Zones 1–4. The presence and position of a hinge line intersecting at the Zone 3/4 border, surface exposure ages ranging from ~12–50 ka, and the distinct geomorphology of a broad arch, dominant sedimentary pebble lithology, and elevated geochemical concentrations of Zone 3 all support a model that suggests Zone 3 records a time of ice sheet thickening and a change in provenance during the LGM. Zone 4 is interpreted to represent pre-LGM deposition or till accumulation, Zone 2 is a record of deglaciation, and Zone 1 is still actively connected to the Law Glacier. This study reveals the importance of using multiple analytical techniques when interpreting till provenance.

Table 1. Analysis per sample.

	SAL	Sample ID	Latitude	Longitude	Till	Till Thickness (cm)	Munsell Color of Dry Till	Pebbles	Particle Size	U/Pb	Geochemistry
	1948	East Crest	-84.11096	162.16574	X	4-5	Greyish Brown		X		X
	---	1I	-84.0979	162.17647		---	---	Cobbles			
	1949	1H	-84.10696	162.05138	X	---	Grey		X		X
	1914	1G	-84.1076	162.05008	X	5	Dark Grey	X	X		
	1971	1G Red/Grey	-84.10816	162.05466	X	---	Dark Grey; Lt. Grey and Lt. Olive Grey		X		
Tail	1969	1F Crest 1	-84.11539	161.90712	X	3	Dark Grey	X	X		
	1970	1F Crest 2	-84.1157	161.90967	X	12	Grey	X	X		
	1913	1E	-84.13533	161.8172	X	2	Dark Grey	X	X		X
	1951	1E Red/Grey	-84.13554	161.84344	X	4-5	Dark Grey and Very Dark Grey	X	X		X
	1968	1D	-84.16523	161.69415	X	1	Light Grey	X	X		
	1967	1C	-84.17773	161.53679	X	1-2	Light Grey	X	X		
Zone 1	1912	1A	-84.1828	161.26768	X	3	Dark Grey	X	X	X	X
	1952	1B	---	---	X	3	Very Dark Grey	X	X		X
Zone 2	1947	2A	-84.1881	161.26773	X	8	Light Grey and Light Olive Grey		X	X	X
	1953	3C	-84.19074	161.28191	X	9-10	Light Grey and Light Olive Grey	X	X		X
	1916	3D	-84.19093	161.27972	X	---	Light Grey and Light Olive Grey	X	X		
Zone 3	1954	3 Dark	-84.19242	161. 28790	X	8	Dark Grey		X		X
	1941	3B	-84.19283	161. 28775	X	11	Light Grey	X	X	X	X
	1915	3A	-84.19307	161. 28751	X	12	Light Grey	X	X		
	1955	3E	-84.19486	161.27872	X	14	Light Olive Grey		X		X
	1921	4L	-84.2017	161.27872	X	> 35	Light Olive Grey	X	X	X	X
	1943	4K	-84.20215	161.33037	X	>30	Light Brownish Grey	X	X	X	X
	1920	4J	-84.20238	161.32782	X	>18	Grey	X	X	X	X
	1960	4I	-84.20473	161.35077	X	---	Pale Yellow and Light Yellowish Brown		X		X
	1959	4G	-84.20892	161.3671	X	34	Pale Yellow and Light Yellowish Brown	X	X		X
Zone 4	1972	4H	-84.20918	161.36667	X	>22	Pale Yellow	X	X		
	1919	4F	-84.21372	161.36685	X	---	Light Yellowish Brown		X		
	1958	4E	-84.21606	161.36421	X	>30	Light Yellowish Brown	X	X		X
	1957	4D	-84.21841	161.36061	X	>28	Pale Yellow		X		X
	1918	4C	-84.21909	161.36067	X	>30	Pale Yellow	X	X		X
	1942	4B	-84.22171	161.35822	X	>30	Pale Yellow	X	X	X	X
	1917	4A	-84.22298	161.355594	X	>45	Pale Yellow	X	X		
	1922	5A	-84.22598	161.27373	X	>15	Pale Yellow and Light Yellowish Brown	X	X		X
	1923	5B	-84.22861	161.27284	X	>15	Pale Yellow and Light Yellowish Brown	X	X	X	X
Zone 5	1962	5C	-84.23213	161.27444	X	---	Pale Yellow and Light Yellowish Brown		X		X
	1924	5D	-84.23618	161.28149	X	---	Greyish Brown		X		X
	1963	5E	-84.22989	161.30516	X	---	Pale Yellow and Light Yellowish Brown		X		X

Table 2. Pebble classification scheme.

Igneous	Felsic/Intermediate	>20% Quartz (Qtz), K-Spar, Plagioclase
	Intermediate/Mafic	<20% Quartz, K-spar, Plagioclase
	Intermediate/Mafic: Different than Others	<20% Quartz, K-spar, F-Spar, but interpreted as not the local dolerite.
Metamorphic	Quartzite	Conchoidal fracture, indistinguishable grain boundaries, cannot be scratched
	Slate/Phyllite	Foliated shale with dull to shiny luster depending on degree of metamorphism
	Marble	Composed primarily of CaCO3; effervesces with 3%HCl; recrystallized grains
Sedimentary	Sandstone	Dominated by quartz or feldspar, any grain roundness and size (>63 μm) with or without cement
	Meta-Sandstone	Sandstones that have undergone varying degree of metamorphism, but not to the level of a quartzite.
	(Meta) Siltstone	Silt (<63 μm), grains too small to determine grade of metamorphism
	(Meta) Black Argillite/Clay/Mudstone	May be weakly metamorphosed, conchoidal fracture common, may contain some silt-size grains, feels waxy on fresh surface, organic- or iron-rich (black/dark grey color)
	(Meta) White Argillite/Clay/Mudstone	May be weakly metamorphosed, conchoidal fracture common, may contain some silt-size grains, feels waxy on fresh surface, silicate-rich (white/tan color)
	Shale	Silt, mud, or clay, bedded or laminated
	Chert	Microcrystalline, conchoidal fracture, cannot be scratched, waxy feel
	Limestone	Composed primarily of $CaCO_3$; effervesces with 3%HCl.
	Coal	Black, layered, brittle, sooty

Table 3. Pebble counts for the Mt. Achernar moraine till. CG = Coarse Grained, FG = Fine Grained, F/S = Faceted and/or Striated.

Site ID		IGNEOUS										METAMORPHIC			
		Felsic/Intermediate				Intermediate/Mafic		Intermediate/Mafic: Different than Others							
		CG	CG F/S	FG	FG F/S	CG	CG F/S	CG	CG F/S	FG	FG F/S	Quartzite	Quartzite F/S	Slate/Phyllite	Marble
	1G					35	8			2					
	1F Crest 1		1			36	10	2	1	2		2			
	1F Crest 2		1		1	31	6	2				1			
Tail	1E	2				56	1	1	1	1		3			
	1E Red/Grey			2		47	6	2				2			
	1D					39	2		1						
	1C		1			22	7			1		2	3		
Zone 1	1A	1				12	11	1	2	1			1		
	1B					20	19	1	1	1	1		1		
Zone 3	3C			1		14			1				2		
	3D					11	2	3	1	1	1				
	3B					6	2	1			1				
	3A					4	1	1			2				
Zone 4	4L	1				21	10	1		3		1	4	1	
	4K	3				52	6	2	2	7	1	5			
	4J			1		28	4			5		1			
	4G					19	4	1		2	1				
	4H					27	9	1		3		1			
	4E					42	4			1		3			
	4C		1			9	7				2		1		
	4B					12	23	3	1		1				
	4A					6	2					5	2		
Zone 5	5A					11	5					2			1
	5B					36	7			1	1	2			2

Table 3 continued. Pebble counts for the Mt. Achernar moraine till. CG = Coarse Grained, FG = Fine Grained, F/S = Faceted and/or Striated.

Site ID		SEDIMENTARY							
		Sandstone	Sandstone F/S	Meta-Sandstone	Meta-Sandstone F/S	(Meta) Siltstone	(Meta) Siltstone F/S	(Meta) Black Argillite/Clay/Mudstone	(Meta) Black Argillite/Clay/Mudstone F/S
Tail	1G	1	1	3		4			2
	1F Crest 1	14		14		7	4		
	1F Crest 2	11	1	2		3	1		
	1E	4		1				1	
	1E Red/Grey	6		14		5	2		
	1D	10		8		8	6	4	5
	1C	6		18	3	3	3	1	1
Zone 1	1A	3	1	4	5	1	1		1
	1B	7		6		2	2	3	
Zone 3	3C	19			1	4	2		
	3D	15		2	1	7	2	1	2
	3B	30		1	1	5	7		
	3A	16				2	1		
Zone 4	4L	1	1			2	4		
	4K			3			2	3	
	4J	8	1	1	3	4		2	1
	4G	4	1	8	2	7	1		
	4H	12		6		4		1	
	4E	1				1		2	1
	4C	1		1	2	5			
	4B					1	2		
	4A	2		10	4	1	1		
Zone 5	5A	1		3		2			
	5B	2		1		1			

Table 3 continued. Pebble counts for the Mt. Achernar moraine till. CG = Coarse Grained, FG = Fine Grained, F/S = Faceted and/or Striated.

Site ID		SEDIMENTARY									TOTAL	%F/S
		(Meta) White Argillite/Clay/Mudstone	(Meta) White Argillite/Clay/Mudstone F/S	Shale	Shale F/S	Limestone	Limestone F/S	Chert	Chert F/S	Coal		
Tail	1G			3				1			1500	19.86
	1F Crest 1			2								
	1F Crest 2	1	2	2					2	1		
	1E							1	1			
	1E Red/Grey							2				
	1D					2						
	1C											
Zone 1	1A											
	1B		4		1				1			
Zone 3	3C			19								
	3D	1		6	1	1						
	3B			5	1							
	3A											
Zone 4	4L	1	1					2				
	4K		2					1	1			
	4J		3					1	1	1		
	4G	1		10								
	4H			11								
	4E			10								
	4C			16								
	4B											
	4A			3								
Zone 5	5A			3		2	1	14				
	5B							5				

Table 4. Particle size data from Mt. Achernar moraine till samples.

%GRAVEL							%FINES					
		%PEBBLE*		%GRANULE	Total	Average	%SAND		%SILT		%CLAY	
Site ID		32-8mm	8-4mm	4-2mm	>2mm		Total	Average	Total	Average	Total	Average
Tail	East Crest	2.6	12.0	4.3	18.9	27.1 ± 11.2	62.8	40.0 ± 9.2	10.8	18.3 ± 8.0	7.6	14.7 ± 5.6
	1H	10.8	9.7	12.0	32.6		44.0		13.8		9.6	
	1G	17.5	18.2	6.8	42.5		31.7		10.4		15.5	
	1G Red/Grey	0.0	6.7	3.6	10.3		36.8		30.8		22.2	
	1F Crest 1	9.3	11.0	11.2	31.5		30.4		17.9		20.2	
	1F Crest 2	3.2	5.9	5.0	14.1		43.4		31.1		11.5	
	1E	6.9	9.6	6.8	23.4		36.0		16.6		24.1	
	1E Red/Grey	2.9	8.4	9.4	20.7		41.2		25.8		12.2	
	1D	6.6	17.5	15.4	39.5		35.4		13.2		11.8	
	1C	10.6	15.3	11.6	37.5		37.9		12.6		12.0	
Zone 1	1A	0.0	13.1	16.6	29.6	27.6 ± 3.0	34.3	29.2 ± 7.2	13.9	22.7 ± 12.4	22.2	20.7 ± 2.2
	1B	13.5	7.3	4.6	25.5		24.1		31.5		19.1	
Zone 2	2A	3.3	11.6	10.1	25.0	25.0	46.0	46.0	15.0	15.0	14.1	14.1
Zone 3	3C	4.5	8.8	8.8	22.0	29.8 ± 4.9	36.9	33.2 ± 4.9	18.4	17.5 ± 1.5	22.7	19.6 ± 2.4
	3D	13.5	9.6	7.2	30.2		31.9		17.6		20.3	
	3 Dark	21.5	5.4	3.8	30.7		31.8		18.2		19.3	
	3B	24.4	2.7	4.0	31.1		36.9		16.7		15.4	
	3A	28.0	4.7	4.3	37.0		24.5		19.0		19.3	
	3E	19.6	3.9	4.2	27.7		37.0		14.8		20.5	
Zone 4	4L	7.8	5.1	10.1	23.0	22.7 ± 13.0	54.6	45.6 ± 12.0	10.9	15.7 ± 8.0	11.4	16.0 ± 11.2
	4K	5.4	8.1	12.1	25.5		43.4		14.0		17.0	
	4J	7.7	16.5	15.7	40.0		32.7		12.6		14.7	
	4I	0.0	1.7	12.0	13.7		56.3		15.8		14.1	
	4G	8.6	5.6	8.1	22.4		45.6		18.8		13.2	
	4H	18.0	3.0	9.0	30.0		48.8		11.7		9.6	
	4F	0.0	1.0	5.5	6.5		16.4		34.4		42.7	
	4E	2.8	4.4	8.5	15.7		60.5		13.8		10.0	
	4D	0.0	0.0	0.0	0.0		39.6		27.6		32.8	
	4C	7.7	24.4	10.9	42.9		44.6		7.6		4.9	
	4B	10.9	3.0	3.2	17.2		51.0		14.0		18.0	
	4A	9.8	9.6	15.9	35.3		53.9		6.7		4.1	
Zone 5	5A	28.1	6.0	7.2	41.3	21.0 ± 15.1	44.8	62.9 ± 11.4	9.1	9.3 ± 2.6	4.8	6.9 ± 3.4
	5B	0.0	8.3	2.8	11.0		73.2		9.4		6.5	
	5C	0.0	2.7	5.6	8.3		71.0		11.3		9.4	
	5D	13.9	7.1	12.0	33.0		59.3		5.0		2.6	
	5E	6.8	0.6	3.8	11.1		66.2		11.6		11.1	

*Pebble data in this table does not include the bulk pebble samples collected for pebble lithology data.

Table 5. Particle size data <2 mm from Mt. Achernar moraine till samples.

		%SAND							%SILT						%CLAY				
	Site ID	V. Coarse	Coarse	Medium	Fine	V. Fine	Total	Average	Coarse	Medium	Fine	V. Fine	Total	Average	Coarse	Medium	Fine	Total	Average
Tail	East Crest	10.7	18.7	23.9	15.9	8.1	77.3	55.2 ± 10.8	3.4	2.5	3.2	4.3	13.3	24.5 ± 7.6	4.3	4.1	1.0	9.3	20.4 ± 7.5
	1H	24.8	16.8	14.2	6.2	3.2	65.2		4.1	4.9	5.4	6.3	20.6		6.7	4.2	3.3	14.2	
	1G	20.1	11.2	13.9	6.7	3.1	55.0		3.5	4.3	4.6	5.5	17.9		6.6	6.0	14.4	27.1	
	1G Red/Grey	8.0	7.7	11.8	8.9	4.6	41.0		3.4	5.9	11.3	13.6	34.3		10.8	5.7	8.2	24.7	
	1F Crest 1	21.5	8.2	7.5	4.5	2.7	44.4		2.4	3.9	8.1	11.8	26.2		11.3	6.6	11.6	29.5	
	1F Crest 2	12.7	11.3	13.7	7.7	5.1	50.5		10.0	10.6	8.2	7.4	36.2		6.7	3.8	2.8	13.3	
	1E	22.6	10.6	8.2	3.3	2.4	47.0		2.8	3.2	6.1	9.6	21.7		9.9	6.3	15.1	31.3	
	1E Red/Grey	16.2	13.5	12.9	4.9	4.5	52.0		9.0	8.8	7.4	7.4	32.6		7.0	4.2	4.3	15.5	
	1D	31.3	12.3	8.2	4.0	2.8	58.6		3.1	5.0	6.6	7.2	21.8		7.1	4.9	7.6	19.6	
	1C	25.8	13.1	9.5	6.7	5.6	60.7		4.1	4.2	5.6	6.4	20.1		6.6	5.0	7.6	19.2	
Zone 1	1A	22.1	8.5	9.1	5.7	3.3	48.8	40.5 ± 11.7	2.2	2.8	5.6	9.0	19.6	30.9 ± 16.0	10.7	7.7	13.2	31.6	28.6 ± 4.3
	1B	10.3	5.3	5.6	3.7	7.2	32.2		13.7	11.5	8.5	8.6	42.3		9.1	6.3	10.2	25.6	
Zone 2	2A	16.3	8.4	12.9	14.4	9.3	61.2	61.2	5.2	4.3	4.8	5.8	20.1	20.1	6.6	5.0	7.0	18.7	18.7
Zone 3	3C	11.1	6.7	11.1	11.7	6.9	47.4	47.1 ± 5.0	4.7	5.0	6.2	7.6	23.6	25.0 ± 3.2	8.5	6.5	13.9	29.0	27.9 ± 2.8
	3D	10.3	5.1	10.1	12.3	7.9	45.7		6.4	5.9	6.2	6.8	25.3		6.8	5.7	16.5	29.1	
	3 Dark	8.3	2.8	9.7	14.0	11.1	45.8		7.1	5.8	6.1	7.3	26.3		8.2	6.4	13.2	27.8	
	3B	7.9	6.1	12.6	16.0	10.9	53.4		6.1	5.0	5.9	7.1	24.1		7.9	6.0	8.6	22.5	
	3A	3.8	4.3	11.7	12.3	6.9	39.0		5.0	6.5	8.8	10.1	30.3		10.2	7.0	13.6	30.8	
	3E	9.1	9.7	15.1	11.6	5.6	51.1		3.1	3.2	5.5	8.7	20.5		10.0	6.9	11.4	28.4	
Zone 4	4L	14.4	12.2	16.7	17.5	10.1	70.9	60.8 ± 17.8	4.0	2.9	3.3	4.1	14.2	19.5 ± 7.2	5.4	4.9	4.6	14.9	19.7 ± 10.9
	4K	16.6	11.0	12.5	10.6	7.5	58.2		4.3	3.7	4.6	6.2	18.9		7.8	6.2	8.9	22.9	
	4J	22.2	6.8	10.1	9.1	6.2	54.4		4.5	3.9	5.4	7.3	21.2		8.3	6.4	9.6	24.4	
	4I	15.3	9.0	13.3	16.8	10.7	65.2		4.8	3.9	4.4	5.3	18.4		6.4	5.0	5.0	16.5	
	4G	10.4	5.9	13.7	17.5	11.3	58.8		6.2	5.5	5.7	6.7	24.1		7.5	5.2	4.4	17.1	
	4H	18.9	12.7	15.7	14.3	8.1	69.7		4.0	3.4	4.1	5.1	16.7		5.8	4.4	3.4	13.6	
	4F	4.6	1.0	1.1	3.4	7.5	17.6		6.0	5.7	10.1	15.1	36.8		17.0	11.4	17.2	45.6	
	4E	13.1	8.4	17.0	20.8	12.4	71.8		4.7	3.4	3.8	4.5	16.3		5.1	4.4	2.3	11.9	
	4D	0.2	3.1	14.3	15.6	6.4	39.6		4.2	5.9	7.4	10.1	27.6		12.1	8.7	12.0	32.8	
	4C	23.1	14.5	16.8	15.1	8.6	78.1		4.0	2.9	3.0	3.4	13.2		3.4	4.1	1.1	8.6	
	4B	2.5	2.9	20.6	26.5	9.1	61.6		2.5	3.0	4.3	6.9	16.8		9.1	6.6	6.0	21.7	
	4A	30.6	14.9	16.8	13.8	7.2	83.3		3.2	2.3	2.3	2.5	10.3		2.5	3.1	0.8	6.4	
Zone 5	5A	9.7	7.6	20.3	24.2	14.4	76.2	79.8 ± 5.7	5.3	3.2	3.3	3.7	15.6	11.8 ± 3.0	3.7	3.6	0.9	8.2	8.4 ± 3.2
	5B	4.7	11.9	33.9	24.9	6.8	82.3		2.8	2.2	2.5	3.0	10.5		3.0	3.3	0.9	7.2	
	5C	14.7	13.5	22.8	18.8	7.6	77.4		3.0	2.5	2.9	4.0	12.4		4.6	4.6	1.1	10.2	
	5D	24.8	22.4	25.3	11.8	4.4	88.7		2.4	1.7	1.6	1.8	7.5		1.7	1.7	0.4	3.9	
	5E	12.0	14.2	24.9	17.6	5.7	74.5		2.4	2.3	3.4	5.0	13.1		5.7	4.8	2.0	12.5	

Particle size data normalized without influence of the coarse fraction reported in Table 4, and is averaged over 3–7 replicates. The 'V. Coarse' sand data is normalized to include the 1–2mm fraction.

Table 6. Geochemical analysis of major, trace, and rare earth elements of the Mt. Achernar moraine tills.

		Major Oxides											
	Analyte Symbol	SiO2	Al2O3	Fe2O3(T)	MnO	MgO	CaO	Na2O	K2O	TiO2	P2O5	LOI	Total
	Unit Symbol	%	%	%	%	%	%	%	%	%	%	%	%
	Detection Limit	0.01	0.01	0.01	0.001	0.01	0.01	0.01	0.01	0.001	0.01	---	0.01
	Analysis Method	FUS-ICP	FUS-ICP	FUS-ICP	FUS-ICP	FUS-ICP	FUS-ICP	FUS-ICP	FUS-ICP	FUS-ICP	FUS-ICP	FUS-ICP	FUS-ICP
Tail	East Crest	58.22	13.91	5.93	0.103	2.75	6.77	1.67	2.16	0.829	0.15	8.32	100.8
	1H	59.72	16.74	6.13	0.105	2.09	2.34	0.96	2.36	0.754	0.11	9.68	101
	1E	58.2	15.44	5.7	0.107	1.92	2.24	0.88	2.22	0.725	0.11	10.73	98.28
	1E Red/Grey	58.16	15.52	5.66	0.106	1.96	2.3	0.99	2.19	0.738	0.1	10.42	98.16
Zone 1	1A	60.2	13.72	4.77	0.099	1.93	4.62	1.45	2.09	0.752	0.14	10.5	100.3
	1B	63.23	13.77	4.82	0.098	2.08	2.97	1.64	2.08	0.781	0.12	8.62	100.2
Zone 2	2A	64.14	14.92	5.01	0.091	1.93	3.24	1.84	2.47	0.872	0.18	5.43	100.1
Zone 3	3C	60.84	16.31	5.46	0.087	1.98	3.09	1.78	2.82	0.851	0.14	6.61	99.96
	3 Dark	61.48	16.95	5.07	0.09	1.79	3.1	1.86	2.83	0.825	0.18	6.75	100.9
	3B	60.71	16.35	5.47	0.087	1.91	2.98	1.7	2.88	0.831	0.13	7.47	100.5
	3E	60.08	15.53	5.34	0.097	2.02	3.56	1.62	2.47	0.83	0.12	8.35	100
Zone 4	4L	57.53	15.3	5.51	0.095	2.19	4.07	1.7	2.3	0.707	0.13	10.56	100.1
	4K	56.65	14.99	5.31	0.094	2.26	4.32	1.73	2.25	0.714	0.15	10.11	98.58
	4J	58.45	15.23	5.06	0.093	1.98	3.85	1.51	2.23	0.678	0.12	11.64	100.8
	4I	58.04	16.12	6.13	0.092	2.56	4.19	1.89	2.51	0.794	0.14	8.05	100.5
	4G	57.76	15.67	5.64	0.095	2.42	4.22	1.99	2.5	0.788	0.14	9.48	100.7
	4E	55.31	15.34	5.8	0.093	2.58	4.64	2.05	2.41	0.759	0.13	10.24	99.36
	4D	55.64	14.73	5.04	0.096	2.3	4.39	2.17	2.07	0.713	0.12	11.38	98.66
	4C	56.95	15.81	5.52	0.083	2.34	3.51	1.89	2.59	0.715	0.15	8.96	98.5
	4B	57.04	14	5.43	0.098	2.42	4.51	1.99	2.15	0.725	0.12	10.13	98.62
Zone 5	5A	50.22	13.57	5.42	0.093	3.27	9.85	1.9	2.04	0.665	0.11	12.67	99.79
	5B	49.64	13.49	5.78	0.096	3.51	8.71	1.99	2.09	0.649	0.11	13.62	99.69
	5C	48.85	16.11	6.14	0.091	3.95	5.55	2.8	2.58	0.628	0.12	14.06	100.9
	5D	47.02	14.92	5.75	0.087	3.05	6.5	3.51	2.24	0.625	0.11	16.92	100.7
	5E	50.71	15.34	5.35	0.086	2.75	5.4	2.08	2.49	0.684	0.12	13.28	98.3
	Average	56.99	15.19	5.49	0.09	2.40	4.44	1.82	2.36	0.75	0.13	10.16	99.82
	Std. Dev.	4.49	1.00	0.39	0.01	0.55	1.88	0.53	0.25	0.07	0.02	2.60	0.97

Table 6 continued. Geochemical analysis of major, trace, and rare earth elements of the Mt. Achernar moraine tills.

		Trace Elements												
	Analyte Symbol	Sc	Be	V	Ba	Sr	Y	Zr	Cr	Co	Ni	Cu	Zn	Ga
	Unit Symbol	ppm	ppm	ppm	ppm	ppm	ppm	ppm	ppm	ppm	ppm	ppm	ppm	ppm
	Detection Limit	1	1	5	3	2	2	4	20	1	20	10	30	1
	Analysis Method	FUS-ICP	FUS-ICP	FUS-ICP	FUS-ICP	FUS-ICP	FUS-ICP	FUS-ICP	FUS-MS	FUS-MS	FUS-MS	FUS-MS	FUS-MS	FUS-MS
Tail	East Crest	18	2	120	568	221	31	411	70	17	30	40	60	16
	1H	19	2	111	607	180	26	227	60	16	30	40	70	19
	1E	18	2	104	590	176	24	226	60	16	30	30	60	17
	1E Red/Grey	18	2	107	580	172	24	262	60	16	30	30	60	18
Zone 1	1A	17	2	106	557	200	26	355	60	15	20	30	50	15
	1B	17	2	108	568	201	28	396	70	15	30	30	50	15
Zone 2	2A	16	2	100	717	268	33	388	70	14	30	30	70	17
Zone 3	3C	17	2	115	806	275	29	316	80	16	30	30	80	20
	3 Dark	16	2	110	807	282	27	310	80	15	20	20	60	19
	3B	17	3	111	810	264	29	285	80	16	30	30	80	20
	3E	18	2	113	706	245	29	345	70	16	30	30	70	18
Zone 4	4L	18	2	110	603	214	27	265	60	15	20	40	70	18
	4K	18	2	109	587	224	26	308	60	16	30	40	70	18
	4J	17	2	104	682	226	25	245	50	14	< 20	30	60	17
	4I	18	2	120	674	287	28	287	80	17	30	40	70	18
	4G	18	2	113	672	252	28	368	80	17	30	40	70	18
	4E	18	2	116	641	299	28	325	70	16	30	40	70	17
	4D	16	2	102	558	279	23	358	60	15	30	30	60	17
	4C	16	2	104	686	259	26	267	70	15	30	30	80	19
	4B	17	2	110	588	230	24	396	60	15	40	30	60	17
Zone 5	5A	18	2	113	528	277	24	283	70	16	30	40	60	15
	5B	19	2	111	548	437	24	227	70	18	40	50	70	16
	5C	19	2	114	586	551	24	189	70	18	30	180	150	18
	5D	18	2	106	542	411	23	248	70	21	40	60	90	18
	5E	16	2	103	633	366	24	270	70	15	40	40	70	19
	Average	17.48	2.04	109.60	633.76	271.84	26.40	302.28	68.00	16.00	30.42	41.20	70.40	17.56
	Std. Dev.	0.96	0.20	5.28	84.50	87.98	2.60	61.91	8.16	1.47	5.50	30.04	19.04	1.42

Table 6 continued. Geochemical analysis of major, trace, and rare earth elements of the Mt. Achernar moraine tills.

		Trace Elements												
	Analyte Symbol	Ge	Rb	Nb	Ag	Sn	Cs	Hf	Ta	W	Tl	Pb	Th	U
	Unit Symbol	ppm	ppm	ppm	ppm	ppm	ppm	ppm	ppm	ppm	ppm	ppm	ppm	ppm
	Detection Limit	1	2	1	0.5	1	0.5	0.2	0.1	1	0.1	5	0.1	0.1
	Analysis Method	FUS-MS	FUS-MS	FUS-MS	FUS-MS	FUS-MS	FUS-MS	FUS-MS	FUS-MS	FUS-MS	FUS-MS	FUS-MS	FUS-MS	FUS-MS
Tail	East Crest	1	85	10	2.4	2	3.5	10.3	0.8	< 1	0.5	15	14.3	3.4
	1H	1	100	9	1	7	6.4	5.8	0.8	< 1	0.5	14	11.2	2.7
	1E	1	94	9	1.3	5	5.9	5.8	0.8	< 1	0.6	15	11.8	2.7
	1E Red/Grey	2	94	10	1	4	6.1	6.2	0.7	< 1	0.6	14	12.6	2.8
Zone 1	1A	1	78	13	1.6	3	4.7	8.6	0.7	< 1	0.6	14	12.7	3.1
	1B	1	81	9	2.3	2	4.6	9.4	0.7	< 1	0.4	13	13	3
Zone 2	2A	2	93	12	2.3	3	4.8	9.5	0.9	< 1	0.5	21	14.3	3.5
Zone 3	3C	1	106	11	1.8	3	5.4	7.7	0.8	< 1	0.5	20	14.6	3.2
	3 Dark	1	91	11	1.1	4	4.8	7.5	0.8	< 1	0.6	20	14.9	3.1
	3B	1	106	11	1.7	3	5.8	7.1	0.8	< 1	0.5	21	14.8	3.3
	3E	1	91	10	1.9	3	4.9	8.9	0.8	< 1	0.5	19	14.3	3.2
Zone 4	4L	1	93	9	1.5	2	5.4	6.5	0.7	< 1	0.5	18	11.6	3
	4K	2	82	10	1.1	2	5.2	7.5	0.6	1	0.6	18	12.2	3
	4J	1	90	9	1.4	2	5.6	6	0.7	< 1	0.4	13	10.9	2.9
	4I	1	95	10	1.5	2	5	7.3	0.8	< 1	0.4	15	13.6	3.3
	4G	1	98	11	2.1	2	5.1	9.1	0.7	17	0.4	14	14.8	3.4
	4E	2	87	9	1.8	2	4.8	8.4	0.7	< 1	0.5	18	13.5	3.5
	4D	2	80	10	1.4	2	5.5	8.8	0.7	2	0.5	14	13.8	3
	4C	2	103	12	1.2	3	5.6	6.9	0.7	< 1	0.7	22	15	3.7
	4B	2	82	10	1.8	4	4.7	9.1	0.7	< 1	0.5	15	13.9	3
Zone 5	5A	2	75	9	1.7	2	3.9	6.8	0.6	< 1	0.4	13	11.3	2.6
	5B	3	81	8	1.3	5	4.6	5.7	0.6	1	0.4	19	10.7	2.5
	5C	3	97	8	0.7	3	6.9	5	0.7	1	0.4	25	11.8	2.9
	5D	3	94	9	1.5	3	6.9	5.8	0.6	2	0.2	12	11.7	2.8
	5E	2	93	10	1.9	2	6.4	6.5	0.7	2	0.5	14	12.7	3
	Average	1.60	90.76	9.96	1.57	3.00	5.30	7.45	0.72	3.71	0.49	16.64	13.04	3.06
	Std. Dev.	0.71	8.60	1.24	0.44	1.26	0.84	1.46	0.08	5.88	0.10	3.47	1.40	0.30

Table 6 continued. Geochemical analysis of major, trace, and rare earth elements of the Mt. Achernar moraine tills.

		Rare Earth Elements													
	Analyte Symbol	La	Ce	Pr	Nd	Sm	Eu	Gd	Tb	Dy	Ho	Er	Tm	Yb	Lu
	Unit Symbol	ppm	ppm	ppm	ppm	ppm	ppm	ppm	ppm	ppm	ppm	ppm	ppm	ppm	ppm
	Detection Limit	0.1	0.1	0.05	0.1	0.1	0.05	0.1	0.1	0.1	0.1	0.1	0.05	0.1	0.04
	Analysis Method	FUS-MS	FUS-MS	FUS-MS	FUS-MS	FUS-MS	FUS-MS	FUS-MS	FUS-MS	FUS-MS	FUS-MS	FUS-MS	FUS-MS	FUS-MS	FUS-MS
Tail	East Crest	42.3	85.1	9.64	36.5	6.8	1.31	6	0.9	5.5	1.1	3.1	0.47	3.3	0.54
	1H	31.4	62.7	7.3	27.6	5.4	1.14	4.7	0.8	4.6	0.9	2.7	0.41	2.8	0.45
	1E	32.1	65.3	7.52	29.1	5.7	1.13	4.8	0.8	4.5	0.9	2.6	0.41	2.8	0.44
	1E Red/Grey	30.1	60.8	7.3	29	5.7	1.07	5	0.8	4.4	0.9	2.6	0.39	2.6	0.43
Zone 1	1A	33.6	67	7.84	30.2	6.2	1.17	5.4	0.9	4.7	1	2.9	0.42	2.9	0.47
	1B	34	70.4	8.23	32	6.3	1.16	5.4	0.9	5	1	2.9	0.45	3	0.49
Zone 2	2A	48.9	96.6	10.9	40.7	7.8	1.51	6.5	1	5.7	1.1	3.2	0.49	3.3	0.54
Zone 3	3C	45.1	89.4	10.1	38.1	6.9	1.49	5.7	0.9	5.2	1	3	0.45	3	0.5
	3 Dark	44.4	84.4	9.8	36.3	7.1	1.45	5.7	0.9	4.9	1	2.9	0.44	2.9	0.46
	3B	45.8	90.8	10.2	37.8	7.1	1.41	5.8	0.9	5	1	2.9	0.43	2.9	0.47
	3E	43.3	88.1	9.85	37.8	6.9	1.48	5.9	0.9	5.5	1.1	3.1	0.48	3.2	0.53
Zone 4	4L	33.2	67.2	7.71	30.3	5.8	1.25	5	0.8	4.8	1	2.8	0.43	3	0.48
	4K	34	65.4	7.6	28.2	5.9	1.13	4.9	0.8	4.7	0.9	2.8	0.42	2.9	0.46
	4J	30.8	63	7.34	28.5	5.5	1.2	4.8	0.8	4.6	0.9	2.7	0.4	2.8	0.45
	4I	42.4	84.1	9.59	35.9	6.8	1.34	5.5	0.9	4.9	1	2.9	0.43	2.8	0.47
	4G	43.4	86.9	9.91	38	7	1.28	5.5	0.9	5	1	2.8	0.43	2.8	0.45
	4E	39.3	78.1	8.92	34.2	6.3	1.29	5.5	0.8	5	1	2.9	0.45	3	0.49
	4D	35.2	68.5	7.91	29.6	6.2	1.05	4.9	0.7	4.4	0.9	2.6	0.4	2.7	0.43
	4C	43.8	83.1	9.4	34.6	6.8	1.26	5.8	0.9	4.8	1	2.9	0.44	3.1	0.48
	4B	35.6	71.2	8.41	32.7	6.1	1.15	5.2	0.8	4.7	0.9	2.7	0.41	2.8	0.45
Zone 5	5A	32.9	66.1	7.59	28.7	5.4	1.1	4.5	0.7	4.4	0.8	2.4	0.37	2.5	0.41
	5B	32.4	64.9	7.43	28.4	5.3	1.09	4.7	0.7	4.2	0.8	2.5	0.36	2.4	0.4
	5C	33.9	67.2	7.55	27.9	5.4	1.12	4.6	0.7	4.3	0.9	2.5	0.39	2.7	0.42
	5D	33.8	66.7	7.49	28.6	5.2	1.01	4.5	0.7	4.2	0.8	2.4	0.36	2.4	0.41
	5E	33.5	66.6	7.81	29.9	5.7	1.13	5.2	0.8	4.5	0.9	2.6	0.4	2.7	0.43
	Average	37.41	74.38	8.53	32.42	6.21	1.23	5.26	0.83	4.78	0.95	2.78	0.42	2.85	0.46
	Std. Dev.	5.72	10.88	1.15	4.13	0.71	0.15	0.53	0.08	0.40	0.09	0.22	0.03	0.24	0.04

Table 7. Percent pebble lithology. F/S indicates the percentage of the pebbles that are faceted and/or striated.

			%Igneous		%Metamorphic		%Sedimentary		TOTAL	%F/S
	Site ID	**# of Pebbles**	**Total**	**F/S**	**Total**	**F/S**	**Total**	**F/S**		
	1G	60	75.0	13.3	0.0	0.0	25.0	5.0		
	1F Crest 1	95	54.7	12.6	2.1	0.0	43.2	4.2		
	1F Crest 2	68	60.3	11.8	1.5	0.0	38.2	8.8		
Tail	1E	73	84.9	2.7	4.1	0.0	11.0	1.4		
	1E Red/Grey	88	64.8	6.8	2.3	0.0	33.0	2.3		
	1D	85	49.4	3.5	0.0	0.0	50.6	12.9		
	1C	71	43.7	11.3	7.0	4.2	49.3	9.9		
	Average	**77.1 ± 12.5**	**61.8 ± 14.4**	**8.9 ± 4.4**	**2.4 ± 2.5**	**0.6 ± 1.6**	**35.7 ± 14.2**	**6.4 ± 4.3**		
	1A	45	62.2	28.9	2.2	2.2	35.6	17.8		
Zone 1	1B	70	61.4	30.0	1.4	1.4	37.1	11.4		
	Average	**57.5 ± 17.7**	**61.8 ± 0.6**	**29.4 ± 0.8**	**1.8 ± 0.6**	**1.8 ± 0.6**	**36.3 ± 1.1**	**14.6 ± 4.5**		
	3C	63	25.4	1.6	3.2	3.2	71.4	4.8		
	3D	58	32.8	6.9	0.0	0.0	67.2	10.3		
Zone 3	3B	60	16.7	5.0	0.0	0.0	83.3	15.0		
	3A	27	29.6	11.1	0.0	0.0	70.4	3.7	**1500**	**19.9**
	Average	**52.0 ± 16.8**	**26.1 ± 7.0**	**6.1 ± 4.0**	**0.8 ± 1.6**	**0.8 ± 1.6**	**73.1 ± 7.1**	**8.5 ± 5.2**		
	4L	54	66.7	18.5	11.1	7.4	22.2	11.1		
	4K	90	81.1	10.0	5.6	0.0	13.3	5.6		
	4J	65	60.0	6.2	1.5	0.0	40.0	13.8		
	4G	61	44.3	8.2	0.0	0.0	55.7	6.6		
Zone 4	4H	75	53.3	12.0	1.3	0.0	45.3	0.0		
	4E	65	72.3	6.2	4.6	0.0	23.1	1.5		
	4C	45	42.2	22.2	2.2	2.2	55.6	4.4		
	4B	43	93.0	58.1	0.0	0.0	7.0	4.7		
	4A	36	22.2	5.6	19.4	5.6	58.3	13.9		
	Average	**54.0 ± 16.9**	**59.5 ± 21.7**	**16.3 ± 16.7**	**5.1 ± 6.4**	**1.7 ± 2.9**	**35.6 ± 19.6**	**6.8 ± 5.1**		
	5A	45	35.6	11.1	6.7	0.0	57.8	2.2		
Zone 5	5B	58	77.6	13.8	6.9	0.0	15.5	0.0		
	Average	**51.5 ± 9.2**	**56.6 ± 29.7**	**12.5 ± 1.9**	**6.8 ± 0.2**	**0.0**	**36.6 ± 29.9**	**1.1 ± 1.6**		

Table 8. K-S test results of Mt. Achernar till and cobbles vs. sandstones* described in Elliot and Fanning (2008).

SITE ID	1A													
2A	**0.081**	2A												
Sandstone	0.036	**0.671**	Sandstone											
3B	**0.173**	**0.417**	**0.749**	3B										
4L	**0.993**	0.002	0.004	**0.112**	4L									
4K	**0.245**	**0.291**	**0.526**	**0.995**	**0.234**	4K								
4J	**0.385**	0.018	0.001	0.023	**0.194**	**0.093**	4J							
4B	**0.202**	**0.787**	**0.698**	**0.998**	**0.094**	**0.832**	0.039	4B						
Tillite	0.001	0.007	0.004	0.001	0.000	0.000	0.000	0.007	Tillite					
5B	**0.375**	**0.378**	**0.229**	**0.833**	**0.219**	**0.455**	**0.209**	**0.980**	0.001	5B				
Granite	0.000	0.000	0.000	0.000	0.000	0.000	0.000	0.000	0.000	0.000	Granite			
Granitoid	0.000	0.000	0.000	0.000	0.000	0.000	0.000	0.000	0.000	0.000	**0.999**	Gneiss		
96-36-4*	**0.909**	0.000	0.000	0.001	0.049	0.002	**0.065**	0.001	0.000	0.010	0.000	0.000	96-36-4*	
96-35-2*	0.000	0.000	0.000	0.000	0.000	0.000	0.000	0.000	0.000	0.000	0.000	0.000	0.000	96-35-2*
96-36-1*	0.000	0.000	0.000	0.000	0.000	0.000	0.000	0.000	0.000	0.000	0.000	0.000	0.000	0.000

p-value >0.05

Table 9. Geochemical ratios from the Mt. Achernar till samples.

Sample Site		Ratios								
		Zr/Sc	Th/Sc	Th/U	Cr/V	Y/Ni	La/Th	Rb/Sr	Sm/Nd	Eu/Eu*
Tail	East Crest	22.83	0.79	4.21	0.58	1.03	2.96	0.38	0.19	0.63
	1H	11.95	0.59	4.15	0.54	0.87	2.80	0.56	0.20	0.69
	1E	12.56	0.66	4.37	0.58	0.80	2.72	0.53	0.20	0.66
	1E Red/Grey	14.56	0.70	4.50	0.56	0.80	2.39	0.55	0.20	0.61
Zone 1	1A	20.88	0.75	4.10	0.57	1.30	2.65	0.39	0.21	0.62
	1B	23.29	0.76	4.33	0.65	0.93	2.62	0.40	0.20	0.61
Zone 2	2A	24.25	0.89	4.09	0.70	1.10	3.42	0.35	0.19	0.65
Zone 3	3C	18.59	0.86	4.56	0.70	0.97	3.09	0.39	0.18	0.73
	3 Dark	19.38	0.93	4.81	0.73	1.35	2.98	0.32	0.20	0.70
	3B	16.76	0.87	4.48	0.72	0.97	3.09	0.40	0.19	0.67
	3E	19.17	0.79	4.47	0.62	0.97	3.03	0.37	0.18	0.71
Zone 4	4L	14.72	0.64	3.87	0.55	1.35	2.86	0.43	0.19	0.71
	4K	17.11	0.68	4.07	0.55	0.87	2.79	0.37	0.21	0.64
	4J	14.41	0.64	3.76	0.48	1.32	2.83	0.40	0.19	0.71
	4I	15.94	0.76	4.12	0.67	0.93	3.12	0.33	0.19	0.67
	4G	20.44	0.82	4.35	0.71	0.93	2.93	0.39	0.18	0.63
	4E	18.06	0.75	3.86	0.60	0.93	2.91	0.29	0.18	0.67
	4D	22.38	0.86	4.60	0.59	0.77	2.55	0.29	0.21	0.58
	4C	16.69	0.94	4.05	0.67	0.87	2.92	0.40	0.20	0.61
	4B	23.29	0.82	4.63	0.55	0.60	2.56	0.36	0.19	0.62
Zone 5	5A	15.72	0.63	4.35	0.62	0.80	2.91	0.27	0.19	0.68
	5B	11.95	0.56	4.28	0.63	0.60	3.03	0.19	0.19	0.67
	5C	9.95	0.62	4.07	0.61	0.80	2.87	0.18	0.19	0.69
	5D	13.78	0.65	4.18	0.66	0.58	2.89	0.23	0.18	0.64
	5E	16.88	0.79	4.23	0.68	0.60	2.64	0.25	0.19	0.63
	Average	17.42	0.75	4.26	0.62	0.92	2.86	0.36	0.19	0.66
	Std. Dev.	3.99	0.11	0.26	0.07	0.23	0.22	0.10	0.01	0.04

Table 10. Discriminant analysis scores of major, trace, and rare earth elements of the Mt. Achernar moraine till.

Major	Axis 1	Axis 2	Axis 3	Axis 4	Axis 5
East Crest	-3.1227	-3.0785	0.66132	1.0189	2.0402
1H	-3.4515	-3.4406	3.9588	0.7766	-0.36403
1E	-3.395	-3.7728	3.5106	1.3859	-0.45871
1E Red/Grey	-2.8661	-2.9051	3.3899	0.90267	-0.46907
1A	-4.388	-1.7907	-3.533	2.2676	-0.16675
1B	-7.3052	-1.5686	-5.5139	1.1228	-1.0686
2A	-9.3518	-0.0054112	-3.6075	-0.95647	1.8586
3C	-3.3748	5.605	0.89712	-0.094093	0.087095
3 Dark	-4.5376	6.165	1.3393	-0.62668	0.604
3B	-2.6877	6.7146	1.1248	1.0502	-1.0115
3E	-3.3701	3.3892	0.97444	1.6038	0.06169
4L	-0.8157	-1.0364	0.66287	-1.1286	-1.2982
4K	-0.63183	-2.4844	-0.17057	-1.9366	0.50663
4J	-0.3382	-1.0188	-2.0104	0.043833	-1.9588
4I	-1.3779	-1.3551	1.5724	-2.0996	0.92789
4G	-1.2333	1.0188	0.48984	0.70841	0.76867
4E	1.215	-0.61513	0.894	-0.57943	0.86663
4D	0.75388	-0.38004	-0.79582	-1.4543	-0.21758
4C	0.64128	-0.39459	-0.77325	-3.4518	-0.19421
4B	-1.4655	-0.22189	0.30058	-1.1692	-1.5774
5A	10.818	1.4462	0.027767	0.025295	-0.3889
5B	9.9483	-1.4751	-0.49815	1.2925	0.028465
5C	11.431	0.21781	-1.0092	0.93613	0.78055
5D	10.362	0.039643	-0.77841	-0.7387	-0.64118
5E	8.543	0.94689	-1.1136	1.1006	1.2846

Trace	Axis 1	Axis 2	Axis 3	Axis 4	Axis 5
East Crest	3.1543	6.3781	5.7252	1.9438	-0.53997
1H	2.9899	7.4351	4.84	2.8285	1.0237
1E	4.4188	5.4698	6.4456	0.67551	1.5432
1E Red/Grey	3.3556	8.5861	5.6613	0.52437	-0.49742
1A	-5.7319	-6.5915	8.8281	-4.3021	0.6461
1B	-5.5352	-5.7974	8.0998	-2.3195	0.53959
2A	-14.217	-13.386	4.7125	3.7321	-2.907
3C	25.36	-6.1115	-3.9763	-0.25673	0.96906
3 Dark	25.009	-5.6252	-1.7535	1.8271	2.0418
3B	20.904	-5.7627	-1.852	1.5331	1.3592
3E	25.077	-2.4826	-2.1168	0.37926	0.75206
4L	7.2014	2.0972	-0.090328	-1.5953	-1.441
4K	7.3492	1.7155	-3.6755	-0.24475	-0.42802
4J	6.8715	2.2655	-2.6451	-0.20936	-1.7637
4I	6.9979	3.2981	-2.0466	-1.2697	2.2368
4G	7.1392	2.0739	-2.1624	-1.0761	-1.5973
4E	7.5727	0.58416	-3.093	-1.0599	-0.98637
4D	5.5937	1.9877	-3.2004	-2.8577	-1.1768
4C	7.73	2.3254	-2.4008	1.0144	-2.1067
4B	7.2434	1.4758	-0.015362	-0.42112	-1.1606
5A	-29.905	-0.21309	-2.7641	-0.66289	-0.1272
5B	-30.432	0.6037	-3.7146	0.46746	1.0845
5C	-29.751	0.036752	-3.1617	0.20195	1.0055
5D	-29.323	-0.16439	-2.6174	0.88243	1.2804
5E	-29.074	-0.19896	-3.0266	0.26527	0.2498

REE	Axis 1	Axis 2	Axis 3	Axis 4	Axis 5
East Crest	1.1595	2.6267	1.5607	1.7245	-0.40149
1H	-1.0632	3.9419	0.00058055	0.74024	0.80784
1E	0.86881	2.2526	1.0577	1.214	0.5055
1E Red/Grey	0.06626	4.7963	2.2204	1.6749	0.94526
1A	6.2159	3.8517	0.33984	-1.6671	1.2268
1B	7.3401	5.3995	2.1208	-1.791	0.28092
2A	3.0402	-5.748	6.1733	-0.12024	-1.6208
3C	2.5943	-6.3925	-1.4598	0.13407	0.70374
3 Dark	0.96568	-6.5636	-1.0848	0.63813	0.52484
3B	-0.24531	-4.3236	0.78643	-0.81331	0.20734
3E	0.62302	-5.4906	0.075697	0.2366	2.3131
4L	3.1618	0.84329	-1.1107	0.91601	-1.0625
4K	3.1688	1.3437	-0.24205	0.5024	-1.5973
4J	1.1923	-0.03594	-1.5301	-1.3151	0.40641
4I	2.9087	-0.37609	-0.67111	-0.23319	2.3227
4G	2.2342	-0.20104	-1.941	-0.1886	-1.4517
4E	0.21919	-0.77774	-1.2275	0.36505	-0.99015
4D	2.2334	-0.046459	-2.4197	-1.5905	-1.7321
4C	1.7804	-0.31924	-0.68468	0.38706	-0.94096
4B	2.0026	1.4726	-2.972	1.7731	-0.24379
5A	-9.2955	-0.81314	1.7528	1.1216	-0.40635
5B	-7.3003	-0.028153	-0.097214	-0.93704	-0.31953
5C	-7.9697	1.8729	-1.0954	0.82779	0.79171
5D	-8.8456	1.7171	-0.50669	-1.3317	-0.73276
5E	-7.0555	0.9979	0.95454	-2.2676	0.46336

Table 11. Discriminant analysis loadings of major, trace, and rare earth elements of the Mt. Achernar moraine till.

Major	Axis 1	Axis 2	Axis 3	Axis 4	Axis 5
SiO2	-0.76583	0.21084	-0.083773	0.084633	-0.1257
Al2O3	-0.031891	0.14426	0.24391	-0.13329	0.098877
Fe2O3(T)	0.026263	-0.032569	0.11568	-0.0084177	0.094218
MnO	-0.00037411	-0.0014074	0.0010074	0.002114	-0.00071559
MgO	0.084458	-0.027026	-0.025399	0.012706	0.13054
CaO	0.24891	-0.039698	-0.17514	0.087403	0.31343
Na2O	0.058982	0.050095	-0.085786	-0.11012	0.082565
K2O	-0.0067873	0.064562	0.027116	-0.026543	0.063764
TiO2	-0.010012	0.0093863	0.0025707	0.0030321	0.024382
P2O5	-0.0017032	0.0022888	-0.0022921	-0.0057378	0.010937
LOI	0.38768	-0.29022	-0.080298	0.25639	-0.61858

REE	Axis 1	Axis 2	Axis 3	Axis 4	Axis 5
Sc	-0.076019	0.10646	-0.051167	0.30453	0.1755
Y	0.28799	-0.36286	0.59055	0.22594	-0.012529
La	0.3797	-1.2793	0.41849	0.33195	-0.27175
Ce	0.76559	-2.3742	0.99831	0.60659	-0.093557
Pr	0.093876	-0.24704	0.1076	0.07063	-0.00322
Nd	0.37325	-0.84241	0.39645	0.28796	0.070165
Sm	0.088928	-0.13295	0.08385	0.020324	-0.023595
Eu	0.013143	-0.034742	0.013444	0.015683	0.024408
Gd	0.062889	-0.084488	0.094644	0.012165	0.012114
Tb	0.012785	-0.0094835	0.016162	0.00028771	0.01303
Dy	0.049811	-0.059692	0.072476	0.050919	0.0097709
Ho	0.012668	-0.0098382	0.011207	0.0076783	0.0094564
Er	0.033755	-0.028467	0.030234	0.013308	0.016842
Tm	0.0050327	-0.0043338	0.0050156	0.0042241	0.0011509
Yb	0.034732	-0.02292	0.033654	0.040025	-0.0047648
Lu	0.0053783	-0.0041485	0.0066862	0.0051015	0.0017639

Trace	Axis 1	Axis 2	Axis 3	Axis 4	Axis 5
V	0.062327	0.2314	-0.227	-0.10229	1.4064
Ba	3.0723	-7.7788	-5.6429	17.377	5.3214
Sr	-2.9832	-2.8307	-11.829	4.4496	15.479
Zr	1.0988	-4.5738	4.3061	-7.325	-16.226
Cr	0.052796	-0.64145	-0.60158	0.89173	2.2012
Co	-0.033714	0.077491	-0.093419	0.086052	0.49305
Ni	-0.15373	0.15448	-0.31645	0.74658	0.47121
Cu	-0.84685	0.49854	-1.5882	0.53054	3.8251
Zn	-0.32755	-0.087065	-1.8768	2.4563	2.2181
Ga	0.037867	-0.00078439	-0.12786	0.34262	0.16056
Ge	-0.023064	0.012797	-0.10401	0.032114	-0.041256
Rb	0.16529	0.020592	-0.35898	2.3299	0.77226
Nb	0.028043	-0.1116	0.045085	-0.018311	-0.20115
Ag	0.0086875	-0.054502	0.054607	-0.032984	-0.12978
Sn	0.0022698	0.053314	0.08355	0.33318	0.32477
Cs	-0.017356	0.051923	-0.059775	0.083011	0.13728
Hf	0.027004	-0.076676	0.016197	-0.17491	-0.35602
Ta	0.0017975	-0.0011787	0.0082163	-0.00026721	0.017909
W	0.0013953	0.060284	-0.11909	-0.27178	-0.55122
Tl	0.016921	-0.012795	-0.0015856	0.0013579	-0.020952
Pb	0.031806	-0.25548	-0.26875	0.69989	0.004547
Th	0.042562	-0.11545	0.043569	0.081244	-0.18373
U	0.023484	-0.027811	-0.019754	0.059762	-0.046363

Table 12. Discriminant analysis classifier of major, trace, and rare earth elements of the Mt. Achernar moraine till.

Major

Point	Given group	Classification	Jackknifed
East Crest	0	0	1
1H	0	0	0
1E	0	0	0
1E Red/Grey	0	0	0
1A	1	1	4
1B	1	1	2
2A	2	2	1
3C	3	3	3
3 Dark	3	3	3
3B	3	3	3
3E	3	3	3
4L	4	4	4
4K	4	4	4
4J	4	4	1
4I	4	4	0
4G	4	4	4
4E	4	4	4
4D	4	4	4
4C	4	4	4
4B	4	4	4
5A	5	5	5
5B	5	5	5
5C	5	5	5
5D	5	5	4
5E	5	5	4

Trace

Point	Given group	Classification	Jackknifed
East Crest	0	2	0
1H	0	2	1
1E	0	2	5
1E Red/Grey	0	2	2
1A	1	2	3
1B	1	2	1
2A	2	5	5
3C	3	5	5
3 Dark	3	5	3
3B	3	5	3
3E	3	5	1
4L	4	2	1
4K	4	2	1
4J	4	2	0
4I	4	2	0
4G	4	2	0
4E	4	2	2
4D	4	2	2
4C	4	2	2
4B	4	2	2
5A	5	2	2
5B	5	2	5
5C	5	2	5
5D	5	2	5
5E	5	2	2

REE

Point	Given group	Classification	Jackknifed
East Crest	0	0	2
1H	0	0	0
1E	0	0	4
1E Red/Grey	0	0	0
1A	1	1	4
1B	1	1	1
2A	2	2	3
3C	3	3	3
3 Dark	3	3	3
3B	3	3	4
3E	3	3	0
4L	4	4	1
4K	4	4	1
4J	4	4	4
4I	4	4	3
4G	4	4	3
4E	4	4	3
4D	4	4	4
4C	4	4	3
4B	4	4	0
5A	5	5	2
5B	5	5	4
5C	5	5	0
5D	5	5	5
5E	5	5	0

Table 13. Discriminant analysis confusion matrix of major, trace, and rare earth elements of the Mt. Achernar moraine till.

Major	0	1	2	3	4	5	Total
0	4	0	0	0	0	0	4
1	0	2	0	0	0	0	2
2	0	0	1	0	0	0	1
3	0	0	0	4	0	0	4
4	0	0	0	0	9	0	9
5	0	0	0	0	0	5	5
Total	4	2	1	4	9	5	25

Trace	0	1	2	3	4	5	Total
0	0	0	4	0	0	0	4
1	0	0	2	0	0	0	2
2	0	0	0	0	0	1	1
3	0	0	0	0	0	4	4
4	0	0	9	0	0	0	9
5	0	0	5	0	0	0	5
Total	0	0	20	0	0	5	25

REE	0	1	2	3	4	5	Total
0	4	0	0	0	0	0	4
1	0	2	0	0	0	0	2
2	0	0	1	0	0	0	1
3	0	0	0	4	0	0	4
4	0	0	0	0	9	0	9
5	0	0	0	0	0	5	5
Total	4	2	1	4	9	5	25

Table 14. Chemical index of alteration (CIA), chemical index of weathering (CIW), and index of compositional variability (ICV) values for the Mt. Achernar moraine tills.

	CIA	CIW	ICV
East Crest	56.8	62.2	1.5
1H	74.7	83.5	0.9
1E	74.3	83.2	0.9
1E Red/Grey	73.9	82.5	0.9
1A	62.7	69.3	1.1
1B	67.3	74.9	1.1
2A	66.4	74.6	1.0
3C	68.0	77.0	1.0
3Dark	68.5	77.4	0.9
3B	68.4	77.7	1.0
3E	67.0	75.0	1.0
4L	65.5	72.6	1.1
4K	64.4	71.2	1.1
4J	66.7	74.0	1.0
4I	65.2	72.6	1.1
4G	64.3	71.6	1.1
4E	62.8	69.6	1.2
4D	63.1	69.2	1.1
4C	66.4	74.5	1.1
4B	61.8	68.3	1.2
5A	49.6	53.6	1.7
5B	51.3	55.8	1.7
5C	59.6	65.9	1.3
5D	54.9	59.8	1.5
5E	60.6	67.2	1.2

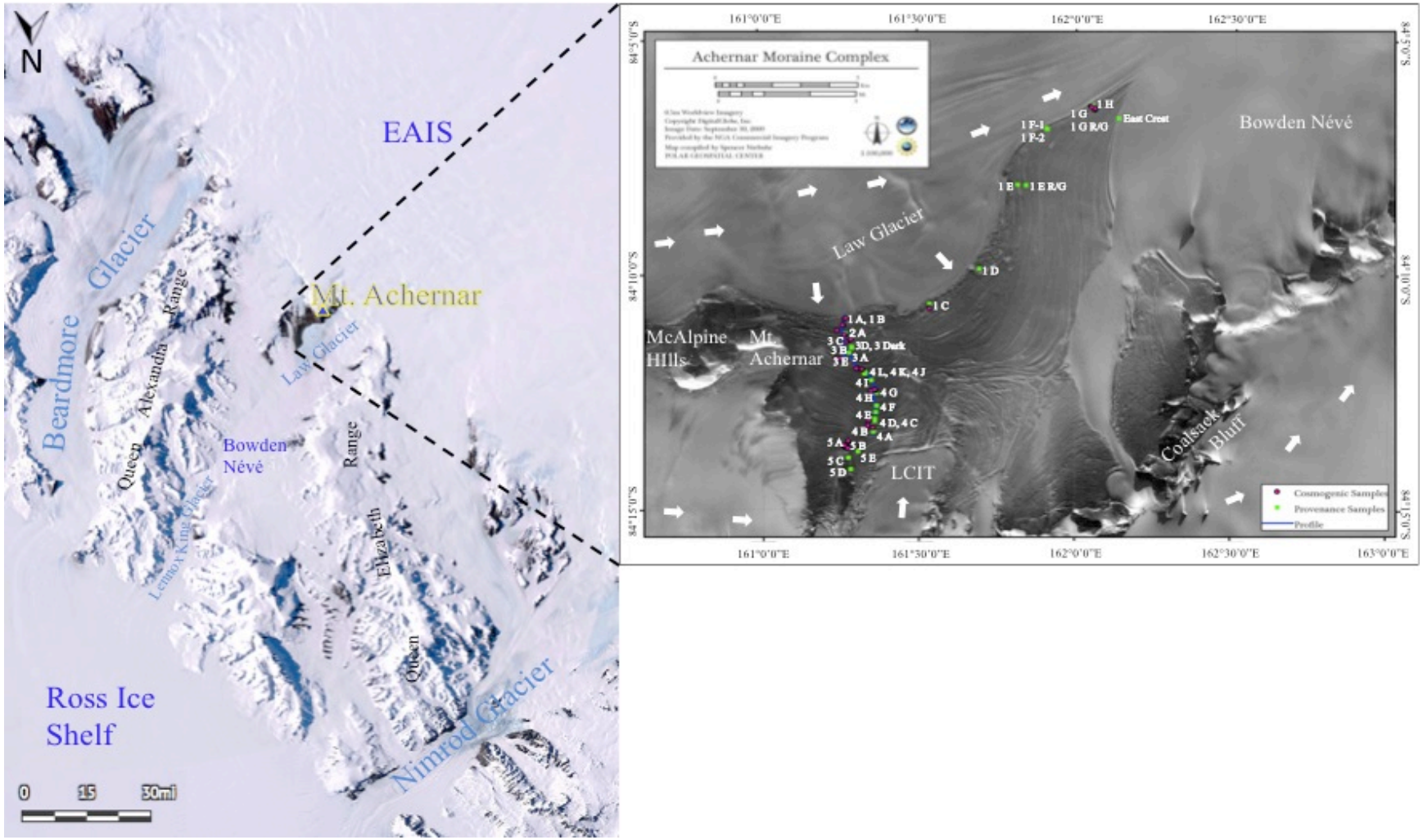

Figure 1: Transect and topographic profile across the Mt. Achernar moraine showing the location of each sample site. LCIT = Lewis Cliff Ice Tongue. Arrows indicate ice flow directions.

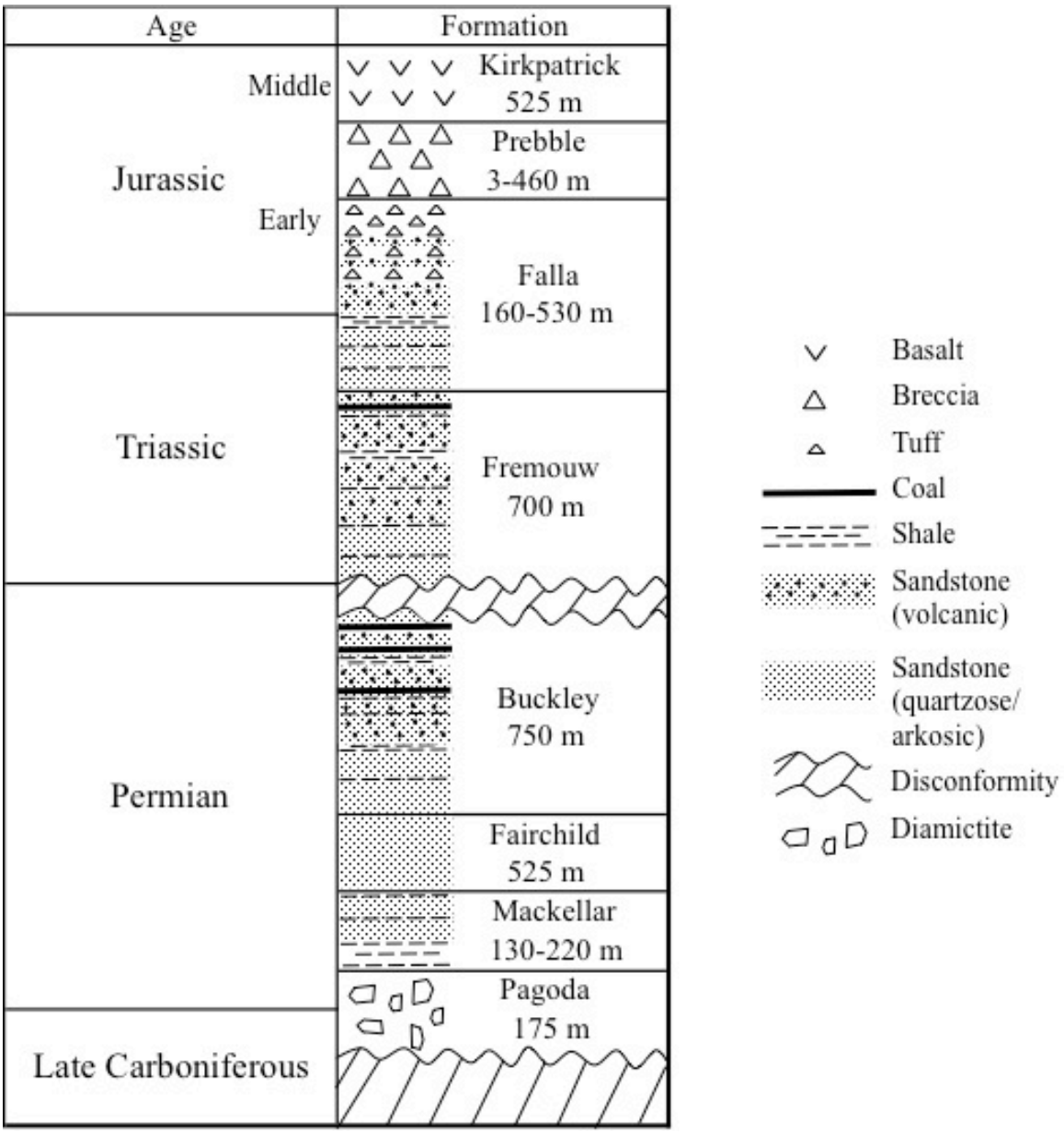

Figure 2: Simplified stratigraphic column of Beacon Supergroup from the central Transantarctic Mountains. Modified from Thomson et al., 1991.

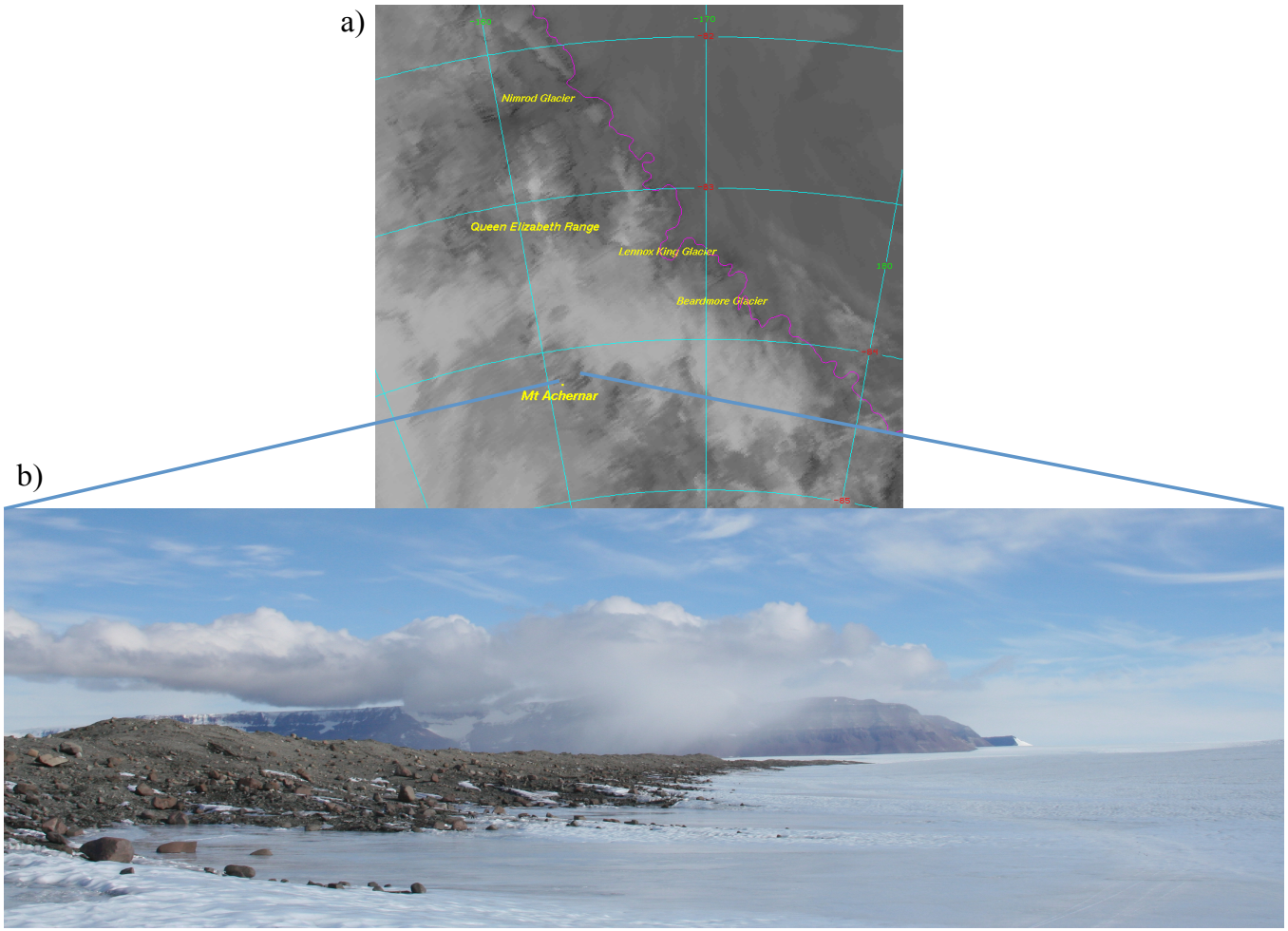

Figure 3: Transantarctic Mountains microclimate. a) Infrared aerial image over the Transantarctic Mountains. In general, the whiter the color, the colder the temperature (and usually the higher up in the atmosphere) clouds are. A light patch of white (i.e. clouds) is seen just north of the Mt. Achernar moraine. b) Microclimate of clouds and snow occurring over the Mt. Achernar moraine while surrounding area was relatively clear.

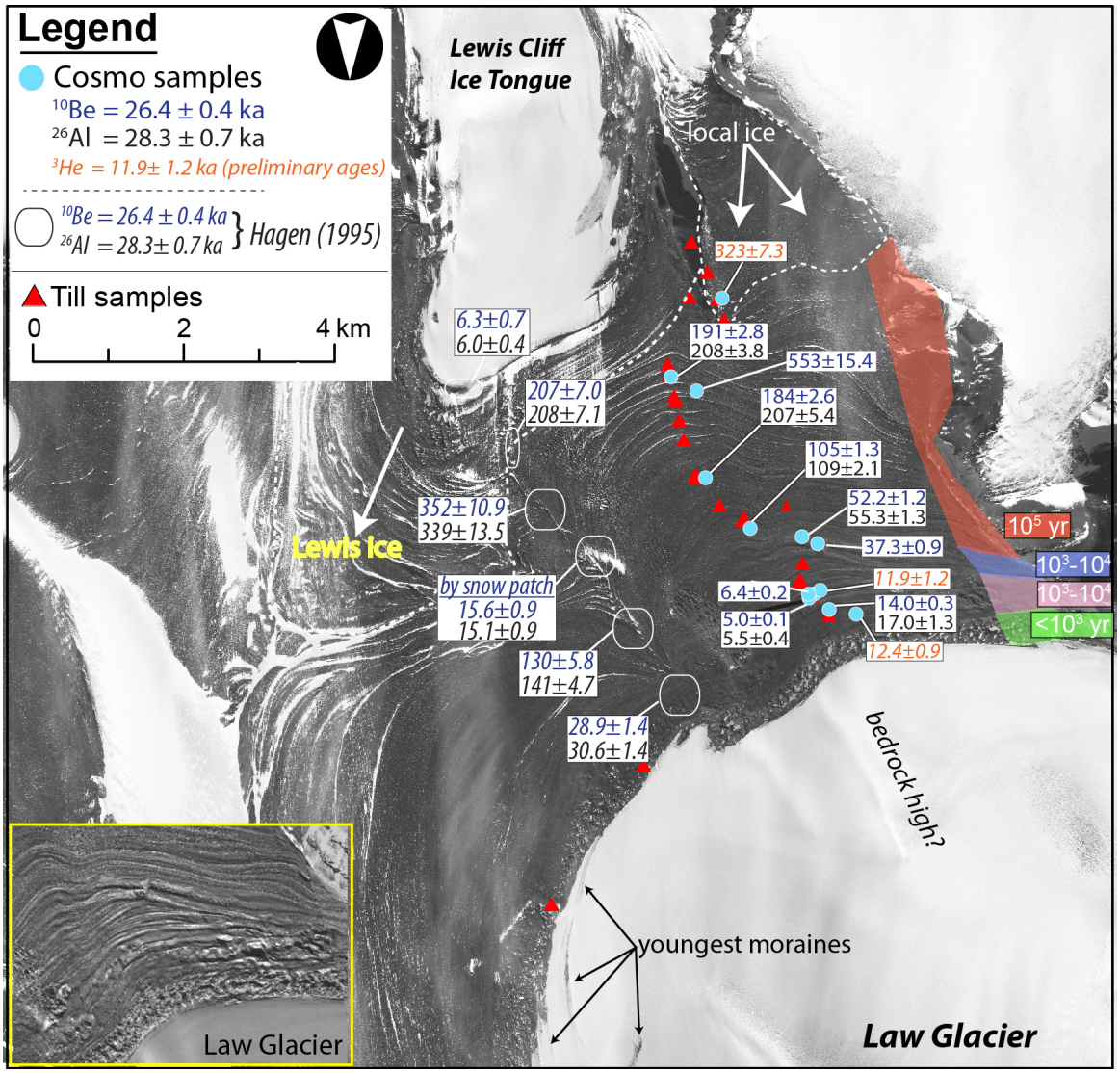

Figure 4: Surface exposure ages of Mt. Achernar moraine reported from Mathieson et al., 2012 and Kaplan, personal communication.

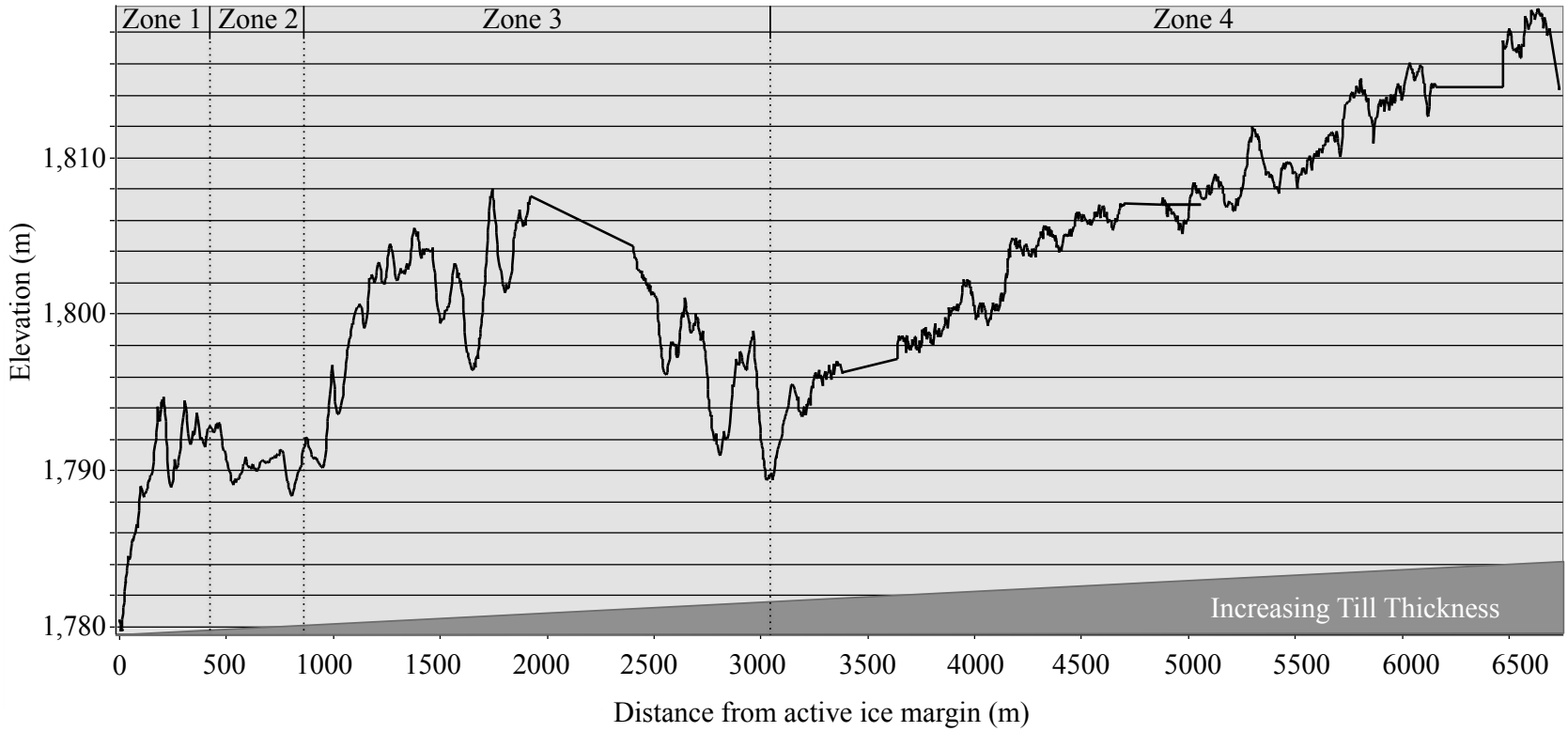

Figure 5: Topographic profile of Mt. Achernar moraine from 2010-2011 field season (See Figure 1 for location). Straight-line segments are regions of missing or insufficient data. Left side is adjacent to Law Glacier. Till thickness is schematic.

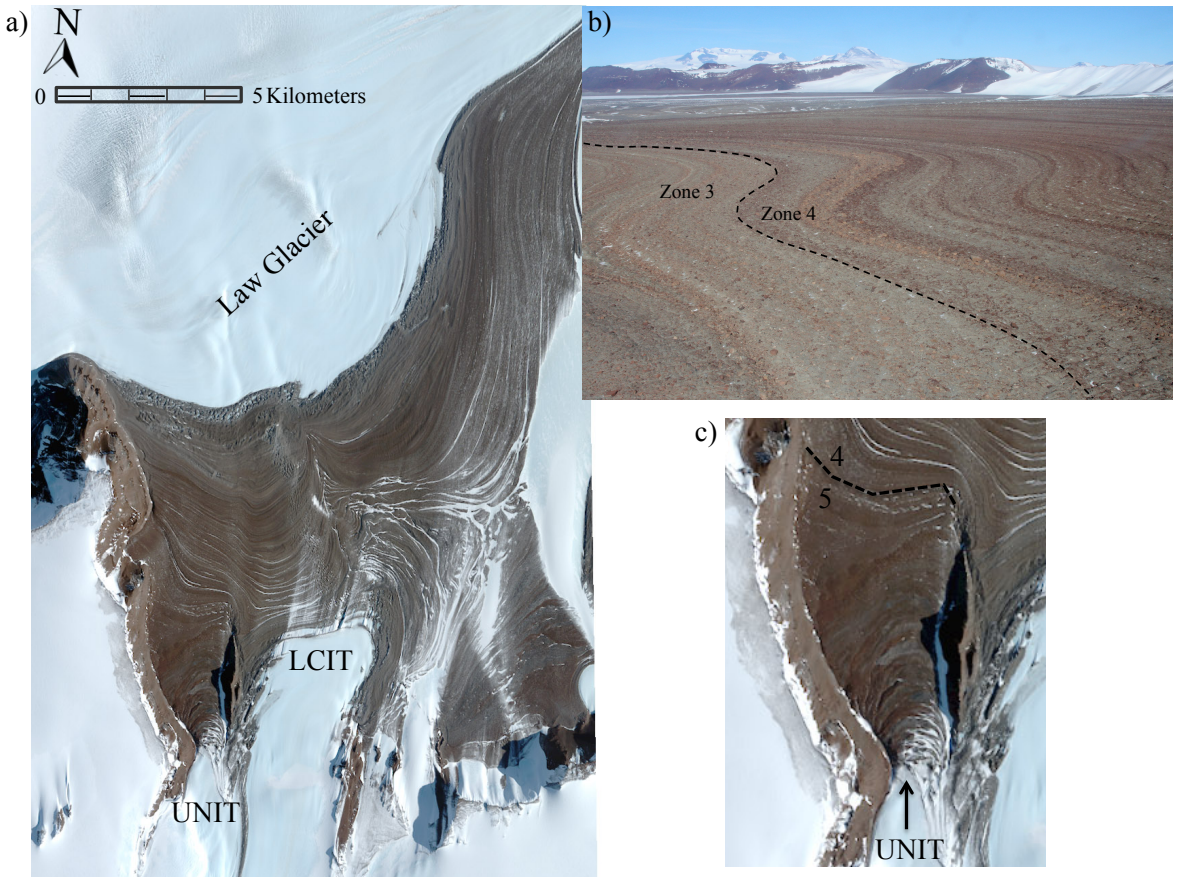

Figure 6: Aerial view of lithologic colored bands and ridges of the Mt. Achernar moraine. a) Distinctly colored lithologic bands across the Mt. Achernar moraine. b) Colored lithologic bands on the Zone 3 and Zone 4 boundary, possibly reflecting a gradational transition between dominantly lithologies of each zone. c) The Zone 4 and Zone 5 boundary that displays the ridges in Zone 5 that are orientated in the opposite direction of those of Zone 4. LCIT = Lewis Cliff Ice Tongue. UNIT = unnamed ice tongue.

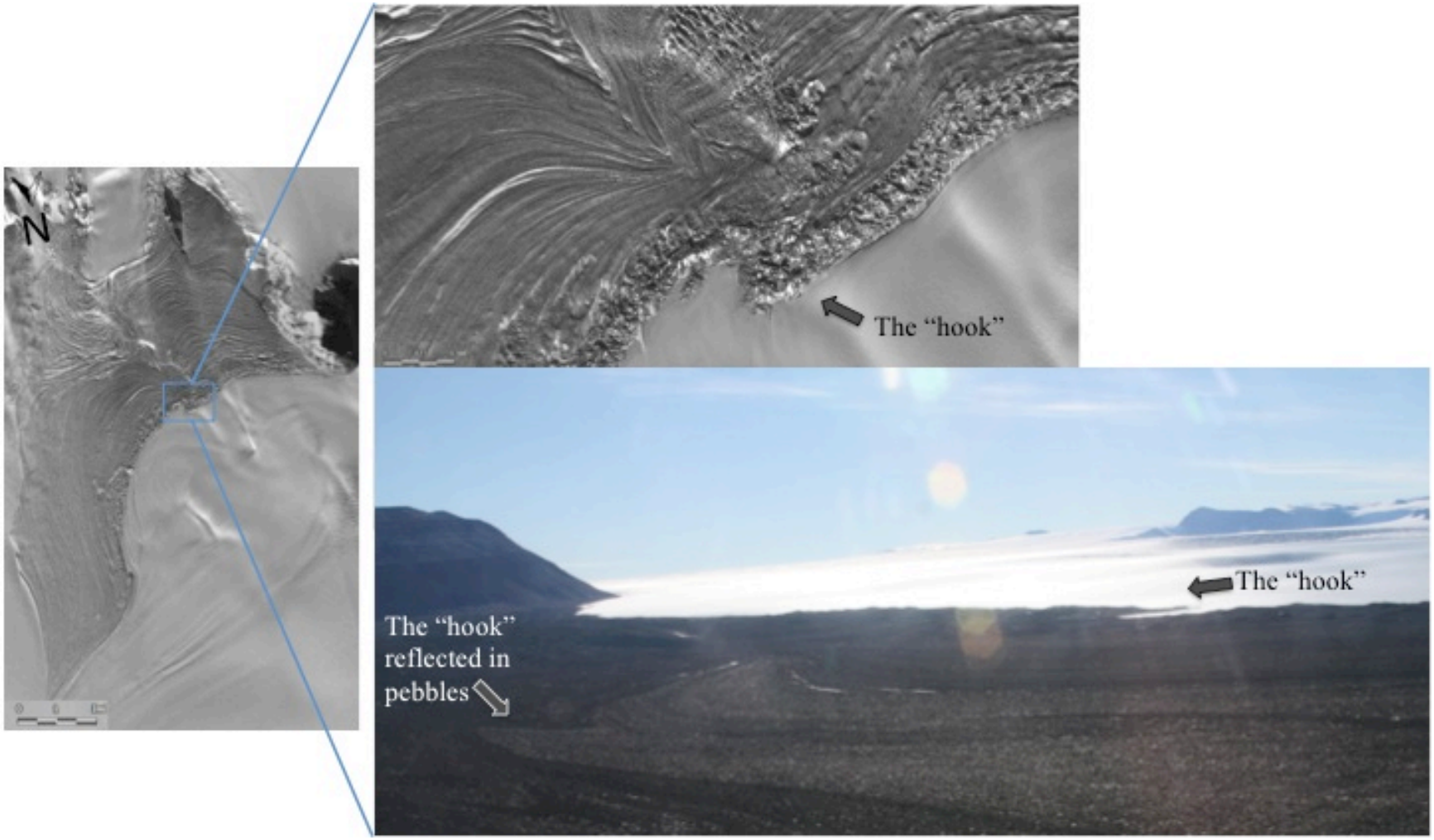

Figure 7: The "hook"/potential fold feature affecting the formation of the Mt. Achernar moraine.

a)

b)

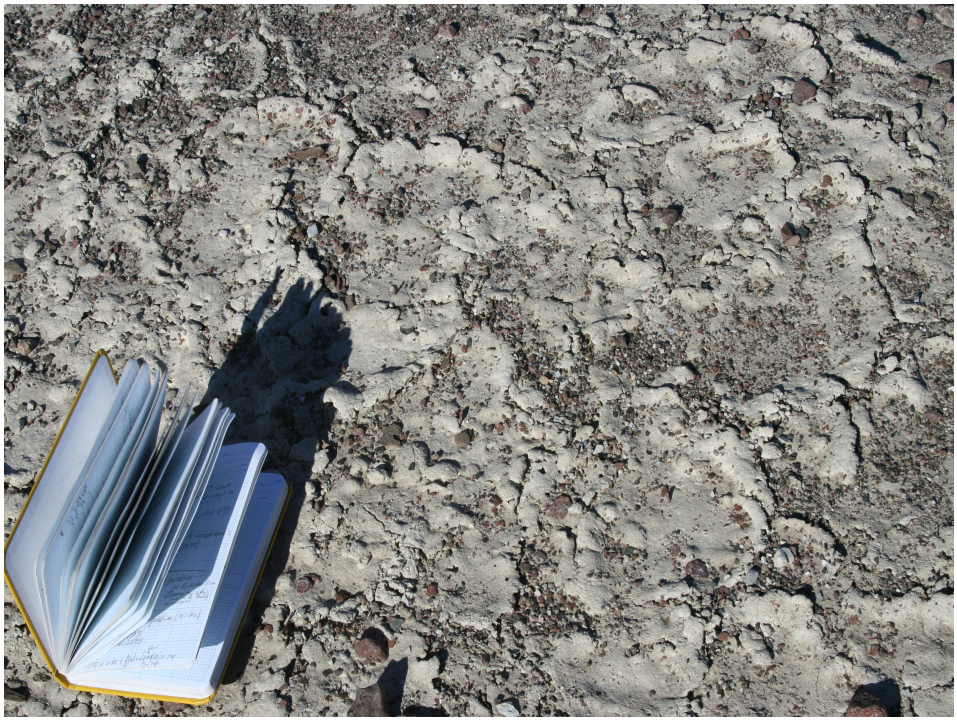

Figure 8: Crusts of sediment on the Mt. Achernar moraine. a) “Knobby” and b) platy crusts of sediment on the top 0.5–1 cm noted throughout Zones 4 and 5.

a)

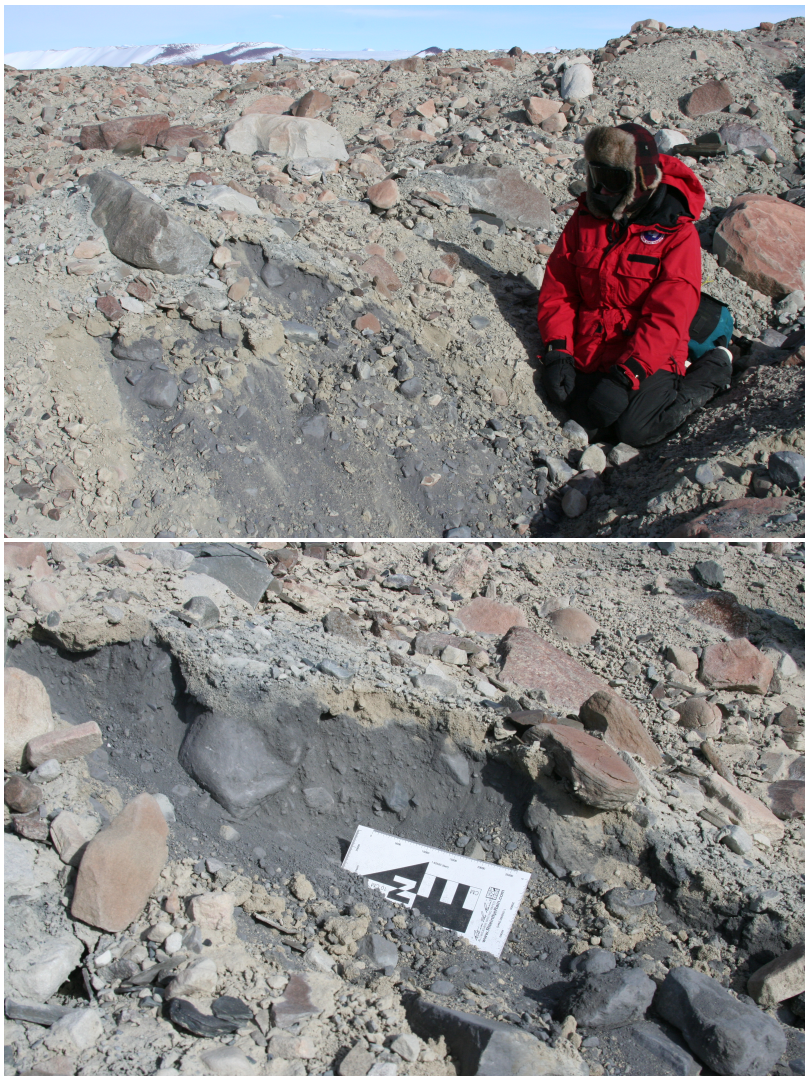

b)

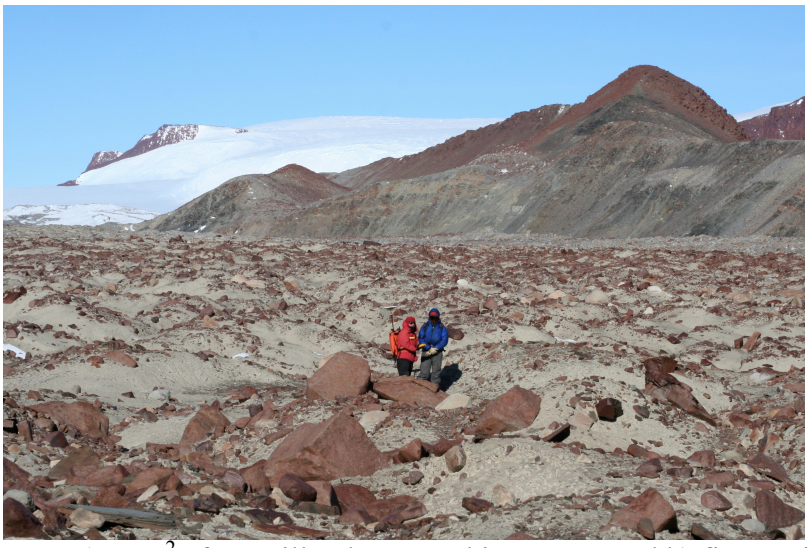

Figure 9: a) ~1m^2 of two till colors noted in Zone 3 and b) fine-grained paths noted in Zone 4 of the Mt. Achernar moraine.

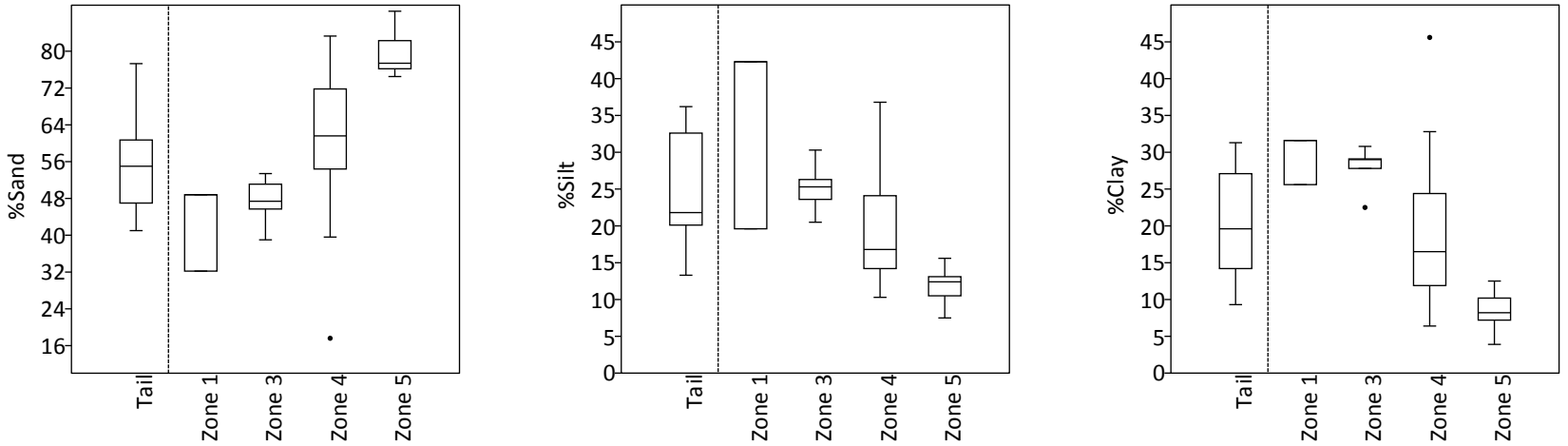

Figure 10: Box plots of <2 mm particle size data by zone (Table 5). The box outlines the middle 50% of data (2nd and 3rd quartiles), the line inside the box represents the median value of the whole data set, and the whiskers show the greatest/least values excluding the outliers, which are defined as data that is greater than 1.5 times the box height. Zone 2 is not included in box plots because only one sample was collected. Dotted line separates the tail from main transect. Tail n=10, Zone 1 n=2, Zone 3 n=6, Zone 4 n=12, Zone 5 n=5.

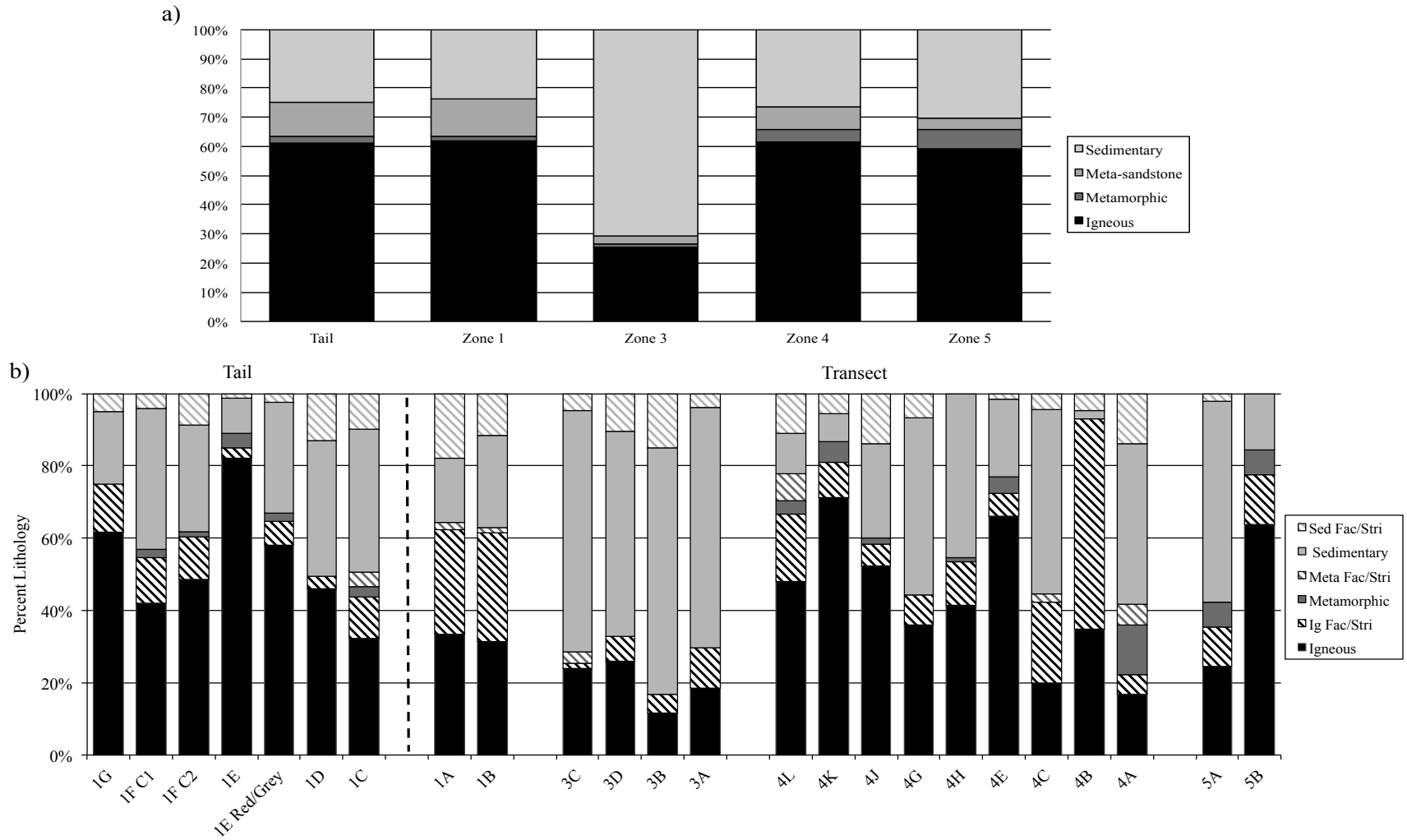

Figure 11: Percent lithology per zone and site. a) Percent lithology per zone; b) Percentage of pebble lithologies present on the Mt. Achernar moraine, including proportion faceted and/or striated. Each sample reflects lithologies collected from $1m^2$. See Table 2 for the classification scheme used to categorize pebbles.

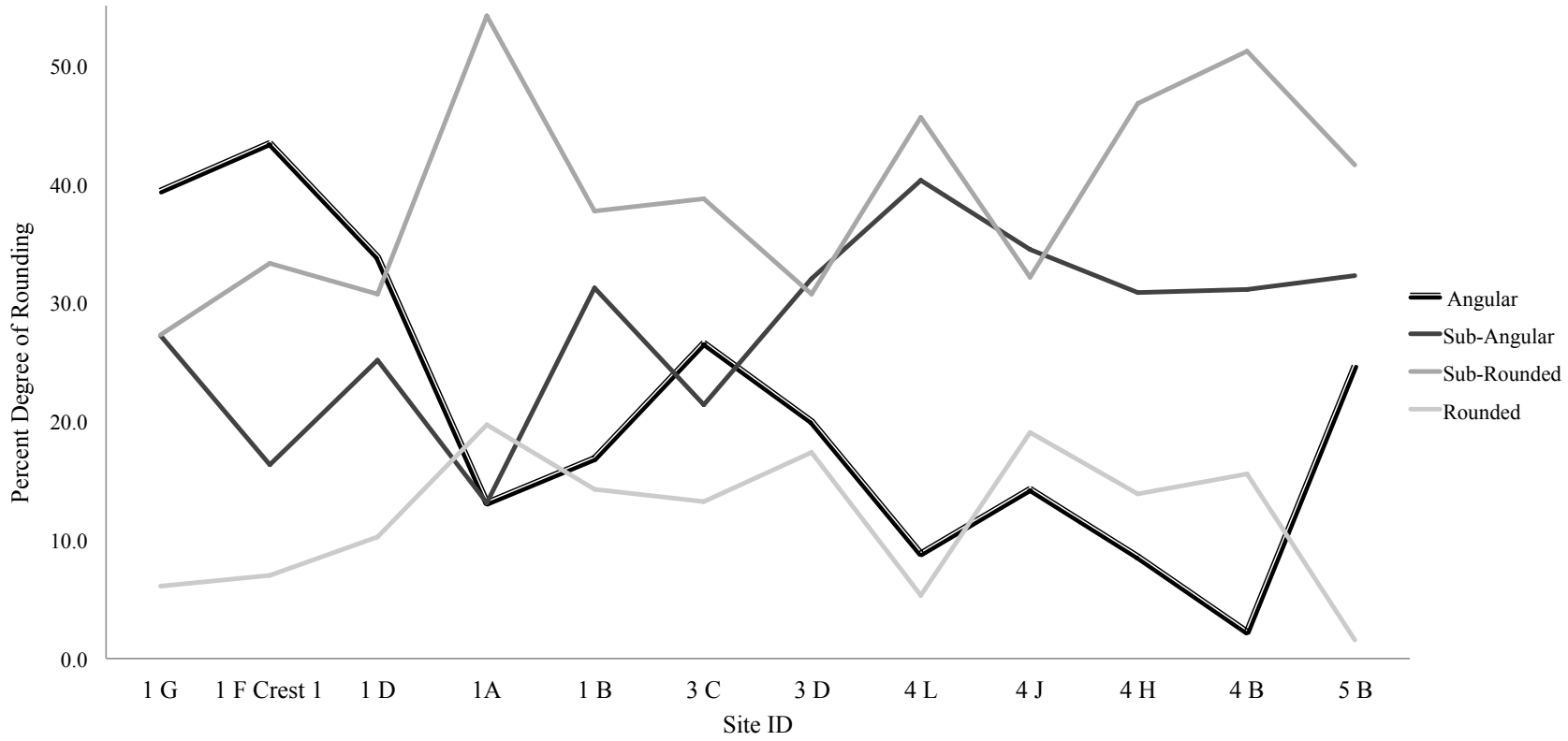

Figure 12: Degree of rounding of pebbles by site.

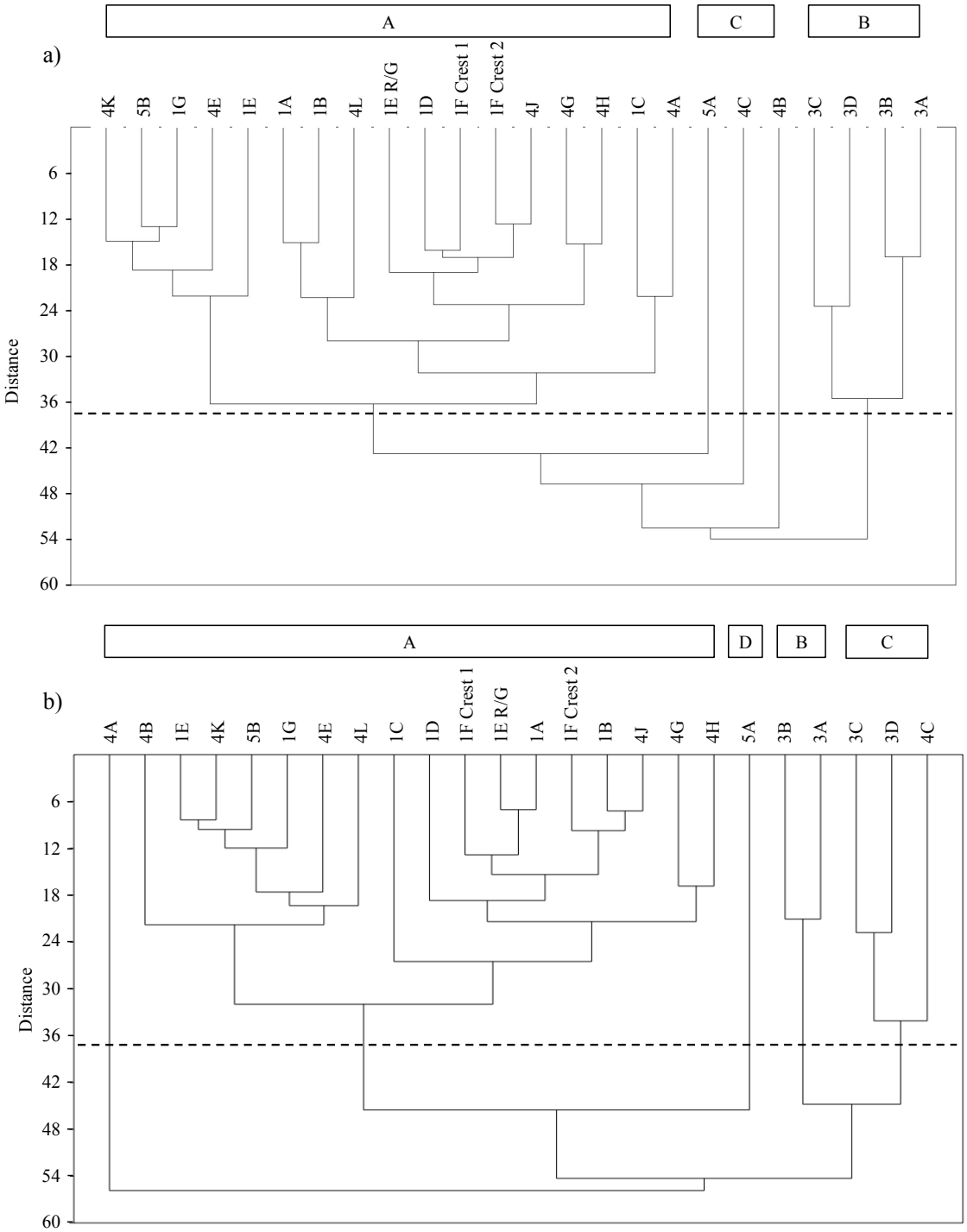

Figure 13: Cluster analysis results based on pebble lithologies listed in Table 2: a) the coarse and fine-grained fraction of the intermediate/mafic igneous rocks and the faceted and/or striated pebble fraction are included as separate categories and can influence the results and b) is based solely on pebble lithologies shown in Table 2; the coarse and fine-grained fraction of the intermediate/mafic igneous rocks and the faceted and/or striated pebble fraction are not separate categories influencing the results.

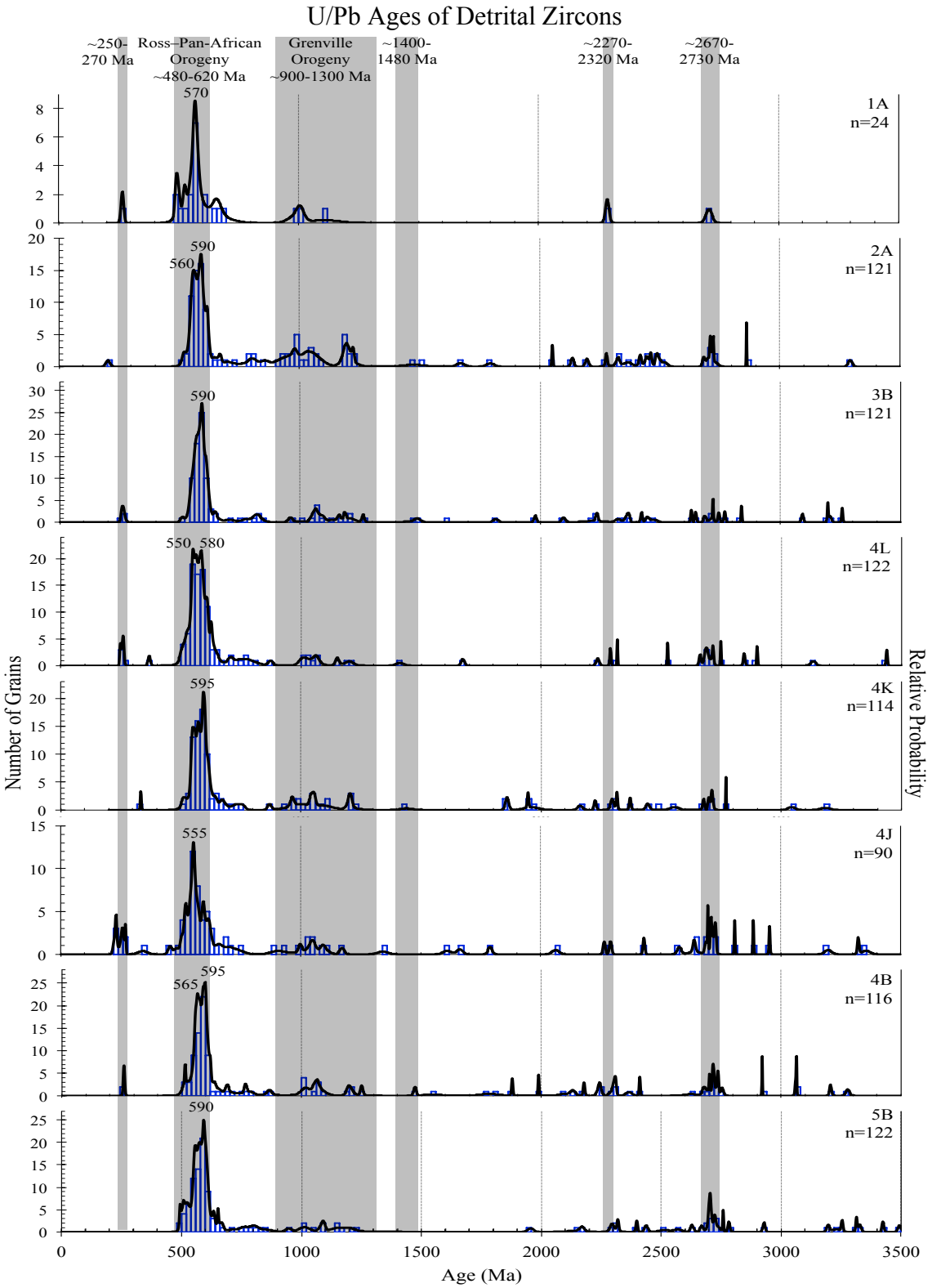

Figure 14: Normalized probability plots and histograms of Mt. Achernar moraine tills. Known geologic event time frames and ages of interest highlighted in grey. Ross/Pan-African and Grenville ranges are taken from Licht et al. (in press) and Goodge et al. (2010) respectively.

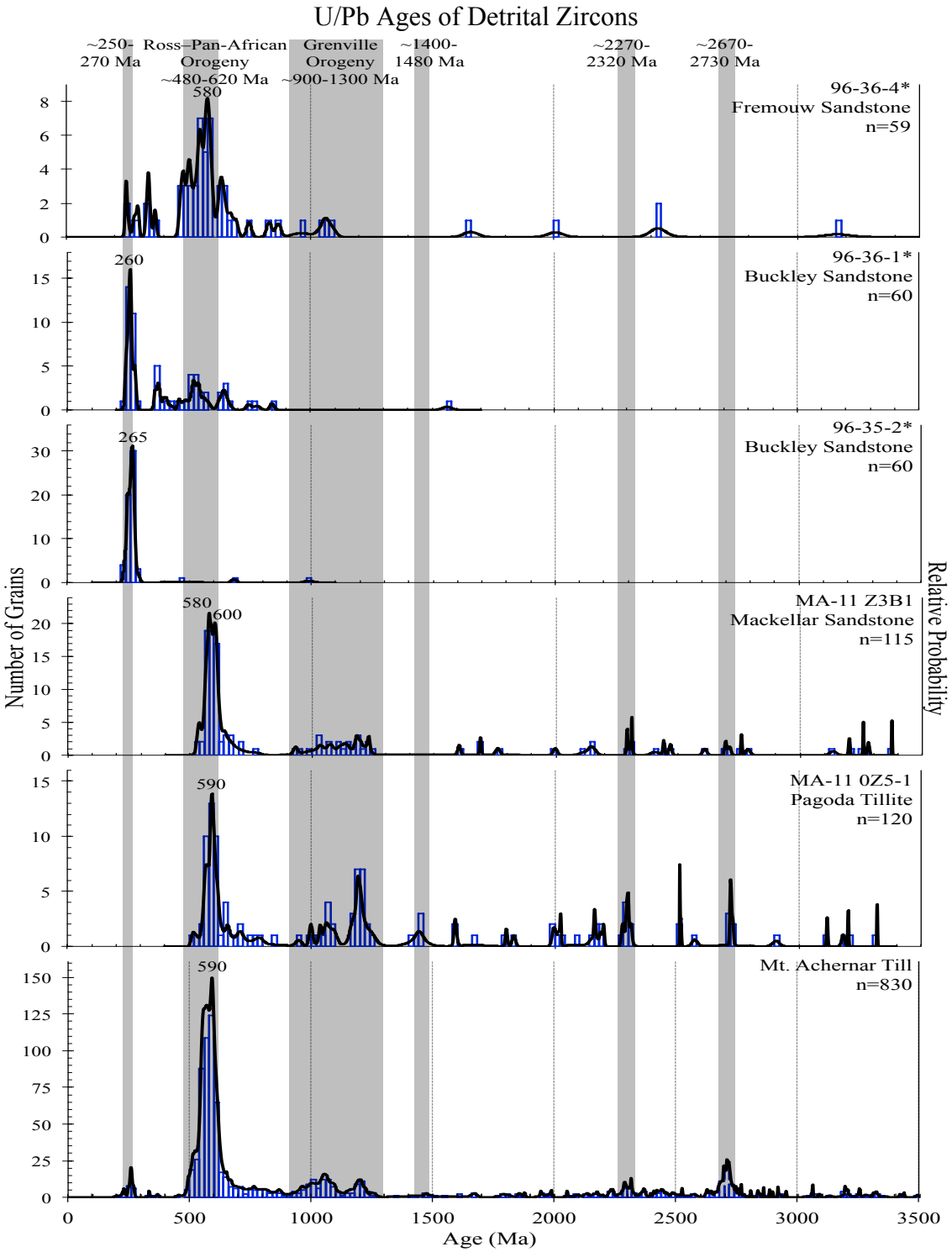

Figure 15: Normalized probability plots and histograms of Mt. Achernar moraine tills and cobbles, as well as sandstone* cobbles described in in Elliot and Fanning (2008). Known geologic event time frames and ages of interest highlighted in grey. Ross/Pan-African and Grenville ranges taken from Licht et al. (in press) and Goodge et al. (2010) respectively. Mackellar inferred based on visual similarity to rocks from known outcrops.

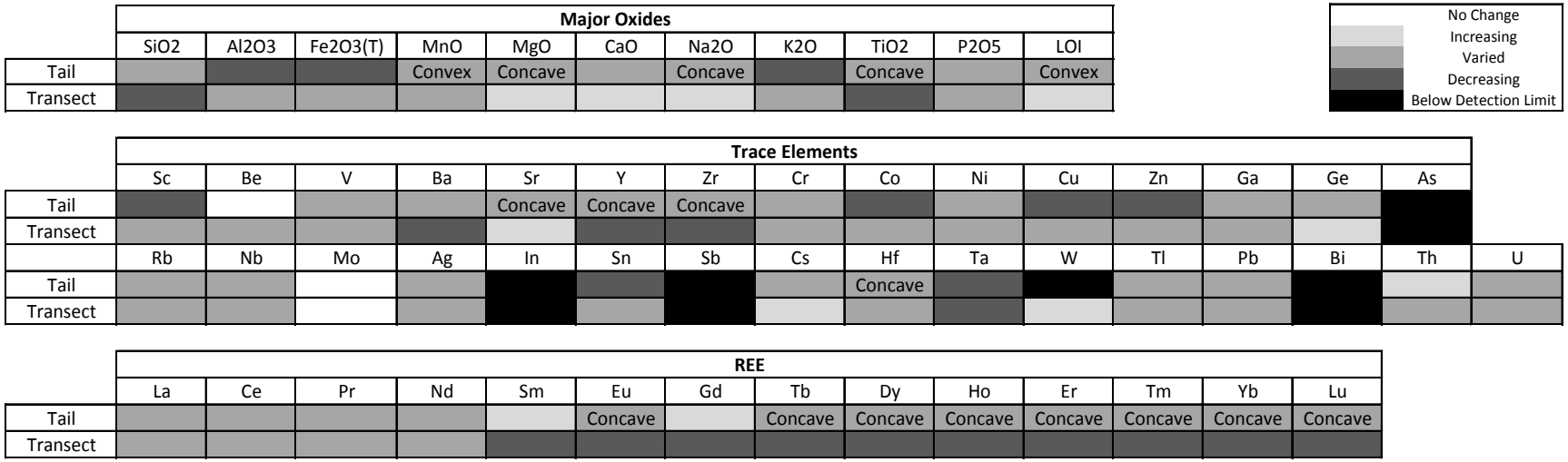

Figure 16: Spatial trends in till geochemistry from the active ice margin back towards the nunatak wall of the Mt. Achernar moraine. Sites 1A and 1B are included in both the "Tail" and "Transect" analyses.

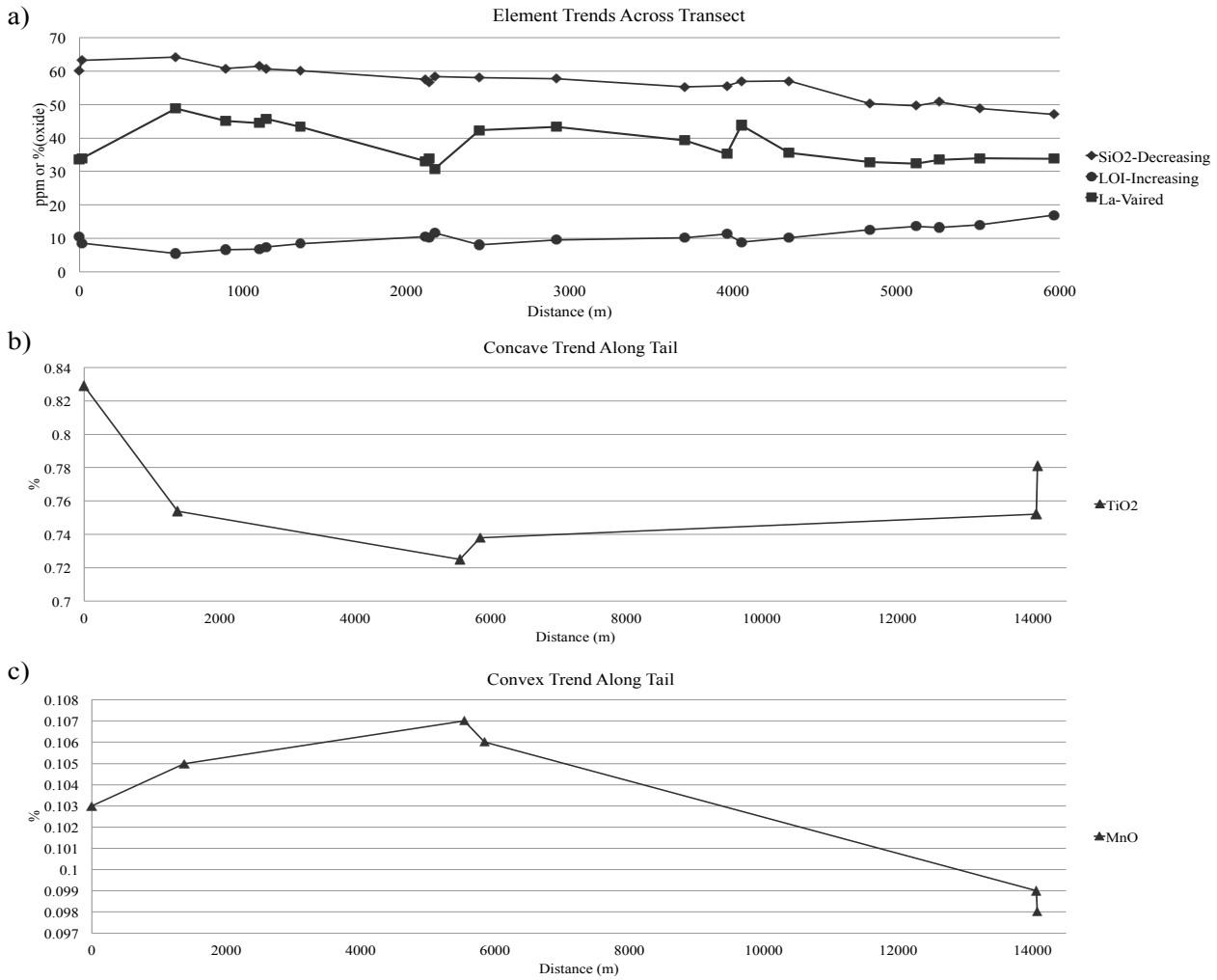

Figure 17: a) Spatial trends in till geochemistry of Mt. Achernar moraine from active ice margin to nunatak. b) and c) Sample distance along tail trends northeast to southwest along the tail of the moraine complex. (East Crest at 0 m, MA-1A and 1B at 14,000 m)

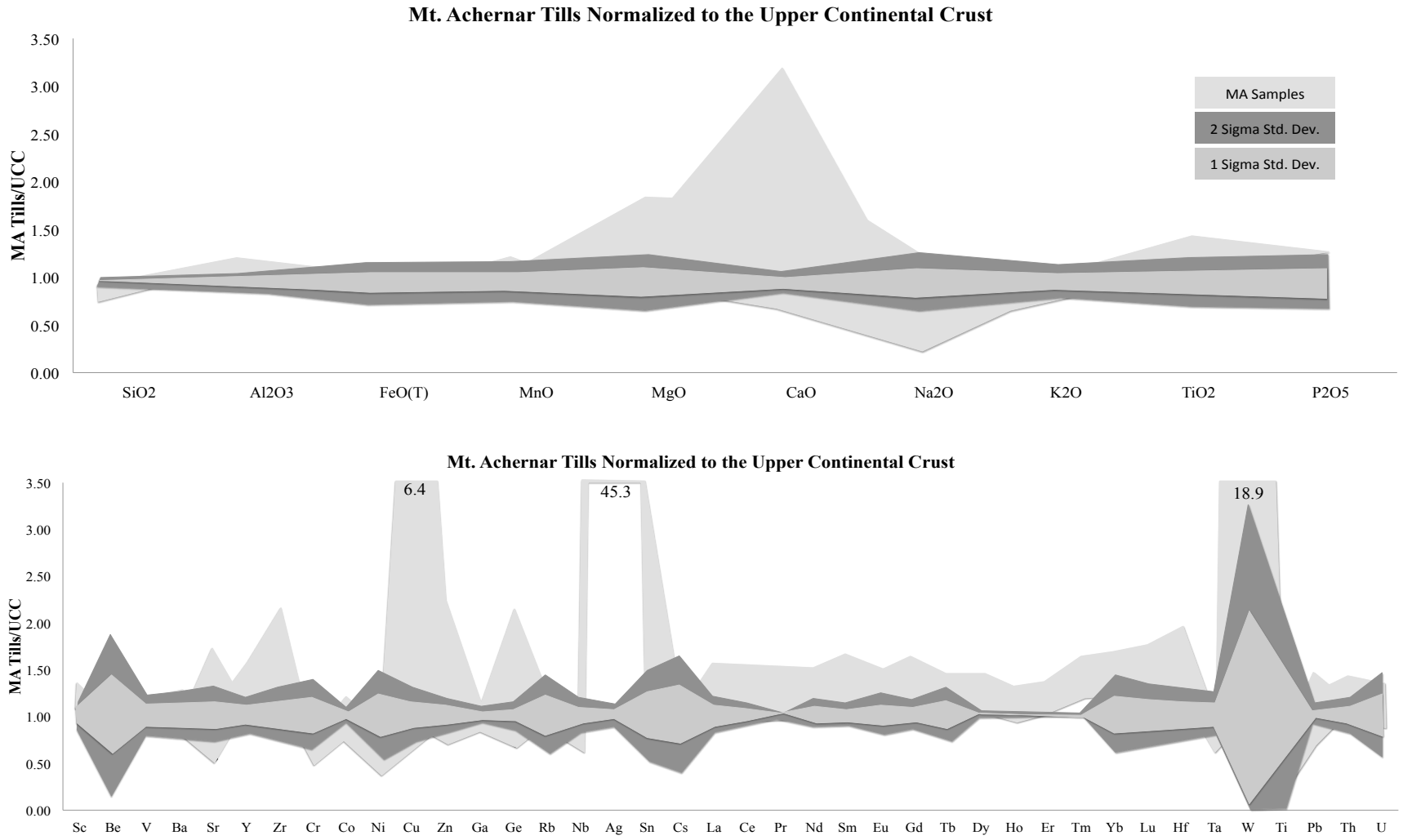

Figure 18: Major, trace, and REE patterns of the range of Mt. Achernar moraine till values normalized to UCC (Rudnick and Gao, 2003). Higest values out of chart range are labeled. Lightest shade of grey represents range of MA till values. Darker shades of grey represent 1 and 2 sigma standard deviaiton values for the UCC.

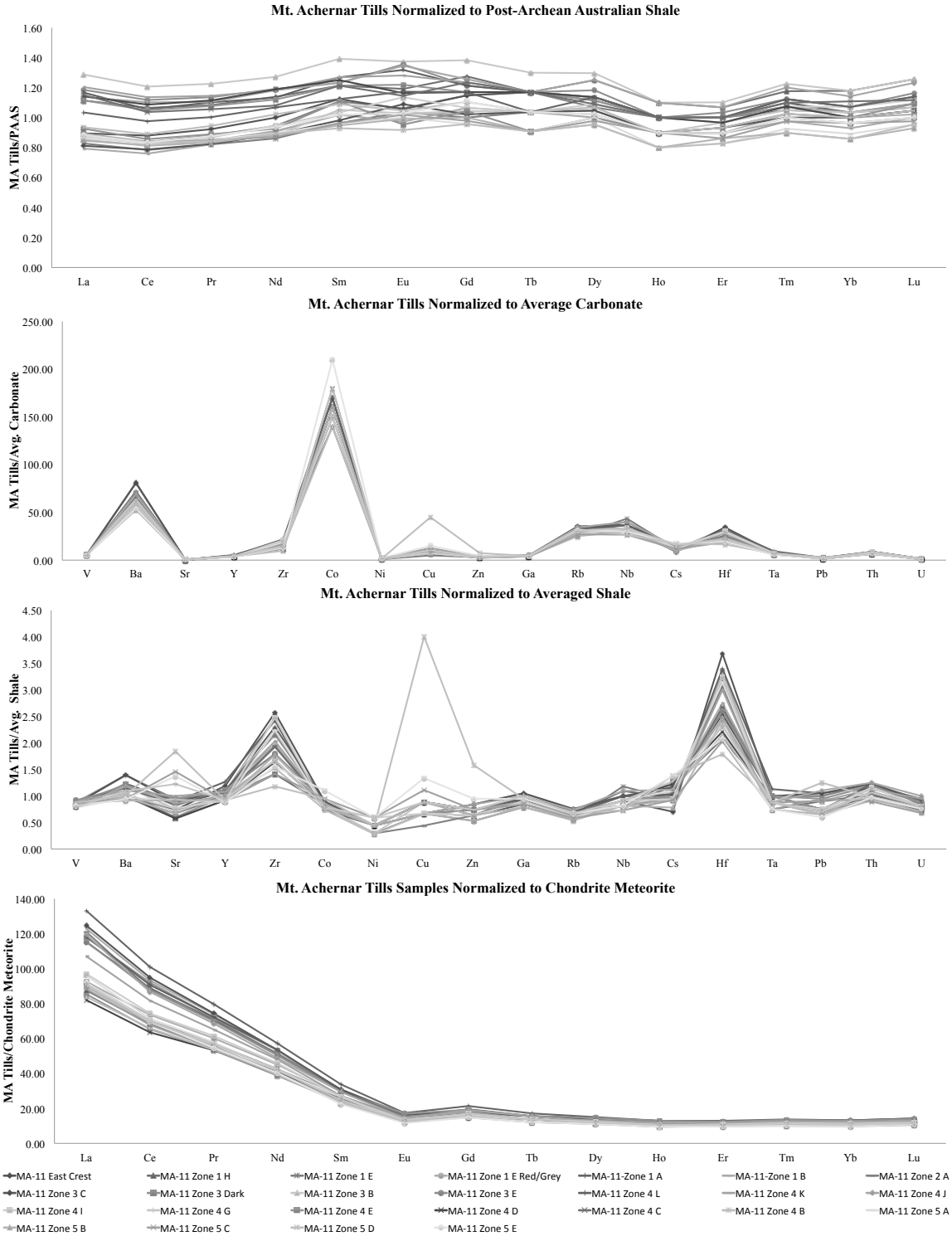

Figure 19: Geochemical patterns for the range of the Mt. Achernar moraine till values normalized to the post-Archean Australian shale (PAAS) (Taylor and McLennan, 1985)., average carbonate (Mason and Moore, 1982), average shale (Mason and Moore, 1982; Krauskopf and Bird, 1994), and chondrite meteorite (Taylor and McLennan, 1985).

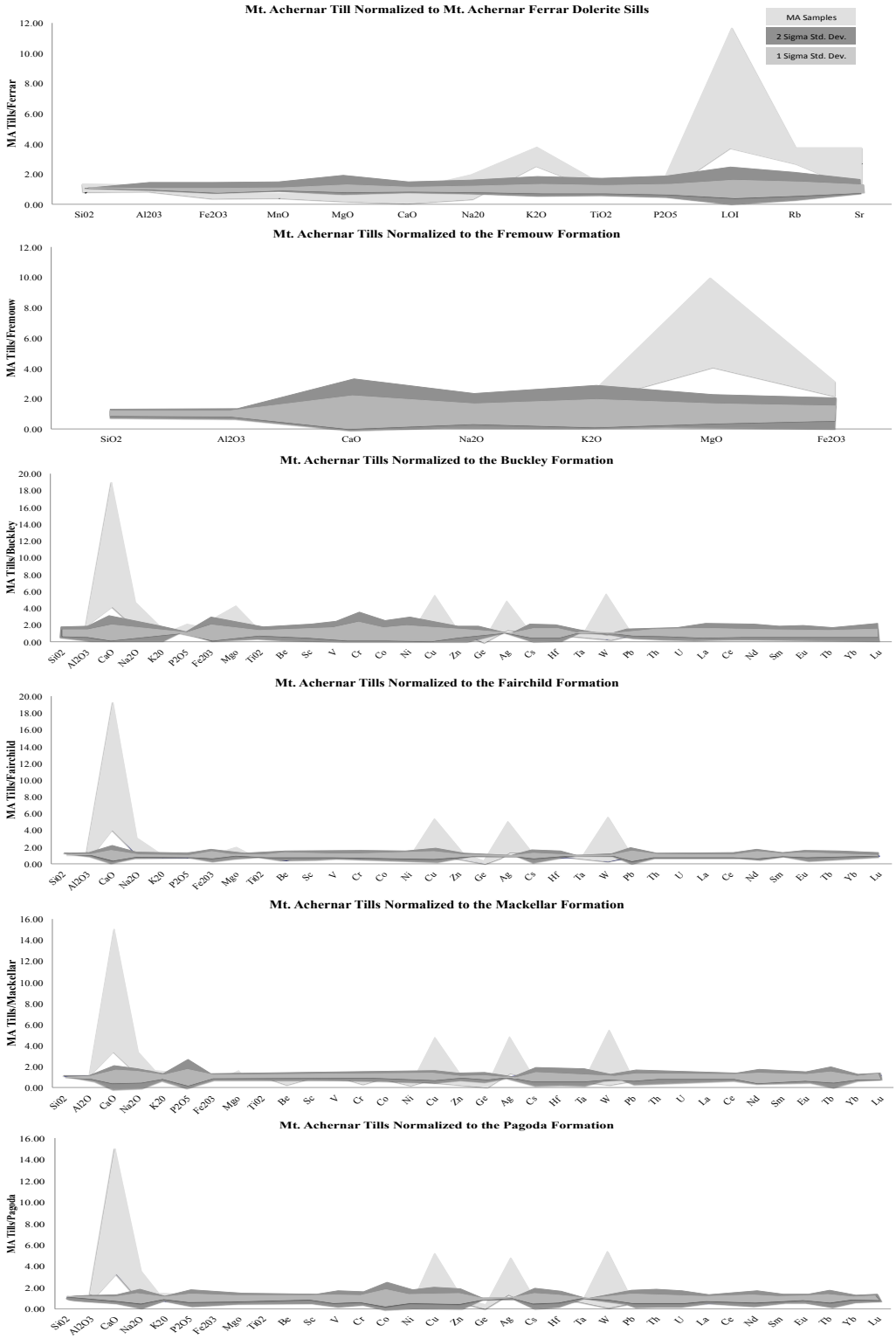

Figure 20: Major, trace, and REE patterns of the range of Mt. Achernar moraine till values normalized to rocks of the Beacon and Ferrar Supergroup (Vavra, 1982; Horner, 1992; Faure and Mensing, 2010). Lightest shade of grey represents range of MA till values. Darker shades of grey represent 1 and 2 sigma standard deviaiton values for the each formation.

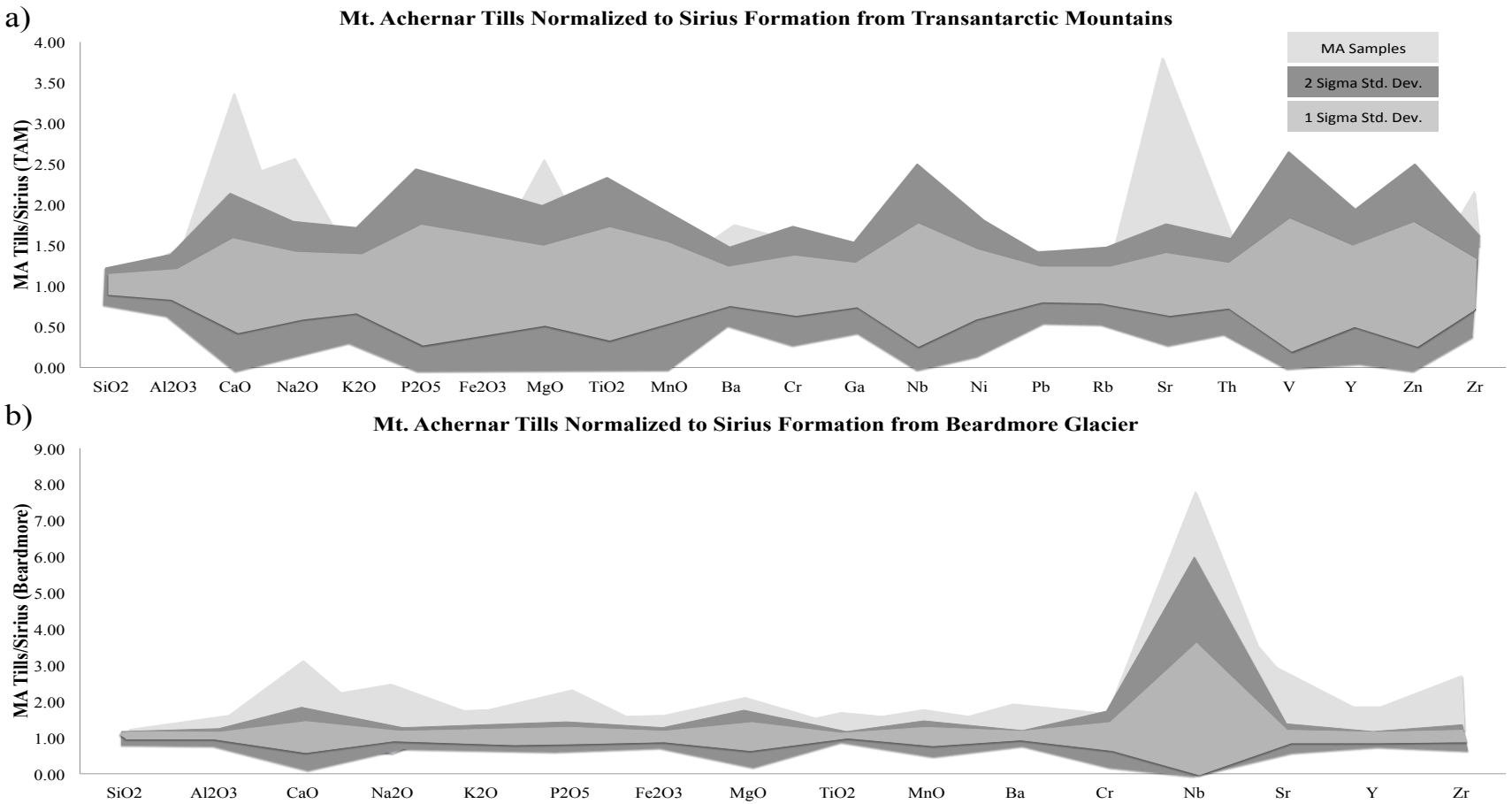

Figure 21: Major and trace element patterns of Mt. Achernar moraine till normalized to tills of the Sirius Formation (Passchier, 2004). Lightest shade of grey represents range of MA till values. Darker shades of grey represent 1 and 2 sigma standard deviaiton values for the each formation. 18a) normalizes the Mt. Achernar moraine till to the overall average of Sirius Formaiton sample averages throughout the TAM, including from the Reedy, Shackleton, Beardrmore, and David Glaciers, as well as the Dry Valleys. 18b) displays the Mt. Achernar moraine till samples normalized to the Sirius Formation averages from the Beardmore Glacier region only.

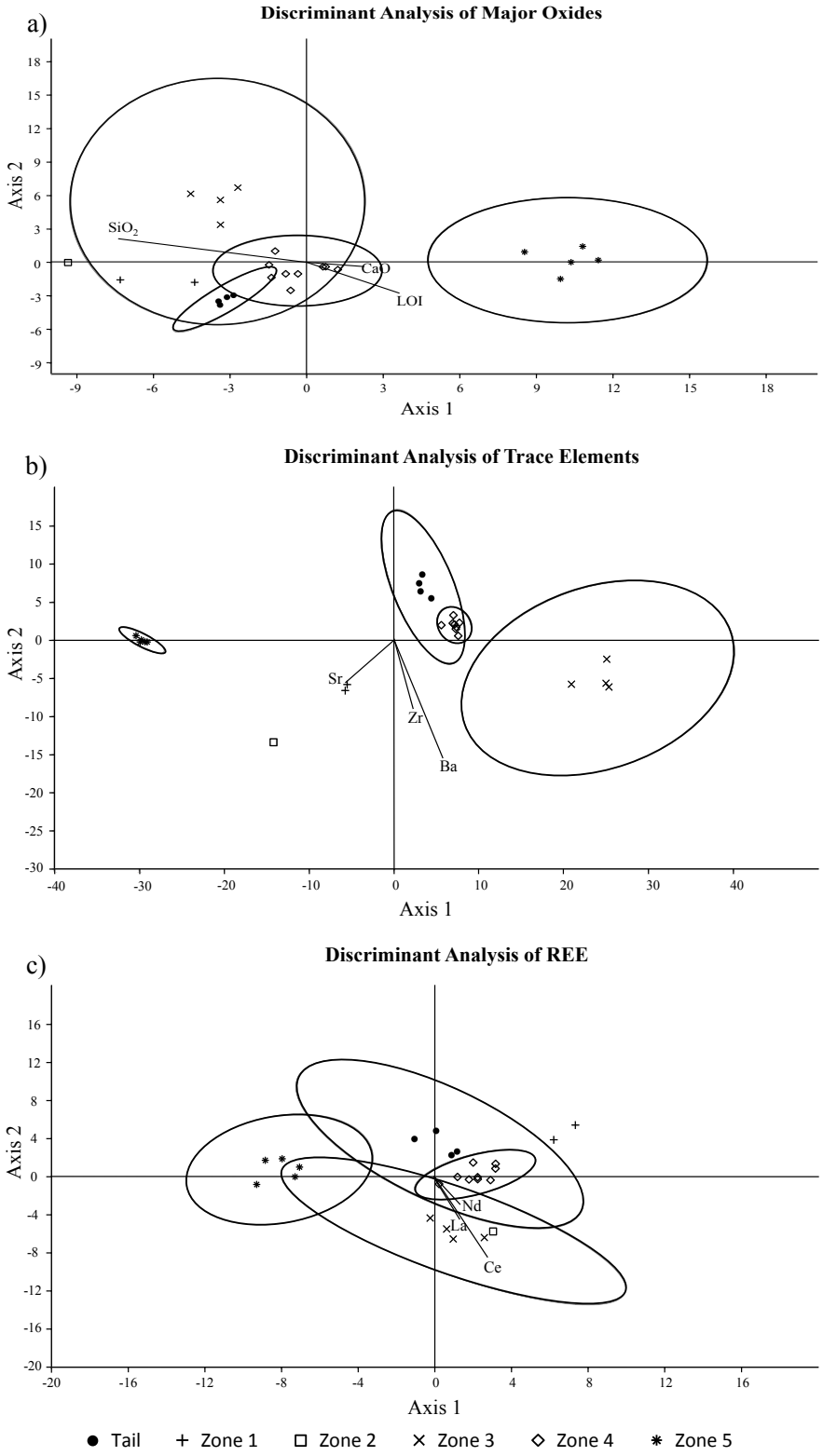

Figure 22: Discriminant analysis (DA) results of the Mt. Achernar moraine till samples (a) major oxides, (b) trace elements, and (c) rare earth elements. DA was run on all geochemical data, but only the three most discriminating elements are listed for the major, trace and REE.

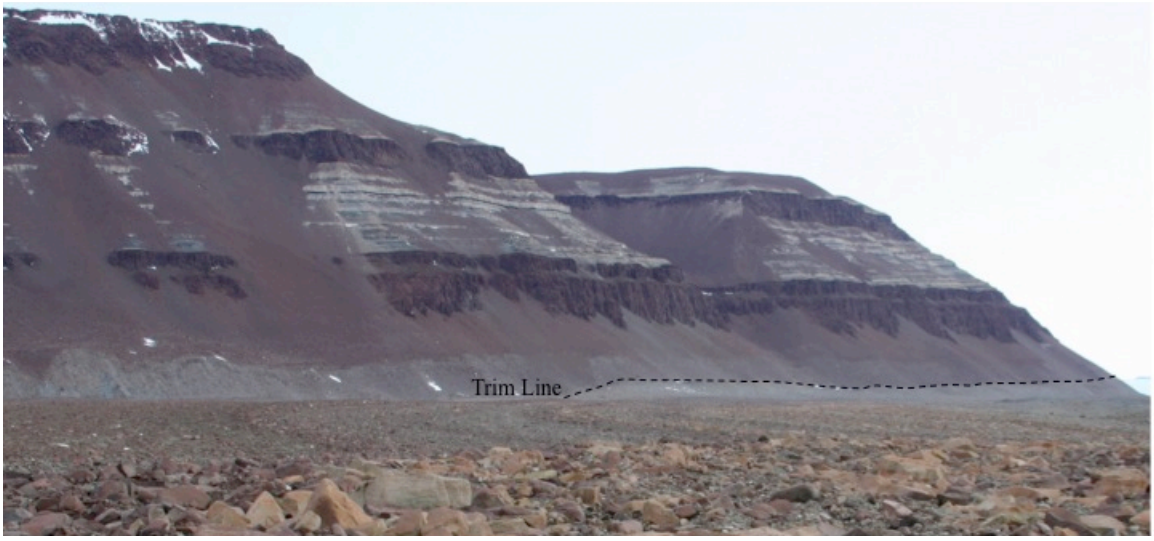

Figure 23: Potential trim line noted at Mt. Achernar.


Figure 24: Debris lines flowing parallel up to the edge of the Mt. Achernar moraine.

a)

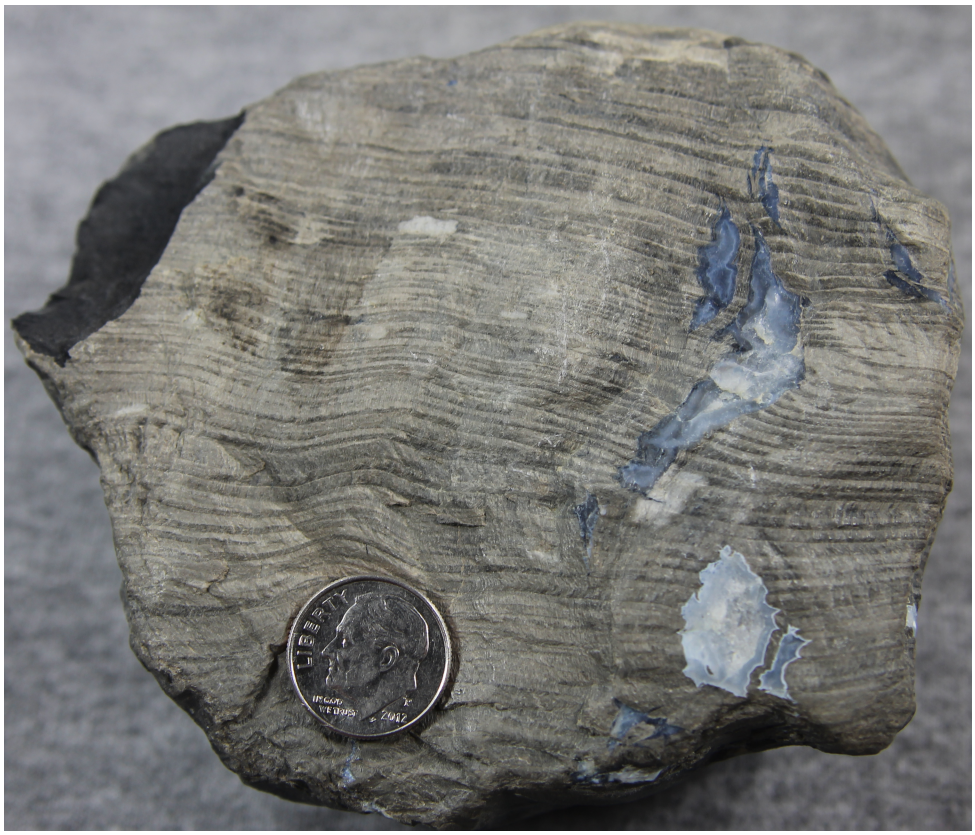

b)

Figure 25: a) A permineralized wood specimen (MA-11 Z1F6) and b) sandstone (MA-11-6) collected from the Mt. Achernar moraine.

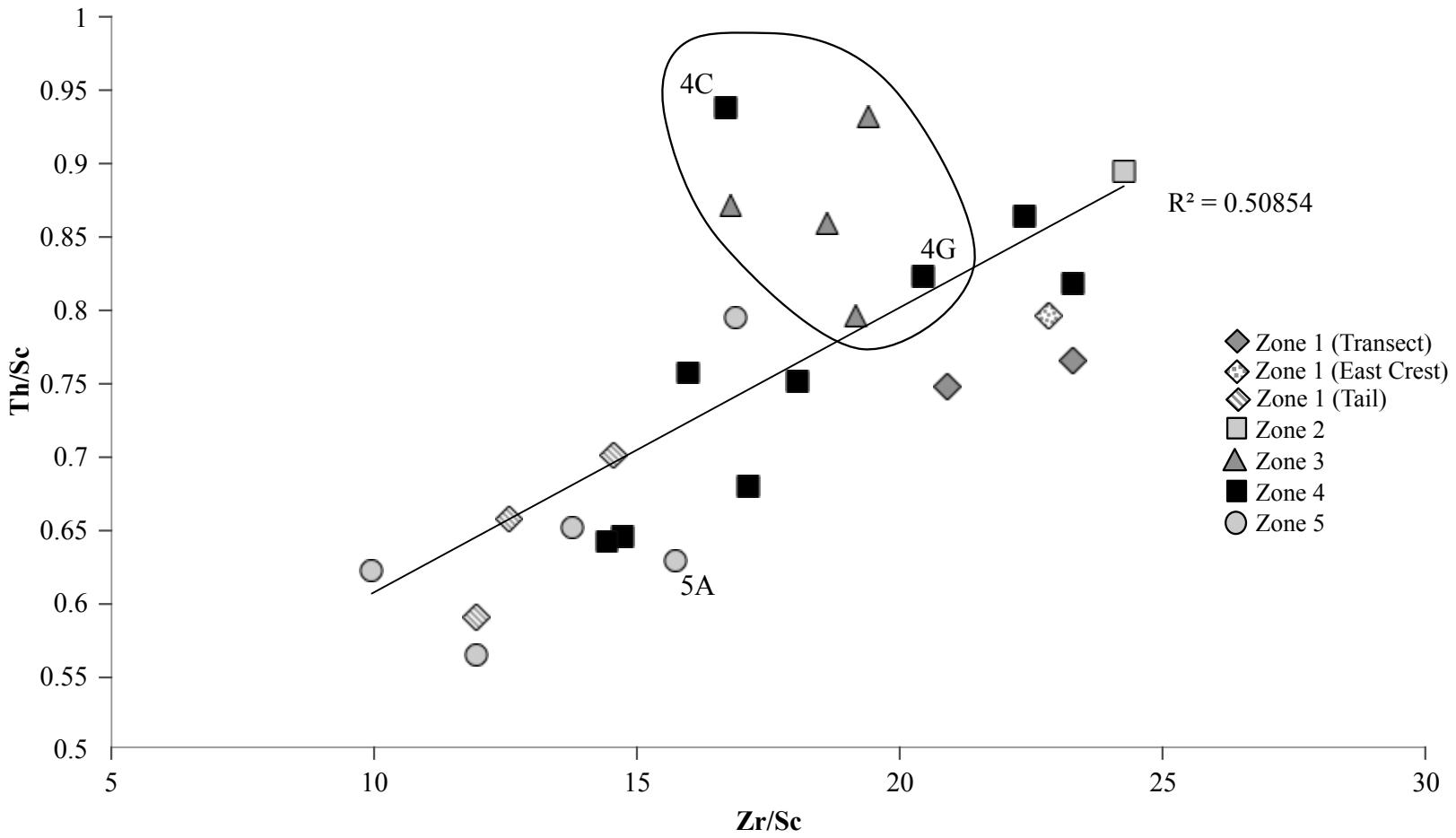

Figure 26: Th/Sc vs. Zr/Sc to explore as provenance tool. Values increase from a more mafic to felsic source. Circled samples and site 5A are samples that are dominated by sedimentary lithologies. Sample sites 4H and 4A are also dominated by sedimentary lithologies, but geochemical data was not analyzed for these sites

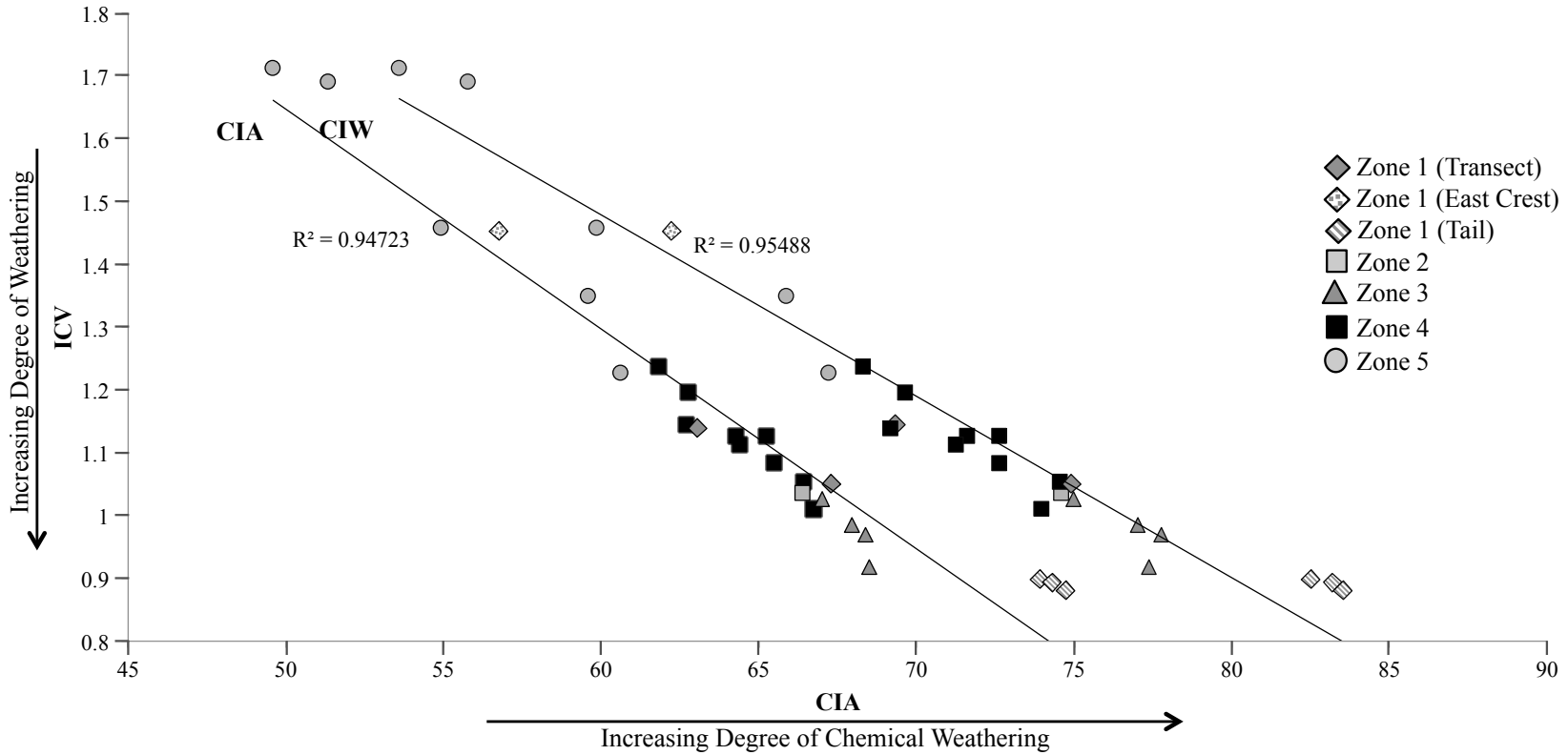

Figure 27: Index of compositional variability (ICV) vs. chemical index of alteration (CIA) and chemical index of weathering (CIW) for the Mt. Achernar moraine tills.

Appendix A. U-Pb analysis results of detrital zircons from the till of the Mt. Achernar moraine.

			Isotope ratios							Apparent ages (Ma)							
U	206Pb	U/Th	206Pb*		207Pb*		206Pb*		error	206Pb*		207Pb*		206Pb*		Best	
(ppm)	204Pb		207Pb*	(%)	235U*	(%)	238U	(%)	corr.	238U*	± (Ma)	235U	± (Ma)	207Pb*	± (Ma)	age	± (Ma)
1A																	
145	9583	1.1	19.6364	7.6	0.2959	7.9	0.0421	2.2	0.28	266.1	5.7	263.2	18.2	237.5	174.4	**266.1**	**5.7**
424	2027	2.1	16.9203	2.2	0.6446	2.5	0.0791	1.2	0.49	490.8	5.8	505.2	10.0	570.8	47.4	**490.8**	**5.8**
113	3990	1.0	16.7549	4.8	0.6632	5.0	0.0806	1.6	0.31	499.6	7.6	516.5	20.4	592.1	103.5	**499.6**	**7.6**
946	12992	5.2	16.9836	0.7	0.6653	5.6	0.0819	5.5	0.99	507.7	27.0	517.8	22.6	562.7	14.5	**507.7**	**27.0**
959	11838	21.6	17.0179	1.5	0.6880	2.0	0.0849	1.3	0.65	525.4	6.5	531.6	8.3	558.3	33.1	**525.4**	**6.5**
141	27908	0.8	17.0812	3.1	0.7258	4.2	0.0899	2.8	0.67	555.0	14.8	554.1	17.8	550.2	67.8	**555.0**	**14.8**
97	26838	1.2	17.6132	3.5	0.7077	4.4	0.0904	2.8	0.63	557.9	14.8	543.4	18.6	482.8	76.2	**557.9**	**14.8**
106	18185	4.2	17.5172	4.1	0.7203	4.9	0.0915	2.7	0.54	564.5	14.5	550.9	21.0	494.9	91.4	**564.5**	**14.5**
89	16238	0.9	16.5075	6.6	0.7660	7.4	0.0917	3.4	0.46	565.7	18.6	577.5	32.8	624.3	142.5	**565.7**	**18.6**
215	68923	2.7	17.1130	2.1	0.7408	2.4	0.0919	1.1	0.47	567.0	6.1	562.9	10.2	546.1	45.6	**567.0**	**6.1**
390	57672	3.3	16.8586	1.7	0.7585	3.3	0.0927	2.9	0.87	571.7	15.7	573.2	14.5	578.7	36.0	**571.7**	**15.7**
107	28598	3.8	16.6566	5.2	0.7685	5.4	0.0928	1.4	0.26	572.3	7.6	578.9	23.8	604.9	112.6	**572.3**	**7.6**
475	142170	2.9	16.5439	1.1	0.7773	4.8	0.0933	4.6	0.97	574.8	25.5	583.9	21.2	619.5	24.2	**574.8**	**25.5**
65	24515	3.4	16.7791	6.6	0.7698	6.9	0.0937	2.0	0.29	577.2	11.0	579.6	30.5	589.0	143.4	**577.2**	**11.0**
192	67259	3.4	16.7360	3.1	0.8060	5.0	0.0978	3.9	0.79	601.7	22.4	600.2	22.5	594.6	66.2	**601.7**	**22.4**
201	13338	2.8	15.6986	4.2	0.8846	7.1	0.1007	5.7	0.81	618.6	33.8	643.5	33.9	731.7	89.5	**618.6**	**33.8**
283	86706	1.9	16.4938	0.9	0.8981	2.6	0.1074	2.5	0.94	657.9	15.4	650.7	12.7	626.1	20.1	**657.9**	**15.4**
339	64937	1.1	15.9381	1.3	0.9389	4.2	0.1085	4.0	0.95	664.2	25.0	672.3	20.5	699.5	27.6	**664.2**	**25.0**
227	59212	2.1	15.3584	1.7	1.0175	7.6	0.1133	7.4	0.98	692.1	48.6	712.6	38.9	777.9	34.9	**692.1**	**48.6**
303	65705	2.8	13.9036	1.4	1.4882	6.4	0.1501	6.3	0.98	901.3	52.7	925.6	39.0	983.8	28.6	**983.8**	**28.6**
334	33908	2.9	13.7522	0.7	1.6714	2.7	0.1667	2.6	0.96	993.9	24.0	997.7	17.2	1006.0	14.9	**1006.0**	**14.9**
59	22257	1.3	13.0736	3.2	1.8829	4.2	0.1785	2.7	0.65	1059.0	26.6	1075.1	27.7	1107.9	63.3	**1107.9**	**63.3**
77	55892	0.6	6.9044	0.4	8.3639	3.3	0.4188	3.3	0.99	2255.1	62.7	2271.3	30.2	2285.8	7.6	**2285.8**	**7.6**
59	34149	1.6	5.3692	0.8	12.1839	2.4	0.4745	2.2	0.94	2503.1	46.5	2618.7	22.3	2709.3	12.9	**2709.3**	**12.9**
2A																	
108	758	0.8	15.0498	18.9	0.2929	19.3	0.0320	4.2	0.22	202.9	8.3	260.8	44.4	820.5	397.0	**202.9**	**8.3**
446	143176	3.5	17.4261	1.3	0.6631	1.8	0.0838	1.3	0.70	518.8	6.5	516.5	7.5	506.3	28.8	**518.8**	**6.5**
59	18963	1.5	17.4291	9.8	0.6778	10.5	0.0857	3.9	0.37	529.9	20.1	525.4	43.2	506.0	215.2	**529.9**	**20.1**
46	8427	0.3	17.6331	12.8	0.6767	13.1	0.0865	3.0	0.23	535.0	15.3	524.8	53.9	480.3	283.8	**535.0**	**15.3**
383	111859	25.3	16.8251	1.6	0.7281	2.0	0.0889	1.2	0.61	548.7	6.4	555.5	8.5	583.0	34.4	**548.7**	**6.4**
44	7382	1.9	18.7496	16.0	0.6546	16.1	0.0890	2.3	0.14	549.7	11.9	511.3	64.9	343.1	363.6	**549.7**	**11.9**
118	29665	1.2	17.3847	8.1	0.7088	8.4	0.0894	2.5	0.29	551.8	13.1	544.0	35.5	511.6	177.3	**551.8**	**13.1**
709	139004	5.9	16.9030	1.0	0.7304	1.6	0.0895	1.2	0.76	552.8	6.4	556.8	6.8	573.0	22.2	**552.8**	**6.4**
479	102198	2.6	16.9371	1.3	0.7316	1.7	0.0899	1.1	0.63	554.8	5.6	557.5	7.3	568.7	28.8	**554.8**	**5.6**
101	27511	1.7	16.9212	4.7	0.7330	5.1	0.0900	2.1	0.41	555.3	11.1	558.3	22.0	570.7	102.1	**555.3**	**11.1**
122	31735	1.3	17.0030	2.7	0.7313	3.4	0.0902	2.1	0.61	556.6	10.9	557.3	14.5	560.2	58.7	**556.6**	**10.9**
340	58095	2.1	16.9605	1.5	0.7337	1.9	0.0902	1.1	0.59	557.0	5.8	558.7	8.0	565.6	32.8	**557.0**	**5.8**
41	7422	1.8	17.2761	10.9	0.7203	11.2	0.0902	2.7	0.24	557.0	14.2	550.8	47.7	525.3	239.2	**557.0**	**14.2**
245	64825	2.6	16.9780	1.5	0.7336	2.3	0.0903	1.7	0.74	557.5	8.9	558.7	9.7	563.4	33.4	**557.5**	**8.9**
162	59676	6.2	17.2943	3.0	0.7231	4.0	0.0907	2.6	0.66	559.7	14.0	552.5	16.9	523.0	65.6	**559.7**	**14.0**
79	32055	0.2	16.8163	5.9	0.7451	6.5	0.0909	2.7	0.41	560.7	14.3	565.4	28.2	584.2	128.8	**560.7**	**14.3**
457	73150	6.6	16.6028	0.9	0.7571	1.7	0.0912	1.5	0.84	562.4	7.8	572.3	7.6	611.9	20.3	**562.4**	**7.8**
244	32734	1.7	17.1548	1.6	0.7346	2.0	0.0914	1.2	0.60	563.8	6.4	559.3	8.5	540.8	34.8	**563.8**	**6.4**
196	65395	1.3	16.3482	1.7	0.7745	7.3	0.0918	7.1	0.97	566.4	38.4	582.4	32.3	645.2	35.7	**566.4**	**38.4**
69	25948	0.2	16.5545	10.7	0.7665	11.0	0.0920	2.4	0.21	567.5	12.8	577.7	48.5	618.1	232.6	**567.5**	**12.8**
204	85718	2.7	17.4337	2.6	0.7287	2.8	0.0921	1.0	0.37	568.1	5.6	555.8	12.1	505.4	58.0	**568.1**	**5.6**
1165	135265	8.4	16.8217	0.8	0.7563	1.7	0.0923	1.5	0.88	568.9	8.1	571.8	7.4	583.5	17.5	**568.9**	**8.1**
112	23483	0.9	16.7500	6.2	0.7596	6.4	0.0923	1.6	0.24	569.0	8.5	573.8	28.0	592.7	134.4	**569.0**	**8.5**
45	11753	0.8	16.7055	15.2	0.7629	16.3	0.0924	5.8	0.35	569.9	31.5	575.7	71.7	598.5	331.7	**569.9**	**31.5**
99	19509	1.0	17.4564	5.1	0.7308	5.5	0.0925	2.0	0.37	570.4	11.1	557.0	23.4	502.5	111.9	**570.4**	**11.1**
1051	9997	10.0	15.4922	1.5	0.8280	3.9	0.0930	3.6	0.92	573.5	19.7	612.5	18.0	759.6	32.0	**573.5**	**19.7**
35	8806	0.3	17.0227	13.6	0.7543	13.7	0.0931	2.0	0.14	574.0	10.9	570.7	59.9	557.7	297.1	**574.0**	**10.9**
28	7629	0.9	17.8674	33.8	0.7214	34.2	0.0935	5.5	0.16	576.1	30.1	551.5	146.5	451.1	769.7	**576.1**	**30.1**
165	30334	2.1	16.9855	5.2	0.7611	5.4	0.0938	1.1	0.21	577.7	6.3	574.6	23.6	562.4	114.4	**577.7**	**6.3**
167	41820	1.1	17.1772	4.2	0.7533	4.6	0.0938	1.8	0.39	578.3	10.0	570.1	20.0	537.9	92.2	**578.3**	**10.0**
203	44566	2.3	16.7948	2.4	0.7772	2.7	0.0947	1.3	0.47	583.1	7.2	583.9	12.1	587.0	52.1	**583.1**	**7.2**
538	127568	2.1	16.6842	1.0	0.7826	1.6	0.0947	1.3	0.79	583.3	7.2	587.0	7.3	601.3	21.4	**583.3**	**7.2**
204	48346	217.0	16.7680	2.5	0.7829	3.0	0.0952	1.7	0.55	586.3	9.3	587.1	13.5	590.4	55.0	**586.3**	**9.3**
171	109746	1.2	16.3096	2.3	0.8060	2.6	0.0953	1.3	0.50	587.1	7.3	600.2	11.8	650.3	48.3	**587.1**	**7.3**
229	60660	3.0	16.7948	2.5	0.7838	2.9	0.0955	1.5	0.53	587.9	8.7	587.7	13.0	587.0	53.6	**587.9**	**8.7**
249	57536	2.1	16.7994	3.5	0.7840	4.0	0.0955	1.9	0.47	588.1	10.6	587.8	17.9	586.4	76.8	**588.1**	**10.6**
711	45039	1.2	16.7565	1.0	0.7862	1.7	0.0956	1.4	0.81	588.3	7.7	589.0	7.5	591.9	21.4	**588.3**	**7.7**
343	110985	2.7	16.6870	1.2	0.7908	2.8	0.0957	2.5	0.90	589.2	13.9	591.6	12.3	600.9	26.2	**589.2**	**13.9**
703	214729	19.9	16.7509	0.7	0.7910	1.1	0.0961	0.9	0.81	591.5	5.2	591.8	5.1	592.6	14.4	**591.5**	**5.2**
387	116697	2.3	16.7139	1.3	0.7933	2.1	0.0962	1.7	0.78	591.9	9.5	593.0	9.6	597.5	28.8	**591.9**	**9.5**
595	200038	1.2	16.6751	0.7	0.7963	1.0	0.0963	0.8	0.76	592.7	4.4	594.7	4.6	602.5	14.4	**592.7**	**4.4**
119	67288	1.0	17.0865	2.9	0.7773	3.2	0.0963	1.3	0.41	592.8	7.5	583.9	14.3	549.5	64.3	**592.8**	**7.5**
604	170333	1.8	16.4002	0.8	0.8105	1.7	0.0964	1.5	0.89	593.3	8.5	602.7	7.7	638.4	16.6	**593.3**	**8.5**
112	28708	0.3	17.2585	4.9	0.7711	5.1	0.0965	1.4	0.28	594.0	8.1	580.4	22.6	527.6	107.7	**594.0**	**8.1**
35	11446	4.8	16.1321	15.6	0.8264	16.4	0.0967	5.2	0.32	594.9	29.7	611.6	75.5	673.7	334.6	**594.9**	**29.7**
162	42173	1.1	17.3316	2.5	0.7729	2.8	0.0972	1.4	0.50	597.7	8.0	581.4	12.5	518.3	53.9	**597.7**	**8.0**
372	76567	2.4	16.6451	1.9	0.8105	2.1	0.0978	0.9	0.43	601.8	5.1	602.7	9.3	606.4	40.0	**601.8**	**5.1**
1304	174590	7.7	16.7800	0.6	0.8059	1.6	0.0981	1.4	0.91	603.2	8.1	600.2	7.0	588.9	13.8	**603.2**	**8.1**
336	128713	3.1	16.7544	1.2	0.8136	1.4	0.0989	0.8	0.53	607.7	4.4	604.4	6.5	592.2	26.3	**607.7**	**4.4**
290	57042	1.6	16.5842	1.1	0.8239	3.9	0.0991	3.8	0.96	609.1	22.0	610.2	18.1	614.3	22.8	**609.1**	**22.0**
887	41542	1.2	16.5361	0.7	0.8360	0.9	0.1003	0.6	0.65	615.9	3.4	616.9	4.2	620.5	14.8	**615.9**	**3.4**
726	397185	2.8	16.6114	0.7	0.8330	1.3	0.1004	1.0	0.82	616.5	6.1	615.3	5.8	610.7	15.6	**616.5**	**6.1**

Appendix A continued. U-Pb analysis results of detrital zircons from the till of the Mt. Achernar moraine.

			Isotope ratios							Apparent ages (Ma)							
U	206Pb	U/Th	206Pb*		207Pb*		206Pb*		error	206Pb*		207Pb*		206Pb*		Best	
(ppm)	204Pb		207Pb*	(%)	235U*	(%)	238U	(%)	corr.	238U*	± (Ma)	235U	± (Ma)	207Pb*	± (Ma)	age	± (Ma)
261	63868	1.7	16.3698	2.2	0.8458	2.6	0.1004	1.5	0.57	616.8	8.8	622.3	12.2	642.4	46.7	**616.8**	**8.8**
207	59343	1.8	16.3852	2.7	0.8461	2.9	0.1005	1.1	0.38	617.6	6.4	622.5	13.4	640.3	57.5	**617.6**	**6.4**
1620	231398	10.2	16.5312	0.4	0.8412	1.2	0.1009	1.1	0.94	619.4	6.7	619.8	5.6	621.2	9.0	**619.4**	**6.7**
138	98123	2.6	16.5049	4.5	0.8527	6.6	0.1021	4.8	0.73	626.6	28.9	626.1	30.8	624.6	96.5	**626.6**	**28.9**
236	71544	2.2	15.6052	3.3	0.9133	5.2	0.1034	4.0	0.77	634.1	24.3	658.8	25.3	744.3	70.4	**634.1**	**24.3**
533	121857	21.2	16.3282	1.3	0.8985	2.2	0.1064	1.7	0.79	651.9	10.7	650.9	10.5	647.8	28.9	**651.9**	**10.7**
289	58648	3.4	15.8907	1.1	0.9506	1.5	0.1096	0.9	0.63	670.2	5.8	678.4	7.2	705.8	24.3	**670.2**	**5.8**
943	23515	10.4	15.9388	1.1	0.9887	2.8	0.1143	2.5	0.92	697.7	16.7	698.1	13.9	699.4	23.6	**697.7**	**16.7**
59	39222	1.0	15.5572	6.6	1.0601	8.0	0.1196	4.5	0.57	728.3	31.3	733.9	42.0	750.8	140.0	**728.3**	**31.3**
205	86136	1.9	14.8707	2.9	1.2041	10.4	0.1299	10.0	0.96	787.1	74.1	802.5	57.8	845.4	60.4	**787.1**	**74.1**
125	82499	0.9	14.7500	2.5	1.2167	5.7	0.1302	5.1	0.89	788.8	37.8	808.3	31.7	862.3	52.9	**788.8**	**37.8**
388	12893	2.3	14.5403	1.2	1.2562	2.2	0.1325	1.9	0.84	802.0	14.0	826.2	12.5	892.0	25.1	**802.0**	**14.0**
79	23075	5.7	14.2932	4.2	1.3010	5.1	0.1349	3.0	0.58	815.6	22.9	846.2	29.5	927.3	85.6	**815.6**	**22.9**
135	49115	4.4	14.8702	2.6	1.3205	3.2	0.1424	1.8	0.57	858.3	14.7	854.7	18.5	845.5	54.7	**858.3**	**14.7**
70	25942	2.2	14.3642	3.9	1.5344	5.0	0.1599	3.2	0.63	956.0	28.0	944.3	30.7	917.1	79.8	**917.1**	**79.8**
205	135908	2.8	14.3121	1.5	1.4508	1.7	0.1506	0.8	0.48	904.3	6.7	910.2	10.0	924.6	29.9	**924.6**	**29.9**
281	35828	1.8	14.2930	1.4	1.4504	3.1	0.1504	2.7	0.88	902.9	22.9	910.0	18.5	927.3	29.7	**927.3**	**29.7**
46	17783	3.6	14.1961	6.4	1.5517	6.6	0.1598	1.9	0.29	955.5	17.0	951.2	41.1	941.3	130.6	**941.3**	**130.6**
315	247508	1.8	14.0921	1.1	1.4113	3.5	0.1442	3.4	0.95	868.6	27.5	893.7	21.1	956.3	21.6	**956.3**	**21.6**
92	30468	1.2	13.9520	2.9	1.3592	10.2	0.1375	9.8	0.96	830.7	76.1	871.5	59.6	976.7	58.8	**976.7**	**58.8**
138	93827	3.5	13.9437	2.2	1.5932	3.9	0.1611	3.3	0.83	963.0	29.1	967.6	24.5	977.9	44.8	**977.9**	**44.8**
517	211969	3.0	13.9239	0.4	1.6238	1.6	0.1640	1.6	0.96	978.8	14.3	979.4	10.2	980.8	8.7	**980.8**	**8.7**
117	3729	3.0	13.9071	3.2	1.5358	4.9	0.1549	3.7	0.76	928.4	32.4	944.8	30.4	983.3	65.4	**983.3**	**65.4**
287	83516	3.9	13.8871	0.9	1.6352	4.6	0.1647	4.5	0.98	982.8	40.7	983.9	28.7	986.2	18.2	**986.2**	**18.2**
133	41752	0.9	13.8540	1.8	1.5313	2.3	0.1539	1.4	0.61	922.6	11.9	943.0	14.1	991.1	37.0	**991.1**	**37.0**
72	18781	1.1	13.8490	4.0	1.5480	5.0	0.1555	3.1	0.61	931.6	26.7	949.7	31.0	991.8	80.8	**991.8**	**80.8**
250	373690	2.1	13.7082	1.4	1.7184	3.3	0.1708	2.9	0.90	1016.8	27.6	1015.4	20.9	1012.5	28.6	**1012.5**	**28.6**
514	60908	3.9	13.6146	0.7	1.5920	2.1	0.1572	2.0	0.95	941.2	17.7	967.1	13.4	1026.4	14.1	**1026.4**	**14.1**
237	100299	2.4	13.4991	0.8	1.8026	1.7	0.1765	1.5	0.87	1047.7	14.2	1046.4	11.0	1043.6	16.8	**1043.6**	**16.8**
163	50391	3.8	13.4590	1.3	1.7273	3.4	0.1686	3.1	0.92	1004.4	28.8	1018.8	21.7	1049.6	26.9	**1049.6**	**26.9**
206	30251	1.9	13.3997	1.9	1.6791	3.6	0.1632	3.1	0.86	974.4	28.2	1000.6	23.2	1058.5	37.9	**1058.5**	**37.9**
305	57877	1.4	13.3733	0.9	1.7917	4.6	0.1738	4.5	0.98	1032.9	43.2	1042.5	30.1	1062.5	18.2	**1062.5**	**18.2**
272	64818	2.1	13.3488	1.1	1.8016	1.9	0.1744	1.6	0.82	1036.4	15.0	1046.0	12.5	1066.2	22.0	**1066.2**	**22.0**
229	78629	1.6	13.1462	1.0	1.8837	1.3	0.1796	0.9	0.67	1064.8	8.4	1075.4	8.5	1096.8	19.2	**1096.8**	**19.2**
211	170990	0.9	12.5463	1.0	2.2176	4.4	0.2018	4.2	0.97	1184.9	46.0	1186.6	30.6	1189.7	20.5	**1189.7**	**20.5**
572	151066	10.2	12.5406	0.6	2.2403	2.1	0.2038	2.0	0.96	1195.5	22.0	1193.7	14.7	1190.6	11.1	**1190.6**	**11.1**
300	91900	1.3	12.5216	0.9	2.2038	1.5	0.2001	1.1	0.79	1176.1	12.3	1182.3	10.2	1193.6	17.8	**1193.6**	**17.8**
646	451503	6.9	12.5112	0.5	2.2200	2.1	0.2014	2.0	0.97	1183.1	22.0	1187.4	14.7	1195.2	10.0	**1195.2**	**10.0**
112	115983	0.9	12.4910	2.0	2.2933	2.3	0.2078	1.1	0.50	1216.8	12.7	1210.2	16.1	1198.4	38.9	**1198.4**	**38.9**
213	108634	4.9	12.4801	0.7	2.2644	1.6	0.2050	1.5	0.90	1201.9	16.1	1201.3	11.5	1200.1	14.0	**1200.1**	**14.0**
387	183779	2.6	12.4195	0.7	2.2672	1.8	0.2042	1.7	0.93	1197.9	18.6	1202.1	12.9	1209.7	13.4	**1209.7**	**13.4**
795	303580	0.5	12.3321	0.2	2.2980	1.0	0.2055	0.9	0.97	1205.0	10.4	1211.7	6.9	1223.6	4.7	**1223.6**	**4.7**
142	99444	1.6	12.3219	1.3	2.1941	2.0	0.1961	1.6	0.77	1154.2	16.5	1179.2	14.1	1225.2	25.1	**1225.2**	**25.1**
193	145571	20.5	10.8433	2.0	2.9700	3.6	0.2336	3.0	0.84	1353.2	37.1	1400.0	27.6	1472.0	37.6	**1472.0**	**37.6**
53	23571	1.3	10.6728	5.3	3.3357	6.8	0.2582	4.3	0.63	1480.6	56.7	1489.4	53.1	1502.0	99.5	**1502.0**	**99.5**
95	83433	1.1	9.7492	0.9	4.2120	2.3	0.2978	2.2	0.93	1680.5	32.0	1676.4	19.1	1671.2	15.9	**1671.2**	**15.9**
159	82803	1.4	9.1124	0.9	4.5008	3.5	0.2975	3.4	0.97	1678.7	50.1	1731.1	29.1	1795.1	16.1	**1795.1**	**16.1**
580	289143	2.8	7.8904	0.1	6.1848	1.9	0.3539	1.9	1.00	1953.4	31.3	2002.3	16.3	2053.2	2.4	**2053.2**	**2.4**
342	751236	4.4	7.5258	0.3	6.5665	3.3	0.3584	3.3	0.99	1974.6	55.5	2054.9	28.9	2136.3	6.1	**2136.3**	**6.1**
132	163337	0.9	7.2677	0.4	7.8641	1.6	0.4145	1.6	0.97	2235.5	30.4	2215.6	14.9	2197.1	6.4	**2197.1**	**6.4**
517	379962	4.1	6.9352	0.2	7.9662	1.5	0.4007	1.5	0.99	2172.2	27.8	2227.2	13.8	2278.1	4.1	**2278.1**	**4.1**
1053	297912	5.0	6.7425	0.4	6.7199	1.5	0.3286	1.5	0.97	1831.7	23.3	2075.2	13.4	2326.6	6.7	**2326.6**	**6.7**
127	203655	1.8	6.7198	2.1	8.2254	6.6	0.4009	6.3	0.95	2173.1	115.6	2256.1	59.8	2332.3	35.3	**2332.3**	**35.3**
285	345096	0.5	6.5754	0.9	6.8053	9.6	0.3245	9.6	1.00	1811.9	151.5	2086.4	85.5	2369.4	14.9	**2369.4**	**14.9**
291	134772	3.9	6.3877	0.3	8.7042	2.1	0.4032	2.1	0.99	2184.0	38.7	2307.5	19.2	2418.7	5.2	**2418.7**	**5.2**
99	102748	1.6	6.3057	1.3	9.7773	7.4	0.4471	7.3	0.98	2382.6	145.5	2414.0	68.5	2440.6	22.7	**2440.6**	**22.7**
150	157448	1.4	6.2823	0.4	8.6720	2.8	0.3951	2.8	0.99	2146.6	50.6	2304.1	25.4	2446.9	6.2	**2446.9**	**6.2**
368	405402	3.7	6.2228	0.2	9.9512	2.1	0.4491	2.1	0.99	2391.3	41.7	2430.3	19.4	2463.0	4.1	**2463.0**	**4.1**
273	297942	3.0	6.1360	0.3	9.4704	2.2	0.4215	2.1	0.99	2267.1	40.9	2384.7	19.9	2486.7	5.4	**2486.7**	**5.4**
132	134079	23.3	6.0997	0.4	9.6667	2.5	0.4276	2.4	0.98	2295.1	46.6	2403.5	22.6	2496.7	7.5	**2496.7**	**7.5**
415	38595	1.6	6.0174	0.7	9.8642	5.2	0.4305	5.1	0.99	2307.9	99.9	2422.2	47.9	2519.6	11.8	**2519.6**	**11.8**
256	197522	1.6	5.4553	0.3	11.0792	2.0	0.4383	1.9	0.99	2343.2	38.1	2529.8	18.3	2683.0	5.4	**2683.0**	**5.4**
75	116294	0.8	5.3982	0.4	12.2361	2.8	0.4791	2.7	0.99	2523.2	57.2	2622.7	26.0	2700.4	6.3	**2700.4**	**6.3**
563	128222	2.1	5.3657	0.1	13.1051	1.5	0.5100	1.5	1.00	2656.6	33.0	2687.2	14.4	2710.4	2.4	**2710.4**	**2.4**
96	132996	1.4	5.3464	0.3	13.1158	1.8	0.5086	1.7	0.98	2650.5	37.9	2688.0	16.7	2716.3	5.2	**2716.3**	**5.2**
247	237938	1.6	5.3262	0.1	12.9444	2.3	0.5000	2.3	1.00	2613.9	49.8	2675.6	21.9	2722.5	2.3	**2722.5**	**2.3**
58	45265	2.0	5.3009	0.7	13.5956	2.5	0.5227	2.4	0.96	2710.6	52.9	2722.0	23.6	2730.4	11.9	**2730.4**	**11.9**
440	353389	1.6	4.8934	0.1	15.1147	2.3	0.5364	2.3	1.00	2768.4	50.7	2822.5	21.5	2861.3	1.2	**2861.3**	**1.2**
37	44564	1.1	3.7351	0.5	22.4421	3.0	0.6079	2.9	0.98	3061.8	71.0	3203.1	28.8	3292.8	8.1	**3292.8**	**8.1**
3B																	
247	234897	1.2	19.4993	2.2	0.2888	2.8	0.0408	1.6	0.60	258.0	4.2	257.6	6.3	253.6	50.7	**258.0**	**4.2**
388	36045	1.4	19.1426	2.9	0.3021	3.4	0.0419	1.7	0.50	264.9	4.4	268.1	7.9	295.9	66.6	**264.9**	**4.4**
95	16938	1.3	21.7950	6.6	0.2664	7.4	0.0421	3.5	0.47	265.9	9.0	239.8	15.9	-8.6	159.3	**265.9**	**9.0**
21	8554	20.6	22.3931	16.8	0.5070	16.8	0.0823	1.5	0.09	510.1	7.6	416.5	57.6	-74.3	412.6	**510.1**	**7.6**
344	91452	1.8	17.0389	1.0	0.7096	2.1	0.0877	1.8	0.86	541.9	9.2	544.5	8.7	555.6	22.9	**541.9**	**9.2**
226	72885	1.2	17.0326	1.6	0.7138	2.8	0.0882	2.3	0.83	544.7	12.2	547.0	11.8	556.4	34.0	**544.7**	**12.2**
187	72225	3.4	17.0802	1.6	0.7151	1.9	0.0886	1.1	0.58	547.2	5.9	547.8	8.1	550.3	33.9	**547.2**	**5.9**
124	39458	1.0	16.8084	1.9	0.7325	3.4	0.0893	2.9	0.84	551.4	15.2	558.0	14.7	585.2	40.4	**551.4**	**15.2**

Appendix A continued. U-Pb analysis results of detrital zircons from the till of the Mt. Achernar moraine.

			Isotope ratios							Apparent ages (Ma)							
U	206Pb	U/Th	206Pb*		207Pb*		206Pb*		error	206Pb*		207Pb*		206Pb*		Best	
(ppm)	204Pb		207Pb*	(%)	235U*	(%)	238U	(%)	corr.	238U*	± (Ma)	235U	± (Ma)	207Pb*	± (Ma)	age	± (Ma)
260	106843	2.1	17.0656	1.0	0.7225	2.0	0.0894	1.8	0.88	552.1	9.5	552.1	8.7	552.2	21.0	**552.1**	**9.5**
313	121282	3.8	17.1191	1.3	0.7206	2.5	0.0895	2.1	0.85	552.4	11.1	551.0	10.5	545.3	28.9	**552.4**	**11.1**
59	19989	1.5	17.2425	5.8	0.7188	6.4	0.0899	2.6	0.41	554.9	13.8	550.0	27.0	529.6	127.4	**554.9**	**13.8**
51	11654	1.4	16.7164	5.7	0.7448	6.0	0.0903	1.7	0.29	557.3	9.3	565.2	25.9	597.1	124.2	**557.3**	**9.3**
102	48542	2.8	17.1432	2.7	0.7267	3.4	0.0904	2.0	0.59	557.7	10.7	554.6	14.5	542.3	60.0	**557.7**	**10.7**
47	14811	0.4	16.2847	10.5	0.7673	10.7	0.0906	1.7	0.16	559.2	8.9	578.2	47.0	653.5	226.3	**559.2**	**8.9**
121	80178	2.4	17.1094	3.1	0.7360	4.1	0.0913	2.7	0.66	563.4	14.5	560.0	17.6	546.6	67.3	**563.4**	**14.5**
22	10776	0.7	18.0432	12.3	0.6990	12.5	0.0915	1.9	0.15	564.3	10.0	538.2	52.2	429.3	276.0	**564.3**	**10.0**
124	51474	1.9	17.4505	1.7	0.7237	2.5	0.0916	1.8	0.72	565.0	9.8	552.9	10.7	503.3	38.1	**565.0**	**9.8**
150	23151	0.9	17.0230	1.7	0.7421	2.1	0.0916	1.1	0.54	565.1	6.0	563.7	8.9	557.6	38.0	**565.1**	**6.0**
153	51221	3.1	16.7406	1.6	0.7547	2.0	0.0916	1.1	0.56	565.2	6.0	570.9	8.6	594.0	35.6	**565.2**	**6.0**
184	75695	1.5	16.9463	1.4	0.7481	2.3	0.0919	1.9	0.80	567.0	10.2	567.1	10.2	567.5	30.6	**567.0**	**10.2**
59	29186	2.3	16.9540	5.6	0.7489	6.0	0.0921	2.2	0.36	567.9	11.7	567.6	26.2	566.5	122.4	**567.9**	**11.7**
536	27678	3.8	16.4405	1.3	0.7729	6.3	0.0922	6.1	0.98	568.3	33.2	581.4	27.7	633.1	29.0	**568.3**	**33.2**
197	74022	1.0	16.8092	1.9	0.7568	2.5	0.0923	1.6	0.63	568.9	8.5	572.2	10.8	585.1	41.6	**568.9**	**8.5**
149	69871	9.4	16.5392	1.1	0.7693	4.6	0.0923	4.5	0.97	569.0	24.6	579.4	20.5	620.1	22.8	**569.0**	**24.6**
398	129504	2.8	16.8688	0.6	0.7568	1.3	0.0926	1.2	0.91	570.9	6.5	572.2	5.7	577.4	12.0	**570.9**	**6.5**
236	14998	1.9	16.6997	3.5	0.7663	4.0	0.0928	2.1	0.51	572.2	11.3	577.6	17.7	599.3	75.0	**572.2**	**11.3**
56	30125	3.9	17.2318	6.7	0.7433	7.1	0.0929	2.4	0.33	572.6	12.9	564.3	30.7	531.0	146.7	**572.6**	**12.9**
29	7636	0.4	16.8195	8.2	0.7644	9.1	0.0932	3.9	0.43	574.7	21.6	576.5	40.1	583.8	178.6	**574.7**	**21.6**
542	210009	7.6	16.9996	0.6	0.7576	1.5	0.0934	1.4	0.92	575.6	7.8	572.6	6.7	560.6	13.1	**575.6**	**7.8**
129	48385	0.9	17.0735	3.0	0.7551	3.3	0.0935	1.3	0.40	576.3	7.3	571.2	14.3	551.2	65.5	**576.3**	**7.3**
93	40273	2.2	17.0335	2.3	0.7574	4.1	0.0936	3.4	0.83	576.6	18.9	572.5	18.0	556.3	49.3	**576.6**	**18.9**
152	42630	0.9	16.9410	1.4	0.7621	1.8	0.0936	1.0	0.59	577.0	5.7	575.2	7.7	568.2	31.0	**577.0**	**5.7**
66	28859	0.3	17.2952	4.8	0.7517	5.4	0.0943	2.4	0.45	580.8	13.5	569.2	23.4	522.9	105.2	**580.8**	**13.5**
155	49421	1.9	16.7954	1.7	0.7761	2.1	0.0945	1.2	0.55	582.3	6.4	583.3	9.3	586.9	37.8	**582.3**	**6.4**
335	79682	6.6	16.7731	1.2	0.7777	2.5	0.0946	2.1	0.88	582.7	12.0	584.1	10.9	589.8	25.7	**582.7**	**12.0**
50	27229	4.9	17.6927	7.6	0.7375	7.9	0.0946	1.9	0.24	582.9	10.7	561.0	33.9	472.9	169.0	**582.9**	**10.7**
603	200120	2.0	16.8184	0.8	0.7772	1.3	0.0948	1.1	0.81	583.8	5.9	583.9	5.8	583.9	16.6	**583.8**	**5.9**
286	41312	3.3	16.4967	1.7	0.7924	3.1	0.0948	2.5	0.83	583.9	14.2	592.5	13.8	625.7	36.8	**583.9**	**14.2**
78	51437	0.3	16.7336	6.5	0.7827	7.0	0.0950	2.8	0.39	585.0	15.5	587.0	31.4	594.9	140.3	**585.0**	**15.5**
82	37750	0.6	16.7821	3.2	0.7817	3.8	0.0951	1.9	0.51	585.9	10.6	586.4	16.7	588.6	70.3	**585.9**	**10.6**
23	9319	1.4	15.7962	8.5	0.8321	8.7	0.0953	1.9	0.22	587.0	10.5	614.8	40.1	718.5	180.7	**587.0**	**10.5**
160	31000	1.2	16.9836	1.1	0.7755	1.6	0.0955	1.2	0.76	588.1	6.9	582.9	7.2	562.6	23.3	**588.1**	**6.9**
106	31470	0.4	16.6265	4.4	0.7940	4.6	0.0957	1.3	0.29	589.4	7.4	593.4	20.5	608.8	94.7	**589.4**	**7.4**
146	31982	1.5	16.4275	2.7	0.8042	3.1	0.0958	1.5	0.48	589.8	8.5	599.2	14.2	634.8	59.1	**589.8**	**8.5**
100	38864	849.9	17.1628	3.3	0.7704	3.4	0.0959	0.9	0.25	590.3	4.8	580.0	15.1	539.8	72.3	**590.3**	**4.8**
565	280505	28.1	16.7404	0.6	0.7902	1.5	0.0959	1.4	0.91	590.6	8.0	591.3	6.9	594.0	13.7	**590.6**	**8.0**
378	134531	9.7	16.6785	0.7	0.7936	1.5	0.0960	1.3	0.87	590.9	7.2	593.2	6.6	602.0	15.7	**590.9**	**7.2**
539	178931	3.6	16.6353	0.6	0.7971	0.9	0.0962	0.7	0.76	591.9	3.9	595.2	4.0	607.6	12.6	**591.9**	**3.9**
132	45254	1.2	16.7327	2.4	0.7930	2.9	0.0962	1.6	0.56	592.3	9.1	592.9	12.8	595.0	51.1	**592.3**	**9.1**
262	116278	0.4	16.7539	1.1	0.7930	1.6	0.0964	1.1	0.71	593.0	6.3	592.9	7.1	592.3	24.1	**593.0**	**6.3**
184	52261	1.6	16.6840	1.7	0.7975	2.1	0.0965	1.1	0.55	593.8	6.5	595.4	9.4	601.3	37.8	**593.8**	**6.5**
134	57326	1.7	16.9184	2.3	0.7868	2.5	0.0965	0.9	0.35	594.1	5.0	589.3	11.1	571.1	50.6	**594.1**	**5.0**
250	52090	1.8	16.6267	1.8	0.8029	5.7	0.0968	5.4	0.95	595.8	30.5	598.5	25.6	608.7	38.7	**595.8**	**30.5**
268	79788	1.6	16.6755	1.1	0.8007	1.3	0.0968	0.8	0.62	595.9	4.7	597.3	6.1	602.4	22.9	**595.9**	**4.7**
155	39499	1.4	16.5972	2.1	0.8072	2.9	0.0972	2.0	0.68	597.8	11.2	600.9	13.0	612.6	45.1	**597.8**	**11.2**
197	224103	10.1	16.1781	1.7	0.8290	3.6	0.0973	3.2	0.88	598.4	18.2	613.1	16.7	667.6	36.9	**598.4**	**18.2**
97	36388	1.0	16.6895	3.4	0.8046	3.7	0.0974	1.5	0.40	599.1	8.4	599.4	16.7	600.6	73.2	**599.1**	**8.4**
135	70319	1.8	16.3556	1.6	0.8246	4.9	0.0978	4.6	0.94	601.6	26.5	610.6	22.5	644.2	35.0	**601.6**	**26.5**
180	79756	3.4	16.7304	1.3	0.8070	1.8	0.0979	1.2	0.68	602.2	7.0	600.8	8.2	595.3	28.8	**602.2**	**7.0**
752	274933	5.2	16.6769	0.5	0.8165	0.8	0.0988	0.7	0.80	607.1	3.9	606.1	3.8	602.2	10.9	**607.1**	**3.9**
522	165542	0.9	16.6386	0.6	0.8187	1.1	0.0988	0.9	0.85	607.3	5.3	607.3	4.9	607.2	12.2	**607.3**	**5.3**
221	44897	0.6	16.8070	2.1	0.8106	2.3	0.0988	0.9	0.40	607.4	5.3	602.8	10.4	585.4	45.4	**607.4**	**5.3**
133	57717	0.9	16.6357	3.1	0.8254	4.0	0.0996	2.6	0.65	612.0	15.2	611.0	18.5	607.6	66.2	**612.0**	**15.2**
209	115319	2.0	16.5919	1.2	0.8278	2.7	0.0996	2.4	0.89	612.1	14.1	612.4	12.5	613.3	26.6	**612.1**	**14.1**
108	58708	1.4	16.6432	2.6	0.8256	3.2	0.0997	1.8	0.57	612.4	10.6	611.2	14.7	606.6	57.0	**612.4**	**10.6**
390	140730	0.9	16.5357	0.5	0.8330	0.8	0.0999	0.7	0.81	613.8	4.0	615.3	3.9	620.6	10.7	**613.8**	**4.0**
224	69801	1.2	16.6824	1.9	0.8267	2.2	0.1000	1.1	0.50	614.6	6.5	611.8	10.1	601.5	41.4	**614.6**	**6.5**
398	211964	1.9	16.6123	0.9	0.8383	1.4	0.1010	1.0	0.74	620.3	5.9	618.2	6.3	610.6	19.7	**620.3**	**5.9**
367	138417	1.6	16.5880	0.8	0.8405	2.5	0.1011	2.3	0.95	621.0	13.9	619.4	11.5	613.8	17.4	**621.0**	**13.9**
111	64549	11.3	15.4825	4.2	0.9026	7.0	0.1013	5.6	0.80	622.3	33.0	653.1	33.6	761.0	88.7	**622.3**	**33.0**
240	60225	3.3	16.4144	1.1	0.8863	1.4	0.1055	0.9	0.67	646.6	5.8	644.4	6.7	636.5	22.7	**646.6**	**5.8**
58	964	1.0	14.9249	8.0	0.9920	8.3	0.1074	2.3	0.28	657.5	14.3	699.8	42.1	837.8	167.0	**657.5**	**14.3**
493	212852	5.4	15.5502	1.1	1.0240	2.7	0.1155	2.5	0.92	704.5	16.9	715.9	14.1	751.7	22.2	**704.5**	**16.9**
60	22326	4.0	15.1209	3.5	1.1300	6.5	0.1239	5.5	0.85	753.1	39.1	767.8	35.0	810.6	72.4	**753.1**	**39.1**
58	21283	3.9	15.0051	3.3	1.1804	3.9	0.1285	2.2	0.55	779.1	15.9	791.5	21.6	826.7	68.6	**779.1**	**15.9**
129	47997	1.1	14.5021	1.6	1.2836	2.2	0.1350	1.5	0.68	816.4	11.3	838.4	12.4	897.4	33.0	**816.4**	**11.3**
156	119499	4.5	14.5660	1.3	1.2863	2.7	0.1359	2.4	0.88	821.4	18.3	839.7	15.3	888.3	26.0	**821.4**	**18.3**
87	42055	2.2	14.2050	2.1	1.3325	2.8	0.1373	1.9	0.67	829.3	14.6	860.0	16.3	940.0	43.0	**829.3**	**14.6**
422	125642	3.4	15.0472	2.2	1.2808	8.3	0.1398	8.0	0.96	843.4	63.0	837.2	47.2	820.8	46.4	**843.4**	**63.0**
297	123458	4.8	14.0664	0.4	1.5528	1.7	0.1584	1.6	0.97	948.0	14.2	951.6	10.3	960.1	8.7	**960.1**	**8.7**
114	67173	1.7	13.7420	2.4	1.5473	6.7	0.1542	6.2	0.93	924.5	53.4	949.4	41.1	1007.5	49.7	**1007.5**	**49.7**
339	139674	5.9	13.4695	0.4	1.7214	1.6	0.1682	1.5	0.97	1002.0	14.1	1016.5	10.1	1048.1	7.8	**1048.1**	**7.8**
505	371215	4.4	13.3698	0.3	1.8287	1.8	0.1773	1.8	0.98	1052.4	17.4	1055.8	12.0	1063.0	6.7	**1063.0**	**6.7**
263	255123	1.8	13.3446	0.5	1.8093	1.9	0.1751	1.9	0.97	1040.2	17.8	1048.8	12.6	1066.8	9.9	**1066.8**	**9.9**
301	113009	1.3	13.2818	0.7	1.8426	1.0	0.1775	0.7	0.73	1053.3	6.8	1060.8	6.4	1076.3	13.3	**1076.3**	**13.3**
229	232423	1.8	13.2632	0.7	1.8785	3.2	0.1807	3.1	0.97	1070.8	30.5	1073.5	21.0	1079.1	14.6	**1079.1**	**14.6**

Appendix A continued. U-Pb analysis results of detrital zircons from the till of the Mt. Achernar moraine.

			Isotope ratios							Apparent ages (Ma)							
U	206Pb	U/Th	206Pb*		207Pb*		206Pb*		error	206Pb*		207Pb*		206Pb*		Best	
(ppm)	204Pb		207Pb*	(%)	235U*	(%)	238U	(%)	corr.	238U*	± (Ma)	235U	± (Ma)	207Pb*	± (Ma)	age	± (Ma)
268	233366	2.3	13.1477	0.5	1.9552	3.4	0.1864	3.3	0.99	1102.1	33.8	1100.2	22.6	1096.6	9.9	**1096.6**	**9.9**
175	112958	2.0	12.9012	0.8	1.8758	2.1	0.1755	1.9	0.92	1042.4	18.5	1072.6	13.8	1134.4	15.9	**1134.4**	**15.9**
344	54215	1.6	12.7157	0.3	2.0314	2.0	0.1873	1.9	0.99	1106.9	19.8	1126.1	13.5	1163.1	6.6	**1163.1**	**6.6**
98	76669	1.5	12.5944	1.5	2.1972	1.9	0.2007	1.2	0.63	1179.1	12.9	1180.2	13.2	1182.1	28.9	**1182.1**	**28.9**
340	309270	2.0	12.5664	0.3	2.1944	1.3	0.2000	1.3	0.98	1175.3	14.1	1179.3	9.3	1186.6	5.0	**1186.6**	**5.0**
133	52121	1.3	12.4098	0.9	2.2560	1.2	0.2030	0.8	0.69	1191.7	9.1	1198.7	8.5	1211.2	17.1	**1211.2**	**17.1**
70	66055	1.0	12.3840	2.2	2.2543	2.5	0.2025	1.2	0.49	1188.6	13.5	1198.1	17.7	1215.4	43.0	**1215.4**	**43.0**
419	71305	1.9	12.0884	0.3	2.3998	1.1	0.2104	1.1	0.97	1231.0	12.1	1242.5	8.0	1262.7	5.0	**1262.7**	**5.0**
39	16352	1.1	10.9007	2.4	3.1636	3.0	0.2501	1.8	0.59	1439.0	22.6	1448.3	22.8	1461.9	45.3	**1461.9**	**45.3**
307	296824	1.5	10.7560	0.6	3.1687	2.5	0.2472	2.4	0.97	1423.9	30.5	1449.6	19.1	1487.3	11.9	**1487.3**	**11.9**
53	21214	0.7	10.0650	3.2	3.2676	4.7	0.2385	3.5	0.74	1379.1	43.6	1473.4	36.7	1612.0	58.8	**1612.0**	**58.8**
351	459318	3.6	9.0154	0.6	4.2601	2.6	0.2786	2.5	0.97	1584.1	35.2	1685.7	21.3	1814.5	11.5	**1814.5**	**11.5**
126	128028	2.2	8.2261	0.3	5.9016	0.8	0.3521	0.7	0.92	1944.6	11.7	1961.5	6.6	1979.3	5.4	**1979.3**	**5.4**
187	185473	1.3	7.6980	0.4	6.4808	1.7	0.3618	1.7	0.97	1990.9	28.7	2043.3	15.2	2096.6	7.6	**2096.6**	**7.6**
196	213128	2.7	7.2028	2.8	7.2658	6.9	0.3796	6.4	0.92	2074.2	113.0	2144.6	62.1	2212.7	48.0	**2212.7**	**48.0**
28	22504	1.7	7.1162	2.6	5.5312	8.0	0.2855	7.6	0.95	1618.9	108.6	1905.5	69.0	2233.7	44.4	**2233.7**	**44.4**
357	408200	0.8	7.1079	0.3	7.0950	2.3	0.3658	2.3	0.99	2009.4	39.3	2123.4	20.4	2235.7	4.9	**2235.7**	**4.9**
216	126870	5.1	6.7513	0.7	6.4581	5.6	0.3162	5.5	0.99	1771.3	85.6	2040.2	49.0	2324.3	11.5	**2324.3**	**11.5**
229	252845	4.0	6.6184	0.5	8.5773	3.4	0.4117	3.4	0.99	2222.8	63.1	2294.2	30.8	2358.3	7.7	**2358.3**	**7.7**
485	345095	3.3	6.5817	0.3	8.4607	2.5	0.4039	2.5	0.99	2186.8	45.8	2281.7	22.6	2367.8	5.5	**2367.8**	**5.5**
250	385530	1.5	6.3773	0.2	8.9815	1.4	0.4154	1.4	0.99	2239.6	26.3	2336.1	12.9	2421.5	3.8	**2421.5**	**3.8**
124	237900	1.8	6.2864	0.4	9.4552	2.3	0.4311	2.2	0.98	2310.6	43.0	2383.2	20.8	2445.8	7.5	**2445.8**	**7.5**
147	147461	2.2	6.1840	0.9	9.4649	6.0	0.4245	5.9	0.99	2280.9	113.8	2384.1	55.0	2473.6	14.8	**2473.6**	**14.8**
210	424756	2.9	5.6370	0.2	10.1424	3.1	0.4147	3.1	1.00	2236.2	59.4	2447.8	29.1	2628.7	3.1	**2628.7**	**3.1**
126	258597	1.0	5.5764	0.2	10.2980	2.2	0.4165	2.2	1.00	2244.5	41.6	2461.9	20.4	2646.6	3.6	**2646.6**	**3.6**
81	42482	0.9	5.4495	0.4	12.0034	5.1	0.4744	5.1	1.00	2502.9	106.5	2604.7	48.3	2684.8	5.8	**2684.8**	**5.8**
74	115858	1.5	5.3554	0.6	14.1002	8.0	0.5477	8.0	1.00	2815.5	181.5	2756.5	75.8	2713.5	9.9	**2713.5**	**9.9**
412	791247	2.5	5.3388	0.1	13.3029	3.9	0.5151	3.9	1.00	2678.4	84.9	2701.4	36.6	2718.7	1.7	**2718.7**	**1.7**
104	363878	3.1	5.2604	0.2	14.0710	1.0	0.5368	1.0	0.97	2770.2	21.9	2754.5	9.5	2743.0	3.8	**2743.0**	**3.8**
131	261414	1.2	5.1811	0.2	13.1942	1.9	0.4958	1.9	0.99	2595.7	40.7	2693.6	18.1	2768.0	3.4	**2768.0**	**3.4**
127	333187	1.0	4.9654	0.1	15.1926	1.2	0.5471	1.2	0.99	2813.2	26.8	2827.4	11.3	2837.5	2.2	**2837.5**	**2.2**
75	156617	6.7	4.2423	0.3	19.3816	1.7	0.5963	1.7	0.99	3015.0	41.2	3061.0	16.7	3091.3	4.3	**3091.3**	**4.3**
158	292326	1.6	3.9699	0.1	21.3512	0.9	0.6148	0.9	0.99	3089.0	22.9	3154.7	9.1	3196.7	2.0	**3196.7**	**2.0**
197	427794	4.7	3.9459	0.4	20.6556	2.6	0.5911	2.6	0.99	2994.0	62.7	3122.6	25.6	3206.3	5.6	**3206.3**	**5.6**
220	341243	2.2	3.8218	0.2	22.8605	2.7	0.6337	2.7	1.00	3164.0	66.6	3221.0	26.0	3256.7	2.7	**3256.7**	**2.7**
4L																	
1205	137679	0.6	19.4799	1.0	0.2771	1.4	0.0392	1.1	0.74	247.6	2.6	248.4	3.2	255.9	22.2	**247.6**	**2.6**
306	25794	1.1	19.8721	2.0	0.2804	3.0	0.0404	2.2	0.74	255.4	5.5	251.0	6.6	209.9	46.2	**255.4**	**5.5**
582	86642	2.1	19.4686	1.3	0.2884	2.4	0.0407	2.0	0.83	257.3	4.9	257.3	5.4	257.2	30.8	**257.3**	**4.9**
126	21146	1.5	19.9523	7.5	0.2849	7.6	0.0412	1.2	0.15	260.4	2.9	254.5	17.1	200.6	174.7	**260.4**	**2.9**
137	49172	1.4	19.0851	4.0	0.4243	4.2	0.0587	1.3	0.31	367.9	4.6	359.1	12.7	302.8	91.4	**367.9**	**4.6**
223	84826	13.5	17.3915	0.4	0.6427	1.7	0.0811	1.6	0.97	502.5	7.7	504.0	6.6	510.7	8.8	**502.5**	**7.7**
253	60298	1.6	17.4180	1.0	0.6495	2.4	0.0821	2.2	0.90	508.4	10.6	508.2	9.6	507.4	23.0	**508.4**	**10.6**
114	36629	1.3	17.4062	3.5	0.6588	4.0	0.0832	2.1	0.52	515.0	10.3	513.9	16.3	508.9	76.2	**515.0**	**10.3**
50	12481	5.9	17.4735	10.3	0.6578	11.2	0.0834	4.4	0.39	516.2	21.8	513.3	45.3	500.4	228.1	**516.2**	**21.8**
75	32512	2.5	17.2127	4.4	0.6770	4.9	0.0845	2.2	0.44	523.0	10.8	525.0	20.1	533.4	96.6	**523.0**	**10.8**
6	1536	10.4	22.8344	30.3	0.5104	31.9	0.0845	9.7	0.30	523.1	48.8	418.7	109.8	-122.3	763.9	**523.1**	**48.8**
222	50212	1.5	17.5630	0.7	0.6651	1.7	0.0847	1.5	0.90	524.2	7.7	517.7	6.9	489.1	16.2	**524.2**	**7.7**
256	32770	1.2	17.0660	1.0	0.6891	2.0	0.0853	1.7	0.86	527.6	8.6	532.3	8.2	552.1	22.0	**527.6**	**8.6**
148	67397	2.1	17.2140	2.3	0.6892	2.8	0.0860	1.7	0.60	532.1	8.6	532.3	11.7	533.2	49.4	**532.1**	**8.6**
62	26248	1.2	17.5568	3.6	0.6816	3.9	0.0868	1.5	0.38	536.5	7.6	527.8	16.1	489.9	80.2	**536.5**	**7.6**
285	30742	2.1	16.3955	1.5	0.7367	4.8	0.0876	4.6	0.95	541.3	23.7	560.5	20.6	639.0	31.2	**541.3**	**23.7**
1325	523560	10.7	17.0685	0.2	0.7126	1.3	0.0882	1.3	0.98	545.0	6.9	546.3	5.6	551.8	5.3	**545.0**	**6.9**
112	30319	3.1	17.3163	2.6	0.7052	3.1	0.0886	1.7	0.53	547.0	8.7	541.9	13.0	520.2	57.3	**547.0**	**8.7**
11	3865	0.3	16.8528	19.7	0.7258	21.0	0.0887	7.3	0.35	547.9	38.4	554.1	89.8	579.5	430.8	**547.9**	**38.4**
174	15439	2.6	17.0408	1.6	0.7182	1.7	0.0888	0.6	0.36	548.2	3.2	549.6	7.1	555.3	34.0	**548.2**	**3.2**
249	109097	1.4	16.9099	1.3	0.7245	1.6	0.0889	1.0	0.61	548.8	5.2	553.3	6.8	572.1	27.5	**548.8**	**5.2**
102	53898	2.8	17.0652	3.3	0.7180	3.5	0.0889	1.2	0.34	548.8	6.1	549.5	14.7	552.2	71.2	**548.8**	**6.1**
255	73414	1.8	17.1176	1.2	0.7172	1.8	0.0890	1.3	0.72	549.9	6.7	549.0	7.5	545.5	26.8	**549.9**	**6.7**
191	56676	4.4	17.1469	1.4	0.7183	1.9	0.0893	1.4	0.71	551.5	7.3	549.6	8.2	541.8	29.8	**551.5**	**7.3**
211	57430	3.1	17.0649	1.0	0.7221	1.6	0.0894	1.3	0.78	551.8	6.6	551.9	6.8	552.3	21.6	**551.8**	**6.6**
144	49578	3.1	16.9810	1.4	0.7263	2.0	0.0894	1.4	0.70	552.3	7.5	554.4	8.6	563.0	31.3	**552.3**	**7.5**
45	15539	1.0	16.4033	5.5	0.7526	5.9	0.0895	2.2	0.38	552.8	11.8	569.7	25.8	638.0	118.1	**552.8**	**11.8**
335	111911	1.8	16.9786	0.9	0.7279	1.5	0.0896	1.3	0.83	553.4	6.8	555.3	6.6	563.3	18.7	**553.4**	**6.8**
488	158487	5.1	17.0629	0.7	0.7245	3.1	0.0897	3.0	0.97	553.5	15.8	553.3	13.1	552.5	16.3	**553.5**	**15.8**
33	8753	0.4	17.0602	11.4	0.7247	12.5	0.0897	5.2	0.41	553.6	27.4	553.4	53.4	552.9	249.5	**553.6**	**27.4**
125	38007	31.3	17.3813	2.2	0.7143	2.6	0.0900	1.3	0.49	555.8	6.8	547.3	10.9	512.0	49.1	**555.8**	**6.8**
272	90307	2.1	16.8805	1.3	0.7363	1.7	0.0901	1.1	0.63	556.4	5.8	560.2	7.4	575.9	28.9	**556.4**	**5.8**
121	60325	3.9	17.3458	2.6	0.7170	3.0	0.0902	1.5	0.49	556.7	7.8	548.9	12.7	516.5	57.2	**556.7**	**7.8**
60	16924	0.8	16.8695	4.1	0.7397	4.7	0.0905	2.4	0.51	558.5	12.7	562.2	20.3	577.4	88.1	**558.5**	**12.7**
324	145209	3.6	16.9326	0.8	0.7407	2.7	0.0910	2.6	0.95	561.3	13.7	562.8	11.6	569.2	18.3	**561.3**	**13.7**
92	46357	312.8	17.0254	2.6	0.7376	3.2	0.0911	1.9	0.58	561.9	10.0	561.0	13.9	557.3	57.4	**561.9**	**10.0**
124	26279	0.9	17.1158	2.7	0.7355	2.8	0.0913	0.9	0.30	563.2	4.6	559.8	12.2	545.8	58.8	**563.2**	**4.6**
220	136714	3.9	16.9434	1.5	0.7443	1.7	0.0915	0.7	0.39	564.2	3.6	564.9	7.3	567.9	33.7	**564.2**	**3.6**
387	171658	4.3	17.0263	0.6	0.7417	2.8	0.0916	2.7	0.97	564.9	14.8	563.4	12.2	557.2	13.7	**564.9**	**14.8**
231	54420	2.4	16.6810	1.8	0.7596	3.4	0.0919	2.9	0.84	566.8	15.5	573.8	14.9	601.7	40.0	**566.8**	**15.5**
66	15803	1.7	16.9639	3.7	0.7475	4.0	0.0920	1.4	0.35	567.2	7.6	566.8	17.3	565.2	81.1	**567.2**	**7.6**
69	55189	0.5	17.0362	1.9	0.7449	2.4	0.0920	1.5	0.63	567.6	8.1	565.3	10.4	556.0	40.6	**567.6**	**8.1**

Appendix A continued. U-Pb analysis results of detrital zircons from the till of the Mt. Achernar moraine.

			Isotope ratios							Apparent ages (Ma)							
U	206Pb	U/Th	206Pb*		207Pb*		206Pb*		error	206Pb*		207Pb*		206Pb*		Best	
(ppm)	204Pb		207Pb*	(%)	235U*	(%)	238U	(%)	corr.	238U*	± (Ma)	235U	± (Ma)	207Pb*	± (Ma)	age	± (Ma)
88	116321	1.4	16.8191	4.4	0.7567	4.7	0.0923	1.6	0.33	569.2	8.4	572.1	20.3	583.8	95.2	**569.2**	**8.4**
96	33397	0.9	16.8121	2.2	0.7598	2.5	0.0926	1.1	0.43	571.1	5.9	573.9	10.9	584.8	48.6	**571.1**	**5.9**
377	81995	5.1	16.9525	0.7	0.7581	1.1	0.0932	0.9	0.76	574.5	4.7	572.9	5.0	566.7	16.1	**574.5**	**4.7**
124	70273	1.3	16.4509	1.5	0.7826	2.5	0.0934	1.9	0.78	575.4	10.6	586.9	11.0	631.7	32.9	**575.4**	**10.6**
74	19805	0.4	17.3577	4.9	0.7424	5.4	0.0935	2.3	0.43	575.9	12.8	563.8	23.3	515.0	106.8	**575.9**	**12.8**
85	24649	6.7	17.0108	3.3	0.7577	3.5	0.0935	1.1	0.30	576.1	5.9	572.7	15.3	559.2	72.9	**576.1**	**5.9**
38	12727	3.1	17.8460	7.5	0.7236	8.0	0.0937	2.8	0.35	577.1	15.5	552.8	34.1	453.8	166.2	**577.1**	**15.5**
463	216192	7.2	16.9186	1.2	0.7636	2.5	0.0937	2.2	0.88	577.4	12.2	576.1	11.0	571.0	25.9	**577.4**	**12.2**
143	25158	0.4	17.1589	3.0	0.7548	4.1	0.0939	2.7	0.67	578.7	15.1	571.0	17.8	540.3	66.1	**578.7**	**15.1**
102	52960	1.0	16.8338	2.3	0.7749	2.5	0.0946	1.0	0.39	582.8	5.4	582.6	11.2	582.0	50.6	**582.8**	**5.4**
85	28115	0.3	16.7710	3.4	0.7781	4.3	0.0946	2.5	0.59	583.0	14.1	584.4	18.9	590.1	74.2	**583.0**	**14.1**
65	24497	0.5	17.1691	3.6	0.7604	3.9	0.0947	1.3	0.34	583.2	7.3	574.2	16.9	538.9	79.4	**583.2**	**7.3**
577	280243	2.9	16.8087	0.3	0.7780	0.8	0.0948	0.7	0.90	584.1	3.8	584.3	3.4	585.2	7.2	**584.1**	**3.8**
384	186476	1.9	16.8618	1.0	0.7764	4.0	0.0950	3.8	0.97	584.8	21.4	583.4	17.6	578.3	22.5	**584.8**	**21.4**
449	332140	2.1	16.8475	0.6	0.7778	1.8	0.0950	1.7	0.94	585.2	9.4	584.2	7.9	580.2	12.9	**585.2**	**9.4**
340	15545	0.9	16.4181	2.5	0.7987	3.5	0.0951	2.5	0.69	585.7	13.7	596.1	15.9	636.0	54.8	**585.7**	**13.7**
524	249444	4.3	16.7361	0.9	0.7836	3.4	0.0951	3.2	0.97	585.7	18.2	587.5	15.0	594.6	18.5	**585.7**	**18.2**
66	14472	1.1	16.3389	5.2	0.8040	5.4	0.0953	1.7	0.32	586.6	9.6	599.1	24.6	646.4	110.7	**586.6**	**9.6**
134	67689	1.7	16.6260	2.1	0.7915	2.4	0.0954	1.0	0.41	587.6	5.4	592.0	10.6	608.8	46.5	**587.6**	**5.4**
108	22247	1.6	17.2371	3.7	0.7638	4.3	0.0955	2.1	0.49	587.9	11.9	576.2	18.9	530.3	81.8	**587.9**	**11.9**
74	35540	1.3	17.0650	3.8	0.7722	4.1	0.0956	1.4	0.34	588.4	7.8	581.0	18.0	552.3	83.8	**588.4**	**7.8**
31	11044	0.3	17.2479	6.3	0.7652	6.9	0.0957	2.7	0.40	589.3	15.5	577.0	30.3	529.0	138.3	**589.3**	**15.5**
98	33021	1.5	17.1087	2.0	0.7728	2.2	0.0959	0.8	0.38	590.3	4.7	581.4	9.7	546.6	44.2	**590.3**	**4.7**
54	38185	0.8	16.7457	2.9	0.7897	3.5	0.0959	2.0	0.58	590.4	11.5	591.0	15.8	593.3	62.0	**590.4**	**11.5**
75	25382	0.5	17.1672	2.1	0.7787	2.4	0.0970	1.3	0.53	596.5	7.3	584.7	10.8	539.2	45.3	**596.5**	**7.3**
43	17643	0.8	17.0753	6.8	0.7829	7.6	0.0970	3.6	0.47	596.6	20.3	587.2	34.1	550.9	147.6	**596.6**	**20.3**
183	38806	0.4	16.9959	1.1	0.7907	3.4	0.0975	3.3	0.95	599.5	18.7	591.6	15.5	561.1	24.2	**599.5**	**18.7**
86	40009	0.7	16.7245	3.3	0.8050	3.5	0.0976	1.0	0.29	600.6	5.8	599.6	15.7	596.1	72.0	**600.6**	**5.8**
203	135407	2.5	16.4026	1.2	0.8250	4.5	0.0981	4.4	0.97	603.5	25.1	610.8	20.7	638.1	25.0	**603.5**	**25.1**
336	97864	1.2	16.7134	0.9	0.8132	1.2	0.0986	0.7	0.63	606.1	4.3	604.3	5.3	597.5	19.6	**606.1**	**4.3**
417	157401	3.0	16.6375	0.8	0.8206	2.2	0.0990	2.1	0.94	608.6	12.2	608.4	10.2	607.3	16.3	**608.6**	**12.2**
478	196595	1.4	16.4898	0.4	0.8282	0.9	0.0990	0.8	0.89	608.8	4.6	612.6	4.1	626.6	8.9	**608.8**	**4.6**
273	204524	3.0	16.6886	0.7	0.8219	0.9	0.0995	0.6	0.67	611.4	3.6	609.1	4.2	600.7	14.6	**611.4**	**3.6**
119	21157	1.7	16.4990	2.8	0.8328	4.1	0.0997	3.1	0.75	612.4	18.2	615.2	19.1	625.4	59.3	**612.4**	**18.2**
366	143605	1.3	16.6114	0.7	0.8302	2.5	0.1000	2.4	0.97	614.5	14.2	613.7	11.5	610.7	14.2	**614.5**	**14.2**
64	30053	30.3	16.6730	3.5	0.8273	4.6	0.1000	3.0	0.65	614.6	17.6	612.1	21.1	602.7	75.5	**614.6**	**17.6**
194	48771	3.3	16.6851	1.6	0.8283	2.9	0.1002	2.4	0.84	615.8	14.4	612.7	13.4	601.2	34.4	**615.8**	**14.4**
112	63644	1.1	16.2795	2.4	0.8525	4.4	0.1007	3.7	0.84	618.2	21.8	626.0	20.6	654.2	51.3	**618.2**	**21.8**
293	109407	2.4	16.6478	0.8	0.8445	1.0	0.1020	0.5	0.55	625.9	3.2	621.6	4.4	606.0	17.2	**625.9**	**3.2**
195	98266	1.8	16.5133	1.6	0.8543	1.9	0.1023	1.0	0.53	628.0	6.0	627.0	9.0	623.5	35.1	**628.0**	**6.0**
900	292693	4.6	16.2859	0.5	0.8808	1.9	0.1040	1.8	0.96	638.0	11.0	641.4	9.0	653.4	11.6	**638.0**	**11.0**
323	176669	1.4	16.4963	0.8	0.8760	3.0	0.1048	2.9	0.97	642.5	17.6	638.8	14.1	625.7	16.8	**642.5**	**17.6**
286	76972	14.2	16.1832	1.2	0.8990	9.4	0.1055	9.3	0.99	646.7	57.4	651.2	45.3	666.9	26.0	**646.7**	**57.4**
211	43203	1.6	14.7630	1.6	0.9896	2.5	0.1060	1.9	0.77	649.2	11.8	698.5	12.5	860.5	32.8	**649.2**	**11.8**
154	102485	13.9	15.5420	2.8	0.9828	9.0	0.1108	8.5	0.95	677.3	54.9	695.0	45.3	752.9	59.5	**677.3**	**54.9**
493	172078	6.4	14.9936	0.8	1.0593	2.6	0.1152	2.5	0.95	702.8	16.6	733.5	13.7	828.3	16.7	**702.8**	**16.6**
86	6309	0.7	15.0430	2.0	1.0646	2.5	0.1162	1.6	0.63	708.4	10.6	736.1	13.2	821.4	40.9	**708.4**	**10.6**
150	86645	1.3	14.7167	1.2	1.1426	2.3	0.1220	1.9	0.85	741.8	13.4	773.7	12.3	867.1	25.1	**741.8**	**13.4**
147	50496	1.0	14.8592	2.5	1.1668	4.9	0.1257	4.2	0.86	763.5	30.6	785.1	26.9	847.0	51.8	**763.5**	**30.6**
581	239505	4.7	14.8476	0.5	1.1848	2.4	0.1276	2.3	0.97	774.1	17.1	793.5	13.3	848.6	11.2	**774.1**	**17.1**
463	224751	7.4	14.7946	0.7	1.2283	3.5	0.1318	3.4	0.98	798.1	25.4	813.6	19.3	856.1	13.7	**798.1**	**25.4**
339	166301	1.7	14.2975	0.7	1.2942	5.2	0.1342	5.2	0.99	811.8	39.4	843.2	29.9	926.7	15.1	**811.8**	**39.4**
212	81440	0.8	14.6394	0.6	1.3668	1.3	0.1451	1.2	0.89	873.6	9.4	874.8	7.6	877.9	12.5	**873.6**	**9.4**
322	112675	5.3	13.7610	0.6	1.5737	7.4	0.1571	7.4	1.00	940.4	64.5	959.9	46.0	1004.7	12.7	**1004.7**	**12.7**
140	51282	2.3	13.7233	1.0	1.6748	2.7	0.1667	2.5	0.93	993.9	23.3	999.0	17.3	1010.3	20.6	**1010.3**	**20.6**
120	82001	1.5	13.5518	1.0	1.8614	2.1	0.1830	1.8	0.87	1083.1	18.3	1067.5	13.9	1035.7	21.0	**1035.7**	**21.0**
141	76670	2.9	13.5460	1.0	1.7166	2.6	0.1686	2.4	0.92	1004.6	22.0	1014.7	16.5	1036.6	20.3	**1036.6**	**20.3**
35	21500	1.2	13.4444	3.3	1.8618	3.9	0.1815	2.1	0.53	1075.4	20.6	1067.6	25.9	1051.8	66.8	**1051.8**	**66.8**
429	333651	2.8	13.3781	0.5	1.7542	1.4	0.1702	1.3	0.93	1013.2	12.5	1028.7	9.2	1061.8	10.2	**1061.8**	**10.2**
165	95591	1.7	13.3285	0.7	1.8166	1.3	0.1756	1.1	0.83	1042.9	10.8	1051.4	8.8	1069.2	15.0	**1069.2**	**15.0**
282	536756	2.3	12.7934	0.3	2.1144	1.0	0.1962	0.9	0.93	1154.8	9.4	1153.5	6.6	1151.1	6.7	**1151.1**	**6.7**
67	49070	0.6	12.5904	1.8	2.1882	2.5	0.1998	1.8	0.71	1174.3	19.4	1177.3	17.7	1182.8	35.2	**1182.8**	**35.2**
98	72155	1.4	12.4666	0.8	2.2914	1.2	0.2072	1.0	0.78	1213.8	10.7	1209.6	8.7	1202.3	15.2	**1202.3**	**15.2**
98	99367	0.5	11.1919	0.9	2.9543	1.6	0.2398	1.4	0.83	1385.7	16.9	1395.9	12.4	1411.7	17.3	**1411.7**	**17.3**
118	111278	1.9	9.7377	0.4	4.2112	1.7	0.2974	1.7	0.98	1678.5	25.0	1676.2	14.2	1673.4	7.0	**1673.4**	**7.0**
101	112934	4.1	7.1114	0.4	7.5429	1.5	0.3890	1.5	0.97	2118.4	26.5	2178.1	13.6	2234.8	6.3	**2234.8**	**6.3**
249	333954	8.6	6.8962	0.2	8.5047	1.3	0.4254	1.3	0.99	2284.8	24.7	2286.4	11.8	2287.9	2.6	**2287.9**	**2.6**
430	818062	1.9	6.7817	0.1	8.7902	0.9	0.4323	0.9	0.99	2316.3	18.1	2316.5	8.5	2316.6	1.7	**2316.6**	**1.7**
525	792938	1.5	5.9947	0.1	10.7581	1.3	0.4677	1.3	1.00	2473.6	26.8	2502.5	12.2	2525.9	1.9	**2525.9**	**1.9**
337	88406	2.2	5.5285	0.3	10.1541	1.5	0.4071	1.4	0.98	2201.9	26.8	2448.9	13.5	2660.9	4.2	**2660.9**	**4.2**
174	85385	2.5	5.4493	0.5	9.5543	2.8	0.3776	2.8	0.99	2065.1	48.7	2392.8	25.7	2684.8	7.7	**2684.8**	**7.7**
56	211519	1.0	5.4396	0.6	12.5418	1.9	0.4948	1.9	0.96	2591.4	39.6	2645.9	18.3	2687.8	9.5	**2687.8**	**9.5**
82	136413	1.9	5.4385	0.4	11.5815	1.8	0.4568	1.8	0.98	2425.5	36.2	2571.2	17.1	2688.1	6.0	**2688.1**	**6.0**
86	226398	1.7	5.3727	0.5	13.0107	4.8	0.5070	4.8	0.99	2643.7	103.9	2680.4	45.5	2708.2	8.3	**2708.2**	**8.3**
125	426453	1.9	5.3508	0.2	13.3948	2.7	0.5198	2.7	1.00	2698.4	60.0	2707.9	25.8	2715.0	2.9	**2715.0**	**2.9**
445	754013	5.4	5.2462	0.1	12.6202	1.6	0.4802	1.6	1.00	2528.1	34.0	2651.7	15.3	2747.5	1.9	**2747.5**	**1.9**
304	346889	1.8	4.9438	0.2	14.0977	2.0	0.5055	2.0	0.99	2637.3	42.7	2756.3	18.8	2844.6	3.7	**2844.6**	**3.7**
139	203438	4.5	4.7820	0.1	14.5047	1.9	0.5031	1.9	1.00	2626.9	40.4	2783.3	17.9	2898.7	2.3	**2898.7**	**2.3**

Appendix A continued. U-Pb analysis results of detrital zircons from the till of the Mt. Achernar moraine.

			Isotope ratios							Apparent ages (Ma)							
U	206Pb	U/Th	206Pb*		207Pb*		206Pb*		error	206Pb*		207Pb*		206Pb*		Best	
(ppm)	204Pb		207Pb*	(%)	235U*	(%)	238U	(%)	corr.	238U*	± (Ma)	235U	± (Ma)	207Pb*	± (Ma)	age	± (Ma)
33	288247	0.9	4.1339	0.6	20.8271	2.5	0.6244	2.4	0.97	3127.5	60.7	3130.6	24.5	3132.5	10.0	**3132.5**	**10.0**
95	269120	4.5	3.4026	0.2	24.1350	2.2	0.5956	2.2	1.00	3012.1	52.3	3273.9	21.3	3438.3	3.0	**3438.3**	**3.0**
4K																	
409	73369	1.1	18.8908	1.5	0.3876	1.7	0.0531	0.7	0.42	333.5	2.3	332.6	4.7	326.0	34.3	**333.5**	**2.3**
623	208739	7.8	17.5285	0.7	0.6470	1.6	0.0823	1.4	0.89	509.6	6.8	506.7	6.2	493.4	15.6	**509.6**	**6.8**
116	21715	7.6	17.6531	3.4	0.6562	5.1	0.0840	3.8	0.75	520.0	19.1	512.3	20.5	477.8	74.5	**520.0**	**19.1**
321	107836	5.1	17.3660	1.3	0.6687	2.1	0.0842	1.7	0.80	521.2	8.6	519.9	8.7	514.0	28.3	**521.2**	**8.6**
7	2126	0.4	27.0132	56.2	0.4382	56.6	0.0859	6.6	0.12	531.0	33.8	369.0	176.8	-555.1	1628.3	**531.0**	**33.8**
102	58066	1.6	17.3908	2.7	0.6962	3.3	0.0878	1.9	0.58	542.6	10.1	536.5	13.9	510.8	59.5	**542.6**	**10.1**
368	137380	7.8	16.9512	0.6	0.7157	1.5	0.0880	1.3	0.90	543.6	6.9	548.1	6.2	566.8	13.6	**543.6**	**6.9**
978	249219	1.8	17.1702	0.5	0.7102	0.9	0.0884	0.8	0.84	546.3	4.1	544.9	3.9	538.8	10.9	**546.3**	**4.1**
110	40919	43.1	17.2874	2.6	0.7062	2.7	0.0885	0.8	0.29	546.9	4.2	542.5	11.4	523.9	57.1	**546.9**	**4.2**
242	153980	1.3	17.1056	1.4	0.7145	1.9	0.0886	1.2	0.63	547.5	6.2	547.4	7.9	547.0	31.7	**547.5**	**6.2**
161	64873	67.6	17.1699	1.9	0.7135	2.2	0.0889	1.1	0.50	548.8	5.9	546.8	9.5	538.8	42.6	**548.8**	**5.9**
169	48060	2.3	16.9121	1.6	0.7258	2.0	0.0890	1.2	0.60	549.7	6.3	554.1	8.5	571.9	34.5	**549.7**	**6.3**
373	117405	1.9	17.1822	0.8	0.7165	1.0	0.0893	0.6	0.60	551.4	3.3	548.6	4.4	537.3	18.3	**551.4**	**3.3**
38	24929	0.9	17.3277	6.1	0.7157	6.4	0.0899	2.0	0.31	555.2	10.6	548.1	27.3	518.8	134.7	**555.2**	**10.6**
30	15112	2.6	16.7507	13.8	0.7412	14.0	0.0900	2.1	0.15	555.8	11.4	563.1	60.5	592.7	300.8	**555.8**	**11.4**
122	47104	2.4	17.2612	2.4	0.7207	2.8	0.0902	1.6	0.55	556.8	8.3	551.1	12.0	527.3	51.8	**556.8**	**8.3**
434	87807	2.3	17.0510	0.7	0.7297	0.9	0.0902	0.6	0.67	557.0	3.4	556.4	4.1	554.0	15.4	**557.0**	**3.4**
333	67114	2.3	17.1230	0.9	0.7275	1.2	0.0904	0.7	0.58	557.6	3.6	555.1	5.0	544.8	20.7	**557.6**	**3.6**
318	64288	1.2	16.8860	0.8	0.7430	1.4	0.0910	1.1	0.80	561.4	5.8	564.2	5.9	575.2	17.9	**561.4**	**5.8**
69	14159	0.7	17.0427	4.6	0.7371	5.0	0.0911	1.8	0.36	562.1	9.6	560.7	21.4	555.1	100.9	**562.1**	**9.6**
99	34679	1.5	16.6380	3.5	0.7584	5.5	0.0915	4.3	0.78	564.5	23.4	573.1	24.3	607.3	74.8	**564.5**	**23.4**
789	330055	5.2	17.0200	0.4	0.7414	0.9	0.0915	0.8	0.90	564.5	4.6	563.2	4.1	558.0	9.1	**564.5**	**4.6**
436	124725	2.0	17.0005	0.6	0.7432	1.1	0.0916	0.9	0.83	565.2	4.8	564.3	4.6	560.5	13.0	**565.2**	**4.8**
14	4924	0.4	15.7974	22.2	0.8085	23.0	0.0926	5.8	0.25	571.1	31.8	601.6	104.7	718.4	477.8	**571.1**	**31.8**
447	382383	2.1	16.9704	1.1	0.7533	1.4	0.0927	0.8	0.58	571.6	4.4	570.2	6.0	564.3	24.5	**571.6**	**4.4**
214	79883	2.3	16.9885	1.5	0.7526	2.7	0.0927	2.2	0.83	571.7	12.1	569.8	11.6	562.0	32.3	**571.7**	**12.1**
45	16552	0.5	16.7038	4.7	0.7661	4.8	0.0928	1.2	0.24	572.2	6.4	577.5	21.2	598.7	101.0	**572.2**	**6.4**
54	21498	0.5	17.2643	9.1	0.7423	9.4	0.0929	2.5	0.26	572.9	13.5	563.7	40.7	526.9	199.3	**572.9**	**13.5**
165	54100	0.2	17.0025	1.5	0.7537	1.7	0.0929	0.7	0.42	572.9	3.9	570.4	7.4	560.2	33.5	**572.9**	**3.9**
76	24347	0.8	16.8791	5.0	0.7600	5.6	0.0930	2.5	0.44	573.5	13.6	574.0	24.5	576.1	108.7	**573.5**	**13.6**
763	27802	12.5	15.9806	1.1	0.8027	5.2	0.0930	5.1	0.98	573.5	28.0	598.4	23.6	693.9	24.4	**573.5**	**28.0**
87	28077	0.4	17.1753	2.2	0.7469	2.5	0.0930	1.2	0.48	573.5	6.6	566.4	11.0	538.2	48.5	**573.5**	**6.6**
286	25945	1.5	16.6290	1.2	0.7737	1.7	0.0933	1.2	0.72	575.1	6.7	581.9	7.5	608.4	25.5	**575.1**	**6.7**
586	196780	1.1	16.8860	0.3	0.7655	0.9	0.0937	0.9	0.94	577.7	4.7	577.2	4.0	575.2	6.9	**577.7**	**4.7**
110	34629	1.5	16.9656	3.2	0.7679	3.5	0.0945	1.6	0.44	582.0	8.7	578.6	15.6	565.0	69.2	**582.0**	**8.7**
165	63481	2.4	16.5903	2.1	0.7862	2.7	0.0946	1.6	0.61	582.6	9.2	589.0	12.0	613.5	45.8	**582.6**	**9.2**
125	61356	0.8	17.0362	2.4	0.7686	2.7	0.0950	1.1	0.42	584.9	6.2	579.0	11.7	556.0	52.5	**584.9**	**6.2**
985	417950	17.2	16.7243	0.5	0.7835	1.0	0.0950	0.9	0.89	585.3	5.1	587.5	4.6	596.1	9.8	**585.3**	**5.1**
367	120493	1.0	16.7527	0.6	0.7857	1.4	0.0955	1.3	0.90	587.8	7.3	588.7	6.4	592.4	13.5	**587.8**	**7.3**
120	56760	0.4	16.8367	2.4	0.7822	2.7	0.0955	1.2	0.44	588.1	6.7	586.7	12.0	581.6	52.4	**588.1**	**6.7**
249	124369	1.9	16.6351	1.1	0.7922	3.8	0.0956	3.6	0.95	588.5	20.2	592.4	16.9	607.7	24.8	**588.5**	**20.2**
739	225857	2.3	16.8078	0.6	0.7896	0.7	0.0963	0.4	0.60	592.4	2.5	591.0	3.3	585.3	12.7	**592.4**	**2.5**
54	19698	1.8	17.3012	4.1	0.7677	4.6	0.0963	2.2	0.47	592.9	12.5	578.5	20.5	522.2	89.9	**592.9**	**12.5**
799	330758	17.9	16.7454	0.5	0.7933	1.0	0.0963	0.9	0.87	592.9	5.0	593.0	4.6	593.4	11.0	**592.9**	**5.0**
258	109219	0.7	16.7172	0.7	0.7979	1.3	0.0967	1.1	0.85	595.3	6.3	595.6	5.9	597.0	15.1	**595.3**	**6.3**
167	142635	1.0	16.3323	1.7	0.8177	2.3	0.0969	1.6	0.68	596.0	9.0	606.8	10.5	647.3	36.2	**596.0**	**9.0**
160	72455	0.8	16.9014	1.8	0.7912	2.0	0.0970	0.9	0.44	596.7	5.0	591.9	8.9	573.3	38.9	**596.7**	**5.0**
115	40969	3.8	16.8586	2.3	0.7934	3.0	0.0970	2.0	0.66	596.8	11.3	593.1	13.5	578.7	49.2	**596.8**	**11.3**
488	205516	1.7	16.5965	0.6	0.8062	2.4	0.0970	2.3	0.97	597.0	13.2	600.3	10.8	612.7	13.2	**597.0**	**13.2**
255	176986	2.0	16.7796	1.4	0.7979	1.6	0.0971	0.9	0.55	597.4	5.0	595.7	7.3	588.9	29.3	**597.4**	**5.0**
195	107046	1.6	16.6161	1.9	0.8059	2.0	0.0971	0.7	0.36	597.5	4.2	600.2	9.2	610.1	40.8	**597.5**	**4.2**
182	87849	0.7	16.5455	1.3	0.8122	1.5	0.0975	0.7	0.47	599.5	3.9	603.7	6.6	619.3	27.7	**599.5**	**3.9**
469	178677	6.0	16.5971	0.9	0.8107	1.3	0.0976	0.9	0.69	600.2	5.0	602.8	5.7	612.6	19.5	**600.2**	**5.0**
281	90443	1.6	16.6765	1.3	0.8089	1.8	0.0978	1.2	0.68	601.7	7.0	601.8	8.1	602.3	28.6	**601.7**	**7.0**
200	67057	1.0	16.6328	1.2	0.8163	1.8	0.0985	1.4	0.75	605.4	7.9	606.0	8.4	608.0	26.3	**605.4**	**7.9**
199	78763	5.6	15.7717	1.5	0.8615	2.7	0.0985	2.3	0.84	605.8	13.1	630.9	12.6	721.8	30.8	**605.8**	**13.1**
148	115176	2.3	16.6528	1.9	0.8175	4.2	0.0987	3.8	0.90	607.0	21.8	606.7	19.2	605.4	40.5	**607.0**	**21.8**
67	24597	1.0	16.4721	4.4	0.8287	5.1	0.0990	2.6	0.51	608.6	15.2	612.9	23.4	628.9	93.9	**608.6**	**15.2**
231	94497	1.9	16.4485	0.6	0.8322	1.9	0.0993	1.8	0.95	610.2	10.5	614.8	8.8	632.0	12.5	**610.2**	**10.5**
321	103797	3.3	16.8019	1.5	0.8189	1.7	0.0998	0.9	0.51	613.2	5.2	607.4	7.9	586.1	32.3	**613.2**	**5.2**
218	128019	1.3	16.6066	1.0	0.8304	1.4	0.1000	1.0	0.73	614.5	6.1	613.8	6.5	611.4	20.9	**614.5**	**6.1**
331	167195	5.8	16.3995	0.7	0.8410	2.0	0.1000	1.9	0.93	614.6	11.2	619.7	9.4	638.5	15.6	**614.6**	**11.2**
44	21801	3.6	16.2870	3.8	0.8559	4.6	0.1011	2.7	0.58	620.9	15.7	627.9	21.5	653.3	80.6	**620.9**	**15.7**
573	305007	14.8	16.4696	0.5	0.8530	1.5	0.1019	1.5	0.95	625.5	8.8	626.3	7.2	629.2	10.0	**625.5**	**8.8**
226	69457	5.2	16.5554	1.8	0.8695	4.9	0.1044	4.5	0.93	640.2	27.6	635.3	23.1	618.0	39.8	**640.2**	**27.6**
330	218397	2.4	16.2845	0.7	0.8898	1.3	0.1051	1.1	0.84	644.2	6.9	646.3	6.4	653.6	15.4	**644.2**	**6.9**
62	50364	6.0	15.2459	2.8	0.9591	7.6	0.1061	7.1	0.93	649.8	43.9	682.8	37.9	793.3	57.7	**649.8**	**43.9**
80	52331	1.7	15.9329	2.6	0.9418	4.2	0.1088	3.3	0.79	666.0	20.8	673.8	20.5	700.2	54.7	**666.0**	**20.8**
160	52034	2.1	15.8623	1.3	0.9570	1.9	0.1101	1.4	0.74	673.3	8.8	681.8	9.3	709.7	26.9	**673.3**	**8.8**
87	40566	3.7	15.1777	2.1	1.0155	7.0	0.1118	6.7	0.95	683.1	43.2	711.7	35.7	802.7	43.8	**683.1**	**43.2**
186	86332	1.9	15.1096	1.7	1.0721	4.3	0.1175	3.9	0.91	716.1	26.3	739.8	22.4	812.2	36.6	**716.1**	**26.3**
147	77143	2.2	15.6545	1.6	1.0609	2.4	0.1204	1.8	0.76	733.1	12.7	734.3	12.7	737.7	33.7	**733.1**	**12.7**
378	188515	2.5	15.5681	0.5	1.1043	1.6	0.1247	1.5	0.94	757.5	10.6	755.4	8.4	749.3	11.0	**757.5**	**10.6**
257	155867	3.5	14.5308	0.9	1.3689	1.3	0.1443	0.9	0.74	868.8	7.7	875.7	7.5	893.3	17.8	**868.8**	**7.7**
138	85857	3.7	14.3272	1.5	1.4481	4.1	0.1505	3.8	0.93	903.6	32.1	909.1	24.6	922.4	30.7	**922.4**	**30.7**

Appendix A continued. U-Pb analysis results of detrital zircons from the till of the Mt. Achernar moraine.

			Isotope ratios							Apparent ages (Ma)							
U	206Pb	U/Th	206Pb*		207Pb*		206Pb*		error	206Pb*		207Pb*		206Pb*		Best	
(ppm)	204Pb		207Pb*	(%)	235U*	(%)	238U	(%)	corr.	238U*	± (Ma)	235U	± (Ma)	207Pb*	± (Ma)	age	± (Ma)
432	139631	6.8	14.0540	0.7	1.5265	5.1	0.1556	5.0	0.99	932.3	43.7	941.1	31.2	961.9	13.6	**961.9**	**13.6**
511	128731	3.0	14.0401	0.3	1.5295	1.5	0.1558	1.5	0.98	933.1	12.8	942.3	9.2	963.9	6.1	**963.9**	**6.1**
142	124022	5.9	13.8687	1.0	1.5193	1.6	0.1528	1.3	0.81	916.8	11.1	938.2	9.9	988.9	19.4	**988.9**	**19.4**
144	82707	2.3	13.8469	1.9	1.5418	4.2	0.1548	3.7	0.89	928.0	32.0	947.2	25.7	992.1	39.1	**992.1**	**39.1**
59	35872	2.4	13.7530	1.3	1.5376	2.4	0.1534	2.0	0.82	919.8	16.7	945.5	14.6	1005.9	27.2	**1005.9**	**27.2**
118	82487	1.5	13.6034	1.1	1.6708	4.4	0.1648	4.2	0.97	983.6	38.4	997.5	27.6	1028.1	22.0	**1028.1**	**22.0**
368	236531	0.7	13.5118	0.3	1.7688	0.7	0.1733	0.6	0.89	1030.5	5.6	1034.1	4.3	1041.7	6.2	**1041.7**	**6.2**
449	179102	2.7	13.4514	0.4	1.7105	4.1	0.1669	4.1	0.99	994.9	37.5	1012.5	26.2	1050.8	8.5	**1050.8**	**8.5**
619	270922	3.1	13.4220	0.3	1.8113	2.0	0.1763	2.0	0.99	1046.9	18.9	1049.5	12.9	1055.2	5.9	**1055.2**	**5.9**
179	126659	1.9	13.3702	1.3	1.7358	9.9	0.1683	9.8	0.99	1002.8	91.4	1021.9	64.0	1063.0	25.2	**1063.0**	**25.2**
131	114133	1.7	13.1660	1.2	1.9171	1.7	0.1831	1.2	0.71	1083.7	12.2	1087.1	11.5	1093.9	24.2	**1093.9**	**24.2**
110	29019	1.1	13.0182	1.7	1.7916	3.1	0.1692	2.6	0.84	1007.4	24.1	1042.4	20.0	1116.4	33.3	**1116.4**	**33.3**
91	41515	2.5	13.0091	2.3	1.5226	7.3	0.1437	6.9	0.95	865.3	56.1	939.5	44.8	1117.8	46.4	**1117.8**	**46.4**
151	63817	1.7	12.4709	0.6	2.3526	4.0	0.2128	3.9	0.99	1243.6	44.1	1228.3	28.2	1201.6	12.6	**1201.6**	**12.6**
268	234249	1.9	12.4597	0.4	2.2132	1.0	0.2000	1.0	0.92	1175.3	10.3	1185.2	7.3	1203.3	8.1	**1203.3**	**8.1**
296	225999	0.8	12.4450	0.3	2.2164	2.6	0.2001	2.6	0.99	1175.6	27.5	1186.2	18.1	1205.7	6.8	**1205.7**	**6.8**
65	44508	1.2	12.3317	1.6	2.3043	3.1	0.2061	2.7	0.85	1207.9	29.3	1213.6	22.1	1223.6	32.1	**1223.6**	**32.1**
57	10271	1.1	11.0294	1.4	3.0264	1.8	0.2421	1.1	0.61	1397.6	13.8	1414.3	13.7	1439.6	26.9	**1439.6**	**26.9**
163	176915	0.9	8.8052	0.4	5.0246	1.1	0.3209	1.0	0.94	1794.0	15.6	1823.5	9.0	1857.3	6.7	**1857.3**	**6.7**
107	158126	0.9	8.7982	0.4	5.1711	1.6	0.3300	1.6	0.97	1838.2	25.5	1847.9	14.0	1858.7	7.5	**1858.7**	**7.5**
225	319015	9.5	8.3839	0.2	5.6901	0.8	0.3460	0.8	0.98	1915.4	13.3	1929.9	7.1	1945.4	3.0	**1945.4**	**3.0**
33	40652	0.6	8.3230	2.0	4.2395	8.9	0.2559	8.7	0.98	1468.9	114.3	1681.7	73.4	1958.4	35.3	**1958.4**	**35.3**
104	123465	1.0	8.3134	1.7	4.7880	5.6	0.2887	5.3	0.95	1635.0	76.9	1782.8	47.0	1960.5	30.0	**1960.5**	**30.0**
99	78226	0.6	7.4163	0.6	7.2246	1.9	0.3886	1.8	0.95	2116.3	32.1	2139.5	16.7	2161.9	10.0	**2161.9**	**10.0**
151	130795	12.0	7.1528	0.3	7.5020	1.1	0.3892	1.0	0.97	2119.1	18.8	2173.2	9.6	2224.8	4.4	**2224.8**	**4.4**
132	226241	2.2	6.8682	0.3	7.9989	3.6	0.3984	3.6	1.00	2161.9	66.3	2230.9	32.7	2294.9	5.3	**2294.9**	**5.3**
844	144091	14.0	6.8428	0.8	8.4595	3.6	0.4198	3.5	0.97	2259.7	66.3	2281.6	32.5	2301.2	14.2	**2301.2**	**14.2**
413	453113	2.6	6.7862	0.2	8.0659	1.2	0.3970	1.2	0.99	2155.2	22.1	2238.4	11.0	2315.5	2.8	**2315.5**	**2.8**
665	246456	4.0	6.5717	0.2	8.3895	2.2	0.3999	2.2	1.00	2168.4	39.7	2274.0	19.7	2370.4	3.7	**2370.4**	**3.7**
171	342980	1.9	6.2954	0.4	9.4629	2.3	0.4321	2.3	0.98	2315.0	43.9	2384.0	21.1	2443.4	7.3	**2443.4**	**7.3**
152	114523	50.9	6.1599	6.1	8.3001	10.7	0.3708	8.8	0.82	2033.2	153.2	2264.3	97.4	2480.2	103.7	**2480.2**	**103.7**
118	22810	0.8	5.8886	1.0	8.4346	5.5	0.3602	5.4	0.98	1983.3	92.0	2278.9	49.7	2555.8	16.1	**2555.8**	**16.1**
197	92637	1.9	5.4771	0.2	11.8034	1.6	0.4689	1.6	0.99	2478.6	32.1	2588.9	14.8	2676.4	4.1	**2676.4**	**4.1**
185	247234	1.9	5.4081	0.2	12.3732	1.0	0.4853	0.9	0.97	2550.4	19.7	2633.1	9.1	2697.4	3.8	**2697.4**	**3.8**
87	255082	1.8	5.3647	0.2	13.1645	0.7	0.5122	0.7	0.96	2666.1	15.2	2691.5	6.8	2710.7	3.4	**2710.7**	**3.4**
44	55080	2.0	5.3617	0.4	13.0863	1.3	0.5089	1.2	0.95	2651.9	26.3	2685.9	12.0	2711.6	6.6	**2711.6**	**6.6**
478	97088	3.9	5.1768	0.1	13.1068	2.2	0.4921	2.2	1.00	2579.8	46.4	2687.4	20.6	2769.3	1.3	**2769.3**	**1.3**
229	714579	3.1	4.3739	0.9	18.1608	2.4	0.5761	2.2	0.93	2932.8	51.8	2998.3	22.8	3042.5	14.2	**3042.5**	**14.2**
325	1343560	2.3	4.0040	1.3	18.9622	2.3	0.5507	1.9	0.81	2827.9	42.6	3039.9	22.2	3183.2	21.3	**3183.2**	**21.3**
4J																	
171	4342	0.7	18.5844	4.6	0.2611	5.2	0.0352	2.4	0.47	222.9	5.3	235.5	11.0	363.0	104.0	**222.9**	**5.3**
279	25991	0.6	20.2157	3.5	0.2484	3.7	0.0364	1.2	0.33	230.6	2.8	225.3	7.5	170.0	81.3	**230.6**	**2.8**
227	61981	1.8	20.0415	4.8	0.2512	5.2	0.0365	2.2	0.42	231.2	5.0	227.5	10.7	190.2	110.8	**231.2**	**5.0**
147	4975	2.2	16.2137	21.0	0.3341	21.3	0.0393	3.7	0.17	248.4	9.0	292.7	54.3	662.9	454.6	**248.4**	**9.0**
153	2615	0.9	18.3637	5.4	0.3031	5.8	0.0404	2.0	0.35	255.1	5.0	268.8	13.6	389.9	121.7	**255.1**	**5.0**
789	65905	2.0	19.4535	0.9	0.2922	1.9	0.0412	1.7	0.90	260.4	4.4	260.3	4.4	259.0	19.6	**260.4**	**4.4**
393	62429	0.8	19.2018	2.2	0.3071	2.3	0.0428	0.8	0.35	270.0	2.2	271.9	5.6	288.9	50.2	**270.0**	**2.2**
165	2777	1.8	15.5036	20.4	0.4850	21.1	0.0545	5.7	0.27	342.3	18.9	401.5	70.2	758.1	433.5	**342.3**	**18.9**
409	103653	1.1	17.7460	0.8	0.5683	1.9	0.0731	1.7	0.91	455.1	7.6	456.9	7.0	466.2	18.0	**455.1**	**7.6**
156	77117	1.2	17.2825	2.6	0.6198	3.5	0.0777	2.3	0.65	482.3	10.6	489.7	13.5	524.5	57.9	**482.3**	**10.6**
142	62812	1.2	17.2405	2.9	0.6499	3.1	0.0813	1.2	0.38	503.7	5.7	508.4	12.3	529.9	62.6	**503.7**	**5.7**
273	61705	2.6	17.3727	1.1	0.6645	1.7	0.0837	1.4	0.79	518.3	6.7	517.4	6.9	513.1	23.1	**518.3**	**6.7**
93	20113	9.1	17.5154	3.5	0.6600	4.4	0.0838	2.7	0.61	519.0	13.4	514.6	17.8	495.1	76.7	**519.0**	**13.4**
118	32282	3.2	17.3611	2.9	0.6667	3.1	0.0839	1.0	0.33	519.6	5.2	518.7	12.6	514.6	64.1	**519.6**	**5.2**
279	101625	0.5	17.1846	0.9	0.6777	1.4	0.0845	1.1	0.76	522.7	5.4	525.4	5.8	537.0	20.1	**522.7**	**5.4**
117	18323	1.5	16.6403	1.8	0.7029	2.9	0.0848	2.2	0.77	524.9	11.1	540.5	12.0	607.0	39.6	**524.9**	**11.1**
265	89223	5.2	16.8916	1.8	0.7006	3.6	0.0858	3.1	0.87	530.8	16.0	539.2	15.1	574.5	38.3	**530.8**	**16.0**
215	102233	1.6	17.1430	1.2	0.7011	1.6	0.0872	1.0	0.64	538.7	5.1	539.4	6.5	542.3	26.0	**538.7**	**5.1**
176	88025	3.3	17.1112	1.8	0.7026	3.1	0.0872	2.5	0.82	538.9	13.0	540.3	12.8	546.3	38.5	**538.9**	**13.0**
56	9736	1.3	17.0474	6.1	0.7098	6.6	0.0878	2.5	0.37	542.3	12.8	544.6	27.7	554.5	133.2	**542.3**	**12.8**
82	26310	3.2	17.8031	3.2	0.6833	3.9	0.0882	2.2	0.57	545.0	11.5	528.8	15.9	459.1	70.2	**545.0**	**11.5**
614	87516	4.1	16.9832	0.8	0.7168	1.6	0.0883	1.4	0.87	545.4	7.1	548.8	6.6	562.7	16.6	**545.4**	**7.1**
104	28458	7.8	17.2865	2.2	0.7081	2.6	0.0888	1.3	0.51	548.3	6.8	543.6	10.8	524.0	48.6	**548.3**	**6.8**
85	20862	14.5	16.8502	3.4	0.7294	3.6	0.0891	1.3	0.36	550.4	6.8	556.2	15.5	579.8	73.3	**550.4**	**6.8**
217	175400	1.9	17.0218	1.3	0.7252	1.5	0.0895	0.8	0.53	552.7	4.2	553.7	6.4	557.8	27.5	**552.7**	**4.2**
146	38712	0.4	17.2033	2.2	0.7182	2.3	0.0896	0.8	0.35	553.2	4.4	549.6	10.0	534.6	48.1	**553.2**	**4.4**
750	47168	9.3	16.8670	0.5	0.7335	1.6	0.0897	1.5	0.94	554.0	7.7	558.6	6.7	577.7	11.5	**554.0**	**7.7**
530	240926	9.3	16.9905	0.7	0.7317	1.2	0.0902	1.0	0.83	556.5	5.5	557.5	5.3	561.8	14.8	**556.5**	**5.5**
171	136423	1.9	16.9233	2.1	0.7365	5.8	0.0904	5.4	0.93	557.9	28.8	560.4	24.9	570.4	46.1	**557.9**	**28.8**
48	22990	2.2	16.8913	8.8	0.7382	9.3	0.0904	3.0	0.33	558.1	16.2	561.3	40.1	574.5	191.6	**558.1**	**16.2**
31	8217	0.6	15.8900	8.4	0.7848	8.5	0.0904	1.5	0.17	558.2	7.9	588.2	38.0	705.9	178.4	**558.2**	**7.9**
533	191679	10.8	16.9054	0.5	0.7409	1.4	0.0908	1.3	0.94	560.5	7.0	562.9	6.0	572.7	10.4	**560.5**	**7.0**
404	51630	8.2	16.2225	2.2	0.7735	5.6	0.0910	5.1	0.92	561.5	27.5	581.8	24.7	661.7	47.9	**561.5**	**27.5**
118	41594	8.3	17.0113	2.6	0.7387	4.3	0.0911	3.4	0.79	562.3	18.2	561.7	18.3	559.1	56.3	**562.3**	**18.2**
86	35093	0.3	16.9700	4.6	0.7406	4.9	0.0911	1.6	0.32	562.3	8.5	562.7	21.2	564.4	101.3	**562.3**	**8.5**
302	164087	3.4	17.1144	0.9	0.7448	2.3	0.0924	2.1	0.91	570.0	11.6	565.2	10.1	545.9	20.7	**570.0**	**11.6**
199	69019	1.1	16.9079	2.0	0.7579	2.3	0.0929	1.1	0.49	572.9	6.2	572.8	10.0	572.4	43.3	**572.9**	**6.2**
442	191901	2.1	16.7683	0.9	0.7645	3.1	0.0930	2.9	0.95	573.1	16.1	576.6	13.5	590.4	19.8	**573.1**	**16.1**

Appendix A continued. U-Pb analysis results of detrital zircons from the till of the Mt. Achernar moraine.

			Isotope ratios							Apparent ages (Ma)							
U	206Pb	U/Th	206Pb*		207Pb*		206Pb*		error	206Pb*		207Pb*		206Pb*		Best	
(ppm)	204Pb		207Pb*	(%)	235U*	(%)	238U	(%)	corr.	238U*	± (Ma)	235U	± (Ma)	207Pb*	± (Ma)	age	± (Ma)
198	86747	0.6	16.7110	1.2	0.7697	2.0	0.0933	1.6	0.80	575.0	9.0	579.6	9.0	597.9	26.2	**575.0**	**9.0**
119	27844	0.7	17.0335	2.9	0.7709	3.9	0.0952	2.6	0.65	586.4	14.3	580.3	17.2	556.3	64.3	**586.4**	**14.3**
398	504584	1.8	16.6726	0.6	0.7954	1.0	0.0962	0.8	0.83	592.0	4.7	594.2	4.5	602.8	12.1	**592.0**	**4.7**
135	80183	0.8	16.5908	2.1	0.8011	3.1	0.0964	2.3	0.75	593.3	13.2	597.5	14.1	613.4	44.7	**593.3**	**13.2**
148	28331	1.3	16.8063	2.1	0.7937	2.3	0.0967	0.9	0.37	595.3	4.9	593.3	10.3	585.5	46.0	**595.3**	**4.9**
526	381336	2.1	16.7058	0.6	0.8061	1.7	0.0977	1.6	0.93	600.7	9.1	600.3	7.8	598.5	13.6	**600.7**	**9.1**
263	104781	16.7	16.5905	1.1	0.8125	1.7	0.0978	1.3	0.78	601.3	7.6	603.9	7.7	613.5	22.9	**601.3**	**7.6**
296	116212	1.0	16.6979	0.9	0.8226	1.9	0.0996	1.7	0.87	612.2	9.7	609.5	8.7	599.5	20.2	**612.2**	**9.7**
200	79473	5.4	15.4072	1.2	0.8975	1.6	0.1003	1.1	0.66	616.1	6.3	650.4	7.8	771.2	25.6	**616.1**	**6.3**
320	58570	1.5	16.5721	1.5	0.8394	2.0	0.1009	1.3	0.66	619.6	7.7	618.8	9.1	615.9	32.1	**619.6**	**7.7**
157	43914	2.3	16.3687	1.5	0.8604	2.1	0.1021	1.6	0.73	626.9	9.3	630.3	10.0	642.5	31.3	**626.9**	**9.3**
449	166137	3.7	16.1603	1.0	0.8808	7.6	0.1032	7.5	0.99	633.3	45.3	641.4	36.1	670.0	22.3	**633.3**	**45.3**
89	44649	3.7	16.4304	3.5	0.8676	5.2	0.1034	3.8	0.73	634.2	22.8	634.2	24.3	634.4	75.9	**634.2**	**22.8**
244	20329	1.6	15.3290	1.4	0.9680	2.4	0.1076	1.9	0.80	658.9	11.7	687.4	11.8	781.9	30.0	**658.9**	**11.7**
123	71610	3.0	15.2441	1.7	1.0206	4.4	0.1128	4.0	0.92	689.2	26.3	714.2	22.4	793.6	35.2	**689.2**	**26.3**
750	174591	20.1	15.0629	1.6	1.0429	3.6	0.1139	3.2	0.90	695.6	21.2	725.4	18.5	818.7	32.4	**695.6**	**21.2**
112	99971	2.0	15.2668	3.4	1.0649	7.1	0.1179	6.3	0.88	718.5	42.9	736.2	37.4	790.5	70.4	**718.5**	**42.9**
903	40310	4.2	14.4666	0.5	1.1597	3.5	0.1217	3.5	0.99	740.2	24.4	781.8	19.3	902.4	10.6	**740.2**	**24.4**
160	109799	1.2	14.5041	1.3	1.4587	2.0	0.1534	1.5	0.75	920.2	12.9	913.5	12.1	897.1	27.5	**897.1**	**27.5**
64	42604	3.1	14.2522	1.9	1.4856	3.5	0.1536	2.9	0.84	920.9	25.1	924.5	21.1	933.2	38.5	**933.2**	**38.5**
557	80332	2.4	13.8066	0.4	1.5461	2.0	0.1548	1.9	0.98	927.9	16.7	948.9	12.1	998.0	7.6	**998.0**	**7.6**
79	29122	2.2	13.5791	2.1	1.7558	2.5	0.1729	1.4	0.54	1028.2	12.9	1029.3	16.2	1031.7	42.4	**1031.7**	**42.4**
164	33471	0.8	13.5418	1.0	1.6360	1.9	0.1607	1.6	0.84	960.6	14.1	984.2	11.9	1037.2	20.6	**1037.2**	**20.6**
336	317556	4.7	13.4541	0.5	1.7951	0.8	0.1752	0.6	0.76	1040.5	5.6	1043.7	5.0	1050.4	10.1	**1050.4**	**10.1**
301	112332	1.2	13.4502	0.7	1.8332	3.0	0.1788	2.9	0.97	1060.5	27.9	1057.4	19.4	1051.0	15.0	**1051.0**	**15.0**
307	46971	2.1	13.1739	0.5	1.8276	1.9	0.1746	1.8	0.96	1037.5	17.5	1055.4	12.5	1092.6	10.3	**1092.6**	**10.3**
111	71320	1.5	13.0935	0.9	1.9493	1.5	0.1851	1.2	0.79	1094.8	12.1	1098.2	10.3	1104.9	18.8	**1104.9**	**18.8**
315	145967	4.0	12.6584	0.5	2.0652	2.2	0.1896	2.2	0.98	1119.2	22.5	1137.3	15.4	1172.1	9.6	**1172.1**	**9.6**
76	77927	1.4	11.6024	1.2	2.5984	2.5	0.2187	2.3	0.89	1274.8	26.1	1300.2	18.6	1342.4	22.3	**1342.4**	**22.3**
137	69246	2.1	10.0711	0.9	2.7017	2.6	0.1973	2.4	0.93	1161.0	25.8	1328.9	19.3	1610.9	17.6	**1610.9**	**17.6**
166	32868	1.1	9.7891	0.6	3.9874	1.1	0.2831	0.9	0.81	1606.9	13.0	1631.6	9.1	1663.6	12.0	**1663.6**	**12.0**
209	265142	3.2	9.1402	0.5	4.7458	1.4	0.3146	1.3	0.94	1763.3	20.3	1775.4	11.7	1789.5	8.4	**1789.5**	**8.4**
385	300069	2.0	7.8490	0.8	5.1044	8.2	0.2906	8.1	0.99	1644.4	118.0	1836.8	69.5	2062.4	14.7	**2062.4**	**14.7**
457	224524	2.9	6.9881	0.3	7.6414	1.8	0.3873	1.8	0.99	2110.2	32.3	2189.7	16.3	2265.0	4.9	**2265.0**	**4.9**
148	153178	1.5	6.8816	0.3	8.1752	0.8	0.4080	0.8	0.94	2205.9	14.3	2250.6	7.4	2291.5	4.8	**2291.5**	**4.8**
256	317992	2.4	6.3439	0.2	8.4022	6.5	0.3866	6.5	1.00	2107.0	116.5	2275.4	58.9	2430.4	3.9	**2430.4**	**3.9**
158	254034	1.0	5.8116	0.5	10.7926	1.4	0.4549	1.3	0.93	2417.0	26.9	2505.4	13.3	2577.9	8.6	**2577.9**	**8.6**
400	63302	13.1	5.5984	0.3	8.7653	3.7	0.3559	3.7	1.00	1962.7	62.8	2313.9	34.0	2640.1	5.3	**2640.1**	**5.3**
76	32283	2.4	5.5900	1.5	9.0019	2.2	0.3650	1.7	0.75	2005.6	28.8	2338.2	20.5	2642.6	24.8	**2642.6**	**24.8**
110	78660	1.4	5.4335	0.3	10.9839	1.7	0.4328	1.7	0.98	2318.6	32.6	2521.8	15.9	2689.6	5.8	**2689.6**	**5.8**
544	419885	2.4	5.4089	0.1	12.2179	2.0	0.4793	2.0	1.00	2524.2	42.4	2621.3	19.1	2697.1	1.5	**2697.1**	**1.5**
256	224233	1.6	5.3691	0.1	12.2731	2.0	0.4779	2.0	1.00	2518.2	40.9	2625.5	18.5	2709.3	2.4	**2709.3**	**2.4**
344	347681	4.6	5.3605	0.8	10.9299	2.6	0.4249	2.5	0.95	2282.8	47.7	2517.2	24.3	2712.0	13.2	**2712.0**	**13.2**
99	158709	1.4	5.3529	0.2	13.0433	0.9	0.5064	0.9	0.97	2641.2	20.0	2682.8	8.9	2714.3	3.7	**2714.3**	**3.7**
149	262630	1.4	5.3200	0.2	13.6596	2.1	0.5270	2.1	0.99	2729.0	46.9	2726.4	20.0	2724.5	3.7	**2724.5**	**3.7**
179	331244	1.7	5.3041	0.2	13.8398	1.6	0.5324	1.6	0.99	2751.6	34.8	2738.8	14.8	2729.4	3.0	**2729.4**	**3.0**
854	717721	1.3	5.0536	0.1	14.8448	0.7	0.5441	0.7	0.99	2800.6	15.7	2805.3	6.7	2808.8	1.9	**2808.8**	**1.9**
454	362245	3.6	4.8187	0.1	15.8547	0.8	0.5541	0.8	0.99	2842.2	18.3	2868.1	7.7	2886.3	1.8	**2886.3**	**1.8**
166	150765	2.3	4.6214	0.1	15.7701	1.3	0.5286	1.3	0.99	2735.5	28.3	2863.0	12.2	2954.0	2.2	**2954.0**	**2.2**
443	367783	7.5	3.9660	0.9	20.7981	1.5	0.5982	1.2	0.80	3022.7	28.9	3129.2	14.5	3198.3	14.3	**3198.3**	**14.3**
43	83996	3.2	3.6624	0.2	22.0458	2.0	0.5856	1.9	0.99	2971.5	46.4	3185.7	19.1	3323.6	3.8	**3323.6**	**3.8**
194	583401	1.5	3.5869	1.1	24.5337	1.7	0.6382	1.3	0.77	3182.1	32.8	3289.8	16.6	3356.2	17.0	**3356.2**	**17.0**
4B																	
311	36430	1.4	19.3271	4.0	0.2911	4.1	0.0408	1.2	0.29	257.8	3.1	259.4	9.5	274.0	90.7	**257.8**	**3.1**
473	52031	1.1	19.5133	1.6	0.2897	2.0	0.0410	1.2	0.61	259.0	3.1	258.3	4.5	252.0	35.7	**259.0**	**3.1**
89	37821	1.5	18.0129	1.9	0.6272	2.8	0.0819	2.0	0.72	507.6	9.9	494.3	10.9	433.0	42.9	**507.6**	**9.9**
354	71560	4.1	17.1500	1.1	0.6655	2.4	0.0828	2.1	0.88	512.6	10.4	517.9	9.6	541.4	24.3	**512.6**	**10.4**
1215	75612	21.9	17.2959	0.3	0.6610	0.6	0.0829	0.5	0.83	513.5	2.4	515.2	2.3	522.8	7.1	**513.5**	**2.4**
47	12684	1.4	18.4321	10.0	0.6371	10.1	0.0852	1.4	0.14	526.9	6.9	500.5	40.0	381.6	225.6	**526.9**	**6.9**
11	4103	1.2	16.0450	34.6	0.7481	35.4	0.0871	7.7	0.22	538.1	39.9	567.1	155.2	685.3	759.9	**538.1**	**39.9**
356	83658	2.9	17.0175	1.1	0.7054	3.2	0.0871	3.0	0.94	538.1	15.4	542.0	13.3	558.3	23.1	**538.1**	**15.4**
1824	16185	1.8	16.7641	0.6	0.7234	1.6	0.0880	1.4	0.92	543.4	7.5	552.7	6.7	590.9	13.6	**543.4**	**7.5**
98	29726	0.7	17.5778	2.7	0.7045	3.1	0.0898	1.5	0.49	554.5	8.1	541.5	13.0	487.2	59.7	**554.5**	**8.1**
277	100573	0.7	16.9567	0.8	0.7329	1.0	0.0901	0.6	0.64	556.3	3.4	558.3	4.3	566.2	16.9	**556.3**	**3.4**
38	9158	1.4	17.2218	11.9	0.7222	12.1	0.0902	1.8	0.15	556.7	9.8	552.0	51.4	532.3	261.6	**556.7**	**9.8**
37	12949	4.5	17.9625	7.7	0.6928	8.0	0.0903	2.1	0.26	557.1	11.2	534.5	33.2	439.3	171.6	**557.1**	**11.2**
99	26457	0.7	17.4819	1.4	0.7124	2.2	0.0903	1.7	0.77	557.5	9.1	546.2	9.4	499.3	31.6	**557.5**	**9.1**
486	159645	11.2	17.0231	0.5	0.7318	2.1	0.0904	2.0	0.96	557.6	10.7	557.6	8.9	557.6	11.9	**557.6**	**10.7**
521	249421	4.4	16.9596	0.6	0.7352	1.2	0.0904	1.0	0.86	558.1	5.3	559.6	5.0	565.7	12.9	**558.1**	**5.3**
81	43414	0.7	17.3295	3.7	0.7208	3.9	0.0906	1.1	0.29	559.1	6.0	551.2	16.6	518.6	82.0	**559.1**	**6.0**
103	32124	1.4	17.2747	5.5	0.7255	5.8	0.0909	2.0	0.34	560.8	10.6	553.9	24.9	525.5	120.4	**560.8**	**10.6**
345	68063	1.5	16.6608	0.7	0.7578	0.9	0.0916	0.6	0.65	564.8	3.3	572.7	4.1	604.3	15.4	**564.8**	**3.3**
404	136784	2.8	16.2156	2.9	0.7798	5.2	0.0917	4.4	0.83	565.7	23.6	585.4	23.3	662.6	62.0	**565.7**	**23.6**
640	207845	2.1	16.9425	0.6	0.7477	1.4	0.0919	1.2	0.88	566.6	6.6	566.9	6.0	568.0	14.1	**566.6**	**6.6**
74	33435	2.1	17.0099	1.7	0.7448	2.2	0.0919	1.4	0.62	566.7	7.4	565.2	9.5	559.3	37.2	**566.7**	**7.4**
56	15199	0.2	16.3069	4.1	0.7795	4.2	0.0922	1.2	0.28	568.5	6.4	585.2	18.9	650.6	87.5	**568.5**	**6.4**
54	23002	0.6	17.0117	5.3	0.7477	6.1	0.0923	3.0	0.50	568.8	16.6	566.9	26.4	559.1	114.7	**568.8**	**16.6**
61	16886	1.6	17.1057	5.5	0.7444	5.7	0.0924	1.5	0.27	569.5	8.4	565.0	24.8	547.0	120.6	**569.5**	**8.4**

Appendix A continued. U-Pb analysis results of detrital zircons from the till of the Mt. Achernar moraine.

			Isotope ratios							Apparent ages (Ma)							
U	206Pb	U/Th	206Pb*		207Pb*		206Pb*		error	206Pb*		207Pb*		206Pb*		Best	
(ppm)	204Pb		207Pb*	(%)	235U*	(%)	238U	(%)	corr.	238U*	± (Ma)	235U	± (Ma)	207Pb*	± (Ma)	age	± (Ma)
98	45949	1.3	17.3201	3.5	0.7367	3.9	0.0925	1.7	0.44	570.5	9.5	560.5	16.8	519.8	76.7	**570.5**	**9.5**
82	25636	1.1	17.1230	3.3	0.7470	3.8	0.0928	1.8	0.49	571.9	10.1	566.5	16.3	544.8	71.8	**571.9**	**10.1**
70	21866	2.0	17.2361	4.7	0.7432	4.9	0.0929	1.4	0.29	572.7	7.9	564.3	21.3	530.5	103.2	**572.7**	**7.9**
277	64161	0.5	16.8509	1.1	0.7606	1.5	0.0930	1.0	0.66	573.0	5.3	574.4	6.5	579.7	23.9	**573.0**	**5.3**
244	128785	1.7	16.9161	1.2	0.7603	1.6	0.0933	1.0	0.67	574.9	5.8	574.2	6.9	571.4	25.5	**574.9**	**5.8**
66	32723	0.4	16.5349	4.9	0.7816	5.0	0.0937	1.0	0.21	577.6	5.7	586.4	22.2	620.7	105.1	**577.6**	**5.7**
180	87101	0.9	17.0194	1.2	0.7641	2.1	0.0943	1.7	0.83	581.0	9.6	576.4	9.2	558.1	25.7	**581.0**	**9.6**
127	24268	1.8	16.3126	2.0	0.7973	2.3	0.0943	1.1	0.50	581.1	6.3	595.3	10.2	649.8	41.9	**581.1**	**6.3**
62	16843	1.4	16.4633	5.0	0.7938	5.2	0.0948	1.5	0.28	583.8	8.2	593.3	23.5	630.1	108.0	**583.8**	**8.2**
70	17754	0.8	17.3929	5.9	0.7526	6.0	0.0949	1.3	0.21	584.7	7.1	569.7	26.2	510.5	128.9	**584.7**	**7.1**
169	27352	0.4	16.5548	1.5	0.7924	1.9	0.0951	1.1	0.58	585.9	6.0	592.5	8.4	618.1	32.8	**585.9**	**6.0**
272	85021	1.9	15.1997	3.6	0.8658	6.5	0.0954	5.4	0.83	587.6	30.3	633.3	30.6	799.7	75.9	**587.6**	**30.3**
878	827683	2.7	16.7618	0.2	0.7855	0.6	0.0955	0.6	0.92	587.9	3.1	588.6	2.7	591.2	5.0	**587.9**	**3.1**
278	149833	1.8	16.8118	1.3	0.7833	3.2	0.0955	3.0	0.92	588.0	16.8	587.4	14.5	584.8	27.5	**588.0**	**16.8**
349	69449	1.4	16.5717	1.3	0.7969	1.7	0.0958	1.0	0.62	589.6	5.8	595.1	7.6	615.9	28.7	**589.6**	**5.8**
46	9350	2.1	16.1534	8.2	0.8217	10.9	0.0963	7.1	0.66	592.5	40.4	609.0	49.8	670.9	175.7	**592.5**	**40.4**
91	66746	1.0	17.0840	2.4	0.7781	3.8	0.0964	2.9	0.77	593.3	16.5	584.4	16.7	549.8	52.2	**593.3**	**16.5**
483	273347	5.1	16.6658	1.0	0.7981	2.7	0.0965	2.5	0.93	593.6	14.0	595.7	11.9	603.7	20.6	**593.6**	**14.0**
305	90851	1.0	16.6202	1.5	0.8007	2.2	0.0965	1.6	0.72	594.0	9.1	597.2	10.0	609.6	33.3	**594.0**	**9.1**
160	65720	0.8	16.6811	2.0	0.7978	2.1	0.0965	0.7	0.35	594.0	4.2	595.6	9.7	601.7	43.5	**594.0**	**4.2**
1031	384112	3.3	16.8312	0.4	0.7925	1.4	0.0967	1.3	0.96	595.3	7.5	592.6	6.2	582.3	8.3	**595.3**	**7.5**
210	45174	1.1	16.6069	1.4	0.8033	1.9	0.0968	1.3	0.68	595.3	7.3	598.7	8.5	611.3	30.0	**595.3**	**7.3**
381	179362	2.7	16.7150	0.9	0.7995	1.3	0.0969	1.0	0.75	596.3	5.8	596.5	6.1	597.3	19.1	**596.3**	**5.8**
89	21359	1.8	17.1304	3.9	0.7809	4.0	0.0970	1.0	0.26	597.0	5.9	586.0	17.9	543.9	84.7	**597.0**	**5.9**
389	73986	1.7	16.5777	1.2	0.8076	4.9	0.0971	4.8	0.97	597.4	27.3	601.1	22.4	615.1	26.0	**597.4**	**27.3**
428	88079	1.5	16.6259	0.9	0.8059	1.7	0.0972	1.4	0.85	597.8	8.1	600.1	7.5	608.8	18.6	**597.8**	**8.1**
203	41529	1.2	16.8507	1.5	0.7965	1.6	0.0973	0.6	0.36	598.8	3.3	594.9	7.3	579.8	33.0	**598.8**	**3.3**
540	53071	1.1	16.6693	0.6	0.8062	2.5	0.0975	2.5	0.97	599.6	14.1	600.3	11.5	603.2	13.6	**599.6**	**14.1**
210	167255	3.4	16.6548	0.9	0.8079	1.4	0.0976	1.1	0.76	600.3	6.2	601.3	6.5	605.1	20.2	**600.3**	**6.2**
1065	344053	4.0	16.5594	0.3	0.8175	1.6	0.0982	1.6	0.98	603.7	9.0	606.6	7.3	617.5	6.4	**603.7**	**9.0**
208	69211	1.5	16.6313	1.3	0.8147	2.7	0.0983	2.3	0.87	604.3	13.4	605.1	12.2	608.2	28.9	**604.3**	**13.4**
118	61971	0.4	16.4560	2.0	0.8268	2.8	0.0987	2.0	0.70	606.7	11.4	611.8	13.0	631.1	43.5	**606.7**	**11.4**
182	21339	1.8	16.5588	3.6	0.8233	7.3	0.0989	6.3	0.87	607.8	36.5	609.9	33.3	617.6	77.9	**607.8**	**36.5**
930	23217	5.8	16.3987	1.2	0.8321	1.7	0.0990	1.2	0.72	608.3	7.2	614.8	8.0	638.6	25.9	**608.3**	**7.2**
196	109590	1.0	16.7517	2.0	0.8157	2.4	0.0991	1.4	0.56	609.2	7.9	605.7	11.1	592.5	44.0	**609.2**	**7.9**
155	52700	0.8	16.5649	2.0	0.8300	2.5	0.0997	1.6	0.63	612.8	9.4	613.6	11.7	616.8	42.5	**612.8**	**9.4**
133	56507	2.6	16.5729	1.9	0.8385	2.0	0.1008	0.6	0.28	619.0	3.3	618.3	9.2	615.8	41.0	**619.0**	**3.3**
584	163961	1.1	16.5467	0.5	0.8626	1.1	0.1035	1.0	0.89	635.0	6.0	631.6	5.2	619.2	11.1	**635.0**	**6.0**
266	105564	2.0	16.4902	1.3	0.8856	2.2	0.1059	1.7	0.81	649.0	10.8	644.0	10.3	626.5	27.2	**649.0**	**10.8**
258	24116	2.1	15.3020	0.9	0.9923	3.0	0.1101	2.8	0.95	673.5	18.1	699.9	15.0	785.6	18.8	**673.5**	**18.1**
547	296875	5.9	15.9417	0.4	0.9769	1.0	0.1129	0.9	0.93	689.8	6.2	692.0	5.1	699.1	8.0	**689.8**	**6.2**
220	91263	2.1	15.0889	0.9	1.0718	4.0	0.1173	3.9	0.97	715.0	26.5	739.6	21.1	815.1	18.7	**715.0**	**26.5**
554	316616	15.1	14.6025	1.4	1.1504	5.6	0.1218	5.5	0.97	741.1	38.2	777.4	30.6	883.2	28.3	**741.1**	**38.2**
293	326790	2.5	15.2756	0.3	1.1372	0.8	0.1260	0.7	0.91	765.0	5.3	771.2	4.4	789.3	7.1	**765.0**	**5.3**
175	157350	2.0	14.8121	0.8	1.2032	2.2	0.1293	2.1	0.94	783.6	15.6	802.1	12.5	853.6	15.9	**783.6**	**15.6**
141	60907	2.3	14.3948	1.3	1.3459	7.4	0.1405	7.3	0.98	847.6	57.8	865.8	43.1	912.7	27.7	**847.6**	**57.8**
440	223794	8.0	14.4646	0.5	1.3688	1.3	0.1436	1.2	0.91	865.0	9.9	875.6	7.8	902.7	11.1	**865.0**	**9.9**
64	36774	1.0	13.7330	4.1	1.6648	4.3	0.1658	1.2	0.27	989.0	10.7	995.2	27.2	1008.9	83.6	**1008.9**	**83.6**
176	135349	1.1	13.7009	0.8	1.6651	1.5	0.1655	1.2	0.83	987.0	11.4	995.3	9.4	1013.6	16.6	**1013.6**	**16.6**
162	91719	1.4	13.6655	0.8	1.7001	5.6	0.1685	5.6	0.99	1003.8	51.6	1008.6	35.9	1018.8	16.9	**1018.8**	**16.9**
138	100975	1.0	13.6617	1.4	1.6091	4.5	0.1594	4.3	0.95	953.7	37.8	973.8	28.2	1019.4	29.1	**1019.4**	**29.1**
516	287234	3.0	13.4464	0.3	1.8186	1.1	0.1774	1.1	0.96	1052.5	10.6	1052.2	7.5	1051.5	6.7	**1051.5**	**6.7**
637	260068	2.4	13.3573	0.3	1.8168	2.4	0.1760	2.4	0.99	1045.1	22.8	1051.5	15.6	1064.9	6.0	**1064.9**	**6.0**
124	57952	1.7	13.3342	1.5	1.8680	1.8	0.1807	1.0	0.58	1070.5	10.2	1069.8	11.8	1068.4	29.2	**1068.4**	**29.2**
253	183208	1.7	13.3101	0.6	1.8943	1.6	0.1829	1.5	0.92	1082.6	14.6	1079.1	10.6	1072.0	12.5	**1072.0**	**12.5**
117	16514	1.3	13.2054	1.0	1.8843	2.4	0.1805	2.2	0.90	1069.6	21.4	1075.6	15.9	1087.9	20.6	**1087.9**	**20.6**
260	331025	3.0	12.5145	0.4	2.1895	2.1	0.1987	2.1	0.98	1168.5	22.3	1177.7	14.8	1194.7	8.1	**1194.7**	**8.1**
158	160596	1.8	12.4520	0.5	2.2900	1.9	0.2068	1.8	0.96	1211.8	20.1	1209.2	13.4	1204.6	10.0	**1204.6**	**10.0**
69	44383	0.8	12.3686	1.9	2.2995	2.3	0.2063	1.2	0.52	1209.0	13.1	1212.1	16.1	1217.8	38.2	**1217.8**	**38.2**
319	171033	1.2	12.1678	0.3	2.4051	0.7	0.2122	0.7	0.94	1240.8	7.7	1244.1	5.3	1249.9	5.0	**1249.9**	**5.0**
230	348008	1.4	10.8404	0.3	3.3241	2.8	0.2613	2.8	0.99	1496.7	37.1	1486.7	21.8	1472.5	5.3	**1472.5**	**5.3**
424	8203	2.2	10.4274	1.9	3.2932	4.3	0.2491	3.8	0.90	1433.6	49.2	1479.4	33.3	1545.8	35.8	**1545.8**	**35.8**
37	70338	1.1	9.1918	1.8	4.8446	2.3	0.3230	1.5	0.63	1804.2	22.9	1792.7	19.5	1779.3	33.0	**1779.3**	**33.0**
739	26412	8.6	9.0311	4.9	4.7349	9.7	0.3101	8.4	0.87	1741.4	127.7	1773.4	81.3	1811.4	88.2	**1811.4**	**88.2**
378	530316	1.6	8.7047	0.2	5.3206	1.7	0.3359	1.6	1.00	1866.9	26.7	1872.2	14.1	1878.0	2.8	**1878.0**	**2.8**
624	572888	4.5	8.1870	0.1	5.7718	1.5	0.3427	1.5	1.00	1899.7	24.8	1942.2	13.1	1987.8	2.3	**1987.8**	**2.3**
32	41104	0.6	7.6888	1.4	6.3379	3.5	0.3534	3.2	0.92	1951.0	54.2	2023.7	30.7	2098.7	24.2	**2098.7**	**24.2**
207	32485	1.0	7.5466	0.6	6.3674	1.8	0.3485	1.7	0.95	1927.5	29.1	2027.8	16.2	2131.5	10.3	**2131.5**	**10.3**
231	451312	2.1	7.3510	0.2	7.1640	1.1	0.3819	1.1	0.98	2085.4	19.1	2132.0	9.7	2177.3	3.6	**2177.3**	**3.6**
74	117885	0.8	7.0872	0.6	7.8243	3.9	0.4022	3.8	0.99	2179.1	70.8	2211.0	34.9	2240.7	9.8	**2240.7**	**9.8**
162	280244	1.5	7.0813	0.3	7.7832	2.4	0.3997	2.4	0.99	2167.8	44.1	2206.3	21.8	2242.2	5.7	**2242.2**	**5.7**
687	613284	2.5	6.8730	0.6	7.3152	3.8	0.3646	3.7	0.99	2004.2	64.3	2150.7	33.8	2293.7	10.2	**2293.7**	**10.2**
147	179835	2.0	6.8385	0.3	8.4817	1.9	0.4207	1.9	0.99	2263.5	35.6	2284.0	17.1	2302.3	4.9	**2302.3**	**4.9**
144	108574	0.8	6.8119	0.2	8.6239	0.9	0.4261	0.9	0.97	2287.9	16.7	2299.1	8.1	2309.0	3.5	**2309.0**	**3.5**
532	1071953	4.7	6.5946	0.8	6.5654	7.4	0.3140	7.4	0.99	1760.4	113.5	2054.7	65.4	2364.5	13.0	**2364.5**	**13.0**
571	220786	2.4	6.4211	0.1	9.0972	1.0	0.4237	1.0	0.99	2277.1	19.4	2347.8	9.4	2409.9	2.5	**2409.9**	**2.5**
10	16231	2.3	5.6534	1.7	12.4544	4.4	0.5107	4.1	0.92	2659.4	88.7	2639.3	41.4	2623.9	27.9	**2623.9**	**27.9**
230	511026	1.5	5.4759	0.4	11.3219	2.3	0.4496	2.3	0.98	2393.7	45.4	2550.0	21.5	2676.8	6.6	**2676.8**	**6.6**

Appendix A continued. U-Pb analysis results of detrital zircons from the till of the Mt. Achernar moraine.

			Isotope ratios							Apparent ages (Ma)							
U	206Pb	U/Th	206Pb*		207Pb*		206Pb*		error	206Pb*		207Pb*		206Pb*		Best	
(ppm)	204Pb		207Pb*	(%)	235U*	(%)	238U	(%)	corr.	238U*	± (Ma)	235U	± (Ma)	207Pb*	± (Ma)	age	± (Ma)
125	111696	2.0	5.4239	0.6	10.3216	6.2	0.4060	6.2	1.00	2196.7	115.4	2464.0	57.7	2692.6	9.2	**2692.6**	**9.2**
60	59310	2.1	5.3948	0.2	12.7609	0.7	0.4993	0.7	0.98	2610.8	15.7	2662.2	7.0	2701.4	2.5	**2701.4**	**2.5**
99	50977	0.9	5.3529	0.2	13.4445	0.8	0.5220	0.8	0.98	2707.5	18.5	2711.4	8.0	2714.3	2.6	**2714.3**	**2.6**
64	139634	1.7	5.3430	0.4	13.1621	1.1	0.5100	1.0	0.94	2656.8	22.6	2691.3	10.4	2717.4	6.0	**2717.4**	**6.0**
63	143277	1.9	5.3370	0.2	12.3231	3.3	0.4770	3.3	1.00	2514.2	69.4	2629.3	31.4	2719.2	3.3	**2719.2**	**3.3**
267	426454	4.8	5.2935	0.3	13.8968	7.4	0.5335	7.4	1.00	2756.3	165.4	2742.7	70.0	2732.7	4.6	**2732.7**	**4.6**
167	823665	1.8	5.2805	0.2	13.8437	1.2	0.5302	1.2	0.99	2742.2	26.5	2739.1	11.4	2736.7	2.6	**2736.7**	**2.6**
215	62353	0.1	5.2289	0.4	12.5527	1.5	0.4760	1.4	0.97	2510.0	29.5	2646.7	13.8	2752.9	5.9	**2752.9**	**5.9**
400	1163887	1.0	4.7176	0.1	16.6424	0.8	0.5694	0.8	1.00	2905.5	19.1	2914.5	7.8	2920.7	1.2	**2920.7**	**1.2**
133	255963	1.4	4.3252	0.2	18.6692	3.2	0.5856	3.2	1.00	2971.7	77.0	3024.9	31.2	3060.4	3.0	**3060.4**	**3.0**
177	285901	1.4	4.3161	0.1	19.0679	2.0	0.5969	2.0	1.00	3017.3	47.7	3045.3	19.1	3063.7	1.4	**3063.7**	**1.4**
91	119323	2.6	3.9479	0.3	17.8435	3.9	0.5109	3.9	1.00	2660.5	85.1	2981.3	37.7	3205.5	4.2	**3205.5**	**4.2**
40	87468	2.1	3.7723	0.5	24.9455	1.8	0.6825	1.7	0.96	3353.9	45.4	3306.1	17.6	3277.2	7.6	**3277.2**	**7.6**
5B																	
67	22068	2.1	17.2395	4.2	0.7188	4.4	0.0899	1.1	0.25	554.8	5.8	549.9	18.5	530.0	92.4	**554.8**	**5.8**
626	228132	3.0	16.5709	0.6	0.8644	2.1	0.1039	2.0	0.96	637.2	12.1	632.5	9.8	616.0	12.9	**637.2**	**12.1**
291	209153	2.0	6.4666	0.2	8.8452	1.5	0.4148	1.4	0.99	2237.0	27.2	2322.2	13.3	2397.9	3.8	**2397.9**	**3.8**
44	35470	2.2	16.3688	7.3	0.8458	7.8	0.1004	2.7	0.34	616.8	15.7	622.3	36.4	642.5	158.2	**616.8**	**15.7**
99	229837	2.5	5.3880	0.6	13.2062	2.6	0.5161	2.5	0.97	2682.4	54.8	2694.5	24.2	2703.5	9.9	**2703.5**	**9.9**
62	21283	1.3	16.8525	5.8	0.7031	6.2	0.0859	2.0	0.33	531.5	10.2	540.7	25.8	579.5	126.7	**531.5**	**10.2**
95	117313	0.8	6.8705	0.4	8.6421	1.5	0.4306	1.5	0.96	2308.6	28.3	2301.0	13.8	2294.3	6.9	**2294.3**	**6.9**
752	17806	3.5	16.2383	3.4	0.7692	3.5	0.0906	0.9	0.27	559.0	5.0	579.3	15.4	659.6	71.9	**559.0**	**5.0**
139	75182	1.0	16.8262	1.6	0.8091	2.6	0.0987	2.1	0.80	607.0	12.1	601.9	11.9	582.9	34.2	**607.0**	**12.1**
107	38435	1.2	17.0021	4.3	0.6669	4.3	0.0822	0.8	0.19	509.5	4.0	518.8	17.6	560.3	92.7	**509.5**	**4.0**
119	43130	0.9	17.0400	2.3	0.7837	2.8	0.0968	1.5	0.55	595.9	8.7	587.6	12.5	555.4	51.0	**595.9**	**8.7**
101	50503	0.6	16.8029	2.4	0.8050	2.7	0.0981	1.1	0.42	603.3	6.6	599.7	12.2	586.0	52.7	**603.3**	**6.6**
65	45075	2.1	3.6543	0.4	21.9306	2.1	0.5812	2.0	0.98	2953.8	48.3	3180.7	20.1	3327.1	6.1	**3327.1**	**6.1**
149	51952	5.8	16.9206	2.3	0.7913	3.2	0.0971	2.2	0.69	597.4	12.4	591.9	14.2	570.8	49.6	**597.4**	**12.4**
43	99493	0.5	6.8437	1.1	8.2706	7.0	0.4105	6.9	0.99	2217.2	129.1	2261.1	63.2	2301.0	18.5	**2301.0**	**18.5**
125	303770	1.9	5.3024	0.8	12.2837	2.1	0.4724	1.9	0.93	2494.0	39.9	2626.3	19.5	2729.9	12.8	**2729.9**	**12.8**
292	293208	3.9	14.1601	0.6	1.5431	1.5	0.1585	1.3	0.92	948.3	11.7	947.8	9.0	946.5	12.0	**946.5**	**12.0**
305	109169	1.2	16.5297	1.0	0.8621	1.2	0.1034	0.7	0.57	634.0	4.3	631.3	5.8	621.4	21.8	**634.0**	**4.3**
110	32836	1.2	17.2807	3.8	0.6815	4.2	0.0854	1.8	0.42	528.4	8.9	527.7	17.3	524.8	84.0	**528.4**	**8.9**
470	235917	5.0	13.1719	0.3	1.8793	2.7	0.1795	2.6	0.99	1064.4	25.9	1073.8	17.6	1092.9	6.0	**1092.9**	**6.0**
155	33042	0.7	16.9380	3.6	0.7685	3.8	0.0944	1.2	0.32	581.6	6.8	578.9	16.6	568.5	77.6	**581.6**	**6.8**
568	245386	2.2	16.4438	0.8	0.8926	0.9	0.1065	0.4	0.48	652.1	2.6	647.8	4.2	632.6	16.4	**652.1**	**2.6**
551	198603	7.2	16.7616	0.6	0.8176	1.0	0.0994	0.8	0.82	610.9	4.9	606.7	4.6	591.3	12.5	**610.9**	**4.9**
25	17199	0.7	12.2909	4.8	2.3941	5.7	0.2134	3.1	0.55	1247.0	35.4	1240.9	41.0	1230.2	94.0	**1230.2**	**94.0**
748	147380	2.9	16.7339	0.6	0.7931	0.8	0.0963	0.5	0.71	592.4	3.1	592.9	3.5	594.9	11.9	**592.4**	**3.1**
126	493246	1.6	3.6857	0.2	26.0096	1.0	0.6953	1.0	0.98	3402.7	26.3	3346.9	9.9	3313.7	3.0	**3313.7**	**3.0**
155	50453	0.7	16.5031	2.2	0.8285	2.6	0.0992	1.4	0.55	609.5	8.4	612.8	12.0	624.9	47.0	**609.5**	**8.4**
336	162593	2.0	16.7185	0.9	0.7944	1.2	0.0963	0.7	0.65	592.8	4.2	593.7	5.2	596.9	19.2	**592.8**	**4.2**
208	123542	1.5	5.3757	0.2	12.5825	2.3	0.4906	2.3	0.99	2573.2	48.0	2648.9	21.4	2707.3	4.0	**2707.3**	**4.0**
29	21506	0.6	17.9474	13.7	0.7182	13.9	0.0935	2.2	0.16	576.1	12.2	549.6	58.9	441.1	305.7	**576.1**	**12.2**
583	156011	5.8	14.6911	0.7	1.2450	2.1	0.1327	1.9	0.93	803.0	14.5	821.1	11.6	870.6	15.3	**803.0**	**14.5**
148	153383	2.0	16.9989	2.7	0.7403	3.4	0.0913	2.1	0.62	563.0	11.3	562.6	14.7	560.7	58.5	**563.0**	**11.3**
269	74173	1.2	17.3390	1.5	0.6619	2.0	0.0832	1.3	0.63	515.4	6.2	515.8	8.0	517.4	33.6	**515.4**	**6.2**
96	37041	2.1	14.8282	1.8	1.2189	3.9	0.1311	3.4	0.89	794.0	25.6	809.3	21.6	851.4	37.3	**794.0**	**25.6**
324	109248	1.0	16.8558	1.3	0.7638	1.9	0.0934	1.3	0.71	575.5	7.3	576.2	8.2	579.1	28.4	**575.5**	**7.3**
367	110579	2.3	16.6466	1.2	0.7842	2.0	0.0947	1.6	0.80	583.1	9.1	587.9	9.1	606.2	26.8	**583.1**	**9.1**
76	23521	1.1	16.6215	2.7	0.7699	3.1	0.0928	1.4	0.47	572.1	7.8	579.7	13.5	609.4	58.4	**572.1**	**7.8**
14	4704	4.5	18.7467	19.4	0.6402	20.0	0.0870	4.8	0.24	538.1	25.0	502.4	79.3	343.4	442.3	**538.1**	**25.0**
103	52338	1.0	14.5628	2.0	1.3421	4.1	0.1417	3.6	0.88	854.5	28.9	864.1	23.9	888.8	40.5	**854.5**	**28.9**
365	71137	2.5	17.3265	0.7	0.6418	1.8	0.0807	1.7	0.92	500.0	8.1	503.4	7.2	518.9	15.6	**500.0**	**8.1**
415	146125	2.5	16.7661	0.7	0.8014	2.3	0.0974	2.2	0.95	599.4	12.8	597.6	10.6	590.7	15.1	**599.4**	**12.8**
194	53377	0.7	17.0166	1.6	0.7279	1.8	0.0898	0.8	0.45	554.6	4.2	555.3	7.6	558.4	34.8	**554.6**	**4.2**
268	261052	2.4	3.4348	0.3	26.3885	1.9	0.6574	1.8	0.99	3257.0	47.1	3361.0	18.2	3423.7	4.3	**3423.7**	**4.3**
14	4614	1.6	22.1297	40.7	0.5492	41.2	0.0881	6.2	0.15	544.5	32.2	444.5	149.3	-45.5	1027.8	**544.5**	**32.2**
172	441693	5.2	7.5087	2.1	6.6530	4.2	0.3623	3.6	0.87	1993.1	62.5	2066.4	37.2	2140.3	36.9	**2140.3**	**36.9**
273	95648	3.6	16.7292	1.0	0.7931	1.5	0.0962	1.2	0.76	592.3	6.5	592.9	6.8	595.5	21.1	**592.3**	**6.5**
117	42954	5.0	17.2443	2.7	0.6806	3.4	0.0851	2.1	0.62	526.6	10.6	527.1	13.9	529.4	58.1	**526.6**	**10.6**
83	92599	1.3	5.5047	0.4	10.8361	4.2	0.4326	4.2	0.99	2317.5	81.6	2509.2	39.2	2668.1	7.0	**2668.1**	**7.0**
213	90249	0.6	16.6485	1.3	0.7996	1.6	0.0966	1.0	0.60	594.2	5.4	596.6	7.2	605.9	27.4	**594.2**	**5.4**
972	299967	4.2	17.3548	0.6	0.6328	0.8	0.0796	0.6	0.68	494.0	2.6	497.8	3.2	515.4	13.2	**494.0**	**2.6**
228	124231	0.6	16.6798	1.5	0.8032	1.7	0.0972	0.9	0.53	597.7	5.3	598.6	7.9	601.8	32.0	**597.7**	**5.3**
360	138066	75.3	17.0211	1.4	0.7258	1.9	0.0896	1.3	0.69	553.2	6.9	554.1	8.0	557.9	29.6	**553.2**	**6.9**
75	217703	1.5	5.3248	0.2	13.5431	1.5	0.5230	1.4	0.99	2712.0	32.1	2718.3	13.9	2723.0	3.9	**2723.0**	**3.9**
120	30192	3.7	16.7378	3.4	0.8428	3.8	0.1023	1.8	0.47	627.9	10.6	620.7	17.6	594.4	72.7	**627.9**	**10.6**
63	176419	1.1	7.3871	0.5	7.4403	2.7	0.3986	2.6	0.98	2162.7	48.0	2165.8	23.9	2168.8	9.6	**2168.8**	**9.6**
193	99386	1.9	17.0827	1.7	0.7424	2.0	0.0920	1.1	0.54	567.2	6.0	563.8	8.8	550.0	37.7	**567.2**	**6.0**
618	115563	8.3	16.7784	0.8	0.7683	1.4	0.0935	1.1	0.80	576.2	6.0	578.8	6.0	589.1	17.6	**576.2**	**6.0**
251	308786	2.2	6.0418	1.3	6.2521	3.3	0.2740	3.0	0.91	1560.9	41.1	2011.8	28.5	2512.8	22.3	**2512.8**	**22.3**
484	247007	1.9	13.2404	0.4	1.8647	2.6	0.1791	2.5	0.98	1061.9	24.9	1068.7	17.1	1082.5	8.9	**1082.5**	**8.9**
157	228837	5.5	6.7719	0.2	6.3407	1.4	0.3114	1.4	0.99	1747.7	21.3	2024.1	12.4	2319.1	3.8	**2319.1**	**3.8**
245	69583	1.1	16.6455	1.1	0.8156	1.6	0.0985	1.1	0.72	605.4	6.5	605.6	7.1	606.3	23.5	**605.4**	**6.5**
134	281620	3.7	3.9703	0.4	15.8143	2.8	0.4554	2.8	0.99	2419.1	56.0	2865.6	26.7	3196.6	6.0	**3196.6**	**6.0**
117	509393	0.9	5.3868	0.2	12.7611	1.0	0.4986	1.0	0.99	2607.6	21.1	2662.2	9.4	2703.9	2.5	**2703.9**	**2.5**
533	157995	2.4	5.4060	0.4	11.7150	1.7	0.4593	1.6	0.96	2436.6	32.9	2581.9	15.7	2698.0	7.3	**2698.0**	**7.3**

Appendix A continued. U-Pb analysis results of detrital zircons from the till of the Mt. Achernar moraine.

			Isotope ratios							Apparent ages (Ma)							
U	206Pb	U/Th	206Pb*		207Pb*		206Pb*		error	206Pb*		207Pb*		206Pb*		Best	
(ppm)	204Pb		207Pb*	(%)	235U*	(%)	238U	(%)	corr.	238U*	± (Ma)	235U	± (Ma)	207Pb*	± (Ma)	age	± (Ma)
142	64434	1.5	16.5790	1.7	0.8140	1.9	0.0979	0.8	0.45	602.0	4.9	604.7	8.5	615.0	35.9	**602.0**	**4.9**
46	13878	1.8	5.3114	0.9	13.4746	2.0	0.5191	1.8	0.89	2695.2	40.4	2713.5	19.4	2727.1	15.1	**2727.1**	**15.1**
232	368028	1.8	8.3354	0.6	5.4034	3.2	0.3267	3.2	0.98	1822.2	50.1	1885.4	27.6	1955.8	11.4	**1955.8**	**11.4**
1138	204211	2.5	16.9994	0.3	0.7426	3.8	0.0916	3.8	1.00	564.7	20.5	563.9	16.4	560.7	6.8	**564.7**	**20.5**
116	82566	1.7	17.2276	3.7	0.7109	4.0	0.0888	1.6	0.38	548.6	8.2	545.3	17.1	531.5	81.9	**548.6**	**8.2**
166	64532	2.9	17.6465	1.9	0.6578	2.2	0.0842	1.2	0.52	521.0	5.8	513.2	9.0	478.6	42.3	**521.0**	**5.8**
13	4592	0.7	24.8471	34.9	0.5274	35.6	0.0951	7.0	0.20	585.3	39.4	430.1	125.5	-335.1	921.8	**585.3**	**39.4**
103	45975	0.4	16.6150	3.4	0.7893	3.5	0.0951	0.9	0.27	585.7	5.3	590.8	15.6	610.3	72.5	**585.7**	**5.3**
502	207748	2.8	17.4282	0.7	0.6365	1.3	0.0805	1.2	0.87	498.8	5.6	500.1	5.3	506.1	14.4	**498.8**	**5.6**
40	18742	3.2	15.3417	5.4	1.1082	7.1	0.1233	4.6	0.65	749.5	32.6	757.3	37.9	780.2	113.7	**749.5**	**32.6**
42	19106	1.1	17.0934	9.9	0.6894	10.0	0.0855	1.8	0.18	528.7	9.2	532.4	41.6	548.6	215.9	**528.7**	**9.2**
54	10852	3.1	17.0402	5.2	0.7309	5.4	0.0903	1.7	0.31	557.5	9.1	557.1	23.3	555.4	112.8	**557.5**	**9.1**
76	14044	1.4	18.2507	6.8	0.6173	6.9	0.0817	1.2	0.17	506.3	5.9	488.1	26.8	403.7	152.4	**506.3**	**5.9**
151	71878	0.7	12.7544	1.1	1.9503	3.0	0.1804	2.8	0.92	1069.2	27.2	1098.5	20.1	1157.1	22.8	**1157.1**	**22.8**
190	161592	1.2	13.6690	0.9	1.5721	2.4	0.1559	2.2	0.93	933.7	19.3	959.3	14.8	1018.3	18.2	**1018.3**	**18.2**
382	103444	1.0	16.8729	1.1	0.7353	1.9	0.0900	1.5	0.80	555.4	8.1	559.6	8.2	576.9	24.7	**555.4**	**8.1**
28	91867	2.1	3.2826	0.4	29.2775	0.8	0.6970	0.7	0.85	3409.4	17.9	3462.9	7.8	3493.9	6.4	**3493.9**	**6.4**
20	3508	1.1	17.3105	16.5	0.7632	17.9	0.0958	7.0	0.39	589.8	39.2	575.9	78.7	521.0	363.6	**589.8**	**39.2**
71	235490	0.5	5.1378	0.3	14.0554	1.4	0.5237	1.4	0.98	2715.0	30.1	2753.4	13.1	2781.7	4.3	**2781.7**	**4.3**
60	26484	4.0	16.1691	6.0	0.8100	6.7	0.0950	3.0	0.45	585.0	16.7	602.5	30.3	668.8	127.5	**585.0**	**16.7**
332	65846	4.9	13.7715	1.0	1.7198	4.2	0.1718	4.1	0.97	1021.9	38.6	1015.9	27.0	1003.2	20.2	**1003.2**	**20.2**
298	130058	2.7	16.6228	1.2	0.7959	1.6	0.0960	1.0	0.64	590.7	5.8	594.5	7.2	609.3	26.7	**590.7**	**5.8**
76	133989	1.8	6.3179	0.4	9.2912	1.6	0.4257	1.6	0.97	2286.5	30.4	2367.1	14.9	2437.3	6.5	**2437.3**	**6.5**
598	219648	8.8	16.1611	0.4	0.9321	1.2	0.1093	1.1	0.96	668.4	7.2	668.7	5.8	669.9	7.5	**668.4**	**7.2**
52	166407	1.4	3.8286	0.2	23.4022	1.0	0.6498	1.0	0.97	3227.5	24.6	3243.8	9.7	3253.9	3.9	**3253.9**	**3.9**
76	31894	0.3	17.2883	4.4	0.7407	4.6	0.0929	1.3	0.28	572.5	6.9	562.8	19.8	523.8	96.6	**572.5**	**6.9**
224	75521	1.1	17.2160	0.9	0.7237	1.4	0.0904	1.1	0.75	557.7	5.7	552.9	6.1	533.0	20.5	**557.7**	**5.7**
90	24098	0.8	16.7576	3.5	0.7671	3.8	0.0932	1.6	0.41	574.6	8.7	578.1	16.8	591.8	75.1	**574.6**	**8.7**
51	24474	0.5	13.4536	2.9	1.8505	4.6	0.1806	3.5	0.77	1070.1	34.9	1063.6	30.3	1050.4	59.0	**1050.4**	**59.0**
109	89061	0.4	12.4498	1.0	2.3306	1.9	0.2104	1.6	0.86	1231.2	18.0	1221.7	13.3	1204.9	19.0	**1204.9**	**19.0**
288	659322	2.0	5.2127	0.1	13.5865	1.5	0.5137	1.5	1.00	2672.2	32.2	2721.3	14.0	2758.0	2.1	**2758.0**	**2.1**
263	72512	0.9	16.8353	0.8	0.7835	2.4	0.0957	2.3	0.94	589.0	13.0	587.5	10.9	581.8	17.9	**589.0**	**13.0**
181	97554	2.5	14.4900	1.6	1.2958	5.5	0.1362	5.3	0.96	823.0	40.7	843.9	31.5	899.1	32.6	**823.0**	**40.7**
141	54279	1.5	16.7543	1.8	0.8068	2.1	0.0980	1.0	0.46	602.9	5.5	600.7	9.4	592.2	40.0	**602.9**	**5.5**
35	9647	1.4	18.7853	7.7	0.6559	8.3	0.0894	3.0	0.37	551.8	16.1	512.1	33.3	338.7	174.3	**551.8**	**16.1**
126	72238	2.5	12.8128	1.7	2.0576	1.9	0.1912	0.9	0.48	1127.9	9.6	1134.8	13.1	1148.1	33.3	**1148.1**	**33.3**
136	65993	5.4	15.1955	1.9	1.0565	4.1	0.1164	3.6	0.89	710.0	24.3	732.1	21.3	800.3	39.4	**710.0**	**24.3**
306	74189	1.1	12.6283	3.2	1.1515	4.0	0.1055	2.4	0.60	646.3	14.5	777.9	21.5	1176.8	62.8	**1176.8**	**62.8**
292	110282	2.0	16.3036	1.9	0.7820	3.4	0.0925	2.8	0.82	570.1	15.0	586.6	15.0	651.0	41.4	**570.1**	**15.0**
72	93380	2.3	14.6352	2.9	1.1824	3.7	0.1255	2.2	0.60	762.2	16.0	792.4	20.3	878.5	60.8	**762.2**	**16.0**
669	175719	143.9	17.2299	0.8	0.7128	1.4	0.0891	1.2	0.85	550.1	6.5	546.4	6.1	531.2	16.4	**550.1**	**6.5**
40	56572	1.4	5.8401	1.1	10.8862	2.6	0.4611	2.4	0.91	2444.4	48.1	2513.5	24.1	2569.7	17.7	**2569.7**	**17.7**
75	23204	0.7	16.8234	3.2	0.7658	3.7	0.0934	1.8	0.49	575.8	9.8	577.3	16.2	583.3	69.7	**575.8**	**9.8**
85	39846	0.5	16.6345	3.0	0.8106	3.5	0.0978	1.8	0.51	601.5	10.1	602.8	15.8	607.7	65.0	**601.5**	**10.1**
75	108993	1.7	3.8869	0.9	23.2314	3.0	0.6549	2.8	0.95	3247.3	71.6	3236.7	28.7	3230.1	14.3	**3230.1**	**14.3**
215	86083	2.3	5.6374	0.4	9.9401	3.6	0.4064	3.6	0.99	2198.5	66.5	2429.2	33.1	2628.6	6.2	**2628.6**	**6.2**
96	38665	1.1	16.5929	3.7	0.8936	4.1	0.1075	1.8	0.43	658.4	11.0	648.3	19.4	613.1	79.0	**658.4**	**11.0**
29	10620	1.6	16.8770	11.8	0.7786	12.4	0.0953	3.9	0.32	586.8	22.1	584.7	55.3	576.4	257.0	**586.8**	**22.1**
169	62612	2.7	16.6205	1.5	0.7657	2.1	0.0923	1.5	0.71	569.1	8.0	577.3	9.1	609.6	31.8	**569.1**	**8.0**
244	158530	1.6	5.4029	0.2	12.2001	1.9	0.4781	1.9	1.00	2518.8	40.2	2619.9	18.2	2699.0	2.9	**2699.0**	**2.9**
158	101454	3.6	16.8857	1.3	0.7541	1.9	0.0924	1.5	0.75	569.5	7.9	570.6	8.5	575.2	28.2	**569.5**	**7.9**
213	83860	2.2	16.8471	1.2	0.7474	2.3	0.0913	2.0	0.85	563.3	10.6	566.7	10.1	580.2	26.7	**563.3**	**10.6**
72	23807	1.9	16.3541	2.8	0.8115	3.2	0.0963	1.4	0.45	592.4	8.0	603.3	14.4	644.4	60.9	**592.4**	**8.0**
110	50452	1.1	16.6425	2.4	0.7460	3.2	0.0900	2.1	0.66	555.8	11.3	565.9	14.0	606.7	52.5	**555.8**	**11.3**
91	28226	0.4	16.4751	3.5	0.7881	3.9	0.0942	1.6	0.41	580.1	8.8	590.1	17.3	628.5	76.0	**580.1**	**8.8**
155	67041	1.4	16.7374	1.6	0.7898	3.2	0.0959	2.8	0.86	590.2	15.7	591.1	14.5	594.4	35.3	**590.2**	**15.7**
61	236166	1.7	4.6951	0.3	16.6383	2.5	0.5666	2.5	0.99	2893.7	57.8	2914.2	23.9	2928.4	4.6	**2928.4**	**4.6**
75	23520	0.8	16.3275	2.8	0.8040	3.2	0.0952	1.6	0.49	586.3	8.8	599.1	14.4	647.9	59.5	**586.3**	**8.8**
Z3B-1																	
Mackellar Sandstone																	
612	610605	63.3	17.1627	0.6	0.6891	1.2	0.0858	1.0	0.85	530.5	5.2	532.3	5.0	539.8	13.9	**530.5**	**5.2**
376	2535	24.8	16.7991	2.5	0.7139	2.6	0.0870	0.9	0.33	537.7	4.5	547.1	11.2	586.4	54.3	**537.7**	**4.5**
302	65989	101.2	17.1676	1.0	0.7031	2.2	0.0875	1.9	0.88	541.0	10.0	540.7	9.2	539.1	22.8	**541.0**	**10.0**
482	169198	2.9	17.2175	0.9	0.7041	1.5	0.0879	1.2	0.80	543.3	6.2	541.3	6.3	532.8	19.8	**543.3**	**6.2**
51	14140	1.1	16.9759	5.5	0.7391	6.5	0.0910	3.4	0.53	561.5	18.5	561.9	28.2	563.6	120.9	**561.5**	**18.5**
160	38183	3.3	16.9232	2.3	0.7447	2.5	0.0914	1.0	0.41	563.8	5.5	565.1	10.8	570.5	49.4	**563.8**	**5.5**
220	92679	6.0	16.4107	2.2	0.7697	3.3	0.0916	2.5	0.75	565.1	13.6	579.6	14.8	637.0	47.5	**565.1**	**13.6**
31	7019	1.2	16.3646	6.6	0.7726	7.3	0.0917	3.0	0.41	565.6	16.3	581.3	32.2	643.0	142.4	**565.6**	**16.3**
144	28621	0.8	16.8778	2.2	0.7502	2.4	0.0918	1.0	0.41	566.4	5.2	568.4	10.3	576.2	47.2	**566.4**	**5.2**
49	29711	1.9	16.6295	5.0	0.7632	5.3	0.0920	1.7	0.32	567.6	9.0	575.8	23.1	608.4	108.1	**567.6**	**9.0**
121	36882	1.7	16.8770	2.4	0.7548	3.6	0.0924	2.6	0.74	569.6	14.4	571.0	15.6	576.3	52.4	**569.6**	**14.4**
223	69830	0.5	16.8303	1.5	0.7577	2.2	0.0925	1.6	0.72	570.2	8.8	572.7	9.7	582.4	33.4	**570.2**	**8.8**
201	248993	3.6	16.8908	1.3	0.7555	2.4	0.0925	2.0	0.84	570.6	10.8	571.4	10.3	574.6	28.1	**570.6**	**10.8**
9	7292	4.1	17.6488	40.7	0.7243	41.1	0.0927	5.9	0.14	571.5	32.4	553.2	177.1	478.3	935.6	**571.5**	**32.4**
106	71009	0.7	16.9284	1.8	0.7558	2.2	0.0928	1.4	0.62	572.1	7.6	571.6	9.8	569.8	38.4	**572.1**	**7.6**
50	26908	0.7	16.4296	5.5	0.7790	5.8	0.0928	2.1	0.36	572.2	11.4	584.9	26.0	634.5	117.6	**572.2**	**11.4**
184	101503	3.1	16.9474	1.2	0.7574	1.6	0.0931	1.1	0.66	573.8	5.9	572.5	7.2	567.3	27.0	**573.8**	**5.9**
135	6336	1.7	16.7346	1.8	0.7699	2.8	0.0934	2.1	0.76	575.9	11.8	579.7	12.4	594.8	39.6	**575.9**	**11.8**

Appendix A continued. U-Pb analysis results of detrital zircons from the till of the Mt. Achernar moraine.

			Isotope ratios							Apparent ages (Ma)							
U	206Pb	U/Th	206Pb*		207Pb*		206Pb*		error	206Pb*		207Pb*		206Pb*		Best	
(ppm)	204Pb		207Pb*	(%)	235U*	(%)	238U	(%)	corr.	238U*	± (Ma)	235U	± (Ma)	207Pb*	± (Ma)	age	± (Ma)
95	30932	0.5	16.8783	2.4	0.7644	3.1	0.0936	2.0	0.63	576.6	10.8	576.6	13.6	576.2	52.4	**576.6**	**10.8**
56	14496	0.6	16.2237	3.7	0.7962	3.9	0.0937	1.2	0.30	577.3	6.4	594.7	17.7	661.6	80.3	**577.3**	**6.4**
357	176144	3.3	16.8014	1.1	0.7691	2.6	0.0937	2.3	0.90	577.5	12.9	579.3	11.4	586.2	24.5	**577.5**	**12.9**
320	138896	0.3	16.8660	1.0	0.7674	1.5	0.0939	1.1	0.72	578.4	6.0	578.2	6.6	577.8	22.6	**578.4**	**6.0**
712	289151	5.2	16.9087	0.5	0.7659	0.7	0.0939	0.5	0.73	578.7	3.0	577.4	3.2	572.3	10.9	**578.7**	**3.0**
45	19502	1.2	17.8042	6.4	0.7333	6.7	0.0947	1.8	0.27	583.2	10.3	558.5	28.8	458.9	143.0	**583.2**	**10.3**
21	12340	0.8	17.1892	14.2	0.7596	15.0	0.0947	5.0	0.33	583.3	28.0	573.8	66.0	536.4	311.5	**583.3**	**28.0**
92	23246	0.3	17.0145	3.2	0.7679	3.4	0.0948	1.2	0.34	583.6	6.5	578.5	15.0	558.7	69.7	**583.6**	**6.5**
144	48941	2.4	16.9336	1.2	0.7735	4.0	0.0950	3.8	0.96	585.0	21.3	581.8	17.6	569.1	25.6	**585.0**	**21.3**
183	19058	1.9	16.4545	4.1	0.7973	4.2	0.0951	0.8	0.19	585.9	4.6	595.3	18.9	631.3	88.6	**585.9**	**4.6**
33	10270	0.5	17.5856	7.9	0.7461	8.7	0.0952	3.7	0.42	585.9	20.5	565.9	37.8	486.3	174.7	**585.9**	**20.5**
115	81503	1.1	16.7633	2.3	0.7834	3.2	0.0952	2.3	0.70	586.5	12.8	587.4	14.4	591.1	49.8	**586.5**	**12.8**
79	29719	0.8	16.8738	3.3	0.7797	3.7	0.0954	1.6	0.43	587.5	9.1	585.3	16.5	576.8	72.6	**587.5**	**9.1**
448	190171	0.9	16.7813	0.7	0.7840	2.2	0.0954	2.1	0.95	587.5	11.8	587.8	9.9	588.7	14.9	**587.5**	**11.8**
64	28445	0.6	16.8790	2.3	0.7801	2.9	0.0955	1.7	0.60	588.0	9.7	585.5	12.7	576.1	49.6	**588.0**	**9.7**
471	21861	4.0	16.6425	0.8	0.7922	1.6	0.0956	1.4	0.88	588.7	7.8	592.4	7.1	606.7	16.3	**588.7**	**7.8**
96	23839	33.7	16.6744	2.6	0.7918	2.9	0.0957	1.2	0.42	589.5	6.8	592.2	12.9	602.6	56.5	**589.5**	**6.8**
16	9933	1.0	20.1743	14.5	0.6555	15.4	0.0959	5.1	0.33	590.4	28.5	511.9	61.9	174.8	340.1	**590.4**	**28.5**
134	53111	2.1	16.7313	2.4	0.7936	2.9	0.0963	1.6	0.55	592.7	9.1	593.2	13.1	595.2	53.0	**592.7**	**9.1**
130	36810	3.2	16.5272	1.9	0.8070	3.6	0.0967	3.0	0.85	595.2	17.2	600.7	16.2	621.7	41.2	**595.2**	**17.2**
214	23409	2.1	16.5655	2.3	0.8065	2.7	0.0969	1.4	0.51	596.2	8.0	600.5	12.4	616.7	50.6	**596.2**	**8.0**
246	5577	6.3	16.5986	1.1	0.8049	1.7	0.0969	1.3	0.78	596.2	7.5	599.6	7.7	612.4	22.9	**596.2**	**7.5**
190	51028	0.4	16.8085	0.9	0.7964	1.6	0.0971	1.3	0.83	597.3	7.5	594.8	7.1	585.2	19.2	**597.3**	**7.5**
82	21041	1.1	16.4851	3.0	0.8158	3.7	0.0975	2.1	0.58	600.0	12.2	605.7	16.7	627.2	64.4	**600.0**	**12.2**
188	48093	1.1	16.6822	1.1	0.8070	2.2	0.0976	1.9	0.87	600.5	10.9	600.7	9.9	601.5	23.2	**600.5**	**10.9**
166	69011	2.3	16.7556	2.5	0.8035	2.8	0.0976	1.3	0.45	600.6	7.3	598.8	12.7	592.0	54.3	**600.6**	**7.3**
585	65072	2.3	16.5915	0.5	0.8129	0.8	0.0978	0.6	0.78	601.6	3.7	604.1	3.7	613.3	11.2	**601.6**	**3.7**
178	43494	2.2	16.8320	1.7	0.8016	3.6	0.0979	3.2	0.89	601.8	18.5	597.7	16.4	582.2	36.3	**601.8**	**18.5**
84	22480	1.1	16.2458	2.7	0.8340	3.0	0.0983	1.3	0.44	604.3	7.5	615.9	13.7	658.6	57.3	**604.3**	**7.5**
120	1905	0.3	15.9271	4.6	0.8541	4.9	0.0987	1.7	0.35	606.6	9.9	626.9	23.0	701.0	98.3	**606.6**	**9.9**
72	42264	1.3	16.5107	5.4	0.8250	5.7	0.0988	1.7	0.30	607.3	9.8	610.8	26.1	623.9	116.9	**607.3**	**9.8**
742	364814	1.2	16.6455	0.5	0.8195	1.1	0.0989	0.9	0.88	608.1	5.5	607.8	4.9	606.3	11.0	**608.1**	**5.5**
610	179873	11.7	16.5560	0.4	0.8245	0.8	0.0990	0.8	0.89	608.5	4.4	610.5	3.9	617.9	8.5	**608.5**	**4.4**
511	260925	2.3	16.6302	0.6	0.8214	1.2	0.0991	1.0	0.84	609.0	5.6	608.8	5.3	608.3	13.4	**609.0**	**5.6**
395	158199	3.6	16.7274	0.6	0.8167	1.9	0.0991	1.8	0.95	609.0	10.5	606.2	8.7	595.7	13.1	**609.0**	**10.5**
114	140882	2.0	16.4352	2.4	0.8316	2.6	0.0991	1.1	0.42	609.3	6.3	614.5	12.1	633.8	51.3	**609.3**	**6.3**
251	5750	0.7	16.1909	3.7	0.8442	5.2	0.0991	3.7	0.70	609.3	21.3	621.4	24.2	665.9	79.3	**609.3**	**21.3**
127	85783	1.4	16.7325	2.8	0.8215	4.1	0.0997	3.0	0.73	612.6	17.3	608.9	18.6	595.0	60.4	**612.6**	**17.3**
335	124451	1.8	16.7053	0.5	0.8262	2.8	0.1001	2.7	0.98	615.0	16.0	611.5	12.8	598.6	10.4	**615.0**	**16.0**
116	66200	1.3	16.4015	1.8	0.8455	2.5	0.1006	1.7	0.68	617.8	10.0	622.2	11.6	638.2	38.9	**617.8**	**10.0**
131	61825	0.6	16.5980	2.8	0.8385	3.1	0.1009	1.4	0.44	619.9	8.0	618.3	14.2	612.5	59.6	**619.9**	**8.0**
187	19309	1.1	16.4254	1.8	0.8476	2.5	0.1010	1.8	0.72	620.1	10.7	623.3	11.8	635.1	37.9	**620.1**	**10.7**
61	53313	1.2	16.2268	3.1	0.8658	5.3	0.1019	4.4	0.82	625.5	26.0	633.3	25.1	661.2	65.9	**625.5**	**26.0**
206	70683	1.0	16.4787	1.1	0.8766	1.5	0.1048	1.1	0.71	642.3	6.5	639.1	7.1	628.0	22.9	**642.3**	**6.5**
845	374238	5.5	16.3780	0.5	0.8932	1.9	0.1061	1.8	0.96	650.0	11.1	648.1	9.0	641.3	11.0	**650.0**	**11.1**
85	32789	1.3	16.3776	3.1	0.9043	4.3	0.1074	3.0	0.70	657.7	18.8	654.0	20.8	641.3	66.2	**657.7**	**18.8**
574	178907	3.9	16.3744	0.4	0.9097	3.1	0.1080	3.1	0.99	661.3	19.6	656.9	15.2	641.8	9.2	**661.3**	**19.6**
371	17761	1.9	15.6054	1.0	0.9582	3.2	0.1084	3.0	0.95	663.7	19.2	682.4	15.9	744.3	21.4	**663.7**	**19.2**
59	24864	5.0	15.8461	4.1	0.9619	5.1	0.1105	3.0	0.59	675.9	19.2	684.3	25.2	711.8	86.8	**675.9**	**19.2**
119	114947	1.7	14.8260	2.0	1.0736	4.1	0.1154	3.6	0.87	704.3	23.8	740.5	21.6	851.7	42.2	**704.3**	**23.8**
53	27491	2.2	15.3897	5.1	1.0516	6.2	0.1174	3.6	0.58	715.5	24.2	729.7	32.3	773.6	106.7	**715.5**	**24.2**
156	35282	6.1	15.3524	1.8	1.1349	3.6	0.1264	3.1	0.87	767.1	22.6	770.1	19.4	778.7	37.7	**767.1**	**22.6**
325	110127	3.0	14.2528	0.4	1.5635	3.8	0.1616	3.7	0.99	965.8	33.6	955.8	23.3	933.1	7.8	**933.1**	**7.8**
108	51290	3.6	14.1093	2.2	1.4911	4.5	0.1526	3.9	0.87	915.4	33.2	926.8	27.1	953.8	44.2	**953.8**	**44.2**
110	24173	4.5	13.8465	1.6	1.6769	5.6	0.1684	5.4	0.96	1003.3	50.0	999.8	35.7	992.2	32.7	**992.2**	**32.7**
110	89902	3.1	13.6402	1.4	1.6194	7.5	0.1602	7.4	0.98	957.9	65.9	977.8	47.3	1022.6	29.0	**1022.6**	**29.0**
92	32146	0.6	13.5574	1.3	1.7091	2.0	0.1681	1.5	0.74	1001.4	13.5	1012.0	12.5	1034.9	26.5	**1034.9**	**26.5**
250	151121	1.7	13.5478	0.5	1.6769	1.3	0.1648	1.2	0.93	983.2	11.0	999.8	8.3	1036.3	9.9	**1036.3**	**9.9**
285	157913	1.5	13.3062	0.5	1.8762	2.0	0.1811	1.9	0.96	1072.8	18.6	1072.7	13.0	1072.6	11.0	**1072.6**	**11.0**
186	167255	2.0	13.2692	0.7	1.9189	1.2	0.1847	0.9	0.77	1092.4	9.0	1087.7	7.8	1078.2	15.0	**1078.2**	**15.0**
331	24064	11.3	13.0705	1.4	1.5245	3.5	0.1445	3.2	0.92	870.1	26.0	940.3	21.4	1108.4	27.8	**1108.4**	**27.8**
182	134538	1.4	13.0050	0.7	1.9143	3.6	0.1806	3.6	0.98	1070.0	35.2	1086.1	24.2	1118.5	13.4	**1118.5**	**13.4**
100	5172	0.8	12.8745	1.5	1.7576	6.9	0.1641	6.8	0.98	979.6	61.6	1030.0	45.0	1138.5	29.8	**1138.5**	**29.8**
212	152389	1.5	12.8577	0.5	1.8194	1.4	0.1697	1.3	0.92	1010.2	12.3	1052.5	9.3	1141.1	10.8	**1141.1**	**10.8**
56	18682	0.8	12.7624	1.4	2.0571	5.6	0.1904	5.4	0.97	1123.6	55.8	1134.7	38.3	1155.9	28.4	**1155.9**	**28.4**
1340	11172	17.3	12.6128	2.0	2.1285	2.1	0.1947	0.6	0.29	1146.8	6.5	1158.1	14.7	1179.3	40.2	**1179.3**	**40.2**
268	284649	1.7	12.5919	0.4	2.2927	1.0	0.2094	1.0	0.93	1225.5	10.7	1210.0	7.2	1182.6	7.2	**1182.6**	**7.2**
282	49290	1.1	12.5752	0.4	2.2145	2.6	0.2020	2.6	0.99	1185.9	28.4	1185.6	18.5	1185.2	7.0	**1185.2**	**7.0**
411	174812	7.4	12.4864	0.3	2.3317	1.3	0.2112	1.3	0.96	1235.0	14.1	1222.0	9.2	1199.1	6.7	**1199.1**	**6.7**
140	149135	2.4	12.3633	0.8	2.2959	2.1	0.2059	1.9	0.93	1206.7	21.2	1211.0	14.6	1218.6	14.8	**1218.6**	**14.8**
138	70042	1.0	12.3192	0.7	2.3137	1.4	0.2067	1.3	0.89	1211.3	13.9	1216.5	10.1	1225.6	12.9	**1225.6**	**12.9**
346	264819	0.9	12.2724	0.2	2.4325	2.1	0.2165	2.1	0.99	1263.4	23.9	1252.3	15.1	1233.2	4.6	**1233.2**	**4.6**
20	1386	0.6	12.1139	7.2	2.4566	7.6	0.2158	2.4	0.32	1259.8	27.9	1259.4	54.8	1258.6	140.7	**1258.6**	**140.7**
434	359713	1.7	10.1091	0.3	3.5951	1.0	0.2636	1.0	0.96	1508.2	13.1	1548.5	8.1	1603.9	5.6	**1603.9**	**5.6**
143	106193	3.1	9.6546	8.3	2.8835	10.4	0.2019	6.2	0.60	1185.6	67.3	1377.6	78.4	1689.2	153.7	**1689.2**	**153.7**
573	812058	2.3	9.6467	0.2	4.1869	1.4	0.2929	1.4	0.99	1656.2	20.3	1671.5	11.5	1690.7	3.1	**1690.7**	**3.1**
105	119999	1.5	9.2825	0.5	4.5685	3.7	0.3076	3.7	0.99	1728.7	56.3	1743.5	31.2	1761.3	8.4	**1761.3**	**8.4**
171	152251	1.5	8.1432	0.5	6.2653	2.2	0.3700	2.1	0.98	2029.5	37.1	2013.6	19.1	1997.3	8.1	**1997.3**	**8.1**

Appendix A continued. U-Pb analysis results of detrital zircons from the till of the Mt. Achernar moraine.

			Isotope ratios							Apparent ages (Ma)							
U	206Pb	U/Th	206Pb*		207Pb*		206Pb*		error	206Pb*		207Pb*		206Pb*		Best	
(ppm)	204Pb		207Pb*	(%)	235U*	(%)	238U	(%)	corr.	238U*	± (Ma)	235U	± (Ma)	207Pb*	± (Ma)	age	± (Ma)
214	207540	2.9	7.6172	1.1	6.5599	2.4	0.3624	2.1	0.89	1993.6	36.5	2054.0	21.0	2115.2	18.8	**2115.2**	**18.8**
63	82900	1.0	7.5001	0.7	7.1561	1.7	0.3893	1.6	0.92	2119.4	28.3	2131.1	15.1	2142.3	11.5	**2142.3**	**11.5**
99	203820	1.0	7.4480	0.8	6.6574	5.6	0.3596	5.6	0.99	1980.4	95.1	2067.0	49.7	2154.5	13.3	**2154.5**	**13.3**
347	1080049	2.4	6.8841	0.1	8.2845	2.3	0.4136	2.3	1.00	2231.5	42.9	2262.6	20.6	2290.9	2.1	**2290.9**	**2.1**
257	340778	2.2	6.8335	0.5	6.1884	3.2	0.3067	3.2	0.99	1724.5	47.7	2002.8	27.9	2303.6	8.3	**2303.6**	**8.3**
689	681714	2.2	6.8064	0.1	8.6498	1.0	0.4270	1.0	1.00	2292.1	19.5	2301.8	9.2	2310.4	1.5	**2310.4**	**1.5**
42	86891	0.9	6.4335	1.0	8.4147	3.0	0.3926	2.8	0.94	2135.0	51.8	2276.8	27.4	2406.6	17.1	**2406.6**	**17.1**
308	233308	1.3	6.3026	0.2	8.7579	2.3	0.4003	2.3	1.00	2170.5	42.3	2313.1	21.0	2441.5	3.8	**2441.5**	**3.8**
202	161853	2.2	6.2035	0.3	9.7585	3.2	0.4391	3.2	1.00	2346.4	62.4	2412.2	29.4	2468.3	5.1	**2468.3**	**5.1**
467	18403	3.0	5.7061	0.5	9.4582	2.8	0.3914	2.8	0.98	2129.4	50.2	2383.5	25.9	2608.4	8.7	**2608.4**	**8.7**
231	463200	2.5	5.4178	0.2	12.2721	3.0	0.4822	3.0	1.00	2536.9	63.7	2625.4	28.6	2694.4	4.0	**2694.4**	**4.0**
181	46160	1.6	5.3682	0.4	12.5607	1.4	0.4890	1.4	0.97	2566.5	29.3	2647.3	13.5	2709.6	6.2	**2709.6**	**6.2**
123	290508	0.9	5.2081	0.2	13.3014	2.1	0.5024	2.1	1.00	2624.2	44.8	2701.3	19.7	2759.4	2.6	**2759.4**	**2.6**
25	77107	1.0	5.1229	0.5	14.8162	2.4	0.5505	2.3	0.97	2827.2	53.6	2803.5	22.9	2786.5	9.0	**2786.5**	**9.0**
879	8541	1.4	4.1287	0.8	18.3083	1.9	0.5482	1.7	0.90	2817.8	38.8	3006.1	18.2	3134.5	13.0	**3134.5**	**13.0**
218	546627	0.7	3.9587	0.2	22.1392	1.1	0.6356	1.1	0.98	3171.8	27.2	3189.9	10.7	3201.2	3.2	**3201.2**	**3.2**
194	470813	2.0	3.8172	0.1	23.4100	2.4	0.6481	2.4	1.00	3220.8	61.7	3244.1	23.7	3258.6	1.6	**3258.6**	**1.6**
277	512953	7.5	3.7670	0.3	20.7634	0.8	0.5673	0.7	0.93	2896.6	16.4	3127.6	7.3	3279.4	4.4	**3279.4**	**4.4**
112	43286	1.1	3.5424	0.1	27.6040	2.2	0.7092	2.2	1.00	3455.4	58.0	3405.1	21.3	3375.7	1.5	**3375.7**	**1.5**
0Z5-1																	
Pagoda Tillite																	
770	431964	5.4	17.4339	0.6	0.6561	1.4	0.0830	1.3	0.91	513.7	6.2	512.2	5.6	505.4	12.3	**513.7**	**6.2**
208	194085	0.9	17.3167	1.4	0.6788	2.1	0.0852	1.5	0.75	527.4	7.8	526.0	8.4	520.2	29.9	**527.4**	**7.8**
86	21249	0.9	16.5184	2.6	0.7546	3.4	0.0904	2.1	0.63	557.9	11.4	570.9	14.7	622.9	56.3	**557.9**	**11.4**
29	16907	3.1	17.5548	9.9	0.7112	10.2	0.0906	2.4	0.23	558.8	12.7	545.5	43.0	490.2	218.8	**558.8**	**12.7**
60	15629	3.1	17.3509	7.1	0.7247	7.4	0.0912	2.1	0.29	562.6	11.5	553.4	31.7	515.8	156.4	**562.6**	**11.5**
647	354359	4.8	17.0144	0.5	0.7408	1.0	0.0914	0.9	0.87	563.9	4.7	562.9	4.4	558.7	10.7	**563.9**	**4.7**
310	179667	6.7	17.0550	1.0	0.7464	1.7	0.0923	1.5	0.83	569.3	7.9	566.1	7.6	553.5	21.2	**569.3**	**7.9**
130	35621	0.6	16.9795	1.4	0.7514	3.3	0.0925	3.0	0.90	570.5	16.2	569.0	14.3	563.2	30.5	**570.5**	**16.2**
165	43235	3.1	16.7070	2.0	0.7637	2.4	0.0925	1.3	0.56	570.5	7.4	576.1	10.6	598.4	43.4	**570.5**	**7.4**
332	73243	3.6	16.9063	0.8	0.7575	1.5	0.0929	1.3	0.86	572.6	7.3	572.6	6.8	572.6	17.2	**572.6**	**7.3**
167	103654	0.9	16.8133	2.4	0.7618	3.4	0.0929	2.4	0.70	572.6	13.1	575.1	14.9	584.6	52.5	**572.6**	**13.1**
113	61698	0.3	17.0080	2.8	0.7554	4.0	0.0932	2.9	0.72	574.3	16.0	571.3	17.7	559.5	61.2	**574.3**	**16.0**
202	138260	3.1	16.8518	1.4	0.7666	1.9	0.0937	1.3	0.67	577.4	7.0	577.8	8.3	579.6	30.2	**577.4**	**7.0**
35	26986	1.4	16.6834	6.5	0.7762	6.8	0.0939	2.0	0.30	578.7	11.2	583.3	30.2	601.4	140.8	**578.7**	**11.2**
105	57788	0.9	16.8087	2.6	0.7832	3.2	0.0955	2.0	0.61	587.9	11.1	587.3	14.4	585.2	55.5	**587.9**	**11.1**
80	45338	1.8	16.3079	2.1	0.8082	2.2	0.0956	0.8	0.36	588.5	4.5	601.4	10.0	650.5	44.2	**588.5**	**4.5**
117	50748	2.3	16.3548	1.5	0.8073	2.2	0.0958	1.7	0.76	589.5	9.5	600.9	10.1	644.3	31.4	**589.5**	**9.5**
327	23448	0.9	16.4547	1.1	0.8033	1.3	0.0959	0.8	0.62	590.1	4.7	598.7	6.1	631.2	22.7	**590.1**	**4.7**
1166	461926	5.1	16.7001	0.3	0.7917	0.9	0.0959	0.9	0.95	590.3	4.9	592.1	4.1	599.2	6.1	**590.3**	**4.9**
98	31748	1.6	16.9618	2.1	0.7798	3.3	0.0959	2.5	0.76	590.5	13.9	585.4	14.5	565.5	46.4	**590.5**	**13.9**
729	209905	26.7	16.7423	0.5	0.7954	0.9	0.0966	0.8	0.87	594.3	4.6	594.2	4.2	593.8	9.8	**594.3**	**4.6**
809	306284	98.8	16.6939	0.5	0.7977	1.1	0.0966	1.0	0.92	594.4	5.9	595.5	5.1	600.0	9.8	**594.4**	**5.9**
104	13782	1.8	16.6580	4.1	0.8025	4.8	0.0970	2.5	0.52	596.6	14.0	598.3	21.5	604.7	88.3	**596.6**	**14.0**
267	102616	1.7	16.7249	0.8	0.7995	1.3	0.0970	1.1	0.82	596.7	6.2	596.5	6.0	596.0	16.7	**596.7**	**6.2**
488	186021	3.3	16.6736	0.9	0.8029	2.6	0.0971	2.5	0.95	597.3	14.2	598.4	11.9	602.7	18.4	**597.3**	**14.2**
520	11552	2.7	16.6211	0.7	0.8072	2.0	0.0973	1.8	0.93	598.6	10.5	600.9	9.0	609.5	15.7	**598.6**	**10.5**
387	202239	2.1	16.6496	0.6	0.8061	1.4	0.0973	1.3	0.91	598.8	7.2	600.3	6.3	605.8	12.7	**598.8**	**7.2**
655	194016	15.4	16.5675	0.6	0.8123	2.6	0.0976	2.6	0.98	600.3	14.8	603.7	12.0	616.4	11.9	**600.3**	**14.8**
302	197003	1.3	16.6322	0.4	0.8114	1.2	0.0979	1.1	0.95	602.0	6.5	603.3	5.4	608.0	8.0	**602.0**	**6.5**
174	56583	0.6	16.6585	1.3	0.8106	2.4	0.0979	2.1	0.85	602.3	11.9	602.8	11.1	604.6	27.8	**602.3**	**11.9**
82	37887	1.0	16.5146	2.1	0.8179	2.7	0.0980	1.6	0.61	602.5	9.5	606.9	12.4	623.4	46.3	**602.5**	**9.5**
306	77190	1.6	16.8365	1.3	0.8035	3.3	0.0981	3.0	0.91	603.4	17.5	598.8	15.0	581.6	29.2	**603.4**	**17.5**
118	77046	0.4	16.7505	1.5	0.8079	1.9	0.0982	1.2	0.60	603.6	6.7	601.3	8.8	592.7	33.6	**603.6**	**6.7**
645	48303	13.8	16.6670	0.5	0.8205	1.9	0.0992	1.8	0.96	609.6	10.3	608.3	8.5	603.5	11.6	**609.6**	**10.3**
221	52634	3.1	16.6569	0.8	0.8302	1.1	0.1003	0.8	0.74	616.1	5.0	613.7	5.3	604.8	16.6	**616.1**	**5.0**
285	97188	1.2	16.4951	1.2	0.8425	2.3	0.1008	2.0	0.86	619.0	11.7	620.5	10.6	625.9	24.9	**619.0**	**11.7**
798	17827	2.4	16.4958	0.4	0.8435	1.7	0.1009	1.6	0.97	619.8	9.7	621.1	7.9	625.8	8.5	**619.8**	**9.7**
292	261683	3.2	16.3543	0.8	0.8746	2.3	0.1037	2.2	0.94	636.3	13.2	638.1	11.0	644.4	17.7	**636.3**	**13.2**
54	17386	0.7	15.7699	5.8	0.9255	10.3	0.1059	8.5	0.82	648.6	52.4	665.3	50.4	722.1	124.2	**648.6**	**52.4**
363	142176	12.7	15.6422	0.9	0.9425	3.3	0.1069	3.2	0.96	654.9	19.7	674.2	16.2	739.3	18.3	**654.9**	**19.7**
312	101430	22.1	16.1193	0.9	0.9188	1.4	0.1074	1.1	0.79	657.8	7.1	661.7	7.0	675.4	18.9	**657.8**	**7.1**
57	22872	3.0	15.4528	2.4	0.9588	3.9	0.1075	3.0	0.78	658.0	18.8	682.7	19.2	765.0	51.3	**658.0**	**18.8**
551	215063	5.0	15.2031	1.0	1.0383	3.2	0.1145	3.0	0.95	698.7	20.0	723.1	16.4	799.2	20.3	**698.7**	**20.0**
544	335137	1.3	14.9427	1.1	1.0719	2.0	0.1162	1.6	0.83	708.5	10.9	739.7	10.2	835.4	22.7	**708.5**	**10.9**
210	178955	3.9	15.3552	0.6	1.0531	3.8	0.1173	3.8	0.99	714.9	25.4	730.4	19.8	778.3	12.0	**714.9**	**25.4**
25	8421	1.2	15.0805	5.2	1.1438	7.6	0.1251	5.5	0.73	759.9	39.7	774.3	41.3	816.2	109.2	**759.9**	**39.7**
164	76258	1.5	14.6954	1.5	1.1856	4.9	0.1264	4.7	0.95	767.1	33.8	793.9	27.0	870.0	30.4	**767.1**	**33.8**
380	165040	4.3	14.9384	0.6	1.1989	2.1	0.1299	2.0	0.96	787.3	15.2	800.1	11.9	836.0	13.2	**787.3**	**15.2**
126	81106	1.4	14.4520	1.4	1.3561	5.9	0.1421	5.8	0.97	856.8	46.4	870.2	34.8	904.5	28.7	**856.8**	**46.4**
300	122921	8.7	14.1441	0.6	1.4510	3.5	0.1488	3.4	0.98	894.5	28.6	910.3	20.9	948.8	12.6	**948.8**	**12.6**
295	99909	1.7	13.8107	0.3	1.5461	2.2	0.1549	2.2	0.99	928.1	18.8	948.9	13.5	997.4	6.3	**997.4**	**6.3**
773	96592	4.0	13.7908	0.3	1.7103	1.7	0.1711	1.6	0.98	1017.9	15.4	1012.4	10.7	1000.3	7.0	**1000.3**	**7.0**
357	250426	2.5	13.5471	0.2	1.7836	1.8	0.1752	1.8	0.99	1040.9	17.1	1039.5	11.6	1036.4	4.7	**1036.4**	**4.7**
227	269510	1.9	13.4628	1.0	1.5919	2.2	0.1554	2.0	0.89	931.4	17.3	967.0	13.9	1049.1	20.3	**1049.1**	**20.3**
322	168889	4.1	13.3773	0.4	1.7915	1.3	0.1738	1.2	0.94	1033.1	11.6	1042.4	8.4	1061.9	8.6	**1061.9**	**8.6**
258	110936	53.6	13.3711	0.7	1.5258	2.4	0.1480	2.4	0.96	889.5	19.6	940.8	15.0	1062.8	13.2	**1062.8**	**13.2**
91	76238	0.7	13.3695	1.8	1.8578	2.4	0.1801	1.7	0.68	1067.7	16.3	1066.2	16.0	1063.1	35.6	**1063.1**	**35.6**

Appendix A continued. U-Pb analysis results of detrital zircons from the till of the Mt. Achernar moraine.

			Isotope ratios							Apparent ages (Ma)							
U	206Pb	U/Th	206Pb*		207Pb*		206Pb*		error	206Pb*		207Pb*		206Pb*		Best	
(ppm)	204Pb		207Pb*	(%)	235U*	(%)	238U	(%)	corr.	238U*	± (Ma)	235U	± (Ma)	207Pb*	± (Ma)	age	± (Ma)
105	62986	2.5	13.2747	0.9	1.8510	1.2	0.1782	0.7	0.60	1057.2	6.9	1063.8	7.7	1077.3	18.7	**1077.3**	**18.7**
129	79603	1.3	13.2243	0.6	1.9003	2.0	0.1823	1.9	0.94	1079.3	18.4	1081.2	13.1	1085.0	13.0	**1085.0**	**13.0**
223	111468	2.0	13.1489	0.6	1.9991	1.1	0.1906	0.9	0.84	1124.9	9.2	1115.2	7.2	1096.4	11.4	**1096.4**	**11.4**
124	139044	2.1	12.7090	0.9	2.0615	2.8	0.1900	2.6	0.95	1121.5	27.0	1136.1	18.9	1164.2	17.3	**1164.2**	**17.3**
152	115265	2.2	12.7084	0.5	2.1855	3.4	0.2014	3.4	0.99	1183.0	36.4	1176.4	23.8	1164.3	10.2	**1164.3**	**10.2**
223	134185	1.3	12.6635	0.5	2.1781	0.9	0.2001	0.8	0.86	1175.6	8.7	1174.1	6.5	1171.3	9.3	**1171.3**	**9.3**
219	40812	4.8	12.5639	0.5	2.0661	1.6	0.1883	1.5	0.95	1112.0	15.4	1137.6	10.8	1186.9	9.3	**1186.9**	**9.3**
349	189452	4.0	12.5442	0.2	2.2208	2.0	0.2020	2.0	0.99	1186.3	21.5	1187.6	14.0	1190.0	4.1	**1190.0**	**4.1**
193	76241	1.9	12.5274	0.6	2.1499	1.7	0.1953	1.6	0.93	1150.2	16.5	1165.0	11.7	1192.7	12.4	**1192.7**	**12.4**
148	118783	1.8	12.5208	0.6	2.2327	1.0	0.2027	0.8	0.82	1190.1	8.7	1191.4	6.9	1193.7	11.2	**1193.7**	**11.2**
190	21791	1.1	12.4965	6.3	2.0297	6.4	0.1840	1.5	0.23	1088.6	15.1	1125.5	43.8	1197.6	123.5	**1197.6**	**123.5**
323	32779	1.1	12.4919	0.5	2.2714	3.0	0.2058	3.0	0.99	1206.3	32.8	1203.5	21.3	1198.3	9.7	**1198.3**	**9.7**
283	11484	1.2	12.4864	0.3	2.2067	1.5	0.1998	1.4	0.98	1174.5	15.2	1183.2	10.1	1199.1	6.2	**1199.1**	**6.2**
128	123185	1.9	12.4657	0.8	2.2197	2.0	0.2007	1.8	0.90	1179.0	19.0	1187.3	13.7	1202.4	16.6	**1202.4**	**16.6**
140	124736	1.3	12.4611	1.0	2.1905	3.3	0.1980	3.1	0.95	1164.4	32.9	1178.0	22.7	1203.1	19.9	**1203.1**	**19.9**
210	208326	2.0	12.4549	0.6	2.1700	1.4	0.1960	1.3	0.91	1153.9	13.2	1171.5	9.6	1204.1	11.4	**1204.1**	**11.4**
90	113766	1.4	12.4535	1.0	2.1991	2.2	0.1986	2.0	0.89	1167.9	21.4	1180.8	15.6	1204.3	19.7	**1204.3**	**19.7**
153	73094	3.4	12.4085	1.4	1.5728	5.2	0.1415	5.0	0.96	853.4	39.7	959.5	32.0	1211.4	27.1	**1211.4**	**27.1**
56	31827	1.7	12.3673	2.3	2.3238	4.3	0.2084	3.7	0.84	1220.5	40.6	1219.6	30.8	1218.0	45.9	**1218.0**	**45.9**
54	36626	0.4	12.3640	1.5	2.3615	3.4	0.2118	3.1	0.90	1238.2	34.8	1231.0	24.3	1218.5	28.5	**1218.5**	**28.5**
121	89250	1.4	12.3047	1.0	2.2853	1.6	0.2039	1.3	0.79	1196.5	13.9	1207.7	11.4	1228.0	19.4	**1228.0**	**19.4**
55	59201	1.5	12.2954	1.7	2.3842	3.7	0.2126	3.2	0.88	1242.7	36.5	1237.9	26.3	1229.4	34.3	**1229.4**	**34.3**
239	34283	2.6	12.1655	0.8	2.2419	2.4	0.1978	2.2	0.95	1163.5	23.9	1194.2	16.7	1250.3	15.0	**1250.3**	**15.0**
112	122999	1.0	11.2395	1.6	2.8419	2.6	0.2317	2.1	0.79	1343.2	25.1	1366.7	19.6	1403.5	30.3	**1403.5**	**30.3**
86	118903	1.6	11.0381	1.1	3.1509	1.7	0.2522	1.3	0.78	1450.1	17.5	1445.2	13.3	1438.1	20.6	**1438.1**	**20.6**
120	97911	1.8	11.0076	0.6	3.0047	1.2	0.2399	1.1	0.86	1386.1	13.3	1408.8	9.5	1443.4	12.3	**1443.4**	**12.3**
45	46407	0.9	10.9708	1.3	3.1827	3.2	0.2532	3.0	0.92	1455.2	38.5	1453.0	24.9	1449.7	24.5	**1449.7**	**24.5**
30	35068	0.7	10.9184	2.0	3.2126	2.6	0.2544	1.7	0.65	1461.1	21.9	1460.2	20.0	1458.8	37.3	**1458.8**	**37.3**
390	172434	1.6	10.1882	0.2	3.7847	0.5	0.2797	0.5	0.90	1589.7	6.6	1589.5	4.2	1589.3	4.3	**1589.3**	**4.3**
234	223624	1.7	10.1698	0.4	3.7505	5.2	0.2766	5.2	1.00	1574.4	72.5	1582.2	41.7	1592.7	6.7	**1592.7**	**6.7**
638	10103	33.7	9.7783	2.7	4.0413	3.0	0.2866	1.2	0.39	1624.5	16.5	1642.5	24.2	1665.7	50.8	**1665.7**	**50.8**
164	195358	3.0	9.0891	0.2	4.7889	2.5	0.3157	2.5	1.00	1768.6	38.9	1783.0	21.2	1799.7	4.2	**1799.7**	**4.2**
314	91831	1.3	8.9375	0.4	4.9861	2.6	0.3232	2.6	0.99	1805.3	40.8	1817.0	22.2	1830.3	6.7	**1830.3**	**6.7**
233	309025	1.3	8.1634	0.4	5.6806	2.5	0.3363	2.4	0.99	1869.0	39.2	1928.4	21.2	1992.9	7.3	**1992.9**	**7.3**
109	176644	1.2	8.1399	0.4	6.1347	1.5	0.3622	1.5	0.97	1992.5	25.0	1995.2	13.2	1998.0	6.9	**1998.0**	**6.9**
216	443328	2.1	8.0661	0.3	5.8960	1.6	0.3449	1.6	0.98	1910.3	26.5	1960.6	14.2	2014.2	5.2	**2014.2**	**5.2**
301	420737	1.8	8.0283	0.1	6.1054	1.4	0.3555	1.4	0.99	1960.8	23.4	1991.0	12.2	2022.5	2.5	**2022.5**	**2.5**
223	171712	1.7	7.7100	2.4	5.4300	4.7	0.3036	4.0	0.86	1709.3	60.3	1889.6	40.1	2093.9	42.0	**2093.9**	**42.0**
94	82435	1.4	7.4648	0.7	7.3752	2.1	0.3993	2.0	0.95	2165.8	36.5	2158.0	18.7	2150.5	11.5	**2150.5**	**11.5**
178	446068	1.1	7.4178	0.2	7.3216	2.6	0.3939	2.6	1.00	2140.9	46.6	2151.4	22.9	2161.6	2.8	**2161.6**	**2.8**
71	131429	0.7	7.3958	0.4	7.1498	1.1	0.3835	1.0	0.91	2092.7	17.2	2130.3	9.4	2166.7	7.5	**2166.7**	**7.5**
136	73561	5.2	7.3118	0.3	5.6536	3.6	0.2998	3.6	1.00	1690.4	52.9	1924.3	30.8	2186.6	5.3	**2186.6**	**5.3**
364	873387	1.2	7.2619	0.2	7.5863	1.9	0.3996	1.9	0.99	2167.0	35.1	2183.2	17.2	2198.5	3.4	**2198.5**	**3.4**
111	185282	1.9	6.9448	0.3	7.9386	2.4	0.3999	2.4	0.99	2168.4	44.0	2224.1	21.7	2275.8	4.4	**2275.8**	**4.4**
190	374438	3.5	6.9119	0.4	8.3862	2.0	0.4204	1.9	0.97	2262.3	37.0	2273.7	18.1	2283.9	7.6	**2283.9**	**7.6**
230	295033	6.3	6.8749	0.2	8.3584	0.8	0.4168	0.7	0.97	2245.8	14.0	2270.7	6.9	2293.2	3.3	**2293.2**	**3.3**
110	219044	0.9	6.8622	0.3	8.5398	1.0	0.4250	0.9	0.97	2283.2	18.1	2290.2	8.9	2296.4	4.4	**2296.4**	**4.4**
161	745650	5.1	6.8494	0.2	8.5717	1.8	0.4258	1.8	1.00	2286.8	34.2	2293.6	16.2	2299.6	2.6	**2299.6**	**2.6**
136	233422	1.0	6.8307	0.6	5.9148	7.8	0.2930	7.8	1.00	1656.6	113.3	1963.4	67.7	2304.2	11.1	**2304.2**	**11.1**
195	303551	3.8	6.8057	0.2	8.3328	1.4	0.4113	1.4	0.99	2220.9	26.4	2267.9	12.9	2310.6	4.2	**2310.6**	**4.2**
514	557299	2.4	6.0488	0.1	10.4507	4.0	0.4585	4.0	1.00	2432.8	81.2	2475.6	37.2	2510.8	0.9	**2510.8**	**0.9**
432	556296	2.0	6.0349	0.2	10.7653	0.8	0.4712	0.8	0.98	2488.8	15.8	2503.1	7.2	2514.7	2.6	**2514.7**	**2.6**
410	107481	18.8	5.8326	0.7	7.9968	2.2	0.3383	2.1	0.95	1878.4	34.1	2230.7	19.8	2571.8	11.0	**2571.8**	**11.0**
45	107560	1.1	5.3720	3.5	9.8792	6.0	0.3849	4.8	0.81	2099.1	86.9	2423.6	55.4	2708.4	58.6	**2708.4**	**58.6**
99	151231	1.4	5.3394	0.2	12.9341	1.9	0.5009	1.9	1.00	2617.6	41.1	2674.9	18.1	2718.5	2.9	**2718.5**	**2.9**
239	31228	3.1	5.3346	0.2	10.2407	2.8	0.3962	2.7	1.00	2151.6	50.3	2456.8	25.5	2720.0	3.7	**2720.0**	**3.7**
80	160614	1.8	5.3333	0.2	13.0387	0.9	0.5043	0.9	0.98	2632.5	19.9	2682.5	8.9	2720.3	3.1	**2720.3**	**3.1**
113	115780	1.7	5.3084	0.2	13.5518	4.8	0.5217	4.8	1.00	2706.6	106.4	2718.9	45.6	2728.1	3.1	**2728.1**	**3.1**
49	103161	65.2	4.7639	0.8	15.8561	3.5	0.5478	3.4	0.97	2816.2	77.6	2868.2	33.4	2904.8	13.3	**2904.8**	**13.3**
203	309012	0.8	4.1797	0.2	19.2063	2.6	0.5822	2.6	1.00	2957.8	62.5	3052.2	25.5	3115.0	2.5	**3115.0**	**2.5**
54	149169	63.1	4.0111	0.4	21.1650	1.9	0.6157	1.8	0.98	3092.9	44.4	3146.2	17.9	3180.4	6.2	**3180.4**	**6.2**
100	298190	11.4	3.9584	0.1	19.0295	1.4	0.5463	1.4	1.00	2809.8	32.3	3043.3	13.8	3201.3	1.9	**3201.3**	**1.9**
425	769377	1.8	3.6712	0.1	24.2811	0.9	0.6465	0.9	0.99	3214.5	21.7	3279.7	8.4	3319.8	1.6	**3319.8**	**1.6**
5cd-1 Granite																	
42	33277	1.8	11.1427	2.8	3.1848	3.9	0.2574	2.7	0.69	1476.4	35.6	1453.5	30.3	1420.1	54.3	**1420.1**	**54.3**
73	55473	2.2	11.1361	1.5	3.1023	2.5	0.2506	1.9	0.79	1441.4	25.2	1433.3	18.9	1421.2	28.7	**1421.2**	**28.7**
98	44069	1.8	11.1097	1.4	3.2091	1.8	0.2586	1.2	0.66	1482.5	16.0	1459.4	14.2	1425.8	26.5	**1425.8**	**26.5**
127	115443	3.4	11.0831	0.9	3.0376	3.5	0.2442	3.4	0.97	1408.3	42.5	1417.1	26.5	1430.3	16.8	**1430.3**	**16.8**
120	54402	1.9	11.0250	0.9	3.1610	1.9	0.2528	1.7	0.88	1452.7	22.3	1447.7	15.0	1440.4	17.4	**1440.4**	**17.4**
56	40563	2.1	11.0063	1.8	3.1700	2.4	0.2530	1.7	0.69	1454.2	21.8	1449.9	18.9	1443.6	33.9	**1443.6**	**33.9**
82	30930	1.6	10.9918	0.7	3.0293	2.3	0.2415	2.2	0.95	1394.5	27.4	1415.0	17.6	1446.1	13.8	**1446.1**	**13.8**
92	111182	1.8	10.9734	1.6	2.9787	2.6	0.2371	2.1	0.80	1371.4	26.2	1402.2	20.1	1449.3	30.0	**1449.3**	**30.0**
44	35946	2.5	10.9652	2.4	3.2187	3.5	0.2560	2.5	0.72	1469.2	33.2	1461.7	27.1	1450.7	46.1	**1450.7**	**46.1**
102	105843	2.0	10.9508	1.4	3.1813	2.7	0.2527	2.3	0.86	1452.2	30.5	1452.6	21.2	1453.2	27.1	**1453.2**	**27.1**
99	59276	1.4	10.9434	1.0	3.1956	2.3	0.2536	2.0	0.90	1457.2	26.7	1456.1	17.7	1454.5	19.2	**1454.5**	**19.2**
192	209919	2.1	10.9386	0.9	3.1245	2.2	0.2479	2.0	0.91	1427.5	25.9	1438.7	17.1	1455.3	17.4	**1455.3**	**17.4**
46	36531	2.6	10.9221	3.1	3.1213	3.5	0.2473	1.5	0.42	1424.3	18.7	1438.0	26.6	1458.2	59.5	**1458.2**	**59.5**

Appendix A continued. U-Pb analysis results of detrital zircons from the till of the Mt. Achernar moraine.

			Isotope ratios							Apparent ages (Ma)							
U	206Pb	U/Th	206Pb*		207Pb*		206Pb*		error	206Pb*		207Pb*		206Pb*		Best	
(ppm)	204Pb		207Pb*	(%)	235U*	(%)	238U	(%)	corr.	238U*	± (Ma)	235U	± (Ma)	207Pb*	± (Ma)	age	± (Ma)
47	34746	1.5	10.9204	3.8	3.1843	4.1	0.2522	1.8	0.42	1449.9	22.9	1453.4	32.1	1458.5	71.4	**1458.5**	**71.4**
83	49923	1.9	10.9203	2.2	3.1844	3.4	0.2522	2.6	0.76	1449.9	33.3	1453.4	26.1	1458.5	41.5	**1458.5**	**41.5**
32	24282	1.5	10.9196	2.9	3.1786	3.7	0.2517	2.3	0.62	1447.4	29.6	1452.0	28.5	1458.6	55.3	**1458.6**	**55.3**
91	95704	1.8	10.9043	1.0	3.2801	1.6	0.2594	1.3	0.81	1486.8	17.8	1476.3	12.8	1461.3	18.1	**1461.3**	**18.1**
40	30744	2.1	10.8709	2.8	3.1368	3.7	0.2473	2.4	0.64	1424.6	30.7	1441.8	28.7	1467.1	54.1	**1467.1**	**54.1**
114	131865	1.9	10.8432	0.8	3.1888	2.0	0.2508	1.8	0.91	1442.5	23.4	1454.4	15.3	1472.0	15.3	**1472.0**	**15.3**
62	26112	2.5	10.8327	5.9	3.2549	6.0	0.2557	1.2	0.20	1467.9	16.0	1470.3	46.8	1473.8	111.9	**1473.8**	**111.9**
5cd-2 Granitoid																	
181	25506	1.5	11.2513	0.9	2.7287	2.3	0.2227	2.1	0.91	1296.0	24.1	1336.3	16.7	1401.5	17.7	**1401.5**	**17.7**
145	23469	1.2	11.2331	1.0	2.9497	1.8	0.2403	1.5	0.83	1388.3	18.9	1394.8	13.9	1404.6	19.8	**1404.6**	**19.8**
64	37999	1.0	11.1943	1.7	2.9655	2.3	0.2408	1.6	0.69	1390.7	20.0	1398.8	17.5	1411.3	31.7	**1411.3**	**31.7**
64	36061	1.3	11.1916	2.1	3.1461	2.3	0.2554	0.9	0.39	1466.1	11.6	1444.0	17.6	1411.7	40.2	**1411.7**	**40.2**
495	14336	1.0	11.1219	0.5	2.8453	2.5	0.2295	2.4	0.98	1331.9	29.3	1367.6	18.8	1423.6	10.4	**1423.6**	**10.4**
113	103272	2.0	11.1089	1.1	3.0323	2.4	0.2443	2.1	0.89	1409.1	26.9	1415.8	18.3	1425.9	21.0	**1425.9**	**21.0**
274	147036	1.5	11.0695	0.5	3.0292	1.2	0.2432	1.1	0.90	1403.3	13.6	1415.0	9.1	1432.7	9.8	**1432.7**	**9.8**
193	79171	1.6	11.0606	0.8	3.1434	1.4	0.2522	1.1	0.81	1449.6	14.3	1443.4	10.5	1434.2	15.1	**1434.2**	**15.1**
85	46663	1.3	11.0564	0.7	3.1078	3.0	0.2492	3.0	0.98	1434.4	38.0	1434.6	23.3	1434.9	12.7	**1434.9**	**12.7**
217	181496	1.9	11.0524	0.6	3.1317	1.3	0.2510	1.2	0.90	1443.8	15.4	1440.5	10.2	1435.6	10.8	**1435.6**	**10.8**
191	128346	1.7	11.0404	0.8	3.2282	1.7	0.2585	1.5	0.89	1482.1	19.8	1463.9	13.0	1437.7	14.5	**1437.7**	**14.5**
150	62096	1.7	11.0325	1.2	3.2005	3.0	0.2561	2.8	0.91	1469.8	36.4	1457.3	23.4	1439.1	23.3	**1439.1**	**23.3**
201	124115	1.6	11.0247	0.6	3.1937	2.4	0.2554	2.3	0.97	1466.1	30.0	1455.6	18.2	1440.4	10.5	**1440.4**	**10.5**
72	56915	1.1	11.0232	2.1	3.1257	3.7	0.2499	3.0	0.82	1437.9	39.0	1439.0	28.4	1440.7	40.4	**1440.7**	**40.4**
181	90608	1.7	11.0209	0.8	3.1832	1.6	0.2544	1.4	0.86	1461.3	18.3	1453.1	12.5	1441.1	15.6	**1441.1**	**15.6**
28	17408	1.8	11.0125	3.9	3.1117	4.7	0.2485	2.6	0.55	1430.9	33.0	1435.6	36.1	1442.5	75.0	**1442.5**	**75.0**
97	77999	1.7	11.0104	1.0	3.1502	3.0	0.2516	2.8	0.94	1446.5	36.9	1445.1	23.3	1442.9	19.6	**1442.9**	**19.6**
106	59012	2.0	10.9974	1.1	3.1874	1.4	0.2542	0.8	0.59	1460.3	10.7	1454.1	10.8	1445.1	21.6	**1445.1**	**21.6**
145	59435	1.2	10.9902	1.0	3.1532	3.8	0.2513	3.6	0.97	1445.3	47.1	1445.8	29.0	1446.4	18.1	**1446.4**	**18.1**
191	214839	1.8	10.9890	0.6	3.1718	1.4	0.2528	1.2	0.91	1452.9	16.1	1450.3	10.6	1446.6	11.1	**1446.6**	**11.1**
117	55162	1.1	10.9862	0.7	3.2202	1.9	0.2566	1.8	0.93	1472.3	23.9	1462.0	15.1	1447.1	13.4	**1447.1**	**13.4**
114	95529	1.2	10.9856	1.0	3.1655	1.8	0.2522	1.5	0.84	1449.9	19.0	1448.8	13.5	1447.2	18.2	**1447.2**	**18.2**
141	218210	1.9	10.9792	0.8	3.2124	2.0	0.2558	1.8	0.91	1468.3	23.9	1460.2	15.5	1448.3	15.5	**1448.3**	**15.5**
107	79779	1.6	10.9759	1.4	3.2204	2.2	0.2564	1.7	0.78	1471.2	22.5	1462.1	16.9	1448.9	26.0	**1448.9**	**26.0**
187	158772	1.1	10.9715	0.7	3.0961	1.7	0.2464	1.6	0.92	1419.7	20.3	1431.7	13.2	1449.6	12.5	**1449.6**	**12.5**
68	15441	1.4	10.9700	1.8	3.1024	3.1	0.2468	2.5	0.81	1422.1	32.4	1433.3	24.0	1449.9	34.7	**1449.9**	**34.7**
148	26626	1.8	10.9675	0.8	3.1376	2.7	0.2496	2.5	0.95	1436.3	32.8	1441.9	20.6	1450.3	15.4	**1450.3**	**15.4**
51	34635	1.1	10.9612	4.4	3.2091	5.3	0.2551	2.8	0.54	1464.8	37.3	1459.4	40.9	1451.4	84.7	**1451.4**	**84.7**
69	29107	1.4	10.9596	1.0	3.1265	1.8	0.2485	1.4	0.81	1430.8	18.4	1439.2	13.7	1451.7	19.9	**1451.7**	**19.9**
89	2772	1.4	10.9590	1.5	3.1175	2.0	0.2478	1.3	0.67	1427.1	17.1	1437.0	15.3	1451.8	28.0	**1451.8**	**28.0**
246	93743	1.7	10.9534	0.4	3.0743	3.8	0.2442	3.8	0.99	1408.7	47.8	1426.3	29.1	1452.8	8.2	**1452.8**	**8.2**
68	53554	1.8	10.9528	1.6	3.1407	2.8	0.2495	2.2	0.81	1435.9	28.8	1442.7	21.3	1452.9	30.9	**1452.9**	**30.9**
66	49089	1.3	10.9467	2.8	3.0939	5.5	0.2456	4.8	0.86	1415.9	60.4	1431.2	42.3	1453.9	53.1	**1453.9**	**53.1**
185	135841	1.0	10.9460	0.9	3.0512	1.6	0.2422	1.4	0.84	1398.3	17.2	1420.5	12.5	1454.1	17.1	**1454.1**	**17.1**
195	28760	1.6	10.9445	0.7	3.1234	2.3	0.2479	2.2	0.95	1427.8	27.9	1438.5	17.7	1454.3	13.9	**1454.3**	**13.9**
168	86961	1.7	10.9425	0.9	3.1840	1.4	0.2527	1.0	0.72	1452.4	12.8	1453.3	10.5	1454.6	17.9	**1454.6**	**17.9**
224	205020	1.7	10.9401	0.7	3.2331	1.6	0.2565	1.4	0.89	1472.1	18.6	1465.1	12.3	1455.1	13.5	**1455.1**	**13.5**
248	110127	1.6	10.9338	0.4	3.2373	1.1	0.2567	1.0	0.92	1473.0	13.4	1466.1	8.6	1456.2	8.4	**1456.2**	**8.4**
244	41638	1.6	10.9336	0.9	3.2272	2.2	0.2559	2.0	0.92	1468.9	26.7	1463.7	17.1	1456.2	16.4	**1456.2**	**16.4**
209	89828	1.7	10.9273	0.8	3.2590	2.7	0.2583	2.5	0.95	1481.0	33.5	1471.3	20.6	1457.3	15.2	**1457.3**	**15.2**
151	87984	1.1	10.9243	0.9	3.1648	1.9	0.2508	1.6	0.87	1442.3	20.8	1448.6	14.3	1457.8	17.5	**1457.8**	**17.5**
87	39710	2.1	10.9240	1.3	3.2478	2.0	0.2573	1.5	0.74	1476.1	19.2	1468.6	15.2	1457.9	24.9	**1457.9**	**24.9**
120	93104	1.8	10.9238	1.3	3.2108	2.0	0.2544	1.4	0.73	1461.0	18.6	1459.8	15.2	1457.9	25.7	**1457.9**	**25.7**
97	58710	1.4	10.9233	1.5	3.1444	4.7	0.2491	4.5	0.95	1433.9	57.9	1443.6	36.5	1458.0	28.3	**1458.0**	**28.3**
44	13014	1.4	10.9182	3.2	3.2288	4.0	0.2557	2.5	0.62	1467.7	32.7	1464.1	31.2	1458.9	60.2	**1458.9**	**60.2**
156	12990	1.6	10.9067	0.9	3.2152	2.2	0.2543	2.1	0.92	1460.8	27.1	1460.8	17.4	1460.9	16.3	**1460.9**	**16.3**
123	77299	1.5	10.9054	0.5	3.2567	1.6	0.2576	1.5	0.95	1477.5	20.3	1470.8	12.5	1461.1	9.3	**1461.1**	**9.3**
104	7152	1.3	10.9036	1.4	3.2042	3.4	0.2534	3.1	0.91	1455.9	40.4	1458.2	26.3	1461.4	26.3	**1461.4**	**26.3**
129	29012	1.5	10.8388	1.4	3.3279	3.4	0.2616	3.1	0.92	1498.1	41.4	1487.6	26.5	1472.8	25.9	**1472.8**	**25.9**
81	44847	1.3	10.7783	1.8	3.3443	3.2	0.2614	2.7	0.83	1497.2	35.9	1491.5	25.3	1483.4	34.1	**1483.4**	**34.1**

Appendix B-1. Normalized values of Mt. Achernar moraine tills to various standards.

	MAM Tills/Upper Continental Crust																							
	SiO2	**Al2O3**	**FeO(T)**	**MnO**	**MgO**	**CaO**	**Na2O**	**K2O**	**TiO2**	**P2O5**	**Sc**	**Be**	**V**	**Ba**	**Sr**	**Y**	**Zr**	**Cr**	**Co**	**Ni**	**Cu**	**Zn**	**Ga**	**Ge**	**Rb**
East Crest	0.96	0.99	1.07	1.13	1.21	2.06	0.56	0.84	1.42	1.09	1.29	0.95	1.24	0.90	0.69	1.48	2.13	0.76	0.98	0.64	1.43	0.90	0.91	0.71	1.04
1H	0.99	1.20	1.11	1.16	0.93	0.72	0.33	0.93	1.31	0.81	1.36	0.95	1.14	0.97	0.56	1.24	1.18	0.65	0.92	0.64	1.43	1.04	1.09	0.71	1.22
1E	1.01	1.16	1.03	1.24	0.90	0.72	0.31	0.92	1.31	0.85	1.29	0.95	1.07	0.94	0.55	1.14	1.17	0.65	0.92	0.64	1.07	0.90	0.97	0.71	1.15
1E Red/Grey	1.01	1.16	1.02	1.22	0.91	0.74	0.35	0.90	1.33	0.77	1.29	0.95	1.10	0.92	0.54	1.14	1.36	0.65	0.92	0.64	1.07	0.90	1.03	1.43	1.15
1A	1.02	1.00	0.86	1.11	0.88	1.45	0.50	0.84	1.32	1.05	1.21	0.95	1.09	0.89	0.63	1.24	1.84	0.65	0.87	0.43	1.07	0.75	0.86	0.71	0.95
1B	1.05	0.99	0.87	1.08	0.92	0.91	0.55	0.82	1.34	0.88	1.21	0.95	1.11	0.90	0.63	1.33	2.05	0.76	0.87	0.64	1.07	0.75	0.86	0.71	0.99
2A	1.03	1.03	0.90	0.97	0.83	0.96	0.60	0.94	1.45	1.28	1.14	0.95	1.03	1.14	0.84	1.57	2.01	0.76	0.81	0.64	1.07	1.04	0.97	1.43	1.13
3C	0.99	1.15	0.98	0.94	0.86	0.93	0.59	1.09	1.44	1.01	1.21	0.95	1.19	1.28	0.86	1.38	1.64	0.87	0.92	0.64	1.07	1.19	1.14	0.71	1.29
3 Dark	0.99	1.18	0.91	0.96	0.77	0.92	0.61	1.08	1.38	1.28	1.14	0.95	1.13	1.29	0.88	1.29	1.61	0.87	0.87	0.43	0.71	0.90	1.09	0.71	1.11
3B	0.99	1.15	0.99	0.94	0.84	0.90	0.56	1.12	1.41	0.94	1.21	1.43	1.14	1.29	0.83	1.38	1.48	0.87	0.92	0.64	1.07	1.19	1.14	0.71	1.29
3E	0.99	1.11	0.96	1.07	0.90	1.09	0.55	0.97	1.43	0.88	1.29	0.95	1.16	1.12	0.77	1.38	1.79	0.76	0.92	0.64	1.07	1.04	1.03	0.71	1.11
4L	0.98	1.12	1.00	1.07	1.00	1.28	0.59	0.93	1.25	0.98	1.29	0.95	1.13	0.96	0.67	1.29	1.37	0.65	0.87	0.43	1.43	1.04	1.03	0.71	1.13
4K	0.97	1.11	0.96	1.08	1.04	1.38	0.61	0.92	1.28	1.14	1.29	0.95	1.12	0.93	0.70	1.24	1.60	0.65	0.92	0.64	1.43	1.04	1.03	1.43	1.00
4J	1.00	1.12	0.91	1.05	0.91	1.22	0.52	0.90	1.20	0.91	1.21	0.95	1.07	1.09	0.71	1.19	1.27	0.54	0.81	0.40	1.07	0.90	0.97	0.71	1.10
4I	0.95	1.14	1.11	1.01	1.13	1.28	0.63	0.98	1.36	1.02	1.29	0.95	1.24	1.07	0.90	1.33	1.49	0.87	0.98	0.64	1.43	1.04	1.03	0.71	1.16
4G	0.96	1.13	1.02	1.05	1.08	1.30	0.67	0.99	1.36	1.03	1.29	0.95	1.16	1.07	0.79	1.33	1.91	0.87	0.98	0.64	1.43	1.04	1.03	0.71	1.20
4E	0.94	1.13	1.05	1.06	1.18	1.47	0.71	0.98	1.35	0.99	1.29	0.95	1.20	1.02	0.93	1.33	1.68	0.76	0.92	0.64	1.43	1.04	0.97	1.43	1.06
4D	0.97	1.11	0.91	1.11	1.08	1.42	0.77	0.86	1.29	0.93	1.14	0.95	1.05	0.89	0.87	1.10	1.85	0.65	0.87	0.64	1.07	0.90	0.97	1.43	0.98
4C	0.97	1.16	1.00	0.94	1.07	1.10	0.65	1.05	1.26	1.13	1.14	0.95	1.07	1.09	0.81	1.24	1.38	0.76	0.87	0.64	1.07	1.19	1.09	1.43	1.26
4B	0.98	1.04	0.98	1.12	1.12	1.44	0.70	0.88	1.30	0.92	1.21	0.95	1.13	0.94	0.72	1.14	2.05	0.65	0.87	0.85	1.07	0.90	0.97	1.43	1.00
5A	0.88	1.03	0.98	1.08	1.53	3.19	0.68	0.85	1.21	0.85	1.29	0.95	1.16	0.84	0.87	1.14	1.47	0.76	0.92	0.64	1.43	0.90	0.86	1.43	0.91
5B	0.88	1.03	1.05	1.13	1.67	2.86	0.72	0.88	1.20	0.87	1.36	0.95	1.14	0.87	1.37	1.14	1.18	0.76	1.04	0.85	1.79	1.04	0.91	2.14	0.99
5C	0.86	1.22	1.11	1.06	1.86	1.81	1.00	1.08	1.15	0.94	1.36	0.95	1.18	0.93	1.72	1.14	0.98	0.76	1.04	0.64	6.43	2.24	1.03	2.14	1.18
5D	0.86	1.18	1.04	1.06	1.49	2.20	1.30	0.97	1.19	0.89	1.29	0.95	1.09	0.86	1.28	1.10	1.28	0.76	1.21	0.85	2.14	1.34	1.03	2.14	1.15
5E	0.91	1.19	0.97	1.03	1.32	1.80	0.76	1.06	1.28	0.96	1.14	0.95	1.06	1.01	1.14	1.14	1.40	0.76	0.87	0.85	1.43	1.04	1.09	1.43	1.13
Plus 1 Sigma Std. Dev.	1.02	1.05	1.11	1.10	1.14	1.06	1.15	1.08	1.13	1.13	1.06	1.43	1.11	1.13	1.14	1.10	1.15	1.18	1.03	1.23	1.14	1.09	1.04	1.07	1.21
Minus 1 Sigma Std. Dev.	0.98	0.95	0.89	0.90	0.86	0.94	0.85	0.92	0.88	0.87	0.94	0.57	0.89	0.87	0.86	0.90	0.85	0.82	0.97	0.77	0.86	0.91	0.96	0.93	0.79
Plus 2 Sigma Std. Dev.	1.04	1.10	1.21	1.20	1.28	1.11	1.29	1.16	1.25	1.27	1.13	1.86	1.23	1.26	1.29	1.19	1.29	1.37	1.07	1.47	1.29	1.18	1.08	1.14	1.41
Minus 2 Sigma Std. Dev.	0.96	0.90	0.79	0.80	0.72	0.89	0.71	0.84	0.75	0.73	0.87	0.14	0.77	0.74	0.71	0.81	0.71	0.63	0.93	0.53	0.71	0.82	0.92	0.86	0.59

Appendix B-1 Continued. Normalized values of Mt. Achernar moraine tills to various standards.

	MAM Tills/Upper Continental Crust																								
	Nb	**Ag**	**Sn**	**Cs**	**La**	**Ce**	**Pr**	**Nd**	**Sm**	**Eu**	**Gd**	**Tb**	**Dy**	**Ho**	**Er**	**Tm**	**Yb**	**Lu**	**Hf**	**Ta**	**W**	**Ti**	**Pb**	**Th**	**U**
East Crest	0.83	45.28	0.95	0.71	1.36	1.35	1.34	1.35	1.45	1.31	1.50	1.29	1.41	1.33	1.35	1.57	1.68	1.74	1.94	0.89	1.00	0.56	0.88	1.36	1.26
1H	0.75	18.87	3.33	1.31	1.01	1.00	1.01	1.02	1.15	1.14	1.18	1.14	1.18	1.08	1.17	1.37	1.43	1.45	1.09	0.89	1.00	0.56	0.82	1.07	1.00
1E	0.75	24.53	2.38	1.20	1.04	1.04	1.04	1.08	1.21	1.13	1.20	1.14	1.15	1.08	1.13	1.37	1.43	1.42	1.09	0.89	1.00	0.67	0.88	1.12	1.00
1E Red/Grey	0.83	18.87	1.90	1.24	0.97	0.97	1.01	1.07	1.21	1.07	1.25	1.14	1.13	1.08	1.13	1.30	1.33	1.39	1.17	0.78	1.00	0.67	0.82	1.20	1.04
1A	1.08	30.19	1.43	0.96	1.08	1.06	1.09	1.12	1.32	1.17	1.35	1.29	1.21	1.20	1.26	1.40	1.48	1.52	1.62	0.78	1.00	0.67	0.82	1.21	1.15
1B	0.75	43.40	0.95	0.94	1.10	1.12	1.14	1.19	1.34	1.16	1.35	1.29	1.28	1.20	1.26	1.50	1.53	1.58	1.77	0.78	1.00	0.44	0.76	1.24	1.11
2A	1.00	43.40	1.43	0.98	1.58	1.53	1.51	1.51	1.66	1.51	1.63	1.43	1.46	1.33	1.39	1.63	1.68	1.74	1.79	1.00	1.00	0.56	1.24	1.36	1.30
3C	0.92	33.96	1.43	1.10	1.45	1.42	1.40	1.41	1.47	1.49	1.43	1.29	1.33	1.20	1.30	1.50	1.53	1.61	1.45	0.89	1.00	0.56	1.18	1.39	1.19
3 Dark	0.92	20.75	1.90	0.98	1.43	1.34	1.36	1.34	1.51	1.45	1.43	1.29	1.26	1.20	1.26	1.47	1.48	1.48	1.42	0.89	1.00	0.67	1.18	1.42	1.15
3B	0.92	32.08	1.43	1.18	1.48	1.44	1.42	1.40	1.51	1.41	1.45	1.29	1.28	1.20	1.26	1.43	1.48	1.52	1.34	0.89	1.00	0.56	1.24	1.41	1.22
3E	0.83	35.85	1.43	1.00	1.40	1.40	1.37	1.40	1.47	1.48	1.48	1.29	1.41	1.33	1.35	1.60	1.63	1.71	1.68	0.89	1.00	0.56	1.12	1.36	1.19
4L	0.75	28.30	0.95	1.10	1.07	1.07	1.07	1.12	1.23	1.25	1.25	1.14	1.23	1.20	1.22	1.43	1.53	1.55	1.23	0.78	1.00	0.56	1.06	1.10	1.11
4K	0.83	20.75	0.95	1.06	1.10	1.04	1.06	1.04	1.26	1.13	1.23	1.14	1.21	1.08	1.22	1.40	1.48	1.48	1.42	0.67	1.11	0.67	1.06	1.16	1.11
4J	0.75	26.42	0.95	1.14	0.99	1.00	1.02	1.06	1.17	1.20	1.20	1.14	1.18	1.08	1.17	1.33	1.43	1.45	1.13	0.78	1.00	0.44	0.76	1.04	1.07
4I	0.83	28.30	0.95	1.02	1.37	1.33	1.33	1.33	1.45	1.34	1.38	1.29	1.26	1.20	1.26	1.43	1.43	1.52	1.38	0.89	1.00	0.44	0.88	1.30	1.22
4G	0.92	39.62	0.95	1.04	1.40	1.38	1.38	1.41	1.49	1.28	1.38	1.29	1.28	1.20	1.22	1.43	1.43	1.45	1.72	0.78	18.89	0.44	0.82	1.41	1.26
4E	0.75	33.96	0.95	0.98	1.27	1.24	1.24	1.27	1.34	1.29	1.38	1.14	1.28	1.20	1.26	1.50	1.53	1.58	1.58	0.78	1.00	0.56	1.06	1.29	1.30
4D	0.83	26.42	0.95	1.12	1.14	1.09	1.10	1.10	1.32	1.05	1.23	1.00	1.13	1.08	1.13	1.33	1.38	1.39	1.66	0.78	2.22	0.56	0.82	1.31	1.11
4C	1.00	22.64	1.43	1.14	1.41	1.32	1.31	1.28	1.45	1.26	1.45	1.29	1.23	1.20	1.26	1.47	1.58	1.55	1.30	0.78	1.00	0.78	1.29	1.43	1.37
4B	0.83	33.96	1.90	0.96	1.15	1.13	1.17	1.21	1.30	1.15	1.30	1.14	1.21	1.08	1.17	1.37	1.43	1.45	1.72	0.78	1.00	0.56	0.88	1.32	1.11
5A	0.75	32.08	0.95	0.80	1.06	1.05	1.05	1.06	1.15	1.10	1.13	1.00	1.13	0.96	1.04	1.23	1.28	1.32	1.28	0.67	1.00	0.44	0.76	1.08	0.96
5B	0.67	24.53	2.38	0.94	1.05	1.03	1.03	1.05	1.13	1.09	1.18	1.00	1.08	0.96	1.09	1.20	1.22	1.29	1.08	0.67	1.11	0.44	1.12	1.02	0.93
5C	0.67	13.21	1.43	1.41	1.09	1.07	1.05	1.03	1.15	1.12	1.15	1.00	1.10	1.08	1.09	1.30	1.38	1.35	0.94	0.78	1.11	0.44	1.47	1.12	1.07
5D	0.75	28.30	1.43	1.41	1.09	1.06	1.04	1.06	1.11	1.01	1.13	1.00	1.08	0.96	1.04	1.20	1.22	1.32	1.09	0.67	2.22	0.22	0.71	1.11	1.04
5E	0.83	35.85	0.95	1.31	1.08	1.06	1.08	1.11	1.21	1.13	1.30	1.14	1.15	1.08	1.13	1.33	1.38	1.39	1.23	0.78	2.22	0.56	0.82	1.21	1.11
Plus 1 Sigma Std. Dev.	1.08	1.06	1.24	1.31	1.10	1.06	1.00	1.07	1.06	1.10	1.08	1.14	1.00	1.00	1.00	1.00	1.20	1.16	1.13	1.11	2.11	1.56	1.03	1.10	1.22
Minus 1 Sigma Std. Dev.	0.92	0.94	0.76	0.69	0.90	0.94	1.00	0.93	0.94	0.90	0.93	0.86	1.00	1.00	1.00	1.00	0.80	0.84	0.87	0.89	--	0.44	0.97	0.90	0.78
Plus 2 Sigma Std. Dev.	1.17	1.11	1.48	1.61	1.19	1.13	1.00	1.15	1.13	1.20	1.15	1.29	1.00	1.00	1.00	1.00	1.41	1.32	1.26	1.22	3.22	2.11	1.06	1.19	1.44
Minus 2 Sigma Std. Dev.	0.83	0.89	0.52	0.39	0.81	0.87	1.00	0.85	0.87	0.80	0.85	0.71	1.00	1.00	1.00	1.00	0.59	0.68	0.74	0.78	--	--	0.94	0.81	0.56

Appendix B-2. Normalized values of Mt. Achernar moraine tills to various standards.

	MAM Tills/PAAS													
	La	**Ce**	**Pr**	**Nd**	**Sm**	**Eu**	**Gd**	**Tb**	**Dy**	**Ho**	**Er**	**Tm**	**Yb**	**Lu**
East Crest	1.11	1.06	1.08	1.14	1.21	1.19	1.28	1.17	1.25	1.10	1.07	1.18	1.18	1.26
1H	0.83	0.78	0.82	0.86	0.96	1.04	1.00	1.04	1.05	0.90	0.93	1.03	1.00	1.05
1E	0.84	0.82	0.84	0.91	1.02	1.03	1.02	1.04	1.02	0.90	0.90	1.03	1.00	1.02
1E Red/Grey	0.79	0.76	0.82	0.91	1.02	0.97	1.06	1.04	1.00	0.90	0.90	0.98	0.93	1.00
1A	0.88	0.84	0.88	0.94	1.11	1.06	1.15	1.17	1.07	1.00	1.00	1.05	1.04	1.09
1B	0.89	0.88	0.92	1.00	1.13	1.05	1.15	1.17	1.14	1.00	1.00	1.13	1.07	1.14
2A	1.29	1.21	1.22	1.27	1.39	1.37	1.38	1.30	1.30	1.10	1.10	1.23	1.18	1.26
3C	1.19	1.12	1.13	1.19	1.23	1.35	1.21	1.17	1.18	1.00	1.03	1.13	1.07	1.16
3 Dark	1.17	1.06	1.10	1.13	1.27	1.32	1.21	1.17	1.11	1.00	1.00	1.10	1.04	1.07
3B	1.21	1.14	1.15	1.18	1.27	1.28	1.23	1.17	1.14	1.00	1.00	1.08	1.04	1.09
3E	1.14	1.10	1.11	1.18	1.23	1.35	1.26	1.17	1.25	1.10	1.07	1.20	1.14	1.23
4L	0.87	0.84	0.87	0.95	1.04	1.14	1.06	1.04	1.09	1.00	0.97	1.08	1.07	1.12
4K	0.89	0.82	0.85	0.88	1.05	1.03	1.04	1.04	1.07	0.90	0.97	1.05	1.04	1.07
4J	0.81	0.79	0.82	0.89	0.98	1.09	1.02	1.04	1.05	0.90	0.93	1.00	1.00	1.05
4I	1.12	1.05	1.08	1.12	1.21	1.22	1.17	1.17	1.11	1.00	1.00	1.08	1.00	1.09
4G	1.14	1.09	1.11	1.19	1.25	1.16	1.17	1.17	1.14	1.00	0.97	1.08	1.00	1.05
4E	1.03	0.98	1.00	1.07	1.13	1.17	1.17	1.04	1.14	1.00	1.00	1.13	1.07	1.14
4D	0.93	0.86	0.89	0.93	1.11	0.95	1.04	0.91	1.00	0.90	0.90	1.00	0.96	1.00
4C	1.15	1.04	1.06	1.08	1.21	1.15	1.23	1.17	1.09	1.00	1.00	1.10	1.11	1.12
4B	0.94	0.89	0.94	1.02	1.09	1.05	1.11	1.04	1.07	0.90	0.93	1.03	1.00	1.05
5A	0.87	0.83	0.85	0.90	0.96	1.00	0.96	0.91	1.00	0.80	0.83	0.93	0.89	0.95
5B	0.85	0.81	0.83	0.89	0.95	0.99	1.00	0.91	0.95	0.80	0.86	0.90	0.86	0.93
5C	0.89	0.84	0.85	0.87	0.96	1.02	0.98	0.91	0.98	0.90	0.86	0.98	0.96	0.98
5D	0.89	0.83	0.84	0.89	0.93	0.92	0.96	0.91	0.95	0.80	0.83	0.90	0.86	0.95
5E	0.88	0.83	0.88	0.93	1.02	1.03	1.11	1.04	1.02	0.90	0.90	1.00	0.96	1.00

Appendix B-3. Normalized values of Mt. Achernar moraine tills to various standards.

	MAM Tills/Average Carbonate																	
	V	**Ba**	**Sr**	**Y**	**Zr**	**Co**	**Ni**	**Cu**	**Zn**	**Ga**	**Rb**	**Nb**	**Cs**	**Hf**	**Ta**	**Pb**	**Th**	**U**
East Crest	6.00	56.80	0.36	4.84	21.63	170.00	1.50	10.00	3.00	4.00	28.33	33.33	8.75	34.33	8.00	1.67	8.41	1.55
1H	5.55	60.70	0.30	4.06	11.95	160.00	1.50	10.00	3.50	4.75	33.33	30.00	16.00	19.33	8.00	1.56	6.59	1.23
1E	5.20	59.00	0.29	3.75	11.89	160.00	1.50	7.50	3.00	4.25	31.33	30.00	14.75	19.33	8.00	1.67	6.94	1.23
1E Red/Grey	5.35	58.00	0.28	3.75	13.79	160.00	1.50	7.50	3.00	4.50	31.33	33.33	15.25	20.67	7.00	1.56	7.41	1.27
1A	5.30	55.70	0.33	4.06	18.68	150.00	1.00	7.50	2.50	3.75	26.00	43.33	11.75	28.67	7.00	1.56	7.47	1.41
1B	5.40	56.80	0.33	4.38	20.84	150.00	1.50	7.50	2.50	3.75	27.00	30.00	11.50	31.33	7.00	1.44	7.65	1.36
2A	5.00	71.70	0.44	5.16	20.42	140.00	1.50	7.50	3.50	4.25	31.00	40.00	12.00	31.67	9.00	2.33	8.41	1.59
3C	5.75	80.60	0.45	4.53	16.63	160.00	1.50	7.50	4.00	5.00	35.33	36.67	13.50	25.67	8.00	2.22	8.59	1.45
3 Dark	5.50	80.70	0.46	4.22	16.32	150.00	1.00	5.00	3.00	4.75	30.33	36.67	12.00	25.00	8.00	2.22	8.76	1.41
3B	5.55	81.00	0.43	4.53	15.00	160.00	1.50	7.50	4.00	5.00	35.33	36.67	14.50	23.67	8.00	2.33	8.71	1.50
3E	5.65	70.60	0.40	4.53	18.16	160.00	1.50	7.50	3.50	4.50	30.33	33.33	12.25	29.67	8.00	2.11	8.41	1.45
4L	5.50	60.30	0.35	4.22	13.95	150.00	1.00	10.00	3.50	4.50	31.00	30.00	13.50	21.67	7.00	2.00	6.82	1.36
4K	5.45	58.70	0.37	4.06	16.21	160.00	1.50	10.00	3.50	4.50	27.33	33.33	13.00	25.00	6.00	2.00	7.18	1.36
4J	5.20	68.20	0.37	3.91	12.89	140.00	0.95	7.50	3.00	4.25	30.00	30.00	14.00	20.00	7.00	1.44	6.41	1.32
4I	6.00	67.40	0.47	4.38	15.11	170.00	1.50	10.00	3.50	4.50	31.67	33.33	12.50	24.33	8.00	1.67	8.00	1.50
4G	5.65	67.20	0.41	4.38	19.37	170.00	1.50	10.00	3.50	4.50	32.67	36.67	12.75	30.33	7.00	1.56	8.71	1.55
4E	5.80	64.10	0.49	4.38	17.11	160.00	1.50	10.00	3.50	4.25	29.00	30.00	12.00	28.00	7.00	2.00	7.94	1.59
4D	5.10	55.80	0.46	3.59	18.84	150.00	1.50	7.50	3.00	4.25	26.67	33.33	13.75	29.33	7.00	1.56	8.12	1.36
4C	5.20	68.60	0.42	4.06	14.05	150.00	1.50	7.50	4.00	4.75	34.33	40.00	14.00	23.00	7.00	2.44	8.82	1.68
4B	5.50	58.80	0.38	3.75	20.84	150.00	2.00	7.50	3.00	4.25	27.33	33.33	11.75	30.33	7.00	1.67	8.18	1.36
5A	5.65	52.80	0.45	3.75	14.89	160.00	1.50	10.00	3.00	3.75	25.00	30.00	9.75	22.67	6.00	1.44	6.65	1.18
5B	5.55	54.80	0.72	3.75	11.95	180.00	2.00	12.50	3.50	4.00	27.00	26.67	11.50	19.00	6.00	2.11	6.29	1.14
5C	5.70	58.60	0.90	3.75	9.95	180.00	1.50	45.00	7.50	4.50	32.33	26.67	17.25	16.67	7.00	2.78	6.94	1.32
5D	5.30	54.20	0.67	3.59	13.05	210.00	2.00	15.00	4.50	4.50	31.33	30.00	17.25	19.33	6.00	1.33	6.88	1.27
5E	5.15	63.30	0.60	3.75	14.21	150.00	2.00	10.00	3.50	4.75	31.00	33.33	16.00	21.67	7.00	1.56	7.47	1.36

Appendix B-4. Normalized values of Mt. Achernar moraine tills to various standards.

	MAM Tills/Average Shale																	
	V	**Ba**	**Sr**	**Y**	**Zr**	**Co**	**Ni**	**Cu**	**Zn**	**Ga**	**Rb**	**Nb**	**Cs**	**Hf**	**Ta**	**Pb**	**Th**	**U**
East Crest	0.92	0.98	0.74	1.19	2.57	0.89	0.44	0.89	0.63	0.84	0.61	0.91	0.70	3.68	1.00	0.75	1.19	0.92
1H	0.85	1.05	0.60	1.00	1.42	0.84	0.44	0.89	0.74	1.00	0.71	0.82	1.28	2.07	1.00	0.70	0.93	0.73
1E	0.80	1.02	0.59	0.92	1.41	0.84	0.44	0.67	0.63	0.89	0.67	0.82	1.18	2.07	1.00	0.75	0.98	0.73
1E Red/Grey	0.82	1.00	0.57	0.92	1.64	0.84	0.44	0.67	0.63	0.95	0.67	0.91	1.22	2.21	0.88	0.70	1.05	0.76
1A	0.82	0.96	0.67	1.00	2.22	0.79	0.29	0.67	0.53	0.79	0.56	1.18	0.94	3.07	0.88	0.70	1.06	0.84
1B	0.83	0.98	0.67	1.08	2.48	0.79	0.44	0.67	0.53	0.79	0.58	0.82	0.92	3.36	0.88	0.65	1.08	0.81
2A	0.77	1.24	0.89	1.27	2.43	0.74	0.44	0.67	0.74	0.89	0.66	1.09	0.96	3.39	1.13	1.05	1.19	0.95
3C	0.88	1.39	0.92	1.12	1.98	0.84	0.44	0.67	0.84	1.05	0.76	1.00	1.08	2.75	1.00	1.00	1.22	0.86
3 Dark	0.85	1.39	0.94	1.04	1.94	0.79	0.29	0.44	0.63	1.00	0.65	1.00	0.96	2.68	1.00	1.00	1.24	0.84
3B	0.85	1.40	0.88	1.12	1.78	0.84	0.44	0.67	0.84	1.05	0.76	1.00	1.16	2.54	1.00	1.05	1.23	0.89
3E	0.87	1.22	0.82	1.12	2.16	0.84	0.44	0.67	0.74	0.95	0.65	0.91	0.98	3.18	1.00	0.95	1.19	0.86
4L	0.85	1.04	0.71	1.04	1.66	0.79	0.29	0.89	0.74	0.95	0.66	0.82	1.08	2.32	0.88	0.90	0.97	0.81
4K	0.84	1.01	0.75	1.00	1.93	0.84	0.44	0.89	0.74	0.95	0.59	0.91	1.04	2.68	0.75	0.90	1.02	0.81
4J	0.80	1.18	0.75	0.96	1.53	0.74	0.28	0.67	0.63	0.89	0.64	0.82	1.12	2.14	0.88	0.65	0.91	0.78
4I	0.92	1.16	0.96	1.08	1.79	0.89	0.44	0.89	0.74	0.95	0.68	0.91	1.00	2.61	1.00	0.75	1.13	0.89
4G	0.87	1.16	0.84	1.08	2.30	0.89	0.44	0.89	0.74	0.95	0.70	1.00	1.02	3.25	0.88	0.70	1.23	0.92
4E	0.89	1.11	1.00	1.08	2.03	0.84	0.44	0.89	0.74	0.89	0.62	0.82	0.96	3.00	0.88	0.90	1.13	0.95
4D	0.78	0.96	0.93	0.88	2.24	0.79	0.44	0.67	0.63	0.89	0.57	0.91	1.10	3.14	0.88	0.70	1.15	0.81
4C	0.80	1.18	0.86	1.00	1.67	0.79	0.44	0.67	0.84	1.00	0.74	1.09	1.12	2.46	0.88	1.10	1.25	1.00
4B	0.85	1.01	0.77	0.92	2.48	0.79	0.59	0.67	0.63	0.89	0.59	0.91	0.94	3.25	0.88	0.75	1.16	0.81
5A	0.87	0.91	0.92	0.92	1.77	0.84	0.44	0.89	0.63	0.79	0.54	0.82	0.78	2.43	0.75	0.65	0.94	0.70
5B	0.85	0.94	1.46	0.92	1.42	0.95	0.59	1.11	0.74	0.84	0.58	0.73	0.92	2.04	0.75	0.95	0.89	0.68
5C	0.88	1.01	1.84	0.92	1.18	0.95	0.44	4.00	1.58	0.95	0.69	0.73	1.38	1.79	0.88	1.25	0.98	0.78
5D	0.82	0.93	1.37	0.88	1.55	1.11	0.59	1.33	0.95	0.95	0.67	0.82	1.38	2.07	0.75	0.60	0.98	0.76
5E	0.79	1.09	1.22	0.92	1.69	0.79	0.59	0.89	0.74	1.00	0.66	0.91	1.28	2.32	0.88	0.70	1.06	0.81

Appendix B-5. Normalized values of Mt. Achernar moraine tills to various standards.

	MAM Tills/Chondrite													
	La	**Ce**	**Pr**	**Nd**	**Sm**	**Eu**	**Gd**	**Tb**	**Dy**	**Ho**	**Er**	**Tm**	**Yb**	**Lu**
East Crest	115.3	88.9	70.4	51.3	29.4	15.1	19.6	15.5	14.4	12.9	12.4	13.2	13.3	14.2
1H	85.6	65.5	53.3	38.8	23.4	13.1	15.4	13.8	12.1	10.6	10.8	11.5	11.3	11.8
1E	87.5	68.2	54.9	40.9	24.7	13.0	15.7	13.8	11.8	10.6	10.4	11.5	11.3	11.5
1E Red/Grey	82.0	63.5	53.3	40.8	24.7	12.3	16.3	13.8	11.5	10.6	10.4	11.0	10.5	11.3
1A	91.6	70.0	57.2	42.5	26.8	13.4	17.6	15.5	12.3	11.8	11.6	11.8	11.7	12.3
1B	92.6	73.6	60.1	45.0	27.3	13.3	17.6	15.5	13.1	11.8	11.6	12.6	12.1	12.9
2A	133.2	100.9	79.6	57.2	33.8	17.4	21.2	17.2	15.0	12.9	12.9	13.8	13.3	14.2
3C	122.9	93.4	73.7	53.6	29.9	17.1	18.6	15.5	13.6	11.8	12.0	12.6	12.1	13.1
3 Dark	121.0	88.2	71.5	51.1	30.7	16.7	18.6	15.5	12.9	11.8	11.6	12.4	11.7	12.1
3B	124.8	94.9	74.5	53.2	30.7	16.2	19.0	15.5	13.1	11.8	11.6	12.1	11.7	12.3
3E	118.0	92.1	71.9	53.2	29.9	17.0	19.3	15.5	14.4	12.9	12.4	13.5	12.9	13.9
4L	90.5	70.2	56.3	42.6	25.1	14.4	16.3	13.8	12.6	11.8	11.2	12.1	12.1	12.6
4K	92.6	68.3	55.5	39.7	25.5	13.0	16.0	13.8	12.3	10.6	11.2	11.8	11.7	12.1
4J	83.9	65.8	53.6	40.1	23.8	13.8	15.7	13.8	12.1	10.6	10.8	11.2	11.3	11.8
4I	115.5	87.9	70.0	50.5	29.4	15.4	18.0	15.5	12.9	11.8	11.6	12.1	11.3	12.3
4G	118.3	90.8	72.3	53.4	30.3	14.7	18.0	15.5	13.1	11.8	11.2	12.1	11.3	11.8
4E	107.1	81.6	65.1	48.1	27.3	14.8	18.0	13.8	13.1	11.8	11.6	12.6	12.1	12.9
4D	95.9	71.6	57.7	41.6	26.8	12.1	16.0	12.1	11.5	10.6	10.4	11.2	10.9	11.3
4C	119.3	86.8	68.6	48.7	29.4	14.5	19.0	15.5	12.6	11.8	11.6	12.4	12.5	12.6
4B	97.0	74.4	61.4	46.0	26.4	13.2	17.0	13.8	12.3	10.6	10.8	11.5	11.3	11.8
5A	89.6	69.1	55.4	40.4	23.4	12.6	14.7	12.1	11.5	9.4	9.6	10.4	10.1	10.8
5B	88.3	67.8	54.2	39.9	22.9	12.5	15.4	12.1	11.0	9.4	10.0	10.1	9.7	10.5
5C	92.4	70.2	55.1	39.2	23.4	12.9	15.0	12.1	11.3	10.6	10.0	11.0	10.9	11.0
5D	92.1	69.7	54.7	40.2	22.5	11.6	14.7	12.1	11.0	9.4	9.6	10.1	9.7	10.8
5E	91.3	69.6	57.0	42.1	24.7	13.0	17.0	13.8	11.8	10.6	10.4	11.2	10.9	11.3

Appendix B-6. Normalized values of Mt. Achernar moraine tills to various standards.

	MAM Tills/Pagoda																
	Si02	**Al2O3**	**CaO**	**Na2O**	**K20**	**P2O5**	**Fe203**	**Mgo**	**Ti02**	**Be**	**Sc**	**V**	**Cr**	**Co**	**Ni**	**Cu**	**Zn**
East Crest	1.00	0.92	9.64	1.53	0.66	0.85	0.93	1.00	1.14	0.37	1.15	0.96	0.69	0.87	0.61	1.15	0.50
1H	1.04	1.12	3.38	0.89	0.73	0.63	0.98	0.77	1.05	0.37	1.21	0.89	0.59	0.82	0.61	1.15	0.59
1E	1.05	1.08	3.37	0.85	0.72	0.66	0.95	0.73	1.05	0.37	1.15	0.83	0.59	0.82	0.61	0.86	0.50
1E Red/Grey	1.05	1.08	3.45	0.96	0.70	0.60	0.94	0.75	1.07	0.37	1.15	0.86	0.59	0.82	0.61	0.86	0.50
1A	1.06	0.93	6.78	1.37	0.66	0.82	0.77	0.72	1.06	0.37	1.08	0.85	0.59	0.77	0.41	0.86	0.42
1B	1.09	0.92	4.27	1.52	0.64	0.69	0.77	0.76	1.08	0.37	1.08	0.87	0.69	0.77	0.61	0.86	0.42
2A	1.07	0.96	4.51	1.65	0.74	1.00	0.77	0.68	1.17	0.37	1.02	0.80	0.69	0.72	0.61	0.86	0.59
3C	1.03	1.07	4.36	1.62	0.85	0.79	0.85	0.71	1.15	0.37	1.08	0.92	0.79	0.82	0.61	0.86	0.67
3 Dark	1.03	1.10	4.34	1.68	0.85	1.01	0.78	0.64	1.11	0.37	1.02	0.88	0.79	0.77	0.41	0.57	0.50
3B	1.03	1.07	4.22	1.55	0.87	0.74	0.86	0.69	1.13	0.56	1.08	0.89	0.79	0.82	0.61	0.86	0.67
3E	1.04	1.03	5.12	1.50	0.76	0.69	0.85	0.74	1.15	0.37	1.15	0.91	0.69	0.82	0.61	0.86	0.59
4L	1.02	1.04	5.99	1.61	0.72	0.77	0.90	0.82	1.00	0.37	1.15	0.88	0.59	0.77	0.41	1.15	0.59
4K	1.01	1.03	6.43	1.66	0.72	0.89	0.87	0.86	1.02	0.37	1.15	0.87	0.59	0.82	0.61	1.15	0.59
4J	1.04	1.04	5.68	1.44	0.70	0.71	0.83	0.74	0.96	0.37	1.08	0.83	0.49	0.72	0.39	0.86	0.50
4I	0.99	1.06	5.97	1.73	0.77	0.80	0.96	0.93	1.09	0.37	1.15	0.96	0.79	0.87	0.61	1.15	0.59
4G	1.00	1.05	6.09	1.85	0.77	0.81	0.90	0.89	1.09	0.37	1.15	0.91	0.79	0.87	0.61	1.15	0.59
4E	0.98	1.05	6.86	1.95	0.76	0.77	0.95	0.97	1.08	0.37	1.15	0.93	0.69	0.82	0.61	1.15	0.59
4D	1.01	1.03	6.63	2.11	0.67	0.72	0.84	0.88	1.04	0.37	1.02	0.82	0.59	0.77	0.61	0.86	0.50
4C	1.01	1.08	5.16	1.79	0.82	0.88	0.90	0.87	1.01	0.37	1.02	0.83	0.69	0.77	0.61	0.86	0.67
4B	1.02	0.97	6.71	1.91	0.69	0.71	0.89	0.92	1.04	0.37	1.08	0.88	0.59	0.77	0.82	0.86	0.50
5A	0.91	0.95	14.89	1.85	0.66	0.67	0.91	1.26	0.97	0.37	1.15	0.91	0.69	0.82	0.61	1.15	0.50
5B	0.91	0.96	13.33	1.96	0.68	0.67	0.98	1.37	0.96	0.37	1.21	0.89	0.69	0.92	0.82	1.43	0.59
5C	0.89	1.13	8.42	2.74	0.84	0.73	1.03	1.52	0.92	0.37	1.21	0.91	0.69	0.92	0.61	5.16	1.26
5D	0.89	1.09	10.22	3.55	0.75	0.69	1.00	1.22	0.94	0.37	1.15	0.85	0.69	1.08	0.82	1.72	0.75
5E	0.94	1.10	8.37	2.08	0.83	0.74	0.92	1.08	1.02	0.37	1.02	0.83	0.69	0.77	0.82	1.15	0.59
Plus 1 Sigma Std. Dev.	1.09	1.14	1.20	1.39	1.14	1.37	1.33	1.25	1.25	1.24	1.24	1.36	1.34	1.74	1.45	1.48	1.47
Minus 1 Sigma Std. Dev.	0.91	0.86	0.80	0.61	0.86	0.63	0.67	0.75	0.75	0.76	0.76	0.64	0.66	0.26	0.55	0.52	0.53
Plus 2 Sigma Std. Dev.	1.18	1.28	1.39	1.78	1.29	1.74	1.65	1.51	1.51	1.48	1.47	1.72	1.67	2.49	1.90	1.96	1.94
Minus 2 Sigma Std. Dev.	0.82	0.72	0.61	0.22	0.71	0.26	0.35	0.49	0.49	0.52	0.53	0.28	0.33	--	0.10	0.04	0.06

Appendix B-6 Continued. Normalized values of Mt. Achernar moraine tills to various standards.

	MAM Tills/Pagoda																
	Ge	**Ag**	**Cs**	**Hf**	**Ta**	**W**	**Pb**	**Th**	**U**	**La**	**Ce**	**Nd**	**Sm**	**Eu**	**Tb**	**Yb**	**Lu**
East Crest	0.10	4.80	0.43	1.72	0.80	0.28	0.65	0.68	0.77	0.68	0.71	0.75	0.91	1.01	0.82	1.14	1.10
1H	0.10	2.00	0.79	0.97	0.80	0.28	0.61	0.54	0.61	0.51	0.53	0.57	0.72	0.88	0.73	0.97	0.92
1E	0.10	2.60	0.73	0.97	0.80	0.28	0.65	0.56	0.61	0.52	0.55	0.60	0.76	0.87	0.73	0.97	0.90
1E Red/Grey	0.20	2.00	0.75	1.03	0.70	0.28	0.61	0.60	0.64	0.49	0.51	0.60	0.76	0.82	0.73	0.90	0.88
1A	0.10	3.20	0.58	1.43	0.70	0.28	0.61	0.61	0.70	0.54	0.56	0.62	0.83	0.90	0.82	1.00	0.96
1B	0.10	4.60	0.57	1.57	0.70	0.28	0.57	0.62	0.68	0.55	0.59	0.66	0.84	0.89	0.82	1.03	1.00
2A	0.20	4.60	0.59	1.58	0.90	0.28	0.91	0.68	0.80	0.79	0.81	0.84	1.04	1.16	0.91	1.14	1.10
3C	0.10	3.60	0.67	1.28	0.80	0.28	0.87	0.70	0.73	0.73	0.75	0.79	0.92	1.15	0.82	1.03	1.02
3 Dark	0.10	2.20	0.59	1.25	0.80	0.28	0.87	0.71	0.70	0.72	0.71	0.75	0.95	1.12	0.82	1.00	0.94
3B	0.10	3.40	0.72	1.18	0.80	0.28	0.91	0.71	0.75	0.74	0.76	0.78	0.95	1.08	0.82	1.00	0.96
3E	0.10	3.80	0.60	1.48	0.80	0.28	0.83	0.68	0.73	0.70	0.74	0.78	0.92	1.14	0.82	1.10	1.08
4L	0.10	3.00	0.67	1.08	0.70	0.28	0.78	0.56	0.68	0.54	0.56	0.63	0.77	0.96	0.73	1.03	0.98
4K	0.20	2.20	0.64	1.25	0.60	0.31	0.78	0.58	0.68	0.55	0.55	0.58	0.79	0.87	0.73	1.00	0.94
4J	0.10	2.80	0.69	1.00	0.70	0.28	0.57	0.52	0.66	0.50	0.53	0.59	0.73	0.92	0.73	0.97	0.92
4I	0.10	3.00	0.62	1.22	0.80	0.28	0.65	0.65	0.75	0.68	0.70	0.74	0.91	1.03	0.82	0.97	0.96
4G	0.10	4.20	0.63	1.52	0.70	5.31	0.61	0.71	0.77	0.70	0.73	0.79	0.93	0.98	0.82	0.97	0.92
4E	0.20	3.60	0.59	1.40	0.70	0.28	0.78	0.65	0.80	0.63	0.65	0.71	0.84	0.99	0.73	1.03	1.00
4D	0.20	2.80	0.68	1.47	0.70	0.63	0.61	0.66	0.68	0.57	0.57	0.61	0.83	0.81	0.64	0.93	0.88
4C	0.20	2.40	0.69	1.15	0.70	0.28	0.96	0.72	0.84	0.71	0.70	0.71	0.91	0.97	0.82	1.07	0.98
4B	0.20	3.60	0.58	1.52	0.70	0.28	0.65	0.67	0.68	0.58	0.60	0.68	0.81	0.88	0.73	0.97	0.92
5A	0.20	3.40	0.48	1.13	0.60	0.28	0.57	0.54	0.59	0.53	0.55	0.59	0.72	0.85	0.64	0.86	0.84
5B	0.30	2.60	0.57	0.95	0.60	0.31	0.83	0.51	0.57	0.52	0.54	0.59	0.71	0.84	0.64	0.83	0.82
5C	0.30	1.40	0.85	0.83	0.70	0.31	1.09	0.56	0.66	0.55	0.56	0.58	0.72	0.86	0.64	0.93	0.86
5D	0.30	3.00	0.85	0.97	0.60	0.63	0.52	0.56	0.64	0.55	0.56	0.59	0.69	0.78	0.64	0.83	0.84
5E	0.20	3.80	0.79	1.08	0.70	0.63	0.61	0.61	0.68	0.54	0.56	0.62	0.76	0.87	0.73	0.93	0.88
Plus 1 Sigma Std. Dev.	1.00	1.00	1.47	1.40	1.00	1.19	1.37	1.41	1.39	1.24	1.27	1.31	1.21	1.23	1.36	1.17	1.18
Minus 1 Sigma Std. Dev.	1.00	1.00	0.53	0.60	1.00	0.81	0.63	0.59	0.61	0.76	0.73	0.69	0.79	0.77	0.64	0.83	0.82
Plus 2 Sigma Std. Dev.	1.00	1.00	1.94	1.80	1.00	1.38	1.74	1.82	1.77	1.49	1.54	1.63	1.43	1.46	1.73	1.34	1.37
Minus 2 Sigma Std. Dev.	1.00	1.00	0.06	0.20	1.00	0.63	0.26	0.18	0.23	0.51	0.46	0.37	0.57	0.54	0.27	0.66	0.63

Appendix B-7. Normalized values of Mt. Achernar moraine tills to various standards.

	MAM Tills/Mackellar																
	Si02	**Al2O3**	**CaO**	**Na2O**	**K20**	**P2O5**	**Fe203**	**Mgo**	**Ti02**	**Be**	**Sc**	**V**	**Cr**	**Co**	**Ni**	**Cu**	**Zn**
East Crest	1.04	0.87	9.77	1.47	0.64	0.71	0.88	0.95	1.12	0.34	1.07	0.93	0.61	0.97	0.56	1.06	0.52
1H	1.08	1.05	3.42	0.86	0.71	0.52	0.92	0.73	1.03	0.34	1.13	0.86	0.52	0.91	0.56	1.06	0.61
1E	1.10	1.01	3.42	0.82	0.70	0.55	0.89	0.70	1.04	0.34	1.07	0.80	0.52	0.91	0.56	0.79	0.52
1E Red/Grey	1.10	1.02	3.50	0.92	0.68	0.50	0.89	0.72	1.05	0.34	1.07	0.83	0.52	0.91	0.56	0.79	0.52
1A	1.11	0.88	6.87	1.31	0.64	0.68	0.73	0.69	1.05	0.34	1.01	0.82	0.52	0.85	0.37	0.79	0.44
1B	1.14	0.86	4.33	1.46	0.62	0.57	0.72	0.73	1.07	0.34	1.01	0.83	0.61	0.85	0.56	0.79	0.44
2A	1.12	0.91	4.57	1.58	0.72	0.83	0.73	0.65	1.15	0.34	0.95	0.77	0.61	0.80	0.56	0.79	0.61
3C	1.08	1.00	4.42	1.55	0.83	0.65	0.80	0.68	1.14	0.34	1.01	0.89	0.70	0.91	0.56	0.79	0.70
3 Dark	1.08	1.04	4.39	1.61	0.82	0.83	0.74	0.61	1.10	0.34	0.95	0.85	0.70	0.85	0.37	0.53	0.52
3B	1.08	1.01	4.27	1.49	0.85	0.61	0.81	0.66	1.12	0.51	1.01	0.86	0.70	0.91	0.56	0.79	0.70
3E	1.09	0.97	5.18	1.44	0.74	0.57	0.80	0.71	1.13	0.34	1.07	0.87	0.61	0.91	0.56	0.79	0.61
4L	1.06	0.98	6.07	1.55	0.70	0.63	0.85	0.78	0.99	0.34	1.07	0.85	0.52	0.85	0.37	1.06	0.61
4K	1.06	0.97	6.52	1.59	0.70	0.74	0.82	0.82	1.01	0.34	1.07	0.84	0.52	0.91	0.56	1.06	0.61
4J	1.09	0.98	5.76	1.38	0.69	0.59	0.78	0.71	0.95	0.34	1.01	0.80	0.44	0.80	0.35	0.79	0.52
4I	1.04	1.00	6.05	1.66	0.74	0.66	0.91	0.89	1.07	0.34	1.07	0.93	0.70	0.97	0.56	1.06	0.61
4G	1.05	0.99	6.17	1.78	0.75	0.67	0.85	0.85	1.08	0.34	1.07	0.87	0.70	0.97	0.56	1.06	0.61
4E	1.03	0.99	6.95	1.87	0.74	0.63	0.89	0.93	1.07	0.34	1.07	0.90	0.61	0.91	0.56	1.06	0.61
4D	1.06	0.97	6.71	2.02	0.65	0.60	0.79	0.85	1.02	0.34	0.95	0.79	0.52	0.85	0.56	0.79	0.52
4C	1.05	1.02	5.23	1.72	0.79	0.73	0.85	0.84	1.00	0.34	0.95	0.80	0.61	0.85	0.56	0.79	0.70
4B	1.07	0.91	6.80	1.83	0.67	0.59	0.84	0.88	1.03	0.34	1.01	0.85	0.52	0.85	0.74	0.79	0.52
5A	0.96	0.90	15.09	1.77	0.64	0.55	0.85	1.20	0.95	0.34	1.07	0.87	0.61	0.91	0.56	1.06	0.52
5B	0.96	0.90	13.51	1.88	0.67	0.56	0.92	1.31	0.94	0.34	1.13	0.86	0.61	1.02	0.74	1.32	0.61
5C	0.93	1.07	8.53	2.62	0.82	0.60	0.97	1.46	0.91	0.34	1.13	0.88	0.61	1.02	0.56	4.75	1.31
5D	0.93	1.02	10.35	3.41	0.73	0.57	0.94	1.17	0.93	0.34	1.07	0.82	0.61	1.19	0.74	1.58	0.78
5E	0.99	1.04	8.48	1.99	0.80	0.61	0.86	1.04	1.01	0.34	0.95	0.80	0.61	0.85	0.74	1.06	0.61
Plus 1 Sigma Std. Dev.	1.07	1.10	1.59	1.48	1.17	1.78	1.18	1.16	1.11	1.15	1.13	1.17	1.15	1.20	1.23	1.28	1.14
Minus 1 Sigma Std. Dev.	0.93	0.90	0.41	0.52	0.83	0.22	0.82	0.84	0.89	0.85	0.88	0.83	0.85	0.80	0.77	0.72	0.86
Plus 2 Sigma Std. Dev.	1.14	1.21	2.17	1.96	1.33	2.57	1.35	1.31	1.23	1.31	1.25	1.33	1.29	1.41	1.45	1.57	1.28
Minus 2 Sigma Std. Dev.	0.86	0.79	--	0.04	0.67	--	0.65	0.69	0.78	0.69	0.75	0.67	0.71	0.59	0.55	0.43	0.72

Appendix B-7 Continued. Normalized values of Mt. Achernar moraine tills to various standards.

	MAM Tills/Mackellar																
	Ge	**Ag**	**Cs**	**Hf**	**Ta**	**W**	**Pb**	**Th**	**U**	**La**	**Ce**	**Nd**	**Sm**	**Eu**	**Tb**	**Yb**	**Lu**
East Crest	0.10	4.80	0.37	1.81	0.73	0.29	0.70	0.69	0.69	0.62	0.68	0.75	0.79	0.87	0.69	1.03	1.02
1H	0.10	2.00	0.68	1.02	0.73	0.29	0.65	0.54	0.55	0.46	0.50	0.57	0.63	0.76	0.62	0.88	0.85
1E	0.10	2.60	0.63	1.02	0.73	0.29	0.70	0.57	0.55	0.47	0.52	0.60	0.66	0.75	0.62	0.88	0.83
1E Red/Grey	0.19	2.00	0.65	1.09	0.64	0.29	0.65	0.61	0.57	0.44	0.49	0.60	0.66	0.71	0.62	0.81	0.81
1A	0.10	3.20	0.50	1.51	0.64	0.29	0.65	0.62	0.63	0.49	0.54	0.62	0.72	0.78	0.69	0.91	0.89
1B	0.10	4.60	0.49	1.65	0.64	0.29	0.60	0.63	0.61	0.50	0.56	0.66	0.73	0.77	0.69	0.94	0.92
2A	0.19	4.60	0.51	1.67	0.82	0.29	0.98	0.69	0.71	0.72	0.77	0.84	0.91	1.01	0.77	1.03	1.02
3C	0.10	3.60	0.57	1.35	0.73	0.29	0.93	0.71	0.65	0.66	0.72	0.79	0.80	0.99	0.69	0.94	0.94
3 Dark	0.10	2.20	0.51	1.32	0.73	0.29	0.93	0.72	0.63	0.65	0.68	0.75	0.83	0.97	0.69	0.91	0.87
3B	0.10	3.40	0.62	1.25	0.73	0.29	0.98	0.72	0.67	0.67	0.73	0.78	0.83	0.94	0.69	0.91	0.89
3E	0.10	3.80	0.52	1.56	0.73	0.29	0.88	0.69	0.65	0.64	0.71	0.78	0.80	0.99	0.69	1.00	1.00
4L	0.10	3.00	0.57	1.14	0.64	0.29	0.84	0.56	0.61	0.49	0.54	0.63	0.67	0.83	0.62	0.94	0.91
4K	0.19	2.20	0.55	1.32	0.55	0.32	0.84	0.59	0.61	0.50	0.52	0.58	0.69	0.75	0.62	0.91	0.87
4J	0.10	2.80	0.60	1.05	0.64	0.29	0.60	0.53	0.59	0.45	0.51	0.59	0.64	0.80	0.62	0.88	0.85
4I	0.10	3.00	0.53	1.28	0.73	0.29	0.70	0.66	0.67	0.62	0.67	0.74	0.79	0.89	0.69	0.88	0.89
4G	0.10	4.20	0.54	1.60	0.64	5.48	0.65	0.72	0.69	0.64	0.70	0.79	0.81	0.85	0.69	0.88	0.85
4E	0.19	3.60	0.51	1.47	0.64	0.29	0.84	0.66	0.71	0.58	0.63	0.71	0.73	0.86	0.62	0.94	0.92
4D	0.19	2.80	0.59	1.54	0.64	0.65	0.65	0.67	0.61	0.52	0.55	0.61	0.72	0.70	0.54	0.84	0.81
4C	0.19	2.40	0.60	1.21	0.64	0.29	1.02	0.73	0.76	0.64	0.67	0.71	0.79	0.84	0.69	0.97	0.91
4B	0.19	3.60	0.50	1.60	0.64	0.29	0.70	0.67	0.61	0.52	0.57	0.68	0.71	0.77	0.62	0.88	0.85
5A	0.19	3.40	0.41	1.19	0.55	0.29	0.60	0.55	0.53	0.48	0.53	0.59	0.63	0.73	0.54	0.78	0.77
5B	0.29	2.60	0.49	1.00	0.55	0.32	0.88	0.52	0.51	0.48	0.52	0.59	0.62	0.73	0.54	0.75	0.75
5C	0.29	1.40	0.73	0.88	0.64	0.32	1.16	0.57	0.59	0.50	0.54	0.58	0.63	0.75	0.54	0.84	0.79
5D	0.29	3.00	0.73	1.02	0.55	0.65	0.56	0.57	0.57	0.50	0.53	0.59	0.60	0.67	0.54	0.75	0.77
5E	0.19	3.80	0.68	1.14	0.64	0.65	0.65	0.62	0.61	0.49	0.53	0.62	0.66	0.75	0.62	0.84	0.81
Plus 1 Sigma Std. Dev.	1.16	1.00	1.39	1.40	1.36	1.06	1.30	1.24	1.24	1.23	1.21	1.34	1.31	1.27	1.46	1.13	1.15
Minus 1 Sigma Std. Dev.	0.84	1.00	0.61	0.60	0.64	0.94	0.70	0.76	0.76	0.77	0.79	0.66	0.69	0.73	0.54	0.88	0.85
Plus 2 Sigma Std. Dev.	1.31	1.00	1.79	1.81	1.73	1.13	1.60	1.48	1.49	1.46	1.42	1.68	1.63	1.53	1.92	1.25	1.30
Minus 2 Sigma Std. Dev.	0.69	1.00	0.21	0.19	0.27	0.87	0.40	0.52	0.51	0.54	0.58	0.32	0.37	0.47	0.08	0.75	0.70

Appendix B-8. Normalized values of Mt. Achernar moraine tills to various standards.

	MAM Tills/Fairchild																
	Si02	**Al2O3**	**CaO**	**Na2O**	**K20**	**P2O5**	**Fe203**	**Mgo**	**Ti02**	**Be**	**Sc**	**V**	**Cr**	**Co**	**Ni**	**Cu**	**Zn**
East Crest	0.99	0.94	12.42	1.38	0.69	1.01	0.98	1.26	1.06	0.36	1.17	0.96	0.67	1.05	0.66	1.23	0.57
1H	1.02	1.15	4.35	0.80	0.76	0.75	1.02	0.97	0.97	0.36	1.23	0.89	0.57	0.99	0.66	1.23	0.66
1E	1.04	1.10	4.34	0.77	0.74	0.79	0.99	0.93	0.98	0.36	1.17	0.83	0.57	0.99	0.66	0.92	0.57
1E Red/Grey	1.04	1.11	4.45	0.86	0.73	0.71	0.98	0.94	0.99	0.36	1.17	0.86	0.57	0.99	0.66	0.92	0.57
1A	1.05	0.96	8.73	1.23	0.68	0.98	0.81	0.91	0.99	0.36	1.10	0.85	0.57	0.93	0.44	0.92	0.47
1B	1.08	0.94	5.50	1.37	0.67	0.82	0.80	0.96	1.00	0.36	1.10	0.86	0.67	0.93	0.66	0.92	0.47
2A	1.06	0.99	5.80	1.48	0.77	1.19	0.81	0.86	1.08	0.36	1.04	0.80	0.67	0.86	0.66	0.92	0.66
3C	1.02	1.09	5.62	1.46	0.89	0.94	0.89	0.90	1.07	0.36	1.10	0.92	0.76	0.99	0.66	0.92	0.76
3 Dark	1.02	1.13	5.58	1.51	0.88	1.20	0.82	0.80	1.03	0.36	1.04	0.88	0.76	0.93	0.44	0.62	0.57
3B	1.02	1.10	5.43	1.40	0.91	0.87	0.90	0.87	1.05	0.55	1.10	0.89	0.76	0.99	0.66	0.92	0.76
3E	1.03	1.06	6.59	1.35	0.79	0.82	0.89	0.93	1.07	0.36	1.17	0.90	0.67	0.99	0.66	0.92	0.66
4L	1.01	1.07	7.71	1.45	0.75	0.91	0.94	1.03	0.93	0.36	1.17	0.88	0.57	0.93	0.44	1.23	0.66
4K	1.00	1.06	8.29	1.49	0.75	1.06	0.91	1.08	0.95	0.36	1.17	0.87	0.57	0.99	0.66	1.23	0.66
4J	1.03	1.07	7.32	1.29	0.73	0.84	0.86	0.94	0.90	0.36	1.10	0.83	0.48	0.86	0.41	0.92	0.57
4I	0.98	1.09	7.69	1.56	0.80	0.95	1.01	1.17	1.01	0.36	1.17	0.96	0.76	1.05	0.66	1.23	0.66
4G	0.99	1.07	7.85	1.67	0.80	0.96	0.94	1.12	1.02	0.36	1.17	0.90	0.76	1.05	0.66	1.23	0.66
4E	0.97	1.08	8.83	1.76	0.79	0.91	0.99	1.22	1.00	0.36	1.17	0.93	0.67	0.99	0.66	1.23	0.66
4D	1.00	1.06	8.54	1.90	0.70	0.86	0.88	1.11	0.96	0.36	1.04	0.82	0.57	0.93	0.66	0.92	0.57
4C	1.00	1.10	6.65	1.61	0.85	1.05	0.94	1.10	0.94	0.36	1.04	0.83	0.67	0.93	0.66	0.92	0.76
4B	1.01	0.99	8.65	1.72	0.71	0.85	0.94	1.16	0.97	0.36	1.10	0.88	0.57	0.93	0.87	0.92	0.57
5A	0.90	0.97	19.18	1.67	0.69	0.79	0.95	1.59	0.90	0.36	1.17	0.90	0.67	0.99	0.66	1.23	0.57
5B	0.90	0.98	17.17	1.77	0.71	0.80	1.02	1.72	0.89	0.36	1.23	0.89	0.67	1.11	0.87	1.54	0.66
5C	0.88	1.16	10.85	2.46	0.87	0.86	1.08	1.92	0.85	0.36	1.23	0.91	0.67	1.11	0.66	5.54	1.42
5D	0.88	1.11	13.16	3.20	0.78	0.82	1.05	1.54	0.88	0.36	1.17	0.85	0.67	1.30	0.87	1.85	0.85
5E	0.93	1.13	10.78	1.87	0.86	0.88	0.96	1.37	0.95	0.36	1.04	0.82	0.67	0.93	0.87	1.23	0.66
Plus 1 Sigma Std. Dev.	1.09	1.11	1.54	1.16	1.12	1.19	1.35	1.17	1.14	1.24	1.23	1.18	1.23	1.30	1.32	1.37	1.17
Minus 1 Sigma Std. Dev.	0.91	0.89	0.46	0.84	0.88	0.81	0.65	0.83	0.86	0.76	0.77	0.82	0.77	0.70	0.68	0.63	0.83
Plus 2 Sigma Std. Dev.	1.18	1.21	2.08	1.32	1.23	1.38	1.70	1.34	1.28	1.47	1.47	1.37	1.45	1.59	1.65	1.74	1.34
Minus 2 Sigma Std. Dev.	0.82	0.79	--	0.68	0.77	0.63	0.30	0.66	0.72	0.53	0.53	0.63	0.55	0.41	0.35	0.26	0.66

Appendix B-8 Continued. Normalized values of Mt. Achernar moraine tills to various standards.

	MAM Tills/Fairchild																
	Ge	**Ag**	**Cs**	**Hf**	**Ta**	**W**	**Pb**	**Th**	**U**	**La**	**Ce**	**Nd**	**Sm**	**Eu**	**Tb**	**Yb**	**Lu**
East Crest	0.10	4.80	0.65	1.24	0.80	0.30	0.87	0.87	0.77	0.69	0.72	0.69	0.91	0.87	0.90	1.03	1.08
1H	0.10	2.00	1.19	0.70	0.80	0.30	0.81	0.68	0.61	0.51	0.53	0.52	0.72	0.76	0.80	0.88	0.90
1E	0.10	2.60	1.09	0.70	0.80	0.30	0.87	0.72	0.61	0.53	0.56	0.55	0.76	0.75	0.80	0.88	0.88
1E Red/Grey	0.20	2.00	1.13	0.75	0.70	0.30	0.81	0.76	0.64	0.49	0.52	0.55	0.76	0.71	0.80	0.81	0.86
1A	0.10	3.20	0.87	1.04	0.70	0.30	0.81	0.77	0.70	0.55	0.57	0.57	0.83	0.78	0.90	0.91	0.94
1B	0.10	4.60	0.85	1.13	0.70	0.30	0.75	0.79	0.68	0.56	0.60	0.60	0.84	0.77	0.90	0.94	0.98
2A	0.20	4.60	0.89	1.14	0.90	0.30	1.21	0.87	0.80	0.80	0.82	0.77	1.04	1.01	1.00	1.03	1.08
3C	0.10	3.60	1.00	0.93	0.80	0.30	1.16	0.88	0.73	0.74	0.76	0.72	0.92	0.99	0.90	0.94	1.00
3 Dark	0.10	2.20	0.89	0.90	0.80	0.30	1.16	0.90	0.70	0.73	0.72	0.68	0.95	0.97	0.90	0.91	0.92
3B	0.10	3.40	1.07	0.86	0.80	0.30	1.21	0.90	0.75	0.75	0.77	0.71	0.95	0.94	0.90	0.91	0.94
3E	0.10	3.80	0.91	1.07	0.80	0.30	1.10	0.87	0.73	0.71	0.75	0.71	0.92	0.99	0.90	1.00	1.06
4L	0.10	3.00	1.00	0.78	0.70	0.30	1.04	0.70	0.68	0.54	0.57	0.57	0.77	0.83	0.80	0.94	0.96
4K	0.20	2.20	0.96	0.90	0.60	0.33	1.04	0.74	0.68	0.56	0.56	0.53	0.79	0.75	0.80	0.91	0.92
4J	0.10	2.80	1.04	0.72	0.70	0.30	0.75	0.66	0.66	0.50	0.54	0.54	0.73	0.80	0.80	0.88	0.90
4I	0.10	3.00	0.93	0.88	0.80	0.30	0.87	0.82	0.75	0.69	0.72	0.68	0.91	0.89	0.90	0.88	0.94
4G	0.10	4.20	0.94	1.10	0.70	5.67	0.81	0.90	0.77	0.71	0.74	0.72	0.93	0.85	0.90	0.88	0.90
4E	0.20	3.60	0.89	1.01	0.70	0.30	1.04	0.82	0.80	0.64	0.66	0.65	0.84	0.86	0.80	0.94	0.98
4D	0.20	2.80	1.02	1.06	0.70	0.67	0.81	0.84	0.68	0.58	0.58	0.56	0.83	0.70	0.70	0.84	0.86
4C	0.20	2.40	1.04	0.83	0.70	0.30	1.27	0.91	0.84	0.72	0.71	0.65	0.91	0.84	0.90	0.97	0.96
4B	0.20	3.60	0.87	1.10	0.70	0.30	0.87	0.84	0.68	0.58	0.61	0.62	0.81	0.77	0.80	0.88	0.90
5A	0.20	3.40	0.72	0.82	0.60	0.30	0.75	0.68	0.59	0.54	0.56	0.54	0.72	0.73	0.70	0.78	0.82
5B	0.30	2.60	0.85	0.69	0.60	0.33	1.10	0.65	0.57	0.53	0.55	0.54	0.71	0.73	0.70	0.75	0.80
5C	0.30	1.40	1.28	0.60	0.70	0.33	1.45	0.72	0.66	0.55	0.57	0.53	0.72	0.75	0.70	0.84	0.84
5D	0.30	3.00	1.28	0.70	0.60	0.67	0.69	0.71	0.64	0.55	0.57	0.54	0.69	0.67	0.70	0.75	0.82
5E	0.20	3.80	1.19	0.78	0.70	0.67	0.81	0.77	0.68	0.55	0.57	0.56	0.76	0.75	0.80	0.84	0.86
Plus 1 Sigma Std. Dev.	1.00	1.00	1.30	1.20	1.00	1.00	1.46	1.15	1.16	1.17	1.16	1.28	1.17	1.27	1.20	1.16	1.14
Minus 1 Sigma Std. Dev.	1.00	1.00	0.70	0.80	1.00	1.00	0.54	0.85	0.84	0.83	0.84	0.72	0.83	0.73	0.80	0.84	0.86
Plus 2 Sigma Std. Dev.	1.00	1.00	1.59	1.41	1.00	1.00	1.91	1.29	1.32	1.34	1.32	1.55	1.35	1.53	1.40	1.31	1.28
Minus 2 Sigma Std. Dev.	1.00	1.00	0.41	0.59	1.00	1.00	0.09	0.71	0.68	0.66	0.68	0.45	0.65	0.47	0.60	0.69	0.72

Appendix B-9. Normalized values of Mt. Achernar moraine tills to various standards.

	MAM Tills/Buckley																
	Si02	**Al2O3**	**CaO**	**Na2O**	**K20**	**P2O5**	**Fe203**	**Mgo**	**Ti02**	**Be**	**Sc**	**V**	**Cr**	**Co**	**Ni**	**Cu**	**Zn**
East Crest	1.12	0.97	12.21	2.01	0.73	1.62	2.57	2.71	1.28	0.42	1.32	1.26	0.77	1.65	0.79	1.22	0.75
1H	1.17	1.18	4.28	1.17	0.81	1.21	2.69	2.08	1.18	0.42	1.40	1.17	0.66	1.55	0.79	1.22	0.88
1E	1.19	1.13	4.27	1.12	0.79	1.26	2.61	2.00	1.18	0.42	1.32	1.09	0.66	1.55	0.79	0.91	0.75
1E Red/Grey	1.18	1.14	4.38	1.26	0.78	1.14	2.58	2.03	1.20	0.42	1.32	1.13	0.66	1.55	0.79	0.91	0.75
1A	1.20	0.98	8.59	1.80	0.73	1.56	2.13	1.96	1.20	0.42	1.25	1.11	0.66	1.46	0.53	0.91	0.63
1B	1.23	0.96	5.41	1.99	0.71	1.31	2.11	2.07	1.22	0.42	1.25	1.14	0.77	1.46	0.79	0.91	0.63
2A	1.21	1.01	5.71	2.16	0.82	1.90	2.12	1.85	1.32	0.42	1.18	1.05	0.77	1.36	0.79	0.91	0.88
3C	1.16	1.12	5.52	2.12	0.94	1.50	2.34	1.93	1.30	0.42	1.25	1.21	0.88	1.55	0.79	0.91	1.01
3 Dark	1.16	1.15	5.49	2.20	0.94	1.91	2.16	1.73	1.25	0.42	1.18	1.16	0.88	1.46	0.53	0.61	0.75
3B	1.16	1.13	5.34	2.03	0.97	1.40	2.35	1.87	1.28	0.63	1.25	1.17	0.88	1.55	0.79	0.91	1.01
3E	1.17	1.09	6.48	1.97	0.84	1.31	2.33	2.01	1.29	0.42	1.32	1.19	0.77	1.55	0.79	0.91	0.88
4L	1.15	1.10	7.58	2.11	0.80	1.45	2.46	2.23	1.13	0.42	1.32	1.16	0.66	1.46	0.53	1.22	0.88
4K	1.14	1.09	8.15	2.18	0.80	1.70	2.40	2.32	1.15	0.42	1.32	1.15	0.66	1.55	0.79	1.22	0.88
4J	1.17	1.10	7.20	1.88	0.78	1.35	2.27	2.02	1.09	0.42	1.25	1.09	0.55	1.36	0.50	0.91	0.75
4I	1.12	1.12	7.56	2.27	0.85	1.52	2.65	2.52	1.23	0.42	1.32	1.26	0.88	1.65	0.79	1.22	0.88
4G	1.13	1.10	7.72	2.43	0.86	1.54	2.48	2.41	1.24	0.42	1.32	1.19	0.88	1.65	0.79	1.22	0.88
4E	1.11	1.10	8.69	2.56	0.85	1.46	2.61	2.63	1.22	0.42	1.32	1.22	0.77	1.55	0.79	1.22	0.88
4D	1.14	1.08	8.39	2.77	0.74	1.38	2.31	2.40	1.17	0.42	1.18	1.07	0.66	1.46	0.79	0.91	0.75
4C	1.13	1.13	6.54	2.35	0.90	1.68	2.47	2.38	1.14	0.42	1.18	1.09	0.77	1.46	0.79	0.91	1.01
4B	1.15	1.02	8.50	2.50	0.76	1.36	2.46	2.49	1.17	0.42	1.25	1.16	0.66	1.46	1.06	0.91	0.75
5A	1.03	1.00	18.86	2.43	0.73	1.26	2.49	3.42	1.09	0.42	1.32	1.19	0.77	1.55	0.79	1.22	0.75
5B	1.03	1.01	16.89	2.57	0.76	1.28	2.69	3.71	1.08	0.42	1.40	1.17	0.77	1.75	1.06	1.52	0.88
5C	1.00	1.19	10.67	3.59	0.93	1.38	2.83	4.14	1.03	0.42	1.40	1.20	0.77	1.75	0.79	5.49	1.88
5D	1.00	1.14	12.94	4.66	0.84	1.31	2.75	3.31	1.07	0.42	1.32	1.11	0.77	2.04	1.06	1.83	1.13
5E	1.06	1.16	10.60	2.72	0.92	1.41	2.52	2.94	1.15	0.42	1.18	1.08	0.77	1.46	1.06	1.22	0.88
Plus 1 Sigma Std. Dev.	1.29	1.37	2.00	1.67	1.44	1.00	1.96	1.64	1.43	1.50	1.51	1.70	2.23	1.78	1.91	1.80	1.51
Minus 1 Sigma Std. Dev.	0.71	0.63	0.00	0.33	0.56	1.00	0.04	0.36	0.57	0.50	0.49	0.30	0.00	0.22	0.09	0.20	0.49
Plus 2 Sigma Std. Dev.	1.58	1.73	3.00	2.33	1.88	1.00	2.92	2.27	1.86	2.00	2.01	2.40	3.46	2.55	2.83	2.59	2.02
Minus 2 Sigma Std. Dev.	0.42	0.27	--	0.00	0.13	1.00	--	--	0.14	--	--	--	--	--	--	--	--

Appendix B-9 Continued. Normalized values of Mt. Achernar moraine tills to various standards.

	MAM Tills/Buckley																
	Ge	**Ag**	**Cs**	**Hf**	**Ta**	**W**	**Pb**	**Th**	**U**	**La**	**Ce**	**Nd**	**Sm**	**Eu**	**Tb**	**Yb**	**Lu**
East Crest	0.09	4.80	0.51	1.98	0.80	0.30	0.78	0.94	0.89	0.89	0.91	0.95	0.99	0.94	0.90	1.00	0.90
1H	0.09	2.00	0.94	1.12	0.80	0.30	0.73	0.74	0.71	0.66	0.67	0.72	0.78	0.81	0.80	0.85	0.75
1E	0.09	2.60	0.87	1.12	0.80	0.30	0.78	0.78	0.71	0.67	0.70	0.76	0.83	0.81	0.80	0.85	0.73
1E Red/Grey	0.19	2.00	0.90	1.19	0.70	0.30	0.73	0.83	0.74	0.63	0.65	0.76	0.83	0.76	0.80	0.79	0.72
1A	0.09	3.20	0.69	1.65	0.70	0.30	0.73	0.84	0.82	0.71	0.72	0.79	0.90	0.84	0.90	0.88	0.78
1B	0.09	4.60	0.68	1.81	0.70	0.30	0.68	0.86	0.79	0.71	0.75	0.83	0.91	0.83	0.90	0.91	0.82
2A	0.19	4.60	0.71	1.83	0.90	0.30	1.09	0.94	0.92	1.03	1.04	1.06	1.13	1.08	1.00	1.00	0.90
3C	0.09	3.60	0.79	1.48	0.80	0.30	1.04	0.96	0.84	0.95	0.96	0.99	1.00	1.06	0.90	0.91	0.83
3 Dark	0.09	2.20	0.71	1.44	0.80	0.30	1.04	0.98	0.82	0.93	0.90	0.95	1.03	1.04	0.90	0.88	0.77
3B	0.09	3.40	0.85	1.37	0.80	0.30	1.09	0.97	0.87	0.96	0.97	0.98	1.03	1.01	0.90	0.88	0.78
3E	0.09	3.80	0.72	1.71	0.80	0.30	0.99	0.94	0.84	0.91	0.94	0.98	1.00	1.06	0.90	0.97	0.88
4L	0.09	3.00	0.79	1.25	0.70	0.30	0.94	0.76	0.79	0.70	0.72	0.79	0.84	0.89	0.80	0.91	0.80
4K	0.19	2.20	0.76	1.44	0.60	0.33	0.94	0.80	0.79	0.71	0.70	0.73	0.86	0.81	0.80	0.88	0.77
4J	0.09	2.80	0.82	1.15	0.70	0.30	0.68	0.72	0.76	0.65	0.68	0.74	0.80	0.86	0.80	0.85	0.75
4I	0.09	3.00	0.74	1.40	0.80	0.30	0.78	0.89	0.87	0.89	0.90	0.93	0.99	0.96	0.90	0.85	0.78
4G	0.09	4.20	0.75	1.75	0.70	5.67	0.73	0.97	0.89	0.91	0.93	0.99	1.01	0.91	0.90	0.85	0.75
4E	0.19	3.60	0.71	1.62	0.70	0.30	0.94	0.89	0.92	0.83	0.84	0.89	0.91	0.92	0.80	0.91	0.82
4D	0.19	2.80	0.81	1.69	0.70	0.67	0.73	0.91	0.79	0.74	0.73	0.77	0.90	0.75	0.70	0.82	0.72
4C	0.19	2.40	0.82	1.33	0.70	0.30	1.15	0.99	0.97	0.92	0.89	0.90	0.99	0.90	0.90	0.94	0.80
4B	0.19	3.60	0.69	1.75	0.70	0.30	0.78	0.91	0.79	0.75	0.76	0.85	0.88	0.82	0.80	0.85	0.75
5A	0.19	3.40	0.57	1.31	0.60	0.30	0.68	0.74	0.68	0.69	0.71	0.75	0.78	0.79	0.70	0.76	0.68
5B	0.28	2.60	0.68	1.10	0.60	0.33	0.99	0.70	0.66	0.68	0.70	0.74	0.77	0.78	0.70	0.73	0.67
5C	0.28	1.40	1.01	0.96	0.70	0.33	1.30	0.78	0.76	0.71	0.72	0.73	0.78	0.80	0.70	0.82	0.70
5D	0.28	3.00	1.01	1.12	0.60	0.67	0.63	0.77	0.74	0.71	0.71	0.74	0.75	0.72	0.70	0.73	0.68
5E	0.19	3.80	0.94	1.25	0.70	0.67	0.73	0.84	0.79	0.70	0.71	0.78	0.83	0.81	0.80	0.82	0.72
Plus 1 Sigma Std. Dev.	1.33	1.00	1.51	1.52	1.00	1.07	1.31	1.39	1.42	1.54	1.52	1.49	1.43	1.43	1.40	1.48	1.50
Minus 1 Sigma Std. Dev.	0.67	1.00	0.49	0.48	1.00	0.93	0.69	0.61	0.58	0.46	0.48	0.51	0.57	0.57	0.60	0.52	0.50
Plus 2 Sigma Std. Dev.	1.67	1.00	2.03	2.04	1.00	1.13	1.61	1.79	1.84	2.08	2.04	1.99	1.87	1.86	1.80	1.97	2.00
Minus 2 Sigma Std. Dev.	0.33	1.00	--	--	--	0.87	0.39	0.21	0.16	--	--	0.01	0.13	0.14	0.20	0.03	--

Appendix B-10. Normalized values of Mt. Achernar moraine tills to various standards.

	MAM Tills/Fremouw						
	SiO2	**Al2O3**	**CaO**	**Na2O**	**K2O**	**MgO**	**Fe2O3**
East Crest	0.95	1.00	1.23	0.84	1.80	6.43	2.77
1H	0.99	1.22	0.43	0.49	1.99	4.94	2.90
1E	1.01	1.18	0.43	0.46	1.95	4.74	2.81
1E Red/Grey	1.00	1.18	0.44	0.52	1.92	4.83	2.79
1A	1.01	1.02	0.87	0.75	1.79	4.65	2.30
1B	1.04	1.00	0.55	0.83	1.75	4.91	2.27
2A	1.03	1.05	0.58	0.90	2.01	4.41	2.29
3C	0.99	1.16	0.56	0.88	2.33	4.58	2.53
3 Dark	0.99	1.20	0.55	0.91	2.32	4.11	2.33
3B	0.99	1.17	0.54	0.84	2.39	4.44	2.54
3E	0.99	1.13	0.65	0.82	2.08	4.76	2.52
4L	0.97	1.14	0.76	0.88	1.98	5.28	2.66
4K	0.97	1.13	0.82	0.90	1.96	5.52	2.59
4J	0.99	1.14	0.73	0.78	1.92	4.79	2.45
4I	0.95	1.16	0.76	0.94	2.09	5.98	2.86
4G	0.96	1.15	0.78	1.01	2.11	5.73	2.67
4E	0.94	1.15	0.88	1.06	2.08	6.26	2.81
4D	0.96	1.12	0.85	1.15	1.83	5.69	2.49
4C	0.96	1.18	0.66	0.97	2.23	5.64	2.66
4B	0.97	1.05	0.86	1.04	1.87	5.91	2.65
5A	0.87	1.04	1.90	1.01	1.80	8.10	2.68
5B	0.87	1.04	1.70	1.07	1.87	8.80	2.90
5C	0.85	1.23	1.07	1.49	2.29	9.82	3.05
5D	0.85	1.18	1.30	1.93	2.06	7.85	2.96
5E	0.90	1.20	1.07	1.13	2.26	6.99	2.72
Plus 1 Sigma Std. Dev.	1.11	1.17	2.10	1.66	1.87	1.62	1.48
Minus 1 Sigma Std. Dev.	0.89	0.83	0.00	0.34	0.13	0.38	0.52
Plus 2 Sigma Std. Dev.	1.22	1.34	3.20	2.32	2.75	2.24	1.95
Minus 2 Sigma Std. Dev.	0.78	0.66	0.00	0.00	0.00	0.00	0.05

Appendix B-11. Normalized values of Mt. Achernar moraine tills to various standards.

	MAM Tills/Ferrar Dolerite												
	Si02	**Al203**	**Fe2O3**	**MnO**	**MgO**	**CaO**	**Na20**	**K2O**	**TiO2**	**P2O5**	**LOI**	**Rb**	**Sr**
East Crest	1.10	0.92	0.60	0.64	0.43	0.64	0.93	2.69	1.28	1.37	5.58	3.04	1.47
1H	1.13	1.10	0.62	0.65	0.33	0.22	0.53	2.94	1.16	1.00	6.49	3.58	1.19
1E	1.10	1.02	0.58	0.66	0.30	0.21	0.49	2.77	1.12	1.00	7.19	3.36	1.17
1E Red/Grey	1.10	1.02	0.57	0.65	0.31	0.22	0.55	2.73	1.14	0.91	6.99	3.36	1.14
1A	1.14	0.90	0.48	0.61	0.30	0.44	0.80	2.61	1.16	1.28	7.04	2.79	1.33
1B	1.19	0.91	0.49	0.60	0.33	0.28	0.91	2.59	1.20	1.09	5.78	2.90	1.33
2A	1.21	0.98	0.51	0.56	0.30	0.31	1.02	3.08	1.34	1.64	3.64	3.33	1.78
3C	1.15	1.07	0.55	0.54	0.31	0.29	0.99	3.52	1.31	1.28	4.43	3.79	1.82
3 Dark	1.16	1.12	0.51	0.56	0.28	0.29	1.03	3.53	1.27	1.64	4.53	3.26	1.87
3B	1.15	1.08	0.56	0.54	0.30	0.28	0.94	3.59	1.28	1.18	5.01	3.79	1.75
3E	1.13	1.02	0.54	0.60	0.32	0.34	0.90	3.08	1.28	1.09	5.60	3.26	1.62
4L	1.09	1.01	0.56	0.59	0.34	0.39	0.94	2.87	1.09	1.18	7.08	3.33	1.42
4K	1.07	0.99	0.54	0.58	0.35	0.41	0.96	2.81	1.10	1.37	6.78	2.93	1.49
4J	1.10	1.00	0.51	0.57	0.31	0.37	0.84	2.78	1.04	1.09	7.80	3.22	1.50
4I	1.09	1.06	0.62	0.57	0.40	0.40	1.05	3.13	1.22	1.28	5.40	3.40	1.90
4G	1.09	1.03	0.57	0.59	0.38	0.40	1.10	3.12	1.21	1.28	6.36	3.51	1.67
4E	1.04	1.01	0.59	0.57	0.40	0.44	1.14	3.01	1.17	1.18	6.87	3.11	1.98
4D	1.05	0.97	0.51	0.59	0.36	0.42	1.20	2.58	1.10	1.09	7.63	2.86	1.85
4C	1.07	1.04	0.56	0.51	0.37	0.33	1.05	3.23	1.10	1.37	6.01	3.69	1.72
4B	1.08	0.92	0.55	0.60	0.38	0.43	1.10	2.68	1.12	1.09	6.79	2.93	1.52
5A	0.95	0.89	0.55	0.57	0.51	0.93	1.05	2.54	1.02	1.00	8.50	2.68	1.84
5B	0.94	0.89	0.59	0.59	0.55	0.83	1.10	2.61	1.00	1.00	9.13	2.90	2.90
5C	0.92	1.06	0.62	0.56	0.62	0.53	1.55	3.22	0.97	1.09	9.43	3.47	3.65
5D	0.89	0.98	0.58	0.54	0.48	0.62	1.95	2.79	0.96	1.00	11.34	3.36	2.72
5E	0.96	1.01	0.54	0.53	0.43	0.51	1.15	3.11	1.05	1.09	8.90	3.33	2.43
Plus 1 Sigma Std. Dev.	1.02	1.06	1.10	1.12	1.26	1.10	1.16	1.24	1.22	1.29	1.49	1.36	1.21
Minus 1 Sigma Std. Dev.	0.98	0.94	0.90	0.88	0.74	0.90	0.84	0.76	0.78	0.71	0.51	0.64	0.79
Plus 2 Sigma Std. Dev.	1.04	1.12	1.19	1.23	1.51	1.21	1.32	1.48	1.44	1.57	1.98	1.72	1.41
Minus 2 Sigma Std. Dev.	0.96	0.88	0.81	0.77	0.49	0.79	0.68	0.52	0.56	0.43	0.02	0.28	0.59

Appendix B-12. Normalized values of Mt. Achernar moraine tills to various standards.

	MAM Tills/Sirius (Beardmore Glacier)															
	SiO2	**Al2O3**	**CaO**	**Na2O**	**K2O**	**P2O5**	**Fe2O3**	**MgO**	**TiO2**	**MnO**	**Ba**	**Cr**	**Nb**	**Sr**	**Y**	**Zr**
East Crest	1.02	1.14	1.95	1.01	1.21	1.84	1.32	1.29	1.52	1.46	1.27	1.25	5.91	1.10	1.65	2.56
1H	1.06	1.38	0.68	0.59	1.34	1.37	1.39	0.99	1.40	1.50	1.36	1.07	5.32	0.90	1.39	1.42
1E	1.07	1.33	0.68	0.56	1.32	1.43	1.35	0.95	1.40	1.60	1.32	1.07	5.32	0.88	1.28	1.41
1E Red/Grey	1.07	1.34	0.70	0.63	1.30	1.29	1.33	0.97	1.43	1.58	1.30	1.07	5.91	0.86	1.28	1.63
1A	1.08	1.15	1.37	0.90	1.21	1.77	1.10	0.93	1.42	1.44	1.25	1.07	7.68	1.00	1.39	2.21
1B	1.11	1.14	0.86	1.00	1.18	1.49	1.09	0.99	1.44	1.40	1.27	1.25	5.32	1.00	1.49	2.47
2A	1.09	1.19	0.91	1.08	1.35	2.16	1.09	0.88	1.56	1.26	1.61	1.25	7.09	1.34	1.76	2.42
3C	1.05	1.32	0.88	1.06	1.57	1.70	1.21	0.92	1.54	1.22	1.81	1.43	6.50	1.37	1.55	1.97
3 Dark	1.05	1.36	0.88	1.10	1.56	2.17	1.11	0.82	1.48	1.25	1.81	1.43	6.50	1.41	1.44	1.93
3B	1.05	1.33	0.85	1.02	1.61	1.59	1.21	0.89	1.51	1.22	1.82	1.43	6.50	1.32	1.55	1.78
3E	1.06	1.28	1.03	0.99	1.40	1.49	1.20	0.96	1.53	1.38	1.58	1.25	5.91	1.22	1.55	2.15
4L	1.04	1.29	1.21	1.06	1.33	1.65	1.27	1.06	1.34	1.39	1.35	1.07	5.32	1.07	1.44	1.65
4K	1.03	1.28	1.30	1.09	1.32	1.92	1.24	1.11	1.37	1.39	1.32	1.07	5.91	1.12	1.39	1.92
4J	1.06	1.29	1.15	0.94	1.30	1.53	1.17	0.96	1.29	1.36	1.53	0.90	5.32	1.13	1.33	1.53
4I	1.01	1.32	1.21	1.14	1.41	1.72	1.37	1.20	1.46	1.30	1.51	1.43	5.91	1.43	1.49	1.79
4G	1.02	1.30	1.23	1.22	1.42	1.74	1.28	1.15	1.46	1.36	1.51	1.43	6.50	1.26	1.49	2.29
4E	1.00	1.30	1.39	1.28	1.40	1.66	1.34	1.26	1.44	1.36	1.44	1.25	5.32	1.49	1.49	2.03
4D	1.03	1.27	1.34	1.39	1.23	1.56	1.19	1.14	1.38	1.44	1.25	1.07	5.91	1.39	1.23	2.23
4C	1.03	1.33	1.04	1.18	1.50	1.90	1.27	1.13	1.35	1.21	1.54	1.25	7.09	1.29	1.39	1.66
4B	1.04	1.19	1.36	1.25	1.26	1.54	1.27	1.19	1.39	1.45	1.32	1.07	5.91	1.15	1.28	2.47
5A	0.93	1.18	3.01	1.22	1.22	1.43	1.29	1.63	1.29	1.40	1.18	1.25	5.32	1.38	1.28	1.76
5B	0.93	1.18	2.70	1.29	1.26	1.45	1.39	1.77	1.28	1.46	1.23	1.25	4.73	2.18	1.28	1.42
5C	0.91	1.40	1.70	1.80	1.54	1.57	1.46	1.97	1.23	1.37	1.31	1.25	4.73	2.75	1.28	1.18
5D	0.91	1.35	2.07	2.34	1.39	1.49	1.42	1.58	1.26	1.36	1.22	1.25	5.32	2.05	1.23	1.55
5E	0.96	1.36	1.69	1.36	1.52	1.60	1.30	1.40	1.36	1.32	1.42	1.25	5.91	1.83	1.28	1.68
Plus 1 Sigma Std. Dev.	1.06	1.09	1.43	1.14	1.16	1.21	1.15	1.38	1.06	1.22	1.10	1.38	3.45	1.19	1.10	1.16
Minus 1 Sigma Std. Dev.	0.94	0.91	0.57	0.86	0.84	0.79	0.85	0.62	0.94	0.78	0.90	0.62	0.00	0.81	0.90	0.84
Plus 2 Sigma Std. Dev.	1.13	1.19	1.85	1.28	1.33	1.42	1.29	1.75	1.12	1.45	1.20	1.76	5.91	1.38	1.20	1.32
Minus 2 Sigma Std. Dev.	0.87	0.81	0.15	0.72	0.67	0.58	0.71	0.25	0.88	0.55	0.80	0.24	0.00	0.62	0.80	0.68

Appendix B-13. Normalized values of Mt. Achernar moraine tills to various standards.

	MAM Tills/Sirius (TAM Average)																						
	SiO2	**Al2O3**	**CaO**	**Na2O**	**K2O**	**P2O5**	**Fe2O3**	**MgO**	**TiO2**	**MnO**	**Ba**	**Cr**	**Ga**	**Nb**	**Ni**	**Pb**	**Rb**	**Sr**	**Th**	**V**	**Y**	**Zn**	**Zr**
East Crest	0.94	1.19	2.14	1.11	1.10	1.42	1.02	1.66	1.18	1.28	1.25	1.41	0.99	1.12	1.23	0.85	0.95	1.50	1.70	0.63	1.18	0.93	2.17
1H	0.98	1.45	0.75	0.65	1.22	1.06	1.07	1.28	1.09	1.33	1.33	1.21	1.17	1.01	1.23	0.79	1.12	1.23	1.33	0.58	0.99	1.09	1.20
1E	0.99	1.39	0.75	0.62	1.19	1.10	1.04	1.23	1.09	1.41	1.30	1.21	1.05	1.01	1.23	0.85	1.05	1.20	1.40	0.54	0.91	0.93	1.19
1E Red/Grey	0.99	1.40	0.77	0.69	1.18	1.00	1.03	1.25	1.11	1.39	1.28	1.21	1.11	1.12	1.23	0.79	1.05	1.17	1.50	0.56	0.91	0.93	1.38
1A	1.00	1.21	1.50	0.99	1.10	1.37	0.85	1.20	1.10	1.27	1.22	1.21	0.93	1.46	0.82	0.79	0.87	1.36	1.51	0.55	0.99	0.78	1.87
1B	1.03	1.19	0.95	1.10	1.07	1.15	0.84	1.27	1.12	1.23	1.25	1.41	0.93	1.01	1.23	0.73	0.90	1.37	1.54	0.56	1.07	0.78	2.09
2A	1.01	1.25	1.00	1.20	1.23	1.67	0.84	1.14	1.21	1.11	1.58	1.41	1.05	1.35	1.23	1.19	1.04	1.82	1.70	0.52	1.26	1.09	2.04
3C	0.97	1.38	0.97	1.17	1.42	1.32	0.93	1.18	1.20	1.07	1.77	1.61	1.24	1.23	1.23	1.13	1.18	1.87	1.74	0.60	1.10	1.24	1.67
3 Dark	0.98	1.42	0.96	1.22	1.42	1.68	0.86	1.06	1.15	1.10	1.77	1.61	1.17	1.23	0.82	1.13	1.02	1.92	1.77	0.57	1.03	0.93	1.63
3B	0.98	1.39	0.94	1.12	1.46	1.23	0.94	1.15	1.18	1.08	1.78	1.61	1.24	1.23	1.23	1.19	1.18	1.80	1.76	0.58	1.10	1.24	1.50
3E	0.98	1.34	1.14	1.09	1.27	1.15	0.93	1.23	1.19	1.22	1.55	1.41	1.11	1.12	1.23	1.07	1.02	1.67	1.70	0.59	1.10	1.09	1.82
4L	0.96	1.35	1.33	1.17	1.21	1.27	0.98	1.37	1.04	1.22	1.33	1.21	1.11	1.01	0.82	1.02	1.04	1.46	1.38	0.57	1.03	1.09	1.40
4K	0.96	1.34	1.43	1.20	1.20	1.49	0.96	1.43	1.06	1.22	1.29	1.21	1.11	1.12	1.23	1.02	0.92	1.53	1.45	0.57	0.99	1.09	1.62
4J	0.98	1.35	1.26	1.04	1.18	1.18	0.91	1.24	1.00	1.20	1.50	1.01	1.05	1.01	0.78	0.73	1.00	1.54	1.30	0.54	0.95	0.93	1.29
4I	0.94	1.38	1.32	1.26	1.28	1.33	1.06	1.55	1.13	1.15	1.48	1.61	1.11	1.12	1.23	0.85	1.06	1.95	1.62	0.63	1.07	1.09	1.51
4G	0.95	1.36	1.35	1.34	1.29	1.35	0.99	1.48	1.14	1.20	1.48	1.61	1.11	1.23	1.23	0.79	1.09	1.72	1.76	0.59	1.07	1.09	1.94
4E	0.93	1.36	1.52	1.42	1.27	1.28	1.04	1.62	1.12	1.20	1.41	1.41	1.05	1.01	1.23	1.02	0.97	2.04	1.60	0.60	1.07	1.09	1.71
4D	0.95	1.33	1.47	1.53	1.12	1.21	0.92	1.47	1.08	1.27	1.23	1.21	1.05	1.12	1.23	0.79	0.89	1.90	1.64	0.53	0.88	0.93	1.89
4C	0.95	1.40	1.15	1.30	1.36	1.47	0.98	1.46	1.05	1.07	1.51	1.41	1.17	1.35	1.23	1.24	1.15	1.76	1.78	0.54	0.99	1.24	1.41
4B	0.96	1.25	1.49	1.38	1.14	1.19	0.98	1.53	1.08	1.28	1.29	1.21	1.05	1.12	1.65	0.85	0.92	1.57	1.65	0.57	0.91	0.93	2.09
5A	0.86	1.23	3.31	1.34	1.10	1.11	0.99	2.10	1.00	1.23	1.16	1.41	0.93	1.01	1.23	0.73	0.84	1.89	1.34	0.59	0.91	0.93	1.49
5B	0.86	1.24	2.96	1.42	1.14	1.12	1.07	2.28	0.99	1.29	1.20	1.41	0.99	0.90	1.65	1.07	0.90	2.98	1.27	0.58	0.91	1.09	1.20
5C	0.84	1.47	1.87	1.98	1.40	1.21	1.13	2.54	0.95	1.21	1.29	1.41	1.11	0.90	1.23	1.41	1.08	3.75	1.40	0.59	0.91	2.33	1.00
5D	0.84	1.41	2.27	2.58	1.26	1.15	1.10	2.03	0.98	1.20	1.19	1.41	1.11	1.01	1.65	0.68	1.05	2.80	1.39	0.55	0.88	1.40	1.31
5E	0.89	1.43	1.86	1.51	1.38	1.24	1.00	1.81	1.06	1.17	1.39	1.41	1.17	1.12	1.65	0.79	1.04	2.49	1.51	0.54	0.91	1.09	1.42
Plus 1 Sigma Std. Dev.	1.11	1.16	1.56	1.40	1.34	1.71	1.60	1.48	1.66	1.48	1.23	1.35	1.26	1.73	1.42	1.22	1.22	1.36	1.29	1.81	1.48	1.74	1.29
Minus 1 Sigma Std. Dev.	0.89	0.84	0.44	0.60	0.66	0.29	0.40	0.52	0.34	0.52	0.77	0.65	0.74	0.27	0.58	0.78	0.78	0.64	0.71	0.19	0.52	0.26	0.71
Plus 2 Sigma Std. Dev.	1.21	1.33	2.12	1.80	1.69	2.41	2.19	1.96	2.32	1.96	1.47	1.71	1.53	2.47	1.83	1.43	1.44	1.73	1.58	2.61	1.95	2.49	1.58
Minus 2 Sigma Std. Dev.	0.79	0.67	0.00	0.20	0.31	0.00	0.00	0.04	0.00	0.04	0.53	0.29	0.47	0.00	0.17	0.57	0.56	0.27	0.42	0.00	0.05	0.00	0.42

REFERENCES CITED

Ackert Jr., R.P., Kurz, M.D., 2004. Age and uplift rates of Sirius Group sediments in the Dominion Range Antarctica, from surface exposure dating and geo-morphology. Glob. Planet. Change 42, p. 207–225.

Ackert Jr., R.P., Mukhopadhyay, S., Parizek, B.R., Borns, H.W., 2007. Ice elevation near the West Antarctic Ice Sheet divide during the Last Glaciation. Geophys. Res. Lett. 34, L21506. http://dx.doi.org/10.1029/2007GL031412.

Ackert Jr., R.P., Mukhopadhyay, S., Pollard, D., DeConto, R.M., Putnam, A.E., Borns, H.W., 2011. West Antarctic Ice Sheet elevations in the Ohio Range: geologic constraints and ice sheet modeling prior to the last highstand. Earth Planet. Sci. Lett. 307, p. 83–93. http://dx.doi.org/10.1016/j.epsl2011.04.015.

Ackert Jr., R.P., Putnam, A.E., Mukhopadhyay, S., Pollard, D., DeConto, R.M., Kurz, M.D., Borns, H.W., 2013. Controls on interior West Antarctic Ice Sheet Elevations: inferences from geologic constraints and ice sheet modeling, Quaternary Science Reviews, 65, p. 26–38.

Allard, S., Hall, B., Denton, G., 2011. History of the Ross Sea ice sheet based on glacial and lake records from Marshall Valley, Antarctica. 18th Annual West Antarctic Ice Sheet meeting, Loveland, CO, http:// www.waisworkshop.org.

Anderson, J.B., Conway, H., Bart, P.J., Kirshner, A.E., Greenwood, S.L., McKay, R.M., Hall, B.L., Ackert, R.P., Licht, K., Jakobsson, M., Stone, J.O., in press. Ross Sea paleo-ice sheet drainage and deglacial history during and since the LGM, Quaternary Science Reviews.

Barker P.F., Filippelli, G.M., Florindo, F., Martin, E.E., Scher, H.D., 2007. Onset and role of the Antarctic circumpolar current. Deep Sea Res II, p. 2388–2398.

Barrett, P.J., 1991. The Devonian to Jurassic Beacon Supergroup of the Transantarctic Mountains and correlatives in other parts of Antarctica. In: Tingey, R.J. (Ed.), The Geology of Antarctica. Oxford University Press, New York, p. 120–152.

Barrett, P.J., Elliot, D.H., Lindsay, J.F., 1986. The Beacon Supergroup (Devonian-Triassic) and Ferrar Group in the Beardmore Glacier area, Antarctica. Antarctic Research Series, 36, p. 339-428.

Bertler, N.A.N., Barrett, P.J., 2010. Vanishing Polar Ice Sheets, Dodson, J. (Ed.), Changing Climates, Earth Systems and Society, International Year of Planet Earth, Springer Science+Business Media B.V., 49. doi: 10.1007/978-90-481-8716-4_4.

Bialas, R.W., Buck, W.R., Studinger, M., Fitzgerald, P.G., 2007. Plateau collapse model for the Transantarctic Mountains-West Antarctic Rift System: Insights from numerical experiments. Geology, 35, p. 687–690.

Bintanja, R., 1999. On the glaciological, meteorological and climatological significance of Antarctic blue ice areas. Rev. Geophys., 37, 3, p. 337–359 doi: 10.1029/1999RG900007.

Black, L., Kamo, S., Allen, C., Davis, D., Aleinikoff, J., Valley, J., Mundil, R., Campbell, I., Korsch, R., Williams, I., and Foudoulis, C., 2004. Improved $^{206}Pb/^{238}U$ microprobe geochronology by the monitoring of a trace-element-related matrix effect; SHRIMP, ID–TIMS, ELA–ICP–MS and oxygen isotope documentation for a series of zircon standards. Chemical Geology, 205, p. 115–140.

Bromley, G.R.M., Hall, B.L., Stone, J.O., Conway, H., Todd, C.E., 2010. Late Cenozoic deposits at Reedy Glacier, Transantarctic Mountains: implications for former thickness of the West Antarctic Ice Sheet. Quaternary Science Reviews 29, p. 384–398.

Canil D., Lacourse, T., 2011. An estimate for the bulk composition of juvenile upper continental crust derived from glacial till in the North American Cordillera. Chemical Geology, 284, p. 229–239.

Chinn, T.J., 1991. Polar glacier margin and debris features. Memorie della Societ a Geologica Italiana, 46, p. 25–44.

Cook, C.P., van de Flierdt, T., Williams, T., Hemming, S.R., Iwai, M., Kobayashi, M., Jimenez-Espejo, F.J., Escutia, C., González, J.J., Khim, B., McKay, R.M., Passchier, S., Bohaty, S.M., Riesselman, C.R., Tauxe, L., Sugisaki, S., Galindo, A.L., Patterson, M.O., Sangiorgi, F., Pierce, E.L., Brinkhuis, H., IODP Expedition 318 Scientists, 2013. Dynamic behavior of the East Antarctic ice sheet during Pliocene warmth. Nature Geoscience, 6, p. 765–769. doi: 10.1038/NGEO1889.

Cox, R., Lowe, D.R., Cullers, R.L., 1995. The influence of sediment recycling and basement composition of evolution of mudrock chemistry in the southwestern United States. Geochimica et Cosmochimica Acta, 59, 14, p. 2919–2940.

Davis, D.W.O., Williams, I.S., Krogh, T.E., 2003. Historical Development of Zircon Geochronology. In: Hanchar, J.M., Hoskin, P.W.O. (Eds.), Zircon: Reviews in Mineralogy and Geochemistry, 53, p. 145–73.

DeConto, R.M., Pollard, D., Wilson, P.A., Palike, H., Lear C.H., Pagani, M., 2008. Thresholds for Cenozoic bipolar glaciation. Nature, 455, p. 652–656.

Denton, G.H., Hughes, T.J., 2002. Reconstructing the Antarctic Ice Sheet at the Last Glacial Maximum. Quaternary Science Reviews 21, p. 193–202.

Denton, G.H., Hughes, T.J., 2000. Reconstruction of the Ross ice drainage system, Antarctica, at the Last Glacial Maximum. Geografiska Annaler, 82, p. 143–166. doi: 10.1111/j.0435-3676.2000.00120.x.

Denton, G.H., Bockheim, J.G., Wilson, S.C., Stuiver, M., 1989. Late Wisconsin and Early Holocene glacial history, inner Ross Emabyment, Antarctica. Quaternary Research 31, p. 151–182.

Dits, T.M., in prep. Characterization of Till from the Mount Howe Blue Ice Moraine: Constraints on East Antarctic Bedrock and Provenance over Multiple Glacial Cycles. M.S. thesis, Indiana University, Indianapolis, IN, USA.

Dits, T., Licht, K.J., Bader, N., Kaplan, M.R., Winckler, G., Schaefer, J., 2012. Uncovering East Antarctic Bedrock Using Detrital Zircon Geochronology and Pebble Lithologies at Mount Howe, Scott Glacier. Abstract PP23C-2073 presented at 2012 Fall Meeting, AGU, San Francisco, CA., 3-7 Dec.

Elliot, D.H., Fanning, C.M., 2008. Detrital zircons from upper Permian and lower Triassic Victoria Group sandstones, Shackleton Glacier region, Antarctica: evidence for multiple sources along the Gondwana plate margin. Gondwana Research 13, p. 259–274. doi: 10.1016/j.gr.2007.05.003.

Elliot, D.H., Fleming, T.H., 2000. Weddell triple junction: the principal focus of Ferrar and Karoo magmatism during initial breakup of Gondwana. Geology, 28, p. 539–542.

Farmer, G.L., Licht, K., Swope, R.J., Andrews, J., 2006. Isotopic constraints on the provenance of fine-grained sediment in LGM tills from the Ross Embayment, Antarctica. Earth and Planetary Science Letters 249, p. 90–107.

Faure, G., 1986. Principles of Isotope Geology, 2nd Edition, John Wiley & Sons, Inc, 608 p.

Faure, G., Mensing, T.M., Johnson, K.S., 1992. Composition of rock clasts in the Mt. Achernar moraine and the Lewis Cliff ice tongue. Antarctic Journal, Ohio State University.

Faure, G., Mensing, T.M., 2010. The Transantarctic Mountains: Rocks, Ice, Metorites, and Water. Springer Science + Business Media B.V. doi: 10.1007/978-90-481-9390-5_10. p. 289–469.

Faure, G., Nishiizumi, K., 1994. Exposure dating of quartz sandstone in the Transantarctic Mountains by cosmogenic ^{10}Be and ^{26}Al. Mineralogical Magazine, 58A, 268–269.

Fedo, C.M., Sircombe, K.N., Rainbird, R.H., 2003. Detrital Zircon Analysis of the Sedimentary Record. In Hanchar, J.M., Hoskin, P.W.O. (Eds.), Zircon: Reviews in Mineralogy and Geochemistry, 53, 277–298.

Fitzgerald, P., 2002. Tectonics and landscape evolution of the Antarctic plate since the breakup of Gondwana, with an emphasis on the West Antarctic Rift System and the Transantarctic Mountains. Royal Society of New Zealand Bulletin, 35, 453–469.

Fogwill, C.J., Hein, A.S., Bentley, M.J., Sugden, D.E., 2012. Do blue-ice moraines in the Heritage Range show that the West Antarctic Ice Sheet survived the last interglacial? Palaeogeography, Palaeoclimatology, Palaeoecology, 335–336, 61–70, http:// dx.doi.org/10.1016/j.palaeo.2011.01.027.

Fretwell, P., Pritchard, H.D., Vaughan, D.G., Bamber, J.L., Barrand, N.E., Bell, R., Bianchi, C., Bingham, R.G., Blankenship, D.D., Casassa, G., Catania, G., Callens, D., Conway, H., Cook, A.J., Corr, H.F.J., Damaske, D., Damm, V., Ferraccioli, F., Forsberg, R., Fujita, S., Gogineni, P., Griggs, J.A., Hindmarsh, R.C.A., Holmlund, P., Holt, J.W., Jacobel, R.W., Jenkins, A., Jokat, W., Jordan, T., King, E.C., Kohler, J., Krabill, W., Riger-Kusk, M., Langley, K.A., Leitchenkov, G., Leuschen, C., Luyendyk, B.P., Matsuoka, K., Nogi, Y., Nost, O.A., Popov, S.V., Rignot, E., Rippin, D. M., Riviera, A., Roberts, J., Ross, N., Siegert, M. J., Smith, A.M., Steinhage, D., Studinger, M., Sun, B., Tinto, B. K., Welch, B.C., Young, D.A., Xiangbin, C., Zirizzotti, A., 2012. Bedmap2: improved ice bed, surface and thickness datasets for Antarctica, The Cryosphere Discuss., 6, 4305–4361, doi:10.5194/tcd-6-4305-2012.

Gehrels, G., Valencia, V., Pullen, A., 2006. Detrital zircon geochronology by laser-ablation multicollector ICPMS at the Arizona Laserchron Center. In: Loszewski, T., Huff, W. (Eds.), Geochronology, Emerging Opportunities, Paleontological Society Papers, 12, 67–76.

Gehrels, G., Valencia, V., Ruiz, J., 2008. Enhanced precision, accuracy, efficiency, and spatial resolution of UePb ages by laser ablation-multicollector-inductively coupled plasma-mass spectrometry. Geochemistry, Geophysics, Geosystems 9, Q03017. http://dx.doi.org/10.1029/2007GC001805.

Gehrels, G., 2012. Detrital zircon U-Pb geochronology: current methods and new opportunities. In: Busby, C., Azor, A. (Eds.), Tectonics of Sedimentary Basins: Recent Advances. Blackwell Publishing, pp. 47–62.

Goodge, J.W., Finn, C.A., 2010. Glimpses of East Antarctica: aeromagnetic and satellite magnetic view from the central Transantarctic Mountains of East Antarctica. Journal of Geophysical Research 115, B09103. http://dx.doi.org/10.1029/2009JB006890.

Goodge, J., Fanning, M., Brecke, D., Licht, K., Palmer, E., 2010. Continuation of the Laurentian Grenville province across the Ross Sea margin of Antarctica. Journal of Geology 118, p. 601–619. doi: 10.1086/656385.

Goodge, J.W., Fanning, C.M., Norman, M.D., Bennett, V.C., 2012. Temporal, isotopic and spatial relations of Early Paleozoic Gondwana-margin arc magmatism, central Transtantarctic Mountains, Antarctica. Journal of Petrology 53, p. 2027–2065.

Gulbranson, E.L., Isbell, J.L., Taylor, E.L., Ryberg, P.E., Taylor, T.N., Flaig, P.P., 2012. Permian polar forests: deciduousness and environmental variation. Geobiology, p. 1–17, doi: 10.1111/j.1472-4669.2012.00338.x.

Hagen, E.H., 1995. A geochemical and petrological investigation of meteorite ablation products in till and ice of Antarctica. M.S. thesis, Ohio State University, Columbus, Ohio, 551 p.

Hall, B., Denton, G., 2000. Radiocarbon chronology of Ross Sea drift, eastern Taylor Valley, Antarctica: evidence for a grounded ice sheet in the Ross Sea at the last glacial maximum. Geografiska Annaler, 82A, p. 305–336.

Hammer, Ø., Harper, D.A.T., Ryan, P.D., 2001. PAST: paleontological statistics software package for education and data analysis. Palaeontologia Electronica 4, p. 1–9. http://palaeo-electronica.org/2001_1/past/issue1_01.htm.

Hodgson, J., Licht, K.J, Swope, J., 2013. Affirmation of Antarctic-Laurentian Rodinian Juxtaposition During the MesoProterozoic. Geological Society of America Abstracts with Programs, 45, 7, p. 585.

Horner, T., 1992, Sedimentologic, mineralogic, and geochemical evaluation of the provenance and paleoclimate record of Permian mudrocks from the Beardmore Glacier area, Antarctica. PhD dissertation, Ohio State University, Columbus, Ohio, 377 p.

Ivy-Ochs, S., Kober, F., 2007. Cosmogenic Nuclides: Exposure Geochronology. In: Elias, S.A. (Eds.), Encyclopedia of Quaternary Sciences, Elsevier, Amsterdam, 436–445.

Joughin, I., Alley, R.B., 2011. Stability of the West Antarctic ice sheet in a warming world. Nature Geoscience 4, p. 506–513.

Kennett, J.P., Hodell, D.A., 1995. Stability or Instability of Antarctic Ice Sheets Durin Warm Climates of the Pliocene? GSA Today, 5, 1, p. 1, 10–13.

Krauskopf, K.B., Bird, D.K., 1994. Introduction to Geochemistry, 3rd Edition. McGraw-Hill, 647 p.

Krissek, L. A., Horner, T.C., 1988. Geochemical record of provenance in fine-grained Permian clastics, central Transantarctic Mountains. Antarctic Journal of the U. S., 23, 5, p. 19-21.

Krissek, L. A., Horner, T.C., 1989. Geochemical geochemical indicators or source lithologies and weathering intensities in fine-grained Permian clastics, central Transantarctic Mountains. Antarctic Journal of the U. S., 23, 5, p. 13–16.

Koffman, T., Hall, B. & Denton, G. 2011. New radio- carbon dates from glacial deposits in Miers Valley constrain the past behavior of the Antarctic Ice Sheet. 18th Annual West Antarctic Ice Sheet Meeting, Loveland, CO, http://www.waisworkshop.org.

Lawver, L.A., Gahagan, L.M., 2003. Evolution of Cenozoic seaways in the circum-Antarctic region. Palaeogeography, Palaeoclimatology, Palaeoecology, 198, p. 11–37.

Licht, K.J., Palmer, E.F., 2013. Erosion and transport by Byrd Glacier, Antarctica during the Last Glacial Maximum. Quaternary Science Reviews, 62, p. 32–48.

Licht K.J., Hennessy, A.J., Welke, B.M., in press. The U/Pb detrital zircon signature of West Antarctic ice stream tills in the Ross Embayment, with implications for LGM ice flow reconstructions. Antarctic Science.

Ludwig, K.R., 2003. Isoplot 3.00: Berkeley Geochronology Center, Special Publication, 4, 70 p.

Manassero, M.J., Cingolani, C.A., Abre, P., 2009. A Silurian–Devonian marine platform-deltaic system in the San Rafael Block, Argentine Precordillera–Cuyania terrane: lithofacies and provenance. In: Konigshof, P., Devonian Change: Case Studies in Palaeogeography and Palaeoecology. The Geological Society, London, Special Publications, 314, p. 215–240.

Mason, B., Moore, C.B., 1982. Principles of Geochemistry, 4th Edition, J. Wiley & Sons Inc, 352 p.

Mathieson, C., Kaplan, M.R., Winckler, G., Schaefer, J., Licht, K.J., Bader, N., Dits, T., 2012. Cosmogenic Dating of Moraines in the Central Transantarctic Mountains to Evaluate Past Behavior of the East Antarctic Ice Sheet. Abstract PP23C-2071 presented at 2012 Fall Meeting, AGU, San Francisco, CA., 3-7 Dec.

McGregor, V.R., 1965. Notes on the geology of the area between the heads of the Beardmore and Shackleton Glacier, Antarctica. New Zealand Journal of Geology and Geophysics, 8, 2, p. 278–291.

McLennan, S.M., 1993. Weathering and global denudation. Journal of Geology, 101, p. 295–303.

McSween, H.Y., Richardson, S.M., Uhle, M.E., 2003. Using Radioactive Isotopes, Geochemistry: Pathways and Processes. 2nd Editon, p. 294–295.

Mielke, J.E., 1979. Composition of the Earth's crust and distribution of the elements. In: Siegel, F.R. (Ed.), Review of Research on Modern Problems in Geochemistry. UNESCO Report, Paris, p. 13–37.

Moecher, D.P., Samson, S.D., 2006. Differential zircon fertility of source terranes and natural bias in the detrital zircon record: implications for sedimentary provenance analysis. Earth and Planetary Science Letters, 247, p. 252–266.

Nesbitt, H.W., Young, G.M.,1982. Early Proterozoic climate and plate motions inferred from major element chemistry of lutites. Nature, 299, p. 715–717.

Palmer, E.F., Licht, K.J., Swope, R.J., Hemming, S.R., 2012. Nunatak moraines as a repository of what lies beneath the East Antarctic ice sheet. In: Rasbury, E.T., Hemming, S.R., Riggs, N.R. (Eds.), Mineralogical and Geochemical Approaches to Provenance. Geological Society of America Special Paper, vol. 487, pp. 97e104. http://dx.doi.org/10.1130/2012.2487(05).

Passchier, S., 2004. Variability in geochemical provenance and weathering history of Sirius Group strata, Transantarctic Mountains: implications for Antarctic glacial history. Journal of Sedimentary Research, 74, 5, p. 607–619.

Pollard, D., DeConto, R.M., 2009. Modeling West Antarctic ice sheet growth and collapse through the past five million years. Nature 458, 329–332. http://dx.doi.org/10.1038/nature07809.

Potter, P.E., Maynard, J.B., Depetris, P.J., 2005. Mud and Mudstones: Introduction and Overview. Springer, p. 157–74.

Rudnick R.L., Gao, S., 2003. Composition of the continental crust. Treatise on Geochemistry, 3, p. 1–64.

Ryberg, P.E., Taylor, E.L., Taylor, T.N., 2012. Permineralized lycopsid from the Permian of Antarctica. Review of Palaeobotany and Palynology, 169, p. 1–6.

Scarrow, J.W., Balks, M.R., Almond, P.C., 2014. Three soil chronosequences in recessional glacial deposits near the polar plateau, in the Central Transantarctic Mountains, Antarctica. Antarctic Science, p. 1–11. doi:10.1017/S0954102014000078.

Schilling, A., 2010. Reconstructing past Antarctic ice flow paths in the Ross Embayment, Antarctica using sand petrography, particle size and detrital zircon provenance. M.S. thesis, Indiana University, Indianapolis, IN, USA.

Siegert, M.J., Carter, S., Tobacco, I., Popov, S., Blankenship, D.D., 2005. A revised inventory of Antarctic subglacial lakes. Antarctic Science, 17, p. 453–460.

Stacey, J.S., Kramers, J.D., 1975. Approximation of terrestrial lead isotope evolution by a two-stage model. Earth and Planetary Science Letters 26, 207–221. doi:10.1016/0012-821X(75) 90088-6.

Stearns, L.A., 2011. Dynamics and mass balance of four large East Antarctic outlet glaciers. Annals of Glaciology 52 (59), 116–126.

Stearns, L.A., Smith, B.E., Hamilton, G.S., 2008. Increased flow speed on a large East Antarctic outlet glacier caused by subglacial floods. Nature Geoscience 1, 827–831. doi: 10.1038/ngeo356.

Stern, T.A., Baxter, A.K., Barrett, P.J., 2005. Isostatic rebound due to glacial erosion within the Transantarctic Mountains. Geology, 33, 3, p. 221–224.

Stickley CE, Brinkhuis H, Schellenberg S, Sluijs A, Roehl U, Fuller M, 2004. Timing and nature of the deepening of the Tasmanian Gateway. Paleoceanography, 19:PA4027.

Stone, J.O., Conway, H., Cowdery, S., Hall, B., Bromley, G., 2009. Deglaciation of the Ross Sea: the view from Scott and Beardmore Glaciers. 16th Annual West Antarctic Ice Sheet Meeting, Eatonville, WA, http://www.waisworkshop.org.

Stump, E., 1995. The Ross Orogen of the Transantarctic Mountains. Cambridge University Press, 284 p.

Taylor, S.R., McLennan, S.M., 1985. The continental crust: its composition and evolution. Blackwell Scientific Publication, Carlton, 312 p.

Taylor, E.L., Taylor, T.N., 1990. Structurally preserved Permian and Triassic floras from Antarctica. In: Taylor, E.L., Thomas, T.N. (Eds.), Antarctic Paleobiology, Springer, p. 149–163.
Thomas, S.G., 2000. Trees: Their Natural History. Cambridge University Press, p. 286, ISBN:978-05-214-59631.
Thomson, M.R.A., Crame, J.A., Thomson, J.W. (Eds), 1991. Geological Evolution of Antarctica. Cambridge University Press, 740 p.
Tingey, R.J., 1991. The regional geology of Archaean and Proterozoic rocks in Antarctica. In: Tingey, R.J. (Ed.), The geology of Antarctica: Oxford Monographs on Geology and Geophysics, 17, Clarenden Press, p. 1–73.
Todd, C., Stone, J., Conway, H., Hall, B.R., Bromley, G., 2010. Late Quaternary evolution of Reedy Glacier, Antarctica. Quat. Sci. Rev. 29, 1328e1341. http://dx.doi.org/10.1016/j.quascirev.2010.02.001.
Vavra, C.L., 1982. Provenance and Alteration of the Triassic Fremouw and Falla Formations, Central Transantarctic Mountains, Antarctica. PhD dissertation, Ohio State University, Columbus, Ohio.
Veevers, J.J., 2003. Pan-African is Pan-Gondwanaland: oblique convergence drives rotation during 650-500 Ma assembly. Geology, 31, p. 501–504.
Whillans, I.M., Cassidy, W.A., 1983. Catch a falling star: Meteorites and old ice: Science, 222, 4619, p. 55–57.
Wingham, D.J., Siegert, M.J., Shepherd, A., Muir, A.S., 2006. Rapid discharge connects Antarctic subglacial lakes. Nature, 440, p. 1033–1036.
Wise, S.W., Fr., Breza, J.R., Harwood, D.M., Wei, W., 1991. Paleogene glacial history of Antarctica. In: McKenzie, J.A., Muller, D.W., Weissert, H. (Eds.), Controversies in Modern Geology, Cambridge: Cambridge University Press, p. 133–171.
Zachos, J., Pagani, M., Sloan, L. Thomas, E., Billups, K., 2001. Trends, Rhythms, and Aberrations in Global Climate 65 Ma to Present, Science, 292, 686-693.

CURRICULUM VITAE

Nicole Ann Bader

Education

June 2014 — Master of Science in Geology
Indiana University Purdue University-Indianapolis (IUPUI)
Indianapolis, IN
Master's Thesis: "Provenance of the Ice-Cored Moraine at Mt. Achernar, Law Glacier, Antarctica"
Advisor: Dr. Kathy Licht

May 2011 — Bachelor of Science
Major: Geology
St. Norbert College (SNC)
DePere, WI
Dean's List: Fall 2007-Spring 2009

Academic Experience

Teaching Experience

- IUPUI Teaching Assistant: G119-Historical Geology Laboratory (2013)
- SNC Teaching Assistant: Introduction to Geology Laboratory (2009-2011)

Lab Experience

- IUPUI Sedimentology Lab
  - Preparation of till samples for the Malvern Mastersizer 2000 laser particle size analyzer and VirTis Benchtop freeze-dryer
  - Preparation of grain mounts and thin sections from samples in East Antarctica
  - Classification of pebbles from East Antarctica
- Arizona LaserChron Center
  - Operated the Nu Plasma HR ICPMS to obtain U/Pb rations of detrital zircons
- Lamont-Doherty Earth Observatory
  - Preparation of rock samples for cosmogenic analysis

Field Experience

- California State University Long Beach 4-week field camp attendee in Ruth, Nevada (2011)
- Transantarctic Mountains, Antarctica field party member, 6 weeks (2010-2011)
- Florida Keys 1-week field course attendee (2009)
- Galapagos Islands 2-week field course attendee (2008)

Professional and Outreach Presentations

- Luxemburg-Casco H.S.: Life of a Graduate Student (Jan. 2014)
- IUPUI Geology Club: My Summer as a GeoCorps Intern (Dec. 2013)

- St. Richards Episcopal School: What is Geology? (March 2013)
- AGU: Provenance of the Ice Cored Moraine Tills at Mt. Achernar, Law Glacier, Antarctica (Dec. 2012)
- Weebelos (Boy Scouts): Intro to Indiana and Antarctic Geology (Nov. 2012)
- AAPG Imperial Barrel Award Program and Indiana Geologists: Exploration Potential of Nova Scotia Sable Sub-basin (May 2012)
- IUPUI College Mentors for Kids: What is Geology? (Feb. 2012)
- Luxemburg-Casco H.S. and St. Norbert College: Travels in Antarctica: A Scientific Adventure (May 2011)

Clubs

- IUPUI Geology Club (2011-2014)
- IUPUI Swing Cats: west coast swing dance club (2011-2014)
- SNC Geology Club (2008-2011)
- SNC Ballroom Dance Club (2007-2011)
- SNC Untouchables: Female Independent Social Organization (2007-2011)
    - Vice President and Homecoming Chair (2010-2011)
    - Social Chair (2009-2010)
    - Clothing Chair (2008-2009)

Employment

May 2013-Sep. 2013	Employer: National Park Service; GeoCorps America Internship; Glacier National Park, MT Title: Geology Interpreter/Educator Supervisor: Diane Sine (406) 250-0169 Duties: Presenting visitors with formal and informal park interpretation, staffing the Many Glacier ranger station information desk, and helping other interpreters learn and teach geological concepts.
Jan. 2013-May 2013	Employer: Indiana University Purdue University-Indianapolis; Indianapolis, IN Title: G119-Historical Geology Teaching Assistant Supervisor: Renata Lafler (317) 274-4946 Duties: Prepare and present each week's material in an efficient yet effective manner by providing students with Powerpoint presentations, handouts, in-class examples, and additional online resources. Grade examinations and weekly labs based on student's effort and quality of work. Offer study sessions for students upon request.
Sep. 2009-May 2011	Employer: Saint Norbert College; DePere, WI Title: Geology Teaching Assistant Supervisor: Tim Flood (920) 403-1356

Duties: Helped students understand introductory geology material and prepare for both lab and class lecture examinations by answering their questions, providing examples, and reviewing the material. Aided with grading of examinations and weekly labs based on student's quality of work.

Sep. 2009-May 2011 — Employer: Saint Norbert College; DePere, WI
Title: Residential Education and Housing Apartment Manager
Supervisor: Michael Peckham (920-403-3360)
Duties: Addressed students' and parents' concerns and questions about campus activities and resources. Completed monthly safety inspections of each residence hall and on-campus apartment and house. Assisted hall directors and office staff with tasks such as answering phones, filing paperwork, and key inventory.

Awards

- GeoCorps America Participant
- IUPUI School of Science Graduate Student Council Grant
- IUPUI Educational Enhancement Grant

Abstract Citations

- Licht, K., Welke, B., **Bader, N.,** Dits, T., Hennessy, A., Palmer, E.F., 2013. Overview of Provenance Signatures, Geologic History, and Ice Sheet Stability Indicated by Detrital Zircon U/Pb and (U-Th)/He Ages from Antarctic Till. Geological Society of America *Abstracts with Programs.* Vol. 45, No. 7, p.745.
- **Bader, N**., Licht, K., Dits, T., Kaplan, M., Schaefer, J., Winckler, G., Flood, T., 2012. Provenance of the Ice Cored Moraine Tills at Mt. Achernar, Law Glacier, Antarctica. Abstract PP23C-2072 presented at 2012 Fall Meeting, AGU, San Francisco, CA., 3-7 Dec.
- Dits, T., Licht, K., **Bader, N**., Kaplan, M.R., Winckler, G., Schaefer, J., 2012. Uncovering East Antarctic Bedrock Using Detrital Zircon Geochronology and Pebble Lithologies at Mount Howe, Scott Glacier. Abstract PP23C-2073 presented at 2012 Fall Meeting, AGU, San Francisco, CA., 3-7 Dec.
- Mathieson, C., Kaplan, M.R., Winckler, G., Schaefer, J., Licht, K., **Bader, N.,** Dits, T., 2012. Cosmogenic Dating of Moraines in the Central Transantarctic Mountains to Evaluate Past Behavior of the East Antarctic Ice Sheet. Abstract PP23C-2071 presented at 2012 Fall Meeting, AGU, San Francisco, CA., 3-7 Dec

Skills

- Operating systems: Advanced skills in a variety of Windows and Mac operating systems.
- Software: Microsoft Office Suite, ESRI ArcGIS, ENVI, PAST, RockJock, Trimble GPS, Garmin GPS, Adobe Photoshop, Audacity: Audio Editor.

- Additional languages: Spanish (written/verbal): 4 semesters of speaking, reading, writing and presenting in the Spanish language.
- American Heart Association Heartsaver CPR/First-Aid certification.

Professional Affiliations

- Geological Society of America
- GeoCorps of America
- American Association of Petroleum Geologists
- American Geophysical Union

Service

- September 2012-August 2013: IUPUI School of Science Earth Science Graduate Student Representative
- Jan. 2012: Volunteer aid for Science Olympiad hosted at IUPUI
- Volunteer aid for USGS-CEES IUPUI Research Exchange July 2012
- June 2012: Volunteer aid for the Transantarctic Mountains Camp (TAM Camp) workshop hosted at IUPUI

Other

- First Wednesday Brown Bag: Teaching to Every Learner: discussed strategies for creating classroom activities and learning opportunities that meet the learning needs of all students.